European Journal of Taxonomy 984: 1–131
https://doi.org/10.5852/ejt.2025.984.2851
ISSN 2118-9773
www.europeanjournaloftaxonomy.eu
2025 · Cicimurri D.J. *et al.*

Monograph

urn:lsid:zoobank.org:pub:7D8BB514-E8B7-403C-9725-B1405E214075

Late Oligocene fishes (Chondrichthyes and Osteichthyes) from the Catahoula Formation in Wayne County, Mississippi, USA

David J. CICIMURRI [1,*], Jun A. EBERSOLE [2], Gary L. STRINGER [3], James E. STARNES [4] & George E. PHILLIPS [5]

[1,*] South Carolina State Museum, 301 Gervais Street, Columbia, South Carolina 29021, USA.
[2] McWane Science Center, 200 19th Street North, Birmingham, Alabama 35203, USA.
[3] University of Louisiana at Monroe, Monroe, Louisiana 71209, USA.
[4] Office of Geology, Mississippi Department of Environmental Quality, 700 North State Street, Jackson, Mississippi 39202, USA.
[5] Mississippi Museum of Natural Science, 2148 Riverside Drive, Jackson, Mississippi 39202, USA.

[*] Corresponding Author: dave.cicimurri@scmuseum.org
[2] Email: jebersole@mcwane.org
[3] Email: stringer@ulm.edu
[4] Email: jstarnes@mdeq.ms.gov
[5] Email: george.phillips@mmns.ms.gov

[1] urn:lsid:zoobank.org:author:F0155EA1-F5D6-49E4-B578-7A14DBB7B902
[2] urn:lsid:zoobank.org:author:D48E2A2F-EC92-4C32-9F2A-2D39716C459E
[3] urn:lsid:zoobank.org:author:4E93392A-5916-44C6-B55A-9053A4F44C76
[4] urn:lsid:zoobank.org:author: D4E14C23-EE57-4D1D-8709-895A1345C8BA
[5] urn:lsid:zoobank.org:author: DFFC9021-05C6-4B56-BCD3-D54BCDE91351

Abstract. Isolated elasmobranch and teleost teeth, jaws, otoliths, scales, vertebrae, and fin spines were recovered from the upper Oligocene (Chattian) Catahoula Formation in Wayne County, Mississippi, USA. A total of 13 551 specimens were examined and 12 340 of these were identified at least to the ordinal level. These remains represent 49 unequivocal fish taxa, viz. 29 elasmobranchs and 20 teleosts. The 3614 elasmobranch remains indicate that Carcharhiniformes is the most diverse group of Elasmobranchii, with 12 taxa belonging to five families. Orectolobiformes and Lamniformes are represented by far fewer taxa (three and four, respectively). *Carcharhinus acuarius* (Probst, 1879) constitutes 49% of the total number of shark teeth in our sample. Ten batoids have been identified within Myliobatiformes (seven taxa) and Rhinopristiformes (three taxa). Partial teeth of durophagous myliobatids (three genera) are the most abundant batoid remains, constituting 41% of the total number of ray fossils. However, teeth of Dasyatidae and *Rhynchobatus* cf. *pristinus* (Probst, 1877) are abundant and represent 36.5% and 15.4%, respectively, of the specimens identified. Herein, we erect five new elasmobranch taxa, including *Galeocerdo platycuspidatum* sp. nov., *Hemipristis intermedia* sp. nov., *Hypanus*? *heterodontus* sp. nov., "*Sphyrna*" *gracile* sp. nov., and "*Sphyrna*" *robustum* sp. nov.

The Catahoula Formation sample includes over 9935 teleost fossils, which constitutes 73% of the total fish sample. Nine bony fish taxa are represented solely by teeth, jaw elements, or fin spines. Although otoliths are much less common than the other identifiable remains (409 versus roughly 8430,

respectively), they allowed us to identify four taxa not known from other skeletal remains. Albulidae, Sciaenidae, and Sparidae are represented by isolated teeth, jaw elements, and otoliths, but we could not ascertain whether the various teeth and jaw elements are conspecific with the otolith-based species we identified. The remains of Sciaenidae (teeth, jaw elements, otoliths) dominate the Catahoula Formation bony fish assemblage, constituting 70% of the teleost specimens identified at least to the ordinal level. Our sample includes the first Oligocene occurrence of Tetraodontidae in the Western Hemisphere.

The vertebrate assemblage within the Catahoula Formation at the study site indicates an estuarine depositional environment, which is consistent with previous interpretations based on lithology. At the study site the Catahoula Formation disconformably overlies the Paynes Hammock Limestone, and we believe the disconformable contact locally represents the Rupelian (early Oligocene)/Chattian (late Oligocene) boundary. The fish fauna described herein is therefore of Chattian age.

Keywords. Elasmobranchii, Teleostei, Paleogene, Oligocene, Chattian, Gulf Coastal Plain, Mississippi.

Cicimurri D.J., Ebersole J.A., Stringer G.L., Starnes J.E. & Phillips G.E. 2025. Late Oligocene fishes (Chondrichthyes and Osteichthyes) from the Catahoula Formation in Wayne County, Mississippi, USA. *European Journal of Taxonomy* 984: 1–131. https://doi.org/10.5852/ejt.2025.984.2851

Contents

Introduction 3
Material and methods 5
Institutional abbreviations 6
Geological and stratigraphical settings 6
Results 8
Brachaeluridae Applegate, 1974 gen. et sp. indet. 8
Genus *Chiloscyllium* Müller & Henle, 1837 9
Genus *Nebrius* Rüppel, 1837 10
Genus *Otodus* Agassiz, 1843 12
Genus *Carcharias* Rafinesque, 1810 13
Genus aff. *Pseudocarcharias* Cadenat, 1963 16
Genus *Alopias* Rafinesque, 1810 17
Genus *Hemipristis* Agassiz, 1835 18
Genus *Physogaleus* Cappetta, 1980a 26
Genus *Rhizoprionodon* Whitley, 1929 30
Genus *Carcharhinus* de Blainville, 1816 31
Genus *Galeorhinus* de Blainville, 1816 34
Genus *Pachyscyllium* Reinecke *et al.*, 2005 36
Genus *Sphyrna* Rafinesque, 1810 38
Genus *Galeocerdo* Müller & Henle, 1837 45
Genus *Rhynchobatus* Müller & Henle, 1837 49
Genus *Pristis* Linck, 1790 51
Genus *Anoxypristis* White & Moy-Thomas, 1941 53
Genus *Hypanus* Rafinesque, 1818 54
Dasyatidae Jordan & Gilbert, 1879 gen. et sp. indet. 63
Genus *Myliobatis* Cuvier, 1816 64
Genus *Aetomylaeus* Garman, 1908 66
Genus *Rhinoptera* Cuvier, 1829 67
Genus *Plinthicus* Cope, 1869 70
Genus *Paramobula* Pfeil, 1981 71

Batomorphi Cappetta, 1980b fam., gen. et sp. indet. 72
Euselachii Hay, 1902 fam., gen. et sp. indet. 74
Lepisosteidae Cuvier, 1825 gen. et sp. indet. 75
Albulidae Bleeker, 1859 gen. et sp. indet. 76
Genus *Protanago* Schwarzhans, Stringer & Takeuchi, 2024 78
Congridae Kaup, 1856 gen. et sp. indet. 80
Siluriformes Cuvier, 1816 fam., gen. et sp. indet. 80
Genus *Sphyraena* Artedi in Röse, 1793 81
Genus *Syacium* Ranzani, 1842 84
Genus *Acanthocybium* Gill, 1862 85
Genus *Scomberomorus* Bleeker, 1859 85
Labridae Cuvier, 1816 gen. et sp. indet. 86
Genus *Allomorone* Dante & Frizzell in Frizzell & Dante 1965 87
Lutjanidae Gill, 1861 gen. et sp. indet. 89
Genus *Aplodinotus* Rafinesque, 1819 90
Genus *Sciaena* Linnaeus, 1758 92
Sciaenidae Cuvier, 1829 gen. et sp. indet. 94
Genus *Diplodus* Rafinesque, 1810 95
Genus *Sparus* Linnaeus, 1758 96
Sparidae Rafinesque, 1818 gen. et sp. indet. 97
Lophiidae Rafinesque, 1810 gen. et sp. indet. 98
Tetraodontidae Bonaparte, 1831 gen. et sp. indet. 99
Teleostei fam., gen. et sp. indet 101
Discussion 101
Characteristics of the Catahoula fish assemblage 101
Biostratigraphic and biogeographic implications of the Catahoula Formation fish assemblage .. 103
Paleoecology and depositional environment of the fossil deposit 105
Conclusions 107
Acknowledgments 107
References 108
Appendices 130

Introduction

Oligocene vertebrate faunas within the Gulf Coastal Plain are relatively unknown. Previous reports of marine vertebrates from Alabama (i.e., Ebersole *et al.* 2021), Louisiana (Stringer & Worley 2003), and Mississippi (Stringer *et al.* 2020c) documented various fish taxa largely based on otoliths, but a limited number of teleosts and elasmobranchs have been identified based on teeth and other skeletal remains, as for example in the Mint Spring Formation in Mississippi (Stringer & Miller 2001). Our understanding of marine vertebrate paleofaunas from this region has recently been improved through the discovery of a highly fossiliferous unit exposed along the banks of a tributary of the Chickasawhay River in eastern Mississippi (Fig. 1A). The fossiliferous unit yielded a significant sample of vertebrate fossils that have provided a unique window into an ancient ecosystem.

Referred to herein as the Jones Branch locality, the fossil site was discovered by avocational collectors in 2012. Jones Branch is a tributary of the Chickasawhay River, and the collecting site is located approximately 1.4 km southwest of the intersection of Mississippi State Highway 184 and Mississippi State Highway 63 (decimal degrees = 31.6618, -88.6564) in Waynesboro, Wayne County, Mississippi, USA (Fig. 1B). The locality is designated as site MS.77.011 by the Mississippi Museum of Natural Science, Jackson, MS, USA. Although access to the locality is possible, the fossil site has been covered with riprap to prevent collapse of the cut bank, and the fossiliferous unit is no longer exposed for study.

Fossils from the site were brought to the attention of GEP who, along with JES, conducted initial investigations at the locality. It was determined that fossils were contained within argillaceous, shelly quartz sand occurring in the lower part of the Oligocene Catahoula Formation. This unit is part of the Jones Branch fossil horizon as utilized by Stults *et al.* (2024), and this informal term is used herein when referring to the fossil bed we sampled. Preliminary analysis of fossils indicated the presence of a diverse vertebrate paleofauna that includes cartilaginous and bony fishes (teeth, skeletal remains, and otoliths), marine and terrestrial mammals, and a herpetofauna containing amphibians and reptiles. Further investigations by the present authors have revealed the true extent of the fossil assemblage,

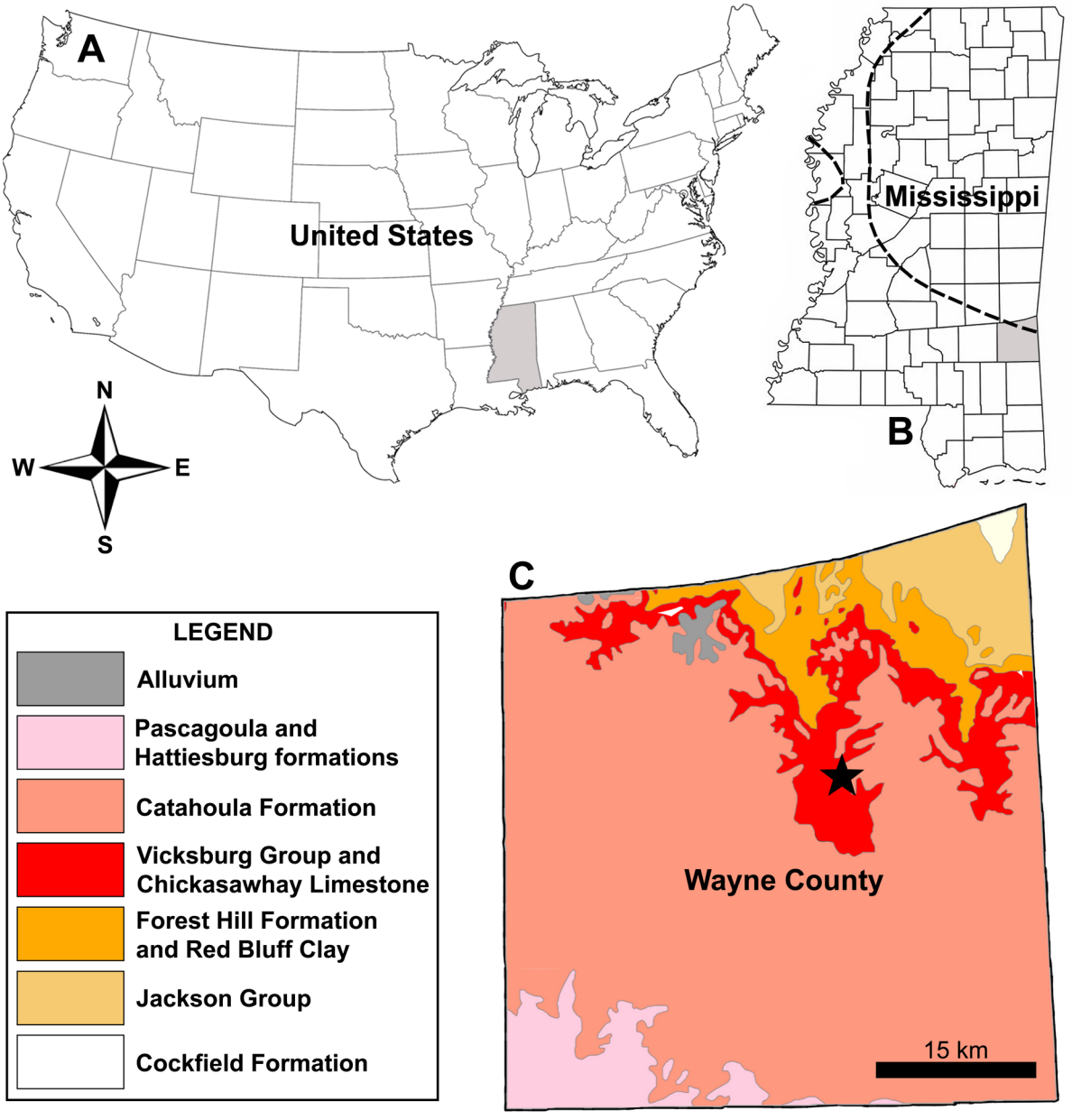

Fig. 1. Geographic location of the Jones Branch fossil site. **A**. State map of the USA showing the location of Mississippi (gray). **B**. County map of Mississippi showing the location of Wayne County (gray). The dotted line represents the Oligocene shoreline based on state-scale surface geology. **C**. Detail map of Wayne County showing the fossil site (designated by solid star at the base of the Catahoula Formation) and the geologic units occurring in the area.

which is dominated by marine fishes. The results of a comprehensive evaluation of the fish assemblage are reported herein, where we describe the various fossils and identify the taxa represented. We also comment on the morphological criteria we used to identify taxa, and we discuss taxonomic issues related to the taxa identified. Furthermore, we comment on the paleobiogeographic and temporal distributions of the taxa, as well as provide a paleoenvironmental evaluation of the fossil-bearing unit based on the associated fossils.

Material and methods

With few exceptions, the specimens discussed herein were obtained from processed matrix samples collected by DJC, GLS and GEP. Approximately 15 kg of bulk matrix from the fossil bed was screened in the creek by DJC using #5, #10 and #20 (0.85 mm) US Standard Soil Sieves. These concentrated fractions were individually bagged and brought to the laboratory, along with an additional 23 kg of unprocessed matrix (wet). This matrix was disaggregated in water and gently screened down to #40 (0.42 mm) mesh size, but material passing through this screen was saved for examination. The remaining concentrations of lithologic material and fossils were sorted under a binocular microscope. These Jones Branch fossils are housed at the South Carolina State Museum in Columbia, USA and are catalogued under accession SC2013.28.

A roughly 75 kg sample (weight was determined after it was air-dried) was collected directly from the fossiliferous bed by GLS. The sample was screen washed with tap water using #5, #10, #20, and #35 (0.5 mm) screens. The remaining residues were examined with a stereoscopic binocular microscope using 6.7–40× magnification. All otoliths that were at least one-half complete were targeted for examination, and taxonomic identification was done by GLS. The otoliths from the GLS collection that are illustrated herein are reposited in the scientific collections at the Mississippi Museum of Natural Science (MMNS) in Jackson, Mississippi, USA.

Specimens exceeding 5.0 mm in greatest dimension were photographed with a Nikon D-80 camera with a Tamron macro-lens. Specimens smaller than 5.0 mm in greatest dimension were photographed with a Wild Photomakroskop M400 microscope with a mounted Canon Eos R50 camera. To account for depth of field, specimens were photographed from several focal lengths and the resulting photographs were stacked and merged in Helicon Focus 8 software. The final plates were produced in Adobe Photoshop ver. 22.5.9. Photographs of sagittae showing the inner surface are oriented with the anterior margin at left, and right sagittae were therefore used as possible. However, when the left sagitta was used we indicated within the figure caption that the image was reversed (so that it appears as if it were a right sagitta)

The classification scheme utilized herein largely follows that of Nelson *et al.* (2016), which was influenced by the molecular research of Betancur-R. *et al.* (2013), but any departure from their hierarchy is noted. Ordinal names were typically based on Wiley & Johnson (2010), and family-group names and authors follow Van der Laan *et al.* (2014). Authorships for genera and species are based primarily on Eschmeyer's *Catalog of Fishes: Genera, Species, References* (Fricke *et al.* 2019). To aid in the anatomical and taxonomic identification of fossils, material was, whenever possible, directly compared to extant elasmobranch jaws and bony fish skeletons housed in the collections at McWane Science Center, Birmingham, Alabama, USA, the South Carolina State Museum, Columbia, USA, and the research collection (otoliths) of one of the authors (GLS).

Institutional Abbreviations

GCVP = Georgia College and State University, Milledgeville, GA, USA
MSC = McWane Science Center, Birmingham, AL, USA
MMNS = Mississippi Museum of Natural Science, Jackson, MS, USA
SC = South Carolina State Museum, Columbia, SC, USA

Geological and stratigraphical settings

The fish fossils described herein were recovered from the upper Oligocene (Chattian) Catahoula Formation at site MS.77.011 in Wayne County, Mississippi, USA. The Catahoula Formation extends from Texas to Alabama in the USA and attains a maximum thickness exceeding 240 m in central Louisiana (Dockery & Thompson 2016). Exposures of the Catahoula Formation are common throughout its outcrop belt, except where it is obscured by post-Pleistocene alluvium. Marginal marine to deltaic impure clays (silty-to-fine sands) occur throughout the section. The clays are interspersed with interbedded distributary channel and thick deltaic sands having grain sizes ranging from fine to coarse and graveliferous. The Catahoula Formation underlies the Hattiesburg Formation of Miocene age, and in western Mississippi it disconformably overlies lower Oligocene (Rupelian) strata of the Vicksburg Group. In western Mississippi the Catahoula Formation is laterally (temporally) equivalent to the Paynes Hammock Limestone, but in the eastern part of the state the Catahoula Formation disconformably overlies the Paynes Hammock Limestone (Fig. 2A).

A stratigraphic test hole, MGS N-12, located near site MS.77.011, was initiated by the Mississippi Geological Survey in 1972 and an electric log was obtained (May *et al.* 1974). The data collected, combined with our observations at the site, demonstrate that the Catahoula Formation and Paynes Hammock Limestone are present at the fossil locality (Figs 1C, 2B). Additionally, the Chickasawhay Limestone (which underlies the Paynes Hammock Limestone) occurs in the subsurface (Starnes & Phillips 2016). The subjacent Chickasawhay Limestone and Paynes Hammock Limestone both contain the planktonic foraminiferan *Chiloguembelina cubensis* (Palmer, 1934), a species whose extinction marks the Rupelian/Chattian stage boundary (King & Wade 2017; Li *et al.* 2023). The age of the boundary at the Global Stratotype Section and Point is between 27.82 and 27.41 Ma (Coccioni *et al.* 2018). The unconformable contact between the Paynes Hammock Limestone and overlying Catahoula Formation demonstrates an abrupt change from carbonate to clastic deposition and is considered herein to represent the Rupelian/Chattian boundary. The Jones Branch fossil horizon at site MS.77.011 is therefore considered by us to be of Chattian age, although no calcareous nannofossils have been described from the Jones Branch fossil horizon to help place exactly when the unit should be correlated, and deposition within Zone NP25 (late Chattian) has been proposed (Starnes & Phillips 2016; Stults *et al.* 2024). If our timing is correct, the disconformable contact between these two lithostratigraphic units could also reflect regression related to Rupelian glaciation (erosion) and subsequent transgression (deposition) during Chattian warming (Van Simaeys *et al.* 2004; Pälike *et al*. 2006). The portion of the Catahoula Formation exposed at the Jones Branch locality stratigraphically occurs well below the last regional occurrence of the benthic foraminifer, *Heterostegina*, a marker taxon for the upper beds of the Catahoula Formation. We note here that this marker horizon was previously placed immediately above the top of the Paynes Hammock Limestone (Dockery & Thompson 2016), but the marker zone and base of the Catahoula Formation are separated by several hundred feet (Fig. 2A).

The Paynes Hammock Limestone consists of glauconitic, sandy-clay marl and soft limestones dominated by thin discontinuous reefs of the large oyster, *Crassostrea blanpiedi* (Howe, 1937). The top of the Paynes Hammock Limestone is marked by a distinctive bed that is a thin, fine-grained, sandy, indurated ledge with well-preserved primary structures of ripple marks on its upper surface. Its upper contact (with the Catahoula Formation) is interpreted as once belonging to a sandy tidal flat truncating the underlying marine deposits of the Paynes Hammock Limestone (Starnes & Phillips 2016).

The Catahoula Formation consists of unweathered dark gray-green, carbonaceous fissile clays. The clays are interrupted by a series of thin coeval sands that are tidally influenced distributary channel lenses along a narrow horizon. Combined, the post-Paynes Hammock deposits represent an emergent delta with brackish water and terrestrial influences grading upwards to massive and more uniform, non-fossiliferous freshwater clays. The clays contain an excellently preserved flora that includes lignitized

Nyssa sp., endocarps and leaf compressions of Lauraceae, palms, and other undescribed morphotypes with entire or toothed margins (a long grass blade is encrusted with barnacles). The flora is indicative of a warm-temperate to subtropical estuarine paleoclimate (Baghai-Riding *et al.* 2018). The sand lenses contain a lag of phosphatic nodules, marine invertebrates (mollusks, crustaceans, brachiopods, echinoderms), and vertebrate remains of both marine (sirenians, cetaceans, elasmobranchs, teleosts) and terrestrial (rodents, ungulates, carnivores, reptiles) taxa. Together, these fossiliferous beds constitute the Jones Branch fossil horizon (sensu Stults *et al.* 2024). One sand lens yielded the Jones Branch paleofauna discussed herein. Although Dockery & Thompson (2016) stated that no vertebrate fossils were known from the Catahoula Formation of Mississippi, specimens that they show in their fig. 893, recovered loose in the stream channel and attributed to the Paynes Hammock Limestone, are now known to have originated from the superjacent Catahoula Formation.

The fossiliferous sand lens of the Jones Branch fossil horizon appears to be somewhat bimodal in deposition, as very well-rounded quartz (nearly spherical) grains constitute a large portion of the mineral clasts. Additionally, fossils of larger marine animals occurring in these channel lags, like oyster valves and dugong ribs, exhibit signs of breakage and heavy abrasion from post mortem transport. The terrestrial vertebrate fossils are comparatively more pristine, and angular quartz grains (including rose quartz) are common, indicating primary deposition.

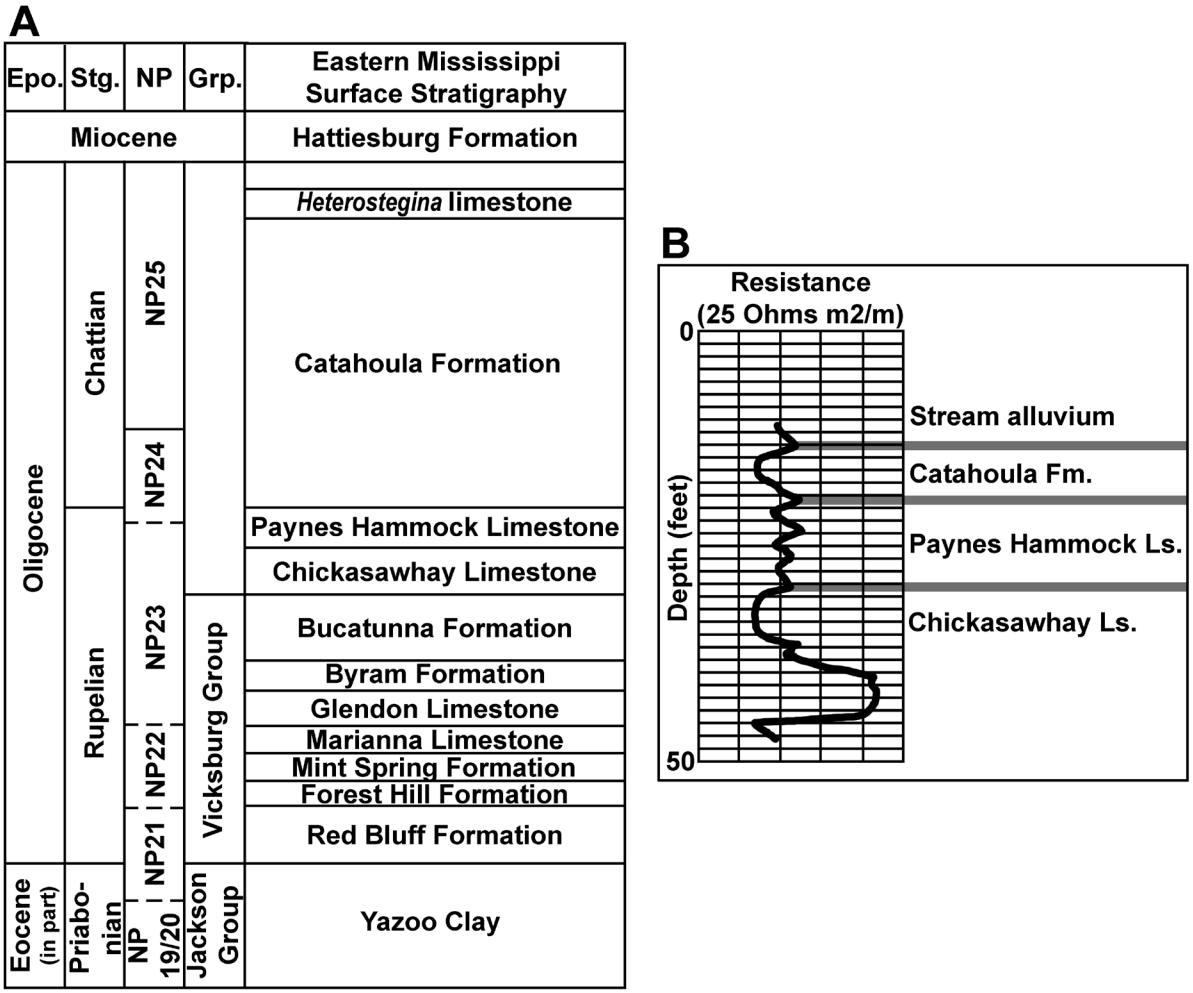

Fig. 2. Lithostratigraphy of eastern Mississippi, USA. **A**. Stratigraphic section showing the relationships among the various Oligo-Miocene lithostratigraphic units occurring in eastern Mississippi. **B**. E-log from near the fossil site showing the lithostratigraphic units occurring in the study location.

Results

Class Chondrichthyes Huxley, 1880
Subclass Euselachii Hay, 1902
Infraclass Elasmobranchii Bonaparte, 1838
Division Selachii Cope, 1871
Superorder Galeomorphi (sensu Nelson, Grande & Wilson 2016)
Suborder Orectoloboidei Applegate, 1974
Order Orectolobiformes Applegate, 1974
Superfamily Orectoloboidea Naylor *et al.*, 2012
Family Brachaeluridae Applegate, 1974

Brachaeluridae gen. et sp. indet.
Fig. 3A–C

Material examined

UNITED STATES OF AMERICA – **Mississippi** • 1 isolated tooth; Catahoula Formation; SC2013.28.54.

Description

This tooth crown measures 2 mm in height and 1.5 mm in width. The crown consists of a tall, rather narrow, triangular main cusp flanked by a single pair of lateral cusplets. The main cusp is conical with indistinct mesial and distal cutting edges (Fig. 3C). In labial view, the main cusp is very slightly distally inclined, and in profile view, it is straight and lingually directed. The labial crown foot is expanded basally into a convex protuberance (aka apron), and there is a diminutive, medially located, basally directed protuberance (Fig. 3A). The lateral cusplets are conical, well-separated from the main cusp, slightly diverging, and located very low on the crown (Fig. 3B). The root is not preserved.

Remarks

Specimen SC2013.28.54 is the only tooth of its kind available to us, but its symmetrical shape indicates that it represents an anterior tooth file. The specimen is clearly distinct from the teeth of two other orectolobiform sharks occurring in the Catahoula Formation (see below). The conical main cusp, single pair of lateral cusplets located low on the crown, and medial protuberance at the labial crown foot are

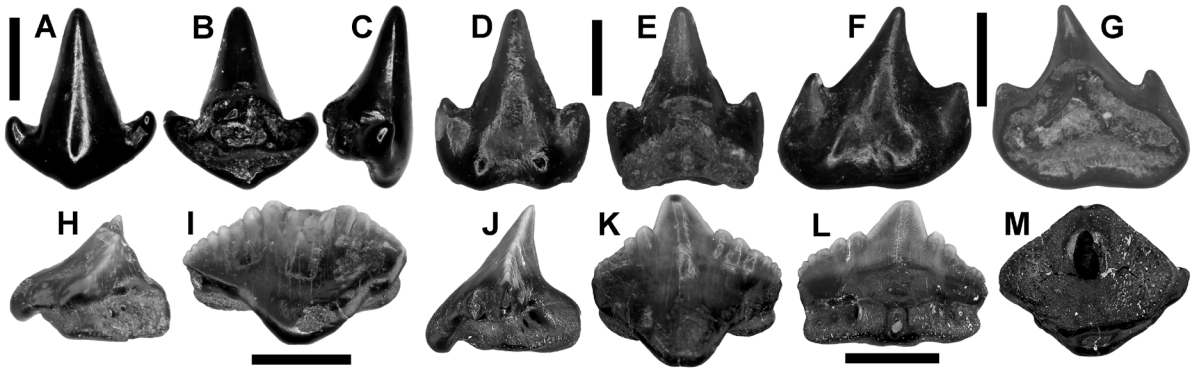

Fig. 3. Brachaeluridae gen. et sp. indet. (A–C), *Chiloscyllium* sp. (D–G), and *Nebrius* sp. (H–M), teeth. **A–C**. SC2013.28.54, Brachaeluridae gen. et sp. indet., anterior tooth. **A**. Labial view. **B**. Lingual view. **C**. Mesial view. **D–E**. SC2013.28.55, *Chiloscyllium* sp., anterior tooth. **D**. Labial view. **E**. Lingual view. **F–G**. SC2013.28.57, *Chiloscyllium* sp., lateral tooth. **F**. Labial view. **G**. Lingual view. **H–I**. MMNS VP-6966, *Nebrius* sp., tooth. **H**. Distal view. **I**. Labial view. **J–M**. MMNS VP-12033, *Nebrius* sp., tooth. **J**. Mesial view. **K**. Labial view. **L**. Lingual view. **M**. Basal view. Scale bars: A–G = 1 mm; H–M = 3 mm.

features occurring on the teeth of Paleogene Brachaeluridae, including *Brachaelurus* and *Eostegostoma* (see Cappetta 2012). The labial protuberance of SC2013.28.54 is not as clearly defined as it is on teeth of the aforementioned taxa, but the dentition of extant *Brachaelurus waddi* (Bloch & Schneider, 1801) shows that the protuberance is less distinct on lateral/posterior teeth compared to anterior teeth (Herman *et al.* 1992). Additional specimens are necessary to accurately ascertain the identity of this orectolobiform taxon.

Superfamily Hemiscyllioidea Naylor *et al.*, 2012
Family Hemiscylliidae Gill, 1862

Genus ***Chiloscyllium*** Müller & Henle, 1837

Type species

Scyllium plagiosum Bennett, 1830, Recent.

Chiloscyllium sp.
Fig. 3D–G

Material examined

UNITED STATES OF AMERICA – **Mississippi** • 12 isolated teeth; Catahoula Formation; MMNS VP-8795 (3 teeth), MMNS VP-12034, SC2013.28.55 (Fig. 3D–E), SC2013.28.56, SC2013.28.57 (Fig. 3F–G), SC2013.28.58 to 28.62.

Description

SC2013.28.55 is the best-preserved specimen and has a crown that measures 2 mm in width and approximately 2.2 mm in height (Fig. 3D–E). The other teeth are broken and/or ablated but appear to have had similar dimensions. The crown of SC2013.28.55 consists of a broadly triangular but sharply tapering main cusp that comprises approximately one-half of the total crown height. The main cusp is flanked by a single pair of short, broad, and slightly diverging lateral cusplets (Fig. 3D). In labial view, the crown is symmetrical, with an erect main cusp, but in profile view the main cusp is slightly lingually inclined. Smooth mesial and distal cutting edges occur on the main cusp that extend onto the lateral sides of the cusplets but do not reach the crown base. The labial face is straight (apico-basally) but slightly convex (mesio-distally), and the crown foot is formed into a broad, bifid protuberance that overhangs the root. The lingual crown face is convex, and a medial protuberance extends onto the upper surface of the root. The root is low in profile view and less wide than the crown (Fig. 3E). In basal view, the root is bilobed, with narrow and widely diverging lobes. The lobes are separated by a deep V-shaped embayment that opens labially, and a very large foramen occurs at the center of the root. Additional foramina occur on the upper root surface on each side of the lingual crown protuberance, and another is located on the lingual-most face of the root. Specimens SC2013.28.59 and SC2013.28.60 (and likely SC2013.28.56) are less well preserved but appear to have been similar to SC2013.28.55.

Specimens SC2013.28.57 (Fig. 3F–G), SC2013.28.58, and SC2013.28.61 differ from the above specimens by their lower overall crown height, lower and distally inclined main cusp, and lower and broader lateral cusplets. Additionally, both mesial and distal cusplets are distally directed (whereas they are diverging on the teeth described above). SC2013.28.62 is highly ablated but notable for the apparent lack of lateral cusplets and the uniformly convex labial apron.

Remarks

These Catahoula Formation teeth are like those of fossil species assigned to *Chiloscyllium* and to extant *Stegostoma* Müller & Henle, 1837, and species of both genera have smooth crown enameloid and typically a pair of large lateral cusplets. However, one conspicuous difference between the genera is

the shape of the teeth, which in extant *Stegostoma* are all symmetrical, from anterior to posterior files (Herman *et al*. 1992; Cappetta 2012). In contrast, teeth of *Chiloscyllium* exhibit monognathic heterodonty, with the main cusp becoming lower and more distally inclined towards the commissure (Herman *et al*. 1992; Noubhani & Cappetta 1997; Cappetta 2012). Adnet *et al*. (2020) recently erected a new tooth-based Eocene species of *Stegostoma* that seemingly contradicts the near homodonty observed in extant representatives. The teeth of their fossil species are comparable to those of *Chiloscyllium*, particularly to Eocene *C. meraense* Noubhani & Cappetta, 1997, but Adnet *et al.* (2020) apparently separated the two genera by the presence or absence of lateral cusplets. In the Eocene *Stegostoma* species, lateral cusplets are present even in posterior positions, whereas they are reduced or absent in distally located teeth of *Chiloscyllium* (i.e., Noubhani & Cappetta 1997). Treating this particular feature as taxonomically significant, the Catahoula Formation specimens are referred to *Chiloscyllium* due to the combination of features that include a single pair of lateral cusplets on anterior and lateral teeth, asymmetrical lateral and posterior teeth, and reduced to absent lateral cusplets on distal lateral and posterior teeth.

The teeth we identify as *Chiloscyllium* sp. bear similarities to those of *Hemiscyllium*, but they differ from the latter by their larger overall size and significantly larger lateral cusplets, particularly on anterior teeth (Herman *et al.* 1992; Cappetta 2012; Adolfssen & Ward 2013; Engelbrecht *et al.* 2017). The Catahoula Formation teeth also differ from the superficially similar Eocene taxon *Notorhamphoscyllium* Engelbrecht *et al.*, 2017 by having conspicuous mesial and distal cutting edges on the main cusp.

The *Chiloscyllium* sp. teeth clearly differ from the Brachaeluridae gen. et sp. indet. tooth in our sample (SC2013.28.54) by their shorter cusp, roughly equal crown height and width dimensions, broader (typically bifid) labial apron, and lateral cusplets occurring much higher on the crown. Teeth of Catahoula Formation *Nebrius* sp. are generally wider than high and have ten or more sets of lateral cusplets that decrease in size distally. Although *Chiloscyllium* has previously been reported from the Cretaceous Gulf Coastal Plain in Alabama (Nicholls & Russell 1990; Ciampaglio *et al*. 2013; Ikejiri *et al*. 2013; Ebersole *et al*. 2024b) and Mississippi (Cicimurri *et al.* 2014), to our knowledge the Catahoula Formation specimens represent the first North American Oligocene record of this genus.

Family Ginglymostomatidae Gill, 1862

Genus ***Nebrius*** Rüppell, 1837

Type species

Nebrius ferrugineus Lesson, 1831, Extant.

Nebrius sp.
Fig. 3H–M

Material examined

UNITED STATES OF AMERICA – **Mississippi** • 8 isolated teeth; Catahoula Formation; MMNS VP-6966 (Fig. 3H–I), MMNS VP-12033 (Fig. 3J–M), SC2013.28.63 to 28.68.

Description

Teeth are wider (mesio-distally) than they are high, with the largest specimen (SC2013.28.63) measuring slightly over 6 mm and 5 mm in these dimensions. In labial view, the broadly triangular, low crown bears a medially located main cusp that is flanked by multiple sets of lateral cusplets (Fig. 3K–L). The main cusp is low, triangular, lingually directed, and may be vertical to distally inclined. Lateral cusplets are much smaller than the main cusp, and cusplet size decreases towards the crown base. Typically, there are

more cusplets on the mesial side than on the distal side (Fig. 3I, K). The mesial and distal cutting edges extend along the lateral cusplets and the main cusp. The labial face is weakly convex mesio-distally, and there is a conspicuous basally directed protuberance that has a rounded or flattened basal margin (Fig. 3I, K). The lingual crown face is convex and bears a medial protuberance that extends lingually onto the root (Fig. 3L). In profile view, the labial face ranges from sinuous to straight (compare Fig. 3H to J), and the main cusp apex is distally directed. The crown enameloid is smooth. The root is low, extends laterally nearly to the crown margin, and is sub-triangular in basal view. A large central foramen occurs within a deeply convex basal attachment surface (Fig. 3M). Additional foramina are located just below the crown on the upper surface of the lingual root face.

Remarks

Based on the dentition of extant *Nebrius ferrugenius* (Lesson, 1831), as illustrated by Herman *et al.* (1992), the sample available to us, although limited, indicates that gradient monognathic heterodonty was developed in the Catahoula Formation *Nebrius* species. Rather narrow and somewhat symmetrical teeth are interpreted to represent anterior jaw positions (Fig. 3K), whereas lateral teeth are wider, have a more distally inclined main cusp, and the longer mesial side bears more cusplets compared to the distal side (Fig. 3I). Teeth from distal lateral to posterior positions have a diminutive and sharply distally inclined main cusp, an elongated and highly convex mesial edge with numerous cusplets, and a comparatively shorter distal edge with significantly fewer cusplets. Additionally, the labial protuberance on the teeth in our sample has either a flat or a rounded basal margin, a phenomenon we also observed in the *N. ferrugenius* dentition, further corroborating the presence of monognathic heterodonty within our sample of fossil *Nebrius* sp. teeth.

The *Nebrius* sp. teeth clearly differ from specimen SC2013.28.54 (Brachaeluridae gen. et sp. indet.) by their wider crowns, prominent labial basal apron, and numerous lateral cusplets. Unfortunately, all the specimens in our sample are damaged and/or ablated, and it is difficult to compare them to ginglymostomatid teeth reported from Oligocene deposits elsewhere. Only a crown fragment referred to Ginglymostomatidae was reported from the Rupelian Ashley Formation of South Carolina (Cicimurri *et al.* 2022), and an incomplete tooth was recovered from the Chattian Chandler Bridge Formation by Cicimurri & Knight (2009). The latter specimen does not differ appreciably from the Catahoula Formation teeth. Müller (1999) identified *Ginglymostoma delfortriei* Daimeries, 1889 from the Oligo-Miocene Belgrade Formation of North Carolina, but all the specimens shown (pl. 2 figs 2–4) are broken apically. We concur with Yabumoto & Uyeno (1994) and assign the *delfortriei* morphology to *Nebrius* because the teeth exhibit significantly more than three sets of lateral cusplets, as opposed to only two or three on *Ginglymostoma* (Cicimurri & Knight 2009; Ebersole *et al.* 2019). Cicimurri & Knight (2009) tentatively identified their single specimen as *N. serra* (Leidy, 1877), but the validity of this taxon is debatable because the stratigraphic and geographic provenance of the original specimen(s) is uncertain. It may be that the Mississippi and North and South Carolina fossil *Nebrius* specimens are conspecific, but larger samples of well-preserved specimens from all these locations are necessary to make this determination.

Order Lamniformes Berg, 1937
Family Otodontidae Glückman, 1964
Genus *Otodus* Agassiz, 1843

Subgenus ***Otodus* (*Carcharocles*)** Hannibal & Jordan in Jordan, 1923 (sensu Cappetta 2012)

Type species

Squalus auriculatus de Blainville, 1818, middle Eocene, Belgium.

***Otodus* (*Carcharocles*)** sp.
Fig. 4

Material examined

UNITED STATES OF AMERICA – **Mississippi •** 1 isolated tooth; Catahoula Formation; MMNS VP-6608.

Description

The specimen was broken upon recovery but has been repaired in its entirety, and it measures 6.2 cm in total height and 4.5 cm in width (mesio-distal). The tooth has a broadly triangular main cusp that is flanked by a pair of relatively small lateral cusplets. The main cusp is slightly distally inclined, and its labial face is flat, but its lingual face is convex, and the enameloid is smooth. In profile view, the main cusp is generally straight but slightly labially curved near the apex. The cutting edges are continuous along the main cusp and lateral cusplets. The mesial and distal cutting edges on the main cusp are somewhat concave at the lower half of the crown, but they become convex apically before converging to form a blunt apex. With respect to the lateral cusplets, the distal cutting edge is elongated and straight to weakly concave, whereas the mesial edge is very short and convex. The cusplets are rather small with respect to main cusp size, they occur very low on the crown, and they are differentiated from the main cusp by a deep notch (Fig. 4A). All cutting edges are serrated, but serration size and complexity vary along each cutting edge. Macroscopically, the serrations appear to be regular but under magnification larger or smaller individual serrae are scattered within lengths of more uniformly sized serrae. The apical and basal margins of individual serrae are sub-parallel, and serrae are separated from each other by deep notches. Some individual serrae are subdivided by one or two additional, smaller serrae. On the lateral cusplets, the serrations on the mesial edge are conspicuously finer than those on the distal edge. A wide, triangular dental band is located between the lingual crown foot and root (Fig. 4B). The root is massive, with rather short but robust mesial and distal lobes having rounded margins. The interlobe area is broadly U-shaped. A prominent lingual boss is perforated by nutritive foramina.

Fig. 4. *Otodus* (*Carcharocles*) sp., MMNS VP-6608, upper left tooth. **A**. Labial view. **B**. Lingual view. Scale bar = 3 cm.

Remarks

Specimen MMNS VP-6608 appears to be an upper left tooth, possibly the second anterior, based on the width and slight distal inclination of the crown, as well as its relatively short root lobes (mesial lobe narrower and more pointed than the distal lobe) and broad U-shaped interlobe area (see also Gottfried & Fordyce 2001). Only one Catahoula Formation otodontid tooth is available to us, but the specimen is comparable to large examples of *Otodus* (*Carcharocles*) *angustidens* (Agassiz, 1835) identified from Oligocene deposits of Europe (i.e., Baut & Génault 1999; Reinecke *et al.* 2001, 2005). The Catahoula tooth differs from those in a sample of small *Otodus* (*Carcharocles*) teeth we examined from the Chattian Chandler Bridge Formation of South Carolina (SC89.240 and SC2006.1). These Chattian teeth were identified as *Carcharocles* sp. by Cicimurri & Knight (2009) and as *Carcharodon subauriculatus* (Agassiz, 1843) by Purdy *et al.* (2001). The rather broad but low lateral cusplets are not as well differentiated from the main cusp cutting edges compared to the Catahoula Formation tooth, a condition that is more similar to that of *Otodus* (*Megaselachus*) *chubutensis* (Ameghino, 1906). The *Otodus* (*Carcharocles*) *subauriculatus* morphotype is synonymous with *O.* (*M.*) *chubutensis*, and in fact Miocene specimens identified as *Carcharodon subauriculatus* by Purdy *et al.* (2001) have been reassigned to *O.* (*M.*) *chubutensis* (Perez *et al.* 2018). Although it is possible that the Chandler Bridge Formation teeth represent a transitional taxon between *O.* (*C.*) *angustidens* and *O.* (*M.*) *chubutensis*, this hypothesis is difficult to test with the single tooth in our sample. The otodontid taxa *O.* (*C.*) *aksuaticus* (Menner, 1928), *O.* (*C.*) *auriculatus* (de Blainville, 1818), *O.* (*C.*) *sokolovi* (Jaekel, 1895), *O.* (*C.*) *angustidens*, and *O.* (*M.*) *chubutensis* may represent a single lineage that culminates with *Otodus* (*Megaselachus*) *megalodon* (Agassiz, 1835) (Applegate & Espinosa-Arrubarrena 1996), but it is also possible that several otodontid lineages may have been present in the Paleogene (Cappetta 2012). The morphological criteria used to identify species can be ambiguous, as demonstrated above by the Catahoula Formation specimen (i.e., "regular" or "irregular" serrations) and within relatively small samples of teeth from one lithostratigraphic unit. Due to these factors, we herein only identified specimen MMNS VP-6608 to the generic level.

Family Carchariidae Müller & Henle, 1838

Genus ***Carcharias*** Rafinesque, 1810

Type species

Carcharias tauras Rafinesque, 1810, Extant.

Carcharias cuspidatus (Agassiz, 1843)
Fig. 5A–N

Lamna cuspidata Agassiz, 1843: 290.

Material examined

UNITED STATES OF AMERICA – **Mississippi •** 240 isolated teeth; Catahoula Formation; MMNS VP-6626 (168 teeth), MMNS VP-12053 (Fig. 5A–B), MMNS VP-12054 (Fig. 5C–D), MMNS VP-12055 (Fig. 5M–N), MMNS VP-12056 (Fig. 5E–F), MMNS VP-12057 (Fig. 5K–L), MMNS VP-12058 (Fig. 5I–J), SC2013.28.272 to 28.283, SC2013.28.284 (Fig. 5G–H), SC2013.28.285 to 28.290, SC2013.28.292 to 28.328, SC2013.28.329 (10 teeth).

Description

Teeth can attain large sizes, with broken specimens estimated to have been more than 3 cm in total height. The tooth crown consists of a very large main cusp that is usually flanked by lateral cusplets. The

main cusp may be mesio-distally narrow, tall, and labio-lingually thick or broadly triangular and labio-lingually thin. Cutting edges are smooth and may or may not extend to the base of the lateral cusplets. The labial face is flat to weakly convex, whereas the lingual crown face is more strongly convex. The crown enameloid is smooth. There is typically a single pair of lateral cusplets, although a poorly developed second cusplet may be present. Cusplets vary from small, narrow, and sharply pointed to low, very broad, and almost heel-like. Some specimens exhibit a denticulated morphology (Fig. 5K–L). Root lobes vary in shape and can be narrow and elongated or short and sub-rectangular, and lobes may be sub-parallel or widely diverging. The interlobe area is U-shaped but varies from deep and narrow to broad and shallow. A robust lingual protuberance may occur on the lingual root face, which is bisected

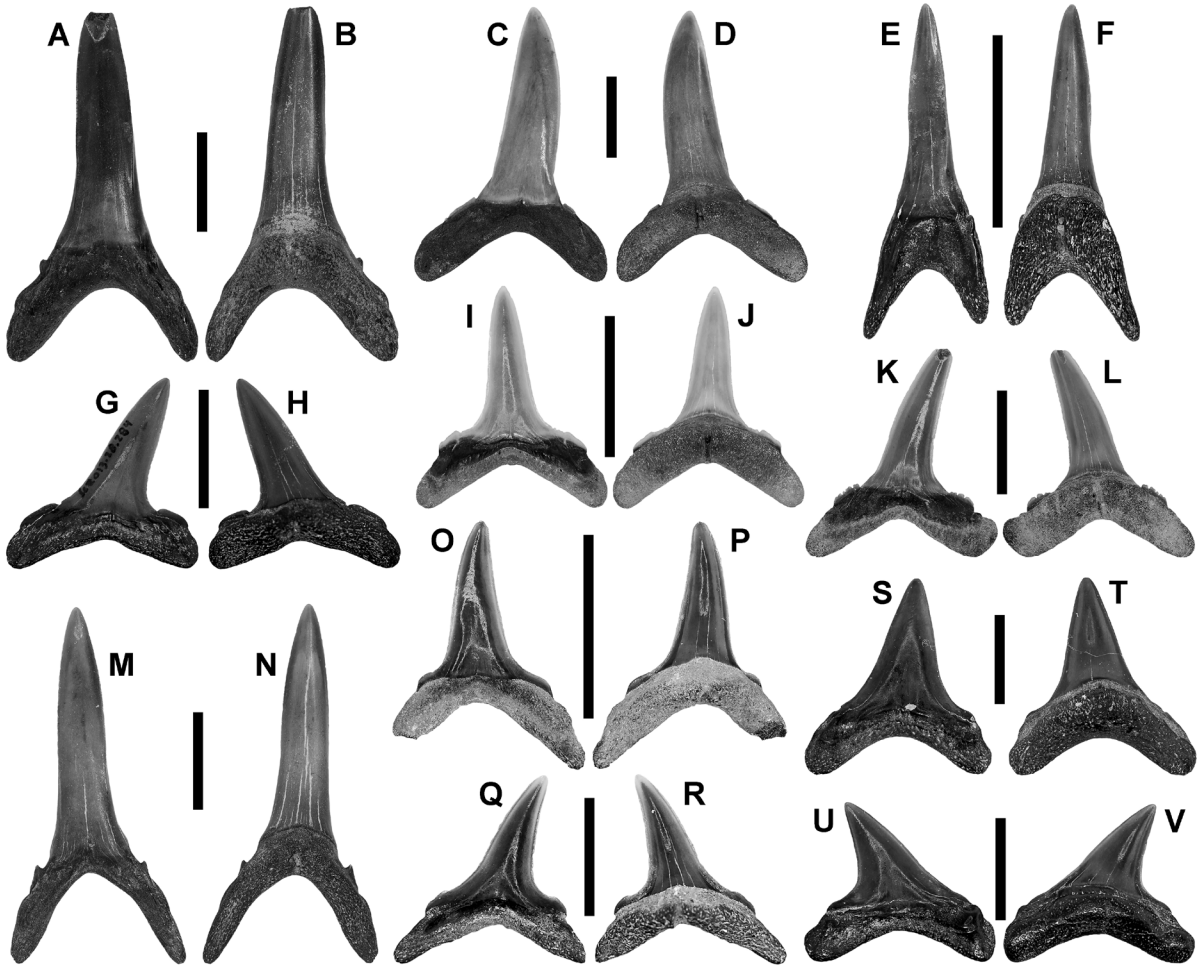

Fig. 5. *Carcharias cuspidatus* (Agassiz, 1843) (A–N), aff. *Pseudocarcharias* sp. (O–R), and *Alopias* sp. (S–V), teeth. **A–B**. MMNS VP-12053, *Carcharias cuspidatus*, upper anterior tooth. **A**. Labial view. **B**. Lingual view. **C–D**. MMNS VP-12054, *C. cuspidatus*, upper right third anterior tooth. **C**. Labial view. **D**. Lingual view. **E–F**. MMNS VP-12056, *C. cuspidatus*, ablated tooth. **E**. Labial view. **F**. Lingual view. **G–H**. SC2013.28.284, *C. cuspidatus*, upper right lateral tooth. **G**. Labial view. **H**. Lingual view. **I–J**. MMNS VP-12058, *C. cuspidatus*, lower right lateral tooth. **I**. Labial view. **J**. Lingual view. **K–L**. MMNS VP-12057, *C. cuspidatus*, upper right lateral tooth. **K**. Labial view. **L**. Lingual view. **M–N**. MMNS VP-12055, *C. cuspidatus*, lower right anterior tooth. **M**. Labial view. **N**. Lingual view. **O–P**. SC2013.28.269, aff. *Pseudocarcharias* sp., anterior tooth. **O**. Labial view. **P**. Lingual view. **Q–R**. SC2013.28.270, aff. *Pseudocarcharias* sp., upper right lateral tooth. **Q**. Labial view. **R**. Lingual view. **S–T**. MMNS VP-7643, *Alopias* sp., anterior tooth. **S**. Labial view. **T**. Lingual view. **U–V**. SC2013.28.271, *Alopias* sp., lateral tooth. **U**. Labial view. **V**. Lingual view. Scale bars: A–P, S–T = 1 cm; Q–R, U–V = 5 mm.

by a narrow and long nutritive groove. Other lingual root surfaces have a more shelf-like appearance but also bear a conspicuous nutritive groove.

Remarks

Monognathic heterodonty is evident in our sample, with anterior teeth having a narrow main cusp with a sinuous profile. The mesial and distal cutting edges do not reach the base of the main cusp, the diminutive cusplets are narrow and pointed, and the root lobes are thin and elongated (Fig. 5A, M). There are variations in upper anterior tooth shape as, for example, demonstrated between the rather vertical crown and moderately diverging root lobes of the second upper anterior position (Fig. 5B) and the mesially curving crown and widely diverging lobes of the third anterior tooth (Fig. 5D). Upper lateral teeth (Fig. 5G–H, K–L) have a broader and labio-lingually thinner main cusp, the cutting edges are complete, and the lateral cusplets are low but very broad. Additionally, well-preserved specimens demonstrate that the root lobes are shorter, sub-rectangular and more divergent. With respect to dignathic heterodonty, the crowns of lower anterior teeth have a strong lingual curvature compared to those of upper anterior teeth, and the root lobes of upper anterior teeth are thicker, shorter, and more divergent compared to those of lower teeth (compare Fig. 5B to N). Additionally, upper lateral teeth are distally inclined, but those of the lower jaw are nearly vertical (compare Fig. 5G to I). Variations in overall tooth size within each tooth file are indicative of ontogenetic heterodonty, where smaller teeth (of juvenile individuals) are simply more gracile versions of larger (adult) teeth. A similar phenomenon was reported for *Mennerotodus* by Cicimurri *et al*. (2020).

The teeth described above compare favorably to those of *Carcharias cuspidatus*, a species commonly reported from the Oligo-Miocene of North America and Europe (Baut & Génault 1999; Müller 1999; Purdy *et al.* 2001; Cappetta 2012; Reinecke *et al.* 2014). Over the past few decades, this species has variably been assigned to *Carcharias* (i.e., Purdy *et al.* 2001) and *Araloselachus* (see Cappetta 2012), with the most recent classification placing it within the former (Hovestadt 2020, 2022). Cappetta (2012) considered *Araloselachus* as distinct from *Carcharias* and other similar taxa, because teeth have smooth enameloid, anterior teeth have a less sigmoidal profile and "small and simple" (Cappetta 2012: 191) lateral cusplets, and lateral teeth have broad but low (sometimes) "pectinate" lateral cusplets. However, the crowns can be more-or-less sigmoidal depending on tooth position within a given jaw (i.e., upper versus lower, first anterior versus third anterior). Additionally, the presence or absence of crown ornamentation on teeth can be variable among individuals within a population of a given species (Purdy *et al.* 2001; Cicimurri *et al.* 2020). Furthermore, the "pectinate" lateral cusplets of lateral teeth, visible on some Catahoula Formation specimens (i.e., MMNS VP-12057), were also noted by Cicimurri *et al.* (2020) on Eocene *Mennerotodus* teeth. Purdy *et al.* (2001) provided some additional tooth characteristics that might prove useful in differentiating *C. cuspidatus* from *C. taurus* (Rafinesque, 1810), but the available sample does not allow us to test those criteria. Our observations regarding dignathic heterodonty are consistent with the work of Hovestadt (2020), who presented a reconstructed dentition of *C. cuspidatus* based on an articulated skeleton (pl. 7 figs 1–22), and familial assignment to Carchariidae is warranted.

Family Pseudocarchariidae Taylor *et al.*, 1983

Genus ***Pseudocarcharias*** Cadenat, 1963

Type species

Carcharias komoharai Matsubara, 1936, Extant.

aff. ***Pseudocarcharias*** sp.
Fig. 5O–R

Material examined

UNITED STATES OF AMERICA – **Mississippi •** 2 isolated teeth; Catahoula Formation; SC2013.28.269 (Fig. 5O–P), SC2013.28.270 (Fig. 5Q–R).

Description

SC2013.28.269 measures 23 mm in total height and 10 mm in width. It bears a tall and rather erect main cusp. Although the cusp is slightly distally inclined, it has a distinct mesial curvature that is the result of the concave mesial cutting edge intersecting apically with the convex distal cutting edge. Both cutting edges are smooth and sharp, and they extend onto mesial and distal shoulders. The transition from main cusp to lateral shoulder is highly curved but not angular. The shoulders are very low and slightly convex at their distal ends, and the mesial shoulder is longer than the distal one (Fig. 5O). The labial crown face is very weakly convex, but the lingual face is very convex, and both faces are smooth. The root is bilobate with strongly diverging lobes that are thin, elongated, and have a pointed extremity (the distal lobe is damaged). The interlobe area is U-shaped. A thin and shelf-like lingual boss bears a very short nutritive groove (Fig. 5P).

SC2013.28.270 is a smaller tooth measuring 7 mm in total height and 7 mm in width, and having a distally inclined and curved main cusp. The smooth and sharp cutting edges extend onto elongated mesial and distal shoulders. The mesial shoulder is not strongly distinguished from the main cusp, whereas the transition from the distal cutting edge to the distal shoulder is a deeply concave line. The shoulders are low, elongated (slightly longer mesially), and their distal ends are somewhat pointed (Fig. 5Q). The labial crown face is weakly convex, the lingual face is strongly convex, and the enameloid is smooth. The strongly bilobate root bears a very short lingual nutritive groove (Fig. 5S). The root lobes are very highly diverging, relatively short, thin, and have pointed extremities. The interlobe area is V-shaped.

Remarks

Although different from each other in terms of overall shape, the features shared by SC2013.28.269 and SC2013.28.270 lead us to conclude that they represent the same species. Specimen SC2013.28.269 (Fig. 5O–P) is reminiscent of a more anteriorly located tooth, whereas SC2013.28.270 (Fig. 5Q–R) is from a lateral jaw position. The smooth cutting edges, curved transition from main cusp to lateral shoulder, and lack of lateral cusplets distinguish these teeth from those of Otodontidae and Carchariidae occurring within the Catahoula Formation.

The two specimens described above are perhaps the most enigmatic within the Catahoula Formation fish assemblage. They are differentiated from comparably-sized teeth of *Carcharias cuspidatus* (see above) by their lack of cusplets and continuous transition from main cusp to lateral shoulders. Specimens SC2013.28.269 and SC2013.28.270 are similar to teeth of Mitsukurinidae, two species of which, *Mitsukurina lineata* (Probst, 1879) and *Woellsteinia oligocaena* Reinecke *et al.*, 2001, have been reported from Oligocene strata elsewhere (Reinecke *et al.* 2005). However, the Catahoula Formation teeth lack the longitudinal ridges on the lingual crown face that characterizes those taxa, and instead have smooth crown enameloid. Specimens SC2013.28.269 and SC2013.28.270 are very weakly cuspidate (particularly the former specimen) and are comparable to teeth within the jaws of male and female *Pseudocarcharias kamoharai* (Matsubara, 1936) as shown by Pollerspöck & Straube (2020: fig. 10), and they bear similarities to *Pseudocarcharias* teeth identified by Cigala Fulgosi (1992) from the Middle Miocene (Serravallian) of Italy. The very weakly cuspidate appearance of the lateral shoulders

on the Catahoula Formation specimens contrasts with the condition of teeth of the Early Miocene (Burdigalian) *P. rigida* (Probst, 1879), which has distinctive lateral cusplets on upper and lower lateral teeth (Bracher & Unger 2007). To our knowledge, *Pseudocarcharias* does not have a pre-Miocene fossil record (also Cappetta 2012), and the Catahoula Formation teeth would represent a significant temporal range extension back to the "middle" Oligocene. Additional specimens, especially distinctive anterior teeth, are necessary to corroborate the identity of these two teeth.

Family Alopiidae Bonaparte, 1840a

Genus ***Alopias*** Rafinesque, 1810

Type species

Alopias macrourus Rafinesque, 1810, Extant.

Alopias sp.
Fig. 5S–V

Material examined

UNITED STATES OF AMERICA – **Mississippi •** 2 isolated teeth; Catahoula Formation; MMNS VP-7643 (Fig. 5S–T), SC2013.28.271 (Fig. 5U–V).

Description

Specimen MMNS VP-7643 has a rather low but broadly triangular main cusp that is weakly distally inclined. In profile the crown is flat. The labial face is convex along the margins but concave medially, and there is a thickening at the crown foot. The lingual face is strongly and uniformly convex. Both crown faces have smooth enameloid. The mesial cutting edge is relatively straight, but the distal edge is weakly convex. Both cutting edges are smooth and extend basally onto short lateral shoulders. The mesial shoulder is more elongated but not well-differentiated compared to the distal heel. The bilobate root has rather short and highly diverging lobes with rounded extremities. The interlobe area is broadly U-shaped.

Tooth SC2013.28.271 has a broad and very distally inclined cusp. The elongated mesial cutting edge is weakly convex apically and extends basally onto an elongated heel. The distal cutting edge is straight but transitions basally through a curved 90° angle onto a short distal heel. The cutting edges are smooth. The labial crown face is weakly convex and has a thickened crown foot. The distal face is more strongly convex, and the crown enameloid on both faces is smooth. The root is bilobate with short but highly diverging lobes that have rounded extremities. There is a conspicuous nutritive pore on a small lingual boss.

Remarks

Although different from each other, MMNS VP-7643 (Fig. 5S–T) and SC2013.28.271 (Fig. 5U–V) both have broadly triangular crowns, smooth cutting edges that extend onto lateral shoulders, and root lobes with rounded extremities. These shared features lead us to conclude that they represent the same taxon and allow us to distinguish them from coeval Otodontidae and Carchariidae teeth in the Catahoula Formation. Additionally, these two teeth differ from aff. *Pseudocarcharias* sp. described above by having shorter but much broader crowns, non-cuspidate lateral shoulders, roots apparently lacking a nutritive groove, and lobes with rounded extremities.

Specimens MMNS VP-7643 and SC2013.28.271 are comparable to teeth in an associated tooth set of extant *Alopias vulpinus* (Bonnaterre, 1788) (SC2015.30.1) and within the jaws of an *A. superciliosus* Lowe, 1841 (SC202.53.12) that we examined. Tooth MMNS VP-7643 appears to represent an anterior jaw position, as it has a rather erect crown with only slight distal inclination (Fig. 5S–T). In contrast, the lower cusp height and greater distal inclination of SC2013.28.271 indicate that it is from a more lateral tooth file (Fig. 5U–V). Neither specimen exhibits a nutritive groove, but this feature is not developed on some anterior teeth in SC2015.30.1 (*A. vulpinus*). Additionally, the root of both specimens is abraded, and it is possible that these structures are simply not preserved. Teeth identified as *Alopias* aff. *vulpinus* in the German Chattian (Reinecke *et al.* 2005: pls 21–22) appear to be more broad-based than the two Catahoula Formation specimens reported herein. The Catahoula Formation *Alopias* specimens have a much wider crown compared to the teeth of *A. exigua* (Probst, 1879), which have been reported from the Oligocene of Europe (i.e., Reinecke *et al.* 2001, 2005).

We note here the taxon *Alopias latidens alabamensis* White, 1956 that was based on teeth derived from upper Eocene (Priabonian) deposits in Alabama (Gulf Coastal Plain of the USA). Ebersole *et al.* (2019) determined that White's taxon was a composite based on multiple taxa, with one being identified as *Negaprion gilmorei* (Leriche, 1942). Within the same volume, White (1956) erected the subspecies *Alopias latidens carolinensis* based on teeth derived from "phosphates" in South Carolina. Interestingly, White's figured holotype (White 1956: pl. 11 fig. 8) is quite similar to specimen SC2013.28.271, and one might consider that the Catahoula Formation and South Carolina material are conspecific. However, the usage of *Alopias latidens carolinensis* for the Catahoula teeth is problematic because the type locality and precise stratigraphic occurrence and age of White's syntypes are unknown, and material from the "phosphates" in South Carolina can range in age from the Eocene to Pliocene (Cicimurri *et al.* 2022). We refrain from identifying the two teeth in our Catahoula Formation sample to species until a greater number of specimens are available for study.

Order Carcharhiniformes Compagno, 1973
Family Hemigaleidae Hasse, 1878

Genus ***Hemipristis*** Agassiz, 1835

Type species

Hemipristis serra Agassiz, 1835, Miocene, Germany.

Hemipristis intermedia sp. nov.
urn:lsid:zoobank.org:act:25CF2AFD-3892-43EC-DE9878B39014
Fig. 6

Diagnosis

Upper lateral teeth are the most common tooth morphology represented, and because they are more diagnostic than the lower teeth, they are utilized herein to diagnose the species. Upper lateral teeth measure up to 2.5 cm in width (mesio-distal) and 2 cm in height (apico-basal). These teeth have a broad, triangular crown and distally directed main cusp. The mesial cutting edge may be smooth or bear up to ten denticles and the distal cutting edge up to 12 denticles, with denticles on both edges increasing in size towards the apex. A smooth-edged cusp constitutes the apical 30%–40% of the crown. Of the fossil *Hemipristis* species we consider valid, the upper lateral teeth of *H. intermedia* sp. nov. differ from those of the Eocene *H. curvatus* Dames, 1883 by attaining larger overall sizes (2.5 cm wide by 2.2 cm high for *H. intermedia* vs 1.5 cm and 1.1 cm, respectively for *H. curvatus*), by having more mesial and

distal denticles (up to four and eight, respectively for *H. curvatus*, and up to 10 and 11, respectively, for *H. intermedia*), and by having mesial denticles that extend higher on the crown (two-thirds the crown height vs. one-half the crown height on *H. curvatus*). *Hemipristis intermedia* sp. nov. upper lateral teeth differ from those of the Miocene to Early Pleistocene *H. serra* Agassiz, 1835 by attaining smaller overall sizes (3.7 cm wide and 3.6 cm height for *H. serra*), by having fewer distal denticles (up to 20 have been observed on *H. serra*), and by having denticles that do not extent as close to the apex, resulting in a cusp that represents more than 20% of the crown height (as opposed to 10% in *H. serra*). These teeth are differentiated from those of the Rupelian *H. tanakai* Tomita, Yabumoto & Kuga, 2023 by having more than five mesial denticles (the maximum number reported for *H. tanakai*), and the apical-most mesial and distal denticles are of nearly equal height on the crown (whereas the distal denticle is generally higher in *H. tanakai*). Finally, the upper lateral teeth of *Hemipristis intermedia* sp. nov. differ from those of the extant *H. elongata* (Klunzinger, 1871) by being mesio-distally wider, by having more conspicuous denticles, and by having a more convex upper one-half of the mesial crown edge. The number of tooth denticles of *Hemipristis intermedia* is greater than the maximum occurring on *H. curvatus* teeth but less than the maximum number known for the Miocene to Early Pleistocene *H. serra* Agassiz, 1835. The proportion of cusp to total crown height is less than in *H. curvatus* but greater than in *H. serra*. The recently named *H. tanakai* (Tomita *et al*. 2023) is considered herein as a nomen dubium (see below), but the tooth size of that taxon overlaps with those of *H. serra* and *H. intermedia*. Additionally, only five mesial denticles occur in *H. tanakai* and the mesial denticles extend closer to the crown apex compared to the distal edge.

Etymology

The species name refers to the transitional tooth morphology between the Eocene *Hemipristis curvatus* and the Miocene to Early Pleistocene *H. serra*.

Material examined

Holotype

UNITED STATES OF AMERICA – **Mississippi** • upper left lateral tooth; Catahoula Formation; SC2013.28.73 (Fig. 6PP–RR).

Paratypes

UNITED STATES OF AMERICA – **Mississippi** • upper left anterior tooth; Catahoula Formation; MMNS VP-12037 (Fig. 6G–I) • lower left anterior tooth; Catahoula Formation; SC2013.28.80 (Fig. 6P–R) • lower right lateral tooth; Catahoula Formation; MMNS VP-12036 (Fig. 6D–F).

Other material

UNITED STATES OF AMERICA – **Mississippi** • 189 isolated teeth; Catahoula Formation; MMNS VP-464 (2 teeth), MMNS VP-6625 (114 teeth), MMNS VP-6625.1 (Fig. 6HH–JJ), MMNS VP-7243 (7 teeth), MMNS VP-7604 (Fig. 6MM–OO), MMNS VP-7691 (9 teeth), MMNS VP-8745, MMNS VP-12035 (Fig. 6A–C), MMNS VP-12038 (Fig. 6J–L), MMNS VP-12039 (Fig. 6M–O), MMNS VP-12040 (Fig. 6S–U), MMNS VP-12041, MMNS VP-12042 (Fig. 6V–X), MMNS VP-12043 (Fig. 6Y–AA), MMNS VP-12044 (Fig. 6BB–CC), MMNS VP-12045 (Fig. 6DD–EE), MMNS VP-12046 (Fig. 6FF–GG), SC2013.28.69 to 28.72, SC2013.28.74 to 28.79, SC2013.28.81 to 28.89, SC2013.28.90 (Fig. 6KK–LL), SC2013.28.91 to 28.101, SC2013.28.102 (10 teeth), SC2013.28.103 (Fig. 6SS–TT), SC2013.28.104 (Fig. 6UU–VV), MMNS VP-7604 (Fig. 6MM–OO).

Stratum typicum

Shelly, argillaceous sand of the Jones Branch fossil horizon, lower Catahoula Formation, Chattian Stage (horizon no longer accessible).

Locus typicus

Site MS.77.011, Jones Branch, tributary flowing into the Chickasawhay River, south of Waynesboro, Wayne County, Mississippi, USA.

Description

Several tooth morphologies are present, including specimens with a triangular, broad-based but apically narrow, slightly distally inclined crown. In profile view (Fig.6C, R, U), the crown on these teeth is flat to weakly sigmoidal, and the labial face is weakly convex, but the lingual face is strongly convex. The crown enameloid is smooth. In profile view, the mesial cutting edge is straight, and in labial/lingual view, it may be straight or concave basally but convex apically. The distal cutting edge is straight basally but overall exhibits a convex appearance due to the distally inclined cusp. The degree of curvature on these edges varies slightly. The mesial edge may be smooth along its entirety or bear up to nine denticles along its lower one- to two-thirds (compare Fig. 6B, E, H). These denticles are apically directed and decrease in size basally, but they do not reach the cusp apex and do not extend to the crown base. The distal edge bears up to nine denticles that decrease in size basally. These denticles do not reach the apex but can extend to the crown foot. The denticles are not serrated. The uppermost one-third of the crown is developed into a triangular cusp that varies slightly in width and degree of distal inclination (compare Fig. 6D to G). The mesial and distal cutting edges of the main cusp are smooth. The root is weakly bilobate with very short and diverging lobes that are separated by a narrow and shallow U-shaped interlobe area. A robust lingual boss (i.e., Fig. 6F) is bisected by a long, shallow but wide nutritive groove.

Other specimens are similar to those described above but have a broader crown that is more strongly distally curved. This broad-based and distally curved morphology is considered diagnostic of the species and a representative specimen was chosen as the holotype (Fig. 6PP–RR). The largest tooth of this type measures 2.5 cm wide and 2 cm in total height. In profile view, the crowns of these teeth are labially curved and labio-lingually thin. The crown enameloid is smooth. The mesial edge is elongated and can be sinuous to uniformly convex (compare Fig. 6Y to 6DD), whereas the distal edge is uniformly concave

Fig. 6 (page 21). *Hemipristis intermedia* sp. nov., teeth. **A–C**. MMNS VP-12035, lower left lateral tooth. **A**. Labial view. **B**. Lingual view. **C**. Mesial view. **D–F**. MMNS VP-12036 (paratype), lower left lateral tooth. **D**. Labial view. **E**. Lingual view. **F**. Mesial view. **G–I**. MMNS VP-12037 (paratype), upper left anterior tooth. **G**. Labial view. **H**. Lingual view. **I**. Mesial view. **J–L**. MMNS VP-12038, lower right anterolateral tooth. **J**. Labial view. **K**. Lingual view. **L**. Mesial view. **M–O**. MMNS VP-12039, lower right anterior tooth. **M**. Labial view. **N**. Lingual view. **O**. Mesial view. **P–R**. SC2013.28.80 (paratype), lower left anterior tooth. **P**. Labial view. **Q**. Lingual view. **R**. Mesial view. **S–U**. MMNS VP-12040, upper left lateral tooth. **S**. Labial view. **T**. Lingual view. **U**. Mesial view. **V–X**. MMNS VP-12042, upper left lateral tooth. **V**. Labial view. **W**. Lingual view. **X**. Mesial view. **Y–AA**. MMNS VP-12043, upper right lateral tooth. **Y**. Labial view. **Z**. Lingual view. **AA**. Mesial view. **BB–CC**. MMNS VP-12044, upper left lateral tooth. **BB**. Labial view. **CC**. Lingual view. **DD–EE**. MMNS VP-12045, upper left lateral tooth. **DD**. Labial view. **EE**. Lingual view. **FF–GG**. MMNS VP-12046, upper left lateral tooth. **FF**. Labial view. **GG**. Lingual view. **HH–JJ**. MMNS VP-6625, lower left symphyseal tooth. **HH**. Labial view. **II**. Lingual view. **JJ**. Mesial view. **KK–LL**. SC2013.28.90, upper right lateral tooth. **KK**. Labial view. **LL**. Lingual view. **MM–OO**. MMNS VP-7604, juvenile lower left anterior tooth. **MM**. Labial view. **NN**. Lingual view. **OO**. Mesial view. **PP–RR**. SC2013.28.73 (holotype), upper right lateral tooth. **PP**. Labial view. **QQ**. Lingual view. **RR**. Mesial view. **SS–TT**. SC2013.28.103, juvenile upper left postero-lateral tooth. **SS**. Labial view. **TT**. Lingual view. **UU–VV**. SC2013.28.104, juvenile upper left lateral tooth. **UU**. Labial view. **VV**. Lingual view. Scale bars: A–U, HH–JJ = 1 cm; MM–OO = 2 mm; V–GG, KK–LL, PP–QQ = 5 mm; RR–UU = 1 mm.

along its length (i.e., Fig. 6T). The degree of curvature of the mesial and distal edges is variable. The mesial edge may be smooth, but it is more typically denticulated, often with 5–6 denticles, but up to ten may be present (compare Fig. 6BB, FF, PP, S). These denticles are usually medially located on the edge, but they may only occur along the lower one-third or extend up to two-thirds of the crown height. Denticles are apically directed but decrease in size basally. The distal edge often bears eight denticles, but up to 11 can occur (compare Fig. 6DD to T). Denticles are apically directed but decrease in size basally, and they extend to the crown foot. Although the distal denticles often extend higher onto the crown compared to the mesial denticles, the mesial denticles sometimes extend beyond the height of the distal ones (compare Fig. 6EE to T). The apical portion of the crown is developed into a triangular cusp that is distally inclined to varying degrees. The mesial and distal cutting edges are smooth. The root is bilobate, with very wide but short sub-rectangular lobes. These are separated by a narrow U-shaped or V-shaped interlobe area. A low lingual boss (Fig. 6AA) is bisected by a long, shallow, and wide nutritive groove.

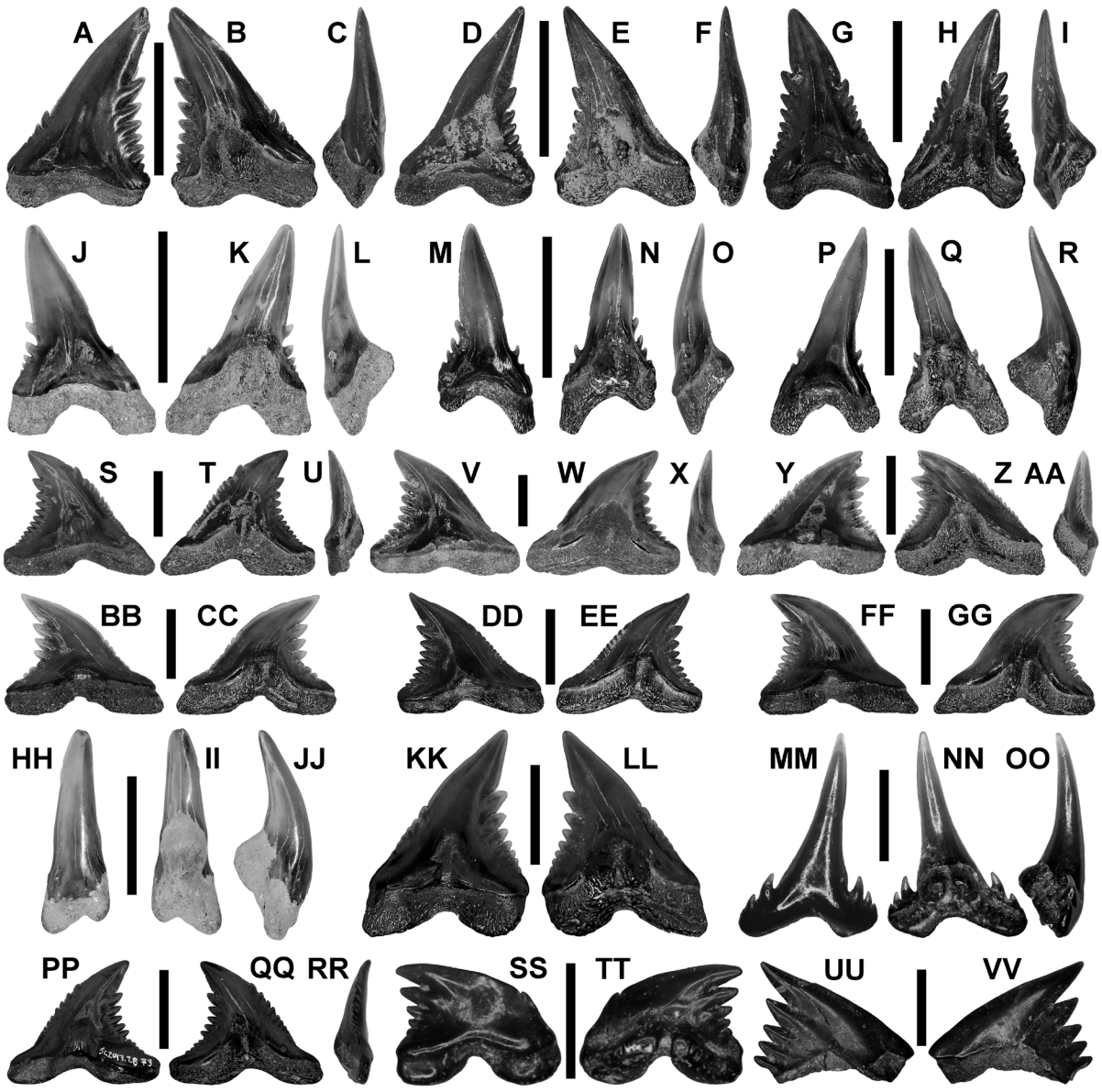

Some specimens are quite distinct from both aforementioned morphotypes, as they are very narrow mesio-distally and have a tall crown (Fig. 6HH). In profile view, the crown may be weakly sinuous, with strong lingual curvature and slight labial curvature of the crown faces (Fig. 6JJ). The labial crown face is moderately convex and the lingual face very convex, which results in a somewhat conical crown. The crown may lack or have apical cutting edges, and no denticles are developed. The root is narrow, weakly bilobate, and has a robust lingual boss bearing a conspicuous nutritive groove. A more common morphology includes teeth with a wider crown that is denticulated. In profile view, the crown is highly lingually curved, and the labial face is convex basally but flatter apically (Fig. 6L, R). The lingual face is very convex, and crown enameloid is smooth on all specimens. The mesial side of the tooth may be rounded or bear a cutting edge that does not extend to the crown foot (Fig. 6JJ). Relatively small and needle-like denticles can occur along the lower one-fourth of the mesial edge, of which up to three have been observed (Fig. 6Q). The distal edge usually bears a smooth cutting edge, which does not reach the crown foot. Two to four small and needle-like denticles occur at the lower one-third of the edge (Fig. 6M, P). The denticles on both sides of the crown are widely separated from each other and may be medially curved. The cutting edges are always smooth and may reach the level of the denticles. The denticle-free portion of the crown is a narrow and triangular cusp that is comparatively larger than those of previously described teeth. The root is bilobate with relatively short, diverging lobes, and the mesial lobe is more elongated and narrower than the distal lobe (Fig. 6H, Q). A robust lingual boss (Fig. 6O, R, JJ) is bisected by a deep but narrow nutritive groove.

Specimens SC2013.28.103 (Fig. 6SS–TT) and SC2013.28.104 (Fig. 6UU–VV) are diminutive teeth that are similar to each other. Both are broad-based and sub-triangular in labial view, with SC2013.28.103 measuring 2 mm in width and SC2013.28.104 just over 3 mm in width as preserved. Both specimens have an elongated and convex mesial cutting edge, and a much shorter (and smooth) distal cutting edge that intersect apically to form a rather small and distally inclined cusp. Although the mesial edge of SC2013.28.104 is smooth, that of SC2013.28.103 bears a diminutive denticle medially (compare Fig. 6VV to TT). Each specimen has an oblique distal heel that bears four triangular denticles that decrease in size basally (Fig. 6SS, UU). Overall, the crown of both specimens is rather straight, with the labial face being relatively flat and the lingual face convex. The crown foot of SC2013.28.104 is not preserved, but that of SC2013.28.103 is thickened and slightly overhangs the root. The root of SC2013.28.103 is higher on the lingual side than on the labial side. The root lobes are very short, sub-rectangular, highly divergent, and separated by a very narrow U-shaped interlobe area. The lingual attachment surface is bisected by a conspicuous nutritive groove.

Specimens SC2013.28.105, MMNS VP-7604, and MMNS VP-8745 are diminutive teeth of comparable morphology. The crowns measure 2.5 mm in width and 4 mm in height. Much of the crown is comprised of the main cusp, which is broad basally but rather needle-like apically. The conical cusp may lack cutting edges (Fig. 6OO) or have mesial and distal cutting edges that are sharp, smooth, and extend to the base of the main cusp. Although the cusp is somewhat distally inclined, the mesial edge is concave and the distal edge is convex, which results in an unusual mesially directed cusp apex (Fig. 6NN). The crown foot at the mesial and distal sides are formed into very short shoulders that each bear two denticles that decrease in size basally (Fig. 6MM). The labial crown foot is very convex and there is a shallow but broad U-shaped embayment. The labial and lingual faces are smooth and convex.

Remarks

The tooth morphology of extant *Hemipristis elongata* (Klunzinger, 1871) is quite variable, and the teeth of the extinct *H. curvatus* Dames, 1883 and *H. serra* Agassiz, 1835 exhibit similar variation. These taxa, as well as the Catahoula Formation *Hemipristis*, exhibit monognathic and dignathic heterodonty. Ontogenetic heterodonty is also evident, as small teeth in our sample are similar to a tooth that Cicimurri & Knight (2009: fig. 5j) recovered from the Chattian Chandler Bridge Formation of South Carolina.

That specimen lacks mesial serrations and was identified as a juvenile upper tooth of *Hemipristis*. Their interpretation is consistent with our evaluation of the Catahoula Formation *Hemipristis* sample, where upper teeth under 7 mm in width lack mesial serration. Specimens SC2013.28.103, SC2013.28.105, MMNS VP-7604, and MMNS VP-8745 are superficially like *Paragaleus* teeth, but our evaluation of four jaws of extant *Hemipristis elongata* (SC84.177.1, SC86.52.1, SC2020.53.9, MSC 42627) leads us to conclude that they are teeth of very small individuals of *H. intermedia* sp. nov. Specimen SC2013.28.103 (Fig. 6SS–TT) is comparable to teeth in the postero-lateral files of *H. elongata*, whereas SC2013.28.105 (Fig. 6UU–VV), MMNS VP-7604 (Fig. 6MM–OO), and MMNS VP-8745 are virtually identical to teeth in the lower anterior files.

Upper anterior teeth in the Catahoula Formation sample are identified by their triangular and rather weakly asymmetrical crown, whereas upper lateral teeth are broadly triangular with a conspicuous distally hooked appearance (compare Fig. 6G to S). Within lateral files, the amount of curvature of the mesial and distal edges, and the degree of distal cusp inclination increase towards the commissure (compare Fig. 6PP to FF). Specimens believed to be lower symphyseal or parasymphyseal (i.e., Fig. 6HH–JJ) teeth are very narrow with a roughly conical crown that lacks denticles and sometimes cutting edges. Lower anterior teeth are much narrower and bear significantly fewer denticles compared to upper anteriors, and the cusp constitutes a comparatively larger portion of the crown (Fig. 6J, P). The root of lower anterior teeth also has a more robust lingual boss compared to the upper teeth. Teeth from lateral positions are broader, have elongated cutting edges that reach the level of the mesial and distal denticles, and have up to five mesial and at least seven distal denticles. Based on our evaluation of extant *H. elongata* jaws (i.e., SC84.177.1, SC86.53.1), upper anterior teeth of *H. intermedia* sp. nov. are distinguished from lower lateral teeth by the greater number of mesial and distal denticles and the comparatively smaller proportion of main cusp to crown height (compare Fig. 6G to E). We chose an upper lateral tooth as the holotype specimen (Fig. 6PP–RR) for the new species because, among the various fossil *Hemipristis* that have been named, this morphology is often the most common and easily identified.

The fossil record of *Hemipristis* extends back to the middle Eocene, with specimens of the globally widespread *H. curvatus* occurring as early as the Lutetian (NP15) (Ebersole *et al.* 2019). The species is well known from North America (i.e., White 1956; Westgate 1984; Parmley & Cicimurri 2003; Cicimurri & Knight 2019; Perez 2022) and Africa (i.e., Adnet *et al.* 2010, 2020; Underwood *et al.* 2011), with rare records from Asia (Tanaka *et al.* 2006; Tomita *et al*. 2023) and possibly Europe (Priem 1912; Ciobanu 1994). *Hemipristis serra* ranges from the Miocene to Early Pleistocene and was nearly globally distributed (Cappetta 2012). *Hemipristis* has also been reported from various Oligocene sites in the USA (Cicimurri & Knight 2009; Ebersole *et al.* 2021; Cicimurri *et al.* 2022) and Asia (Adnet *et al.* 2007), with specimens having been tentatively assigned to *H. serra* or altogether not speciated. Although Chandler *et al.* (2006) indicated that there was no evidence for the existence of Paleogene and Neogene species of *Hemipristis* other than *H. curvatus* and *H. serra*, Adnet *et al.* (2007) and Ebersole *et al.* (2021) suggested that Oligocene teeth represent a transitional species between the two.

Although the gross morphology of *Hemipristis* teeth has remained stable, even to the present day, large samples of *H. curvatus* teeth from the middle Eocene of Alabama (MSC collection), Bartonian of South Carolina (SC2022.27) and Georgia (SC2004.34, SC2013.44), along with samples of *H. serra* from the Middle Miocene (Langhian) of North Carolina (contained within accession SC98.46) and Gelasian (Early Pleistocene) of South Carolina (accessions SC89.240, SC2006.1), and jaws of extant *H. elongata* reveal significant differences among the various taxa. With respect to *H. curvatus*, *H. intermedia* sp. nov. attains a larger overall size (2.5 cm wide by 2.2 cm high vs 1.5 cm and 1.1 cm), and the latter species consistently has more extensively denticulated mesial and distal edges. Whereas the upper lateral teeth of *H. curvatus* exhibit fewer than four mesial and up to eight distal denticles, the teeth of *H. intermedia*

have up to 10 mesial and 11 distal denticles. Additionally, the mesial denticles of *H. curvatus* are limited to the lower one-half of the crown, whereas they extend up to two-thirds of the crown height of *H. intermedia*. The cusp of *H. curvatus* teeth constitutes a larger proportion of the crown compared to *H. intermedia*. Variations in the number of mesial and distal denticles in *H. curvatus* and *H. intermedia* were also observed among the three jaws of *H. elongatus*, but the maximum number of denticles present and their distributions along the mesial and distal edges are taxonomically significant.

Hemipristis serra upper lateral teeth attain a significantly larger size than those of *H. intermedia* sp. nov., with the largest specimen available to us measuring 3.7 cm wide and 3.6 cm in height. In contrast, the largest tooth of *H. intermedia* sp. nov. in our sample measures only 2.5 cm and 2.2 cm in these dimensions, respectively. Additionally, the mesial and distal edges of *H. serra* teeth have a greater number of denticles, with at least 13 occurring on the distal side but more than 20 are common. On the mesial edge, the denticles are largest and most conspicuous along the upper one-half of the crown, but basally the edge appears more regularly serrated (serration/denticulation also consistently reaches the base of the edge). The denticles on *H. serra* teeth also extend closer to the apex, and the cusp comprises a very small portion of the crown compared to in *H. intermedia*. On the former, the cusp can represent as little as 10% of the total tooth height, whereas on the latter it represents at least 20%. Furthermore, small teeth of *H. serra* are as regularly serrated/denticulated as large teeth, whereas in *H. intermedia* these features are generally more extensive on large specimens.

Upper anterior teeth of each of the Paleogene and Neogene taxa are similar in gross morphology but can be separated based on the combination of maximum tooth size, degree of mesial denticulation and location of mesial denticles, degree of denticulation of the distal edge, and size of the cusp with respect to overall tooth size. The overall trend through time is an increase in maximum tooth size and number of mesial and distal denticles and a decrease in cusp size (in relation to total crown size). We found that the morphologies of lower anterior teeth of the Paleogene and Neogene taxa overlap and are largely differentiable by crown size and robustness. These teeth are not considered to be taxonomically useful for species determination.

For completeness, we also evaluated the teeth of extant *H. elongata*. All four *H. elongata* jaws we examined are of the same size and have similar tooth sizes, and none of the upper lateral teeth approach the largest *H. curvatus* in our sample (1 cm wide and 0.9 cm high vs 1.5 cm and 1.1 cm in these dimensions), let alone the largest *H. intermedia* sp. nov. tooth. In general, the upper lateral teeth of *H. elongata* are narrower and the mesial denticles (up to ten) are much less conspicuous compared to teeth of the extinct species. Additionally, the lower half of the tooth is the most convex, whereas it is most convex along the upper one-half on the fossil teeth. Interestingly, the cusp of *H. elongata* teeth constitutes slightly more than 20% of the total tooth height.

The Catahoula Formation *Hemipristis* teeth were compared to Oligocene specimens from the southeastern Atlantic Coastal Plain and Gulf Coastal Plain of the USA, including material from the Glendon Limestone Member of the Byram Formation of Alabama (Rupelian Stage, circa 30 Ma, NP23), the Old Church Formation of Virginia (Rupelian, roughly 29 Ma), the Ashley Formation of South Carolina (Rupelian, approximately 28.5 Ma), and the Chandler Bridge Formation of South Carolina (Chattian Stage, about 24.5 Ma). The Glendon Limestone Member specimen, documented by Ebersole *et al.* (2021), is a lower anterior tooth that is taxonomically uninformative beyond the generic level. Specimens from the Ashley Formation were identified as *H. serra* by Müller (1999) and Cicimurri *et al.* (2022). The specimens shown by Müller (1999: pl. 8 fig. 9) and Cicimurri *et al.* (2022: fig. 5a) are both comparable in size to the Catahoula Formation teeth, and the mesial edges are more extensively denticulated compared to in *H. curvatus.* Visually, the proportion of cusp to tooth height appears to be greater than that of *H. serra*.

We examined five teeth from the Old Church Formation of Virginia that are included within accession SC2020.43, as well as illustrations of four specimens provided by Müller (1999: pl. 8 figs 12–15). In general, the teeth are similar to those of the Catahoula Formation with respect to the number of denticles and the size of the cusp compared to overall tooth size. However, one specimen shown by Müller (1999: pl. 8 fig. 12) exhibits a large number of mesial/distal denticles and a relatively small cusp, features more consistent with *H. serra*. Ten teeth from the Chandler Bridge Formation contained within SC2005.2 were examined, as were two specimens identified as *H. serra* by Cicimurri & Knight (2009). The Chandler Bridge Formation sample is variable and contains specimens that are similar to the Catahoula Formation teeth, as well as specimens that are comparable to *H. serra* (i.e., Cicimurri & Knight 2009: fig. 5i).

The Catahoula Formation *Hemipristis* teeth are comparable to *Hemipristi*s specimens from the Ashley Formation and, for the most part, the Old Church Formation. The Ashley and Old Church formations are slightly older than the Rupelian/Chattian Stage boundary, whereas the Catahoula Formation teeth are slightly younger than that boundary. The morphological and age similarities among the samples from these three units indicate that the *Hemipristis* teeth occurring in each unit are conspecific, and herein assigned to *H. intermedia* sp. nov. However, the *Hemipristis* teeth within the Chandler Bridge Formation, roughly four million years younger than the aforementioned units, are more similar to Miocene *H. serra*.

Adnet *et al.* (2007) reported a sample of 10 *Hemipristis* teeth from the Rupelian of Balochistan that they tentatively referred to *H. serra*. The two teeth they illustrated (figs 6, 15–17) are larger than and have more extensive mesial denticulation compared to Eocene *H. curvatus*, and they are smaller than and less denticulated than Miocene and younger *H. serra*. Those authors indicated that the teeth could represent a transitional morphology between the two species. The two teeth illustrated by Adnet *et al.* (2007) are both upper lateral teeth, and they fall within the range of variation we observed in the Catahoula Formation *Hemipristis* sample. However, as we found the dentition of the Catahoula Formation sample to be highly variable, we refrain from associating the Balochistan taxon with *Hemipristis intermedia* sp. nov. until other tooth morphologies (i.e., upper anterior and lower lateral teeth) can be examined and directly compared to those of the new species.

One additional taxon, *H. tanakai* Tomita, Yabumoto & Kuga, 2023, was recently erected based on a total of five teeth from widely disparate localities. The holotype is a complete tooth from the lower Oligocene (Rupelian) Yamaga Formation in Japan, and the paratype, a broken tooth preserved in labial view, may or may not be from the same lithostratigraphic unit and locality as the holotype. The authors also included in this species the specimens reported by Adnet *et al.* (2007) as well as a tooth from South Carolina. Unfortunately, this species may be considered a nomen dubium for several reasons. Firstly, one of the three criteria used to differentiate *H. tanakai* from other species is tooth height, which for *H. tanakai* is apparently at least 1.5 cm. We note here that although the total height in the *H. curvatus* we examined measured up to 1.2 cm, tooth height in *H. serra* can also measure 1.5 cm. Another characteristic attributed to *H. tanakai* is that the mesial edge purportedly bears up to five denticles. This morphology is comparable to that of *H. curvatus*, where the mesial edge may completely lack denticulation or have up to five denticles. The Catahoula Formation *Hemipristis* teeth, as well as those from the Old Church and Ashley formations (Müller 1999; Cicimurri *et al.* 2022) can have a far greater number of mesial denticles (8+), indicating that the fossils from these units are not conspecific with *H. tanakai*.

As mentioned earlier, Tomita *et al*. (2023: fig. 3) assigned a tooth from South Carolina to *H. tanakai*. Unfortunately, the stratigraphic occurrence of the specimen is listed as "(Upper Oligocene) Chandler Bridge Formation, Ashley Marl." The Ashley Formation (Rupelian Stage) and Chandler Bridge Formation (Chattian Stage) are two different lithostratigraphic units separated by approximately five million years of time. Although the authors provided color images of the specimen (Tomita *et al.* 2023: fig. 3a–e), shark teeth from the Ashley and Chandler Bridge formations can have similar coloration (DJC, pers. obs.). Additionally, although the tooth shown has five distinct mesial denticles, there are

several indistinct crenulations that could be counted as additional denticles (thereby increasing the number to at least seven and exceeding the number attributed to *H. tanakai*).

Thirdly, according to Tomita *et al.* (2023) the apical-most denticle on the mesial cutting edge in *H. tanakai* is located higher on the crown compared to the distal cutting edge. Although this may be true for the holotype specimen of *H. tanakai* shown by Tomita *et al*. (2023: fig. 2), it is not the case for the South Carolina specimen illustrated in their fig. 3a–e, and the mesial edge of their paratype specimen (fig. 3j) is not preserved. We suggest that the South Carolina specimen and broken paratype specimen be excluded from the *H. tanakai* hypodigm, as the stratigraphic and temporal occurrence of the former is ambiguous, and the latter specimen is poorly preserved (and only exposed from the matrix in labial view). Additionally, the morphological features attributed to *H. tanakai* are ambiguous and based only on the upper lateral morphology. In any event, the features of *H. tanakai* are inconsistent with those of the Catahoula Formation taxon (i.e., greater than ten mesial denticles, apical-most denticle of the distal edge is usually located higher than that on the mesial edge of the latter) and, if considered a valid species, does not appear to be conspecific with *H. intermedia* sp. nov.

Family Carcharhinidae Jordan & Evermann, 1896

Genus ***Physogaleus*** Cappetta, 1980

Type species

Trigonodus secundus Winkler, 1874, Lutetian, Belgium.

Physogaleus contortus (Gibbes, 1849)
Fig. 7A–DD

Galeocerdo contortus Gibbes, 1849: 193.

Material examined

UNITED STATES OF AMERICA – **Mississippi •** 15 isolated teeth; Catahoula Formation; MMNS VP-6623 (3 teeth), MMNS VP-6623.1 (Fig. 7D–F), MMNS VP-6623.2 (Fig. 7J–L), MMNS VP-6623.3 (Fig. 7M–O), MMNS VP-6623.4 (Fig. 7P–R), MMNS VP-6623.5 (Fig. 7S–U), MMNS VP-6623.6 (Fig. 7V–X), MMNS VP-6623.7 (Fig. 7Y–AA), MMNS VP-6623.8 (Fig. 7BB–DD), MMNS VP-12047 (Fig. 7A–C), SC2013.28.106 (Fig. 7G–I), SC2013.28.107, SC2013.28.108.

Description

Teeth are broad-based and moderately high-crowned, with the largest specimens measuring 15 mm in mesio-distal width and 12 mm in apico-basal height. The crown of each specimen consists of a conspicuous cusp and distal heel. The mesial cutting edge is elongated and sinuous, with the basal portion being concave and the apical portion convex; the degree of curvature in these areas is variable (i.e., weakly to strongly). The cutting edge is also serrated to varying degrees, and it may be finely and evenly serrated along nearly its entire length or coarse along a portion but fine along another portion of the same edge. Serrations are often coarse basally but fine apically. In mesial view, the cutting edge is usually very sinuous, and the apical portion of the cusp has a twisted appearance that is particularly conspicuous in mesial view (Fig. 7C, I, AA). The distal cutting edge is comparatively much shorter, distally inclined, and finely serrated. The mesial and distal cutting edges intersect apically to form a rather narrow, elongated, and distally inclined cusp. The serrations on the distal cutting edge are coarsest basally but fine apically. Serrations on the mesial and distal cutting edges are simple. The transition from distal cutting edge to distal heel is marked by a sharp curve or a notch (compare Fig. 7BB to 7G), and on the former serrations occur within the curve and onto the apical edge of the first denticle on the

heel (Fig. 7M). On the latter, the apical portion of the first denticle on the heel is serrated (Fig. 7V). The distal heel is low, elongated, oblique to a vertical plane, and denticulated. Typically, there are at least four conspicuous denticles that decrease in size distally, where they blend into serrations near the crown margin. Denticles on the distal heel are often weakly serrated on their apical edges. The root is bilobate with thin, short but widely separated lobes. The prominent lingual root boss on each specimen is ablated but was bisected by a nutritive groove (Fig. 7T, CC).

Remarks

Cicimurri *et al.* (2022) reported similar specimens from the Rupelian Ashley Formation of South Carolina, and they discussed the stratigraphic and temporal ambiguity surrounding the morphology of *P. contortus* as originally described by Gibbes (1849). In short, Gibbes noted that his South Carolina specimens originated from "newer Eocene" deposits, which, based on fossil content, almost certainly belong to the Ashley Formation due to the Rupelian age of the associated invertebrates he identified. Gibbes (1849) specifically noted the twisted appearance of the mesial cutting edge (Fig. 7C, F), and the specimens he illustrated, particularly as seen in his figs 71–72, have coarse distal heel denticles. This latter morphology conforms to the Oligocene specimens we collected from the Catahoula Formation, as well as to the material reported by Cicimurri *et al.* (2022). We examined Miocene and Pliocene teeth typically assigned to *P. contortus* that were collected from North and South Carolina and Florida, and specimens of this age have a more evenly serrated heel compared to the Oligocene counterparts. We must therefore take into consideration the possibility that Gibbes' original concept of the *contortus* morphology was for Oligocene Ashley Formation specimens. That the distal cutting edge serrations of the Catahoula Formation specimens are already encroaching onto the distal heel foreshadows the development of a uniformly serrated heel in the Mio-Pliocene descendants of the Oligocene taxon. The specimens in our sample represent the first occurrence of *P. contortus* from the northern Gulf Coastal Plain of the USA

The Catahoula Formation *P. contortus* teeth exhibit monognathic heterodonty, with anterior teeth being mesio-distally narrow and having a rather erect cusp (Fig. 7D–E), and lateral teeth being wider and having a more distally inclined cusp (Fig. 7A–B). Additionally, cusp inclination increases but height decreases towards the commissure (compare Fig. 7J and P). The teeth vary considerably in the width of the cusp and the convexity of the mesial cutting edge, which we believe reflects dignathic heterodonty. Teeth that may be from upper files are those shown in Fig. 7A, G, and V, whereas those from lower files are shown in Fig. 7M, S, and Y.

The Catahoula Formation *P. contortus* teeth can be separated from *Galeocerdo* (see below) by their elongated and narrow cusp, simple serrations, lack of serrations at the cusp apex, and the "twisted" nature of the mesial cutting edge. The teeth of *Galeocerdo* that we examined, including fossil and extant specimens, have a straight mesial cutting edge (in mesial and occlusal views), and most of the *Galeocerdo* species have compound serrations (Türtscher *et al.* 2021). The Oligocene *P. contortus* morphology should therefore be separable from specimens identified as the "narrow crowned" morphology of *G. aduncus* (Agassiz, 1835) (i.e., Türtscher *et al.* 2021) by this contorted apical portion of the cusp. The Catahoula Formation *P. contortus* teeth differ from those we assigned to *Physogaleus* sp. (see below) by being larger in overall size and by having a more elongated and usually sinuous cusp, conspicuous mesial serrations extending more than two-thirds along the edge, more numerous and well-developed distal denticles, and fine serrations that extend nearly to the apex of the distal cutting edge of the main cusp. Pollerspöck and Unger (2023) recently suggested *P. contortus* be placed within Galeocerdonidae, which was followed by Höltke et al. (2024). However, doing so necessitates placing all other species of *Physogaleus*, which are quite different from *Galeocerdo*, within the family, or assigning the *contortus* morphology to *Galeocerdo*. Based on the criteria we utilized to differentiate *P. contortus* from *Galeocerdo*, we maintain the former taxon within Carcharhinidae.

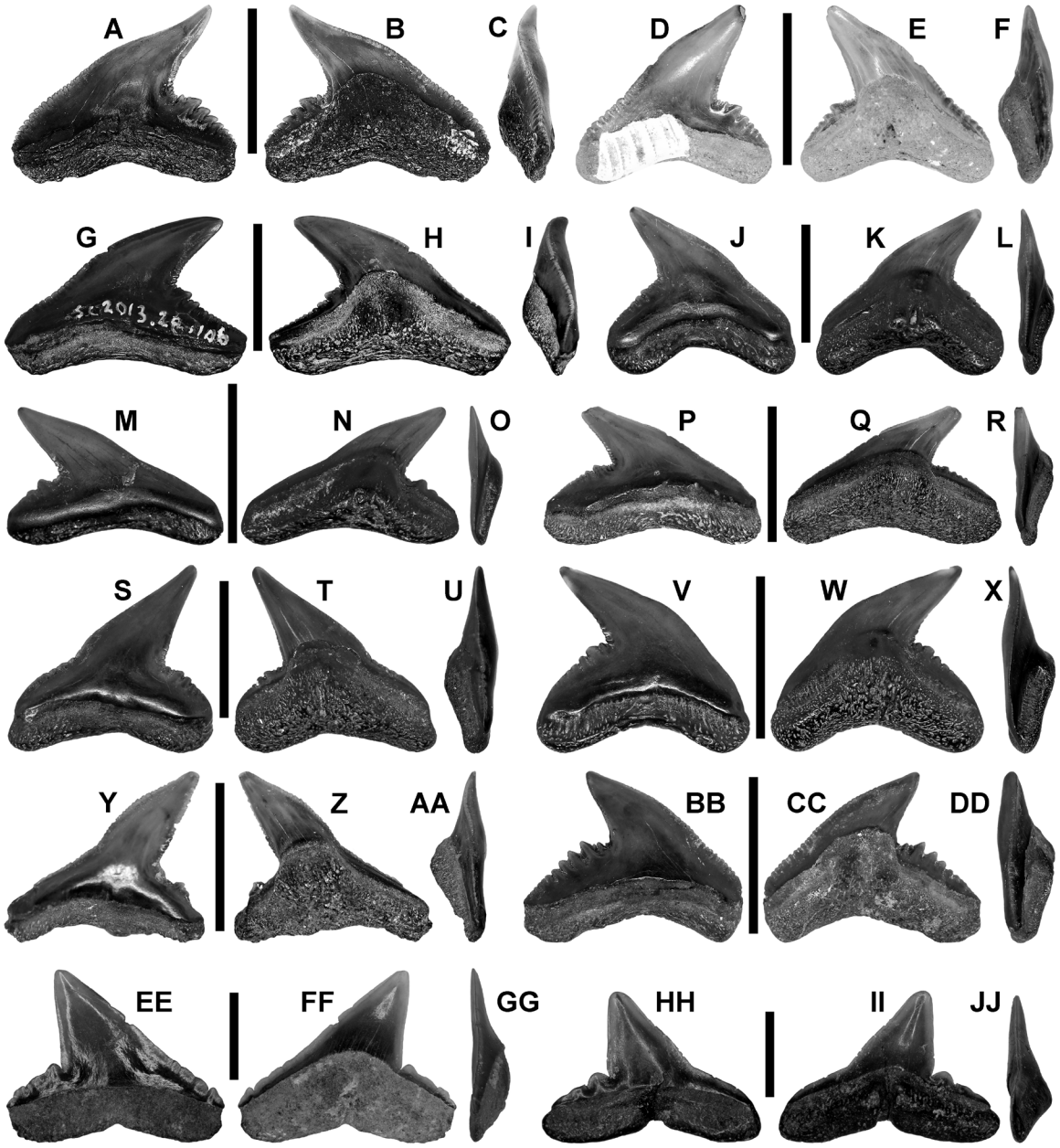

Fig. 7. *Physogaleus contortus* (Gibbes, 1849) (A–DD) and *Physogaleus* sp. (EE–JJ), teeth. **A–C**. MMNS VP-12047, *Physogaleus contortus*, antero-lateral tooth. **A**. Labial view. **B**. Lingual view. **C**. Mesial view. **D–F**. MMNS VP-6623.1, *P. contortus*, anterior tooth. **D**. Labial view. **E**. Lingual view. **F**. Mesial view. **G–I**. SC2013.28.106, *P. contortus*, lateral tooth. **G**. Labial view. **H**. Lingual view. **I**. Mesial view. **J–L**. MMNS VP-6623.2, *P. contortus*, anterior tooth. **J**. Labial view. **K**. Lingual view. **L**. Mesial view. **M–O**. MMNS VP-6623.3, *P. contortus*, lateral tooth. **M**. Labial view. **N**. Lingual view. **O**. Mesial view. **P–R**. MMNS VP-6623.4, *P. contortus*, lateral tooth. **P**. Labial view. **Q**. Lingual view. **R**. Mesial view. **S–U**. MMNS VP-6623.5, *P. contortus*, anterior tooth. **S**. Labial view. **T**. Lingual view. **U**. Mesial view. **V–X**. MMNS VP-6623.6, *P. contortus*, anterior tooth. **V**. Labial view. **W**. Lingual view. **X**. Mesial view. **Y–AA**. MMNS VP-6623.7, *P. contortus*, lateral tooth. **Y**. Labial view. **Z**. Lingual view. **AA**. Mesial view. **BB–DD**. MMNS VP-6623.8, *P. contortus*, antero-lateral tooth. **BB**. Labial view. **CC**. Lingual view. **DD**. Mesial view. **EE–GG**. SC2013.28.134, *Physogaleus* sp., tooth. **EE**. Labial view. **FF**. Lingual view. **GG**. Mesial view. **HH–JJ**. SC2013.28.136, *Physogaleus* sp., tooth. **HH**. Labial view. **II**. Lingual view. **JJ**. Mesial view. Scale bars: A–DD = 1 cm; EE–JJ = 2 mm.

Physogaleus sp.
Fig. 7EE–II

Material examined

UNITED STATES OF AMERICA – **Mississippi** • 14 isolated teeth; Catahoula Formation; SC2013.28.134 (Fig. 7EE–GG), SC2013.28.135, SC2013.28.136 (Fig. 7HH–II), SC2013.28.137 to 28.143, SC2013.28.144 (4 teeth).

Description

The teeth are small, measuring up to 6 mm in mesio-distal width and less than 5 mm in apico-basal height. The crown consists of a prominent cusp and a distal heel. The elongated mesial cutting edge of the cusp is sharp and smooth (Fig. 7HH), but weak denticulation occurs at the base of the edge on SC2013.28.134 (Fig. 7EE). The mesial edge ranges from straight, to sinuous, to weakly convex or weakly concave (Fig. 7FF, II). The distal cutting edge is also smooth but much shorter and may be vertical to distally inclined. The mesial and distal edges intersect apically to form a sharp apex. The distal heel is low and bears two or three denticles. These denticles decrease in size distally, and the distal-most denticle is very inconspicuous. The labial crown face is smooth and flat, whereas the lingual crown face is smooth and convex (Fig. 7JJ). The root is bilobate, with elongated, highly divergent sub-rectangular lobes that are separated by a broad V-shaped interlobe area. The teeth have a thin, medially located lingual nutritive groove (Fig. 7FF, II).

Remarks

Our small sample appears to reflect monognathic and dignathic heterodonty within the dentition of this taxon. Anterior teeth are mesio-distally narrower than lateral teeth, and the cusp of anterior teeth is more erect. Additionally, the main cusp becomes more inclined towards the jaw commissure. The distal heel of lateral teeth is more horizontal than that of anterior teeth, and it is more elongated, with a greater number of denticles. Teeth that we believe are from the lower dentition have a narrower main cusp with a more concave mesial cutting edge (Fig. 7HH) compared to upper teeth (Fig. 7EE).

These teeth differ from those of *Physogaleus contortus* and *Galeocerdo* from the Catahoula Formation by lacking serrated mesial and distal cutting edges. Additionally, they can be separated from the teeth of *Rhizoprionodon* and Sphyrnidae (see below) by having denticles at the base of the mesial cutting edge and on the distal heel. Ebersole *et al.* (2021) reported a single *Physogaleus* sp. tooth from the Glendon Limestone Member of the Byram Formation (NP23) in southwestern Alabama that is comparable to the Catahoula Formation material. Cicimurri *et al.* (2022) later reported two specimens from the Rupelian Ashley Formation of South Carolina that they considered to be conspecific with the *Physogaleus* sp. specimens previously documented by Cicimurri & Knight (2009) from the Chattian Chandler Bridge Formation in South Carolina. The Catahoula Formation sample is younger than the Alabama occurrence and bracketed in age by the two South Carolina Oligocene occurrences, but it is possible that all the material is conspecific. Although the Catahoula Formation sample is rather small and imperfectly preserved, the teeth appear to differ from those of Eocene *P. secundus* (Winkler, 1874) by the weakly crenulated lower portion of their mesial cutting edge and the poorly developed distal heel denticles. They also differ from the Eocene *P. alabamensis* (Leriche, 1942) and Oligocene *P. latus* (Storms, 1894) by their smaller size and poorly developed mesial cutting edge and distal heel denticles (Reinecke *et al*. 2014; Ebersole *et al*. 2019). Larger samples from both the Gulf and Atlantic coastal plains are necessary to make more precise comparisons and identifications of the Oligocene *Physogaleus* sp. teeth.

Genus ***Rhizoprionodon*** Whitley, 1929

Type species

Carcharias crenidens Klunzinger, 1880, Extant.

Rhizoprionodon sp.
Fig. 8A–D

Material examined

UNITED STATES OF AMERICA – **Mississippi** • 36 isolated teeth; Catahoula Formation; MMNS VP-8396 (6 teeth), MMNS VP-8737, SC2013.28.145 (Fig. 8A–B), SC2013.28.146, SC2013.28.147, SC2013.28.148 (Fig. 8C–D), SC2013.28.149, SC2013.28.150, SC2013.28.151 (7 teeth), SC2013.28.152 (9 teeth), SC2013.28.153 (7 teeth).

Description

Teeth are small and generally measure approximately 5 mm in width (mesio-distal). The crown consists predominantly of a main cusp and a much smaller distal heel. The cusp varies in height, degree of distal inclination, and width (compare Fig. 8A to C). The labial crown face is rather flat, but the lingual face is convex, and enameloid is smooth. The mesial cutting edge is elongated, smooth, and may be straight, weakly convex, or concave to varying degrees. The distal cutting edge is smooth and approximately one-half as long as the mesial edge, and it may be straight or convex (compare Fig. 8B to D). The distal heel is low and varies in length, and it may be uniformly convex or somewhat cuspidate. The distal heel is separated from the distal cutting edge by a distinct notch (Fig. 8A). The root is bilobate with short but widely diverging lobes being separated by a prominent lingual nutritive groove (Fig. 8B).

Remarks

These teeth are of small size and most of them are imperfectly preserved, which inhibits our ability to accurately identify them taxonomically. However, we believe that the sample demonstrates monognathic, dignathic, and gynandric heterodonty within the taxon based on the morphological criteria recently presented by Ebersole *et al*. (2023). With respect to monognathic heterodonty, the teeth increase in width but decrease in height from the symphysis to the commissure. Dignathic heterodonty is apparent in cusp width, with that of upper teeth being more than twice as large as that of lower teeth (compare Fig. 8B to D). Anterior teeth of mature, breeding season males have a much more concave mesial cutting edge compared to non-breeding male teeth and female teeth (gynandry). The Catahoula Formation specimens can be differentiated from sphyrnid teeth in our sample (see below) based on their smaller size, shorter main cusp, and shorter and more convex distal heel. However, several authors have commented on the difficulty in differentiating isolated teeth of extant *Rhizoprionodon* from those of taxa within Sphyrnidae (i.e., Purdy *et al.* 2001; Ward & Bonavia 2001), as there is morphological dental overlap between some of the species within these genera (Ebersole *et al.* 2023).

The Catahoula teeth in our sample are morphologically similar to those of two named fossil species, including the Eocene *Rhizoprionodon ganntourensis* (Arambourg, 1952) and the Miocene *R. ficheuri* (Joleaud, 1912). The former species has been documented in lower-to-middle Eocene deposits in the Gulf Coastal Plain of Alabama and Mississippi (Ebersole *et al*. 2019, 2023). The Catahoula Formation sample is not large enough to determine morphological similarity to *R. ganntourensis* and, in any case, the *R. ganntourensis* morphology has not been documented from any fossil deposits that are stratigraphically younger than the middle Eocene. Additionally, there are a number of taxonomic issues surrounding *R. ficheuri* from the type locality that warrant further evaluation of this species (see Ebersole *et al*. 2023

for a discussion of this taxon). We refrain from assigning the Catahoula Formation teeth to any particular species of *Rhizoprionodon* due to our small sample size.

Genus ***Carcharhinus*** de Blainville, 1816

Type species

Carcharhinus melanopterus Quoy & Gaimard, 1824, Extant.

Carcharhinus acuarius (Probst, 1879)
Fig. 8E–H, Q–S

Alopecias acuarius Probst, 1879: 140.

Material examined

UNITED STATES OF AMERICA – **Mississippi** • 986 isolated teeth; Catahoula Formation; SC2013.28.188 to 28.193, SC2013.28.194 (Fig. 8G–H), SC2013.28.195 (Fig. 8E–F), SC2013.28.196

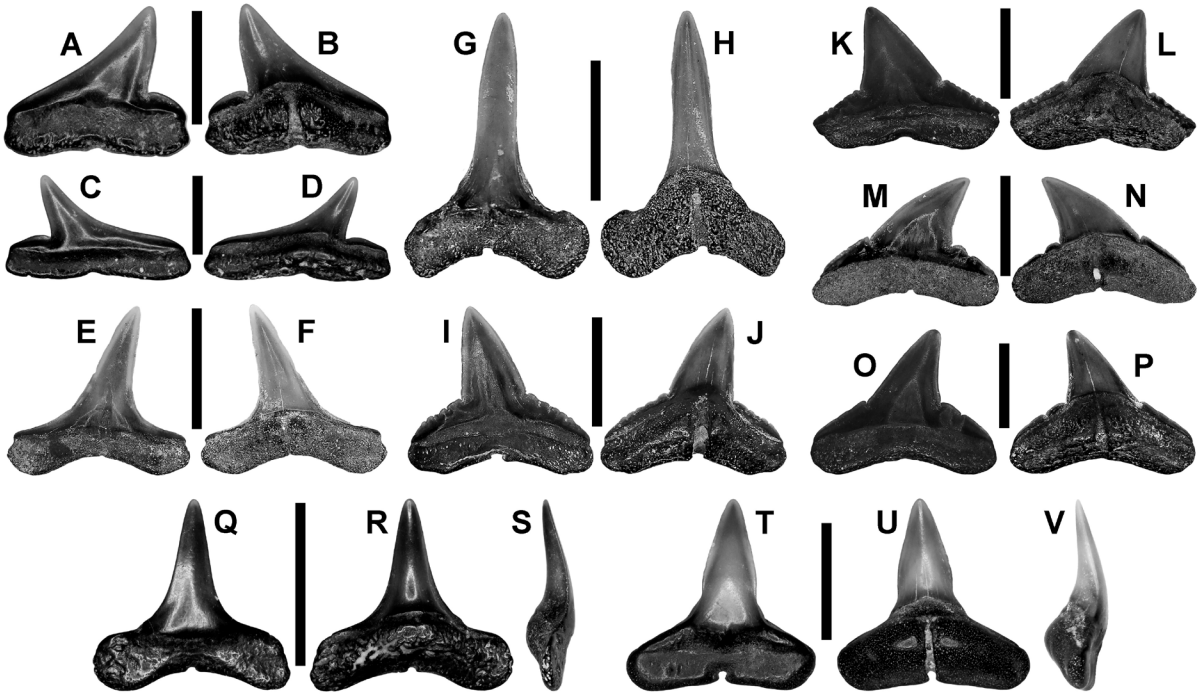

Fig. 8. *Rhizoprionodon* sp. (A–D), *Carcharhinus acuarius* (Probst, 1879) (E–H, Q–S), and *C. elongatus* (Leriche, 1910) (I–P, T–V), teeth. **A–B**. SC2013.28.145, *Rhizoprionodon* sp., upper right anterior tooth. **A**. Labial view. **B**. Lingual view. **C–D**. SC2013.28.148, *Rhizoprionodon* sp., lower right lateral tooth. **C**. Labial view. **D**. Lingual view. **E–F**. SC2013.28.195, *Carcharhinus acuarius*, upper right lateral tooth. **E**. Labial view. **F**. Lingual view. **G–H**. SC2013.28.194, *C. acuarius*, upper right anterior tooth. **G**. Labial view. **H**. Lingual view. **I–J**. SC2013.28.211, *C. elongatus*, upper left anterolateral tooth. **I**. Labial view. **J**. Lingual view. **K–L**. SC2013.28.215, *C. elongatus*, upper left lateral tooth. **K**. Labial view. **L**. Lingual view. **M–N**. SC2013.28.235, *C. elongatus*, upper right posterolateral tooth. **M**. Labial view. **N**. Lingual view. **O–P**. SC2013.28.251, *C. elongatus*, upper right lateral tooth. **O**. Labial view. **P**. Lingual view. **Q–S**. SC2013.28.201, *C. acuarius*, lower tooth. **Q**. Labial view. **R**. Lingual view. **S**. Mesial view. **T–V**. SC2013.28.244, *C. elongatus*, lower tooth. **T**. Labial view. **U**. Lingual view. **V**. Mesial view. Scale bars: A–B = 3 mm; C–D = 2 mm; E–V = 5 mm.

to 28.200, SC2013.28.201 (Fig. 8Q–S), SC2013.28.202 to 28.204, SC2013.28.205 (149 teeth), SC2013.28.206 (206 teeth), SC2013.28.207 (169 teeth), SC2013.28.208 (305 teeth), SC2013.28.209 (121 teeth), SC2013.28.266 (3 teeth), SC2013.28.267 (16 teeth).

Description

The largest teeth in our sample measure 10 mm in apico-basial height and 8 mm in mesio-distal width. The crown consists of a cusp and low lateral shoulders. The cusp varies considerably in height and width, ranging from tall and narrow (mesio-distally) to rather low and broad. In profile the tall and narrow teeth have a slight lingual curvature, but broader teeth are erect. The labial face is flat to weakly convex, whereas the lingual face is convex. The crown enameloid is smooth. The mesial and distal cutting edges are smooth and extend from the cusp apex and onto the lateral shoulders. The shoulders are rather low, vary in length (even between the mesial and distal sides of a given tooth), and may be straight to somewhat convex. The root is bilobate with the lobes being elongated, narrow and somewhat closely spaced, or somewhat rectangular and widely diverging. The U-shaped interlobe area is correspondingly deep or shallow. The thickened lingual root face is bisected by a long and deep nutritive groove.

Remarks

We observed variation in tooth shape and size in the Catahoula Formation sample that we believe reflects heterodonty within a single species. A parasymphyseal tooth (i.e., located adjacent to the jaw symphysis) is small in overall size, has a tall and narrow crown and robust root with short lobes, and the root is equal in height to the crown (see an equivalent tooth in Cappetta 1970: pl. 17). Anterior teeth have a tall and narrow cusp with elongated root lobes, and the lateral shoulders are rather short and oblique. Lateral teeth have a somewhat broader and lower cusp, the lateral shoulders are more elongated and perpendicular to cusp height, and the shorter root lobes are more rectangular and widely diverging. Upper anterior teeth (Fig. 8G–H) have shorter root lobes compared to lower anteriors. Upper lateral teeth have broader and more distally inclined cusps than lower laterals (compare Fig. 8E–F to Q–S). We also observed ontogenetic heterodonty in our sample, as small teeth of presumed juvenile individuals appear to be gracile versions of their larger (adult) counterparts.

These teeth differ from those of superficially similar *Carcharias cuspidatus* teeth in our sample by their much smaller overall size, much shorter root lobes, and lack of lateral cusplets. Additionally, teeth of aff. *Pseudocarcharias* sp. are larger and have a more robust crown, root lobes are more elongated and pointed at their extremities, and a short nutritive groove is limited to the rather thin lingual boss. *Alopias* sp. teeth are comparatively larger and have broader, more robust crowns.

Probst (1879) originally assigned his new Early Miocene *acuarius* species to *Alopecias*, and Cappetta (1970), who identified the species as *Aprionodon*, illustrated additional specimens (his pl. 17) that provided a more comprehensive overview of heterodonty within the species. Although the species was subsequently synonymized with *Isogomphodon* (i.e., Bolliger *et al.* 1995), da Silva Rodrigues-Filho *et al.* (2023) recently determined that extant *Isogomphodon* is genetically inseparable from, and should be synonymized with, *Carcharhinus*, which we follow herein. With their inclusion in *Carcharhinus*, the various fossil species formerly assigned to *Isogomphodon* are herein referred to as the daggernose shark species-group within *Carcharhinus*.

The Catahoula Formation teeth conform in both size range and morphology to *C. acuarius*. This taxon was apparently widely distributed during the Miocene (see Carrillo-Briceño *et al.* 2016, 2019; Fialho *et al.* 2019; Perez 2022; Villafaña *et al.* 2020). Cicimurri & Ebersole (2021) and Ebersole & Cicimurri (in press) identified *Isogomphodon* sp. in the lower Oligocene (Rupelian) Rosefield Formation of Louisiana, and comparison of the material they illustrated to the much larger Catahoula Formation sample indicates that the records are conspecific.

The unique body shape of the extant daggernose shark, *C. oxyrhynchus* (Valenciennes in Müller & Henle, 1839), has been proposed as an adaptation to life within the Amazon River estuary, where conditions are highly turbid (Compagno 1984). The late Eocene (Priabonian) daggernose shark, *Carcharhinus aikenensis* (Cicimurri & Knight, 2019), and the Catahoula Formation species also apparently preferred a similar environment (see Discussion below).

Carcharhinus elongatus (Leriche, 1910)
Fig. 8I–P, T–V

Sphyrna elongata Leriche, 1910: 300–301.

Material examined

UNITED STATES OF AMERICA – **Mississippi** • 291 isolated teeth; Catahoula Formation; MMNS VP-6627 (92 teeth), SC2013.28.210, SC2013.28.211 (Fig. 8I–J), SC2013.28.212 to 28.214, SC2013.28.215 (Fig. 8K–L), SC2013.28.216 to 28.218, SC2013.28.219 (6 teeth), SC2013.28.220 (2 teeth), SC2013.28.221 (9 teeth), SC2013.28.222 (7 teeth), SC2013.28.223 to 28.234, SC2013.28.235 (Fig. 8M–N), SC2013.28.236 to 28.238, SC2013.28.239 (4 teeth), SC2013.28.240 (4 teeth), SC2013.28.241 (6 teeth), SC2013.28.242 (8 teeth), SC2013.28.243, SC2013.28.244 (Fig. 8T–V), SC2013.28.245 to 28.247, SC2013.28.248 (16 teeth), SC2013.28.249 (7 teeth), SC2013.28.250, SC2013.28.251 (Fig. 8O–P), SC2013.28.252, SC2013.28.253, SC2013.28.254 (4 teeth), SC2013.28.255 (7 teeth), SC2013.28.256 to 28.259, SC2013.28.260 (4 teeth), SC2013.28.261 (7 teeth), SC2013.28.262 (61 teeth), SC2013.28.263 (9 teeth).

Description

Two tooth morphologies are present, the most common of which has a broadly triangular main cusp that is flanked by mesial and distal heels (Fig. 8I–P). These teeth are typically mesio-distally wider than tall (apico-basally), measuring up to 15 mm and 12 mm, respectively, in these dimensions. However, some specimens are taller than wide. The cusp is broadly triangular, although width differs among the teeth, and it may be vertical but is more often distally inclined. The labial face is virtually flat, whereas the lingual face is convex, and enameloid on both sides is smooth. The mesial and distal cutting edges are smooth and complete along the cusp. The mesial and distal shoulders vary in length, even between the mesial and distal sides of a tooth, and they may be horizontal or oblique. The cutting edges of the shoulders can be serrated, although serration density and size vary, even along a single cutting edge. The shoulders are separated from the main cusp by a tiny notch. The root is low, particularly in labial view, and strongly bilobate. The root lobes are elongated, highly divergent, and separated by a shallow but broad U-shaped or V-shaped interlobe area. The lobes can be described as sub-rectangular with their distal ends ranging from rounded to pointed. The thickened lingual root face is bisected by a wide but shallow nutritive groove that forms a basal notch on some specimens.

The second morphology includes roughly T-shaped teeth. The crowns of these teeth bear a cusp that is somewhat tall and rather narrow, but cusp height varies, and it may be vertical or distally inclined to varying degrees. The cutting edges of these teeth are straight and smooth and extend onto lateral shoulders (Fig. 8T). These shoulders may be oblique or perpendicular to cusp height. The root has rather short lobes that are very widely diverging (Fig. 8U), with the basal margin being flat to only weakly concave. The lingual nutritive groove is thin and long.

Remarks

Monognathic, dignathic, and ontogenetic heterodonty are represented in our sample of teeth. Upper anterior teeth are taller than wide and symmetrical (or nearly so), whereas lateral teeth are wider than

tall and have a distally inclined cusp. Inclination of the main cusp increases towards the jaw commissure and tooth height correspondingly decreases (compare Fig. 8I–J, K–L and M–N). Upper teeth have a much broader cusp and larger root compared to those in lower files (compare Fig. 8K to U). Lower teeth lack or bear only very weak serrations on the lateral shoulders, and the basal root margin is straighter (compare Fig 8T to O). Ontogenetic heterodonty is expressed as a difference in stoutness among the different tooth size classes, with small teeth being relatively gracile (presumed juveniles) compared to the large, robust specimens (presumed adults). Serration size and density on the lateral shoulders is also variable and may be virtually absent (Fig. 8O), weakly developed (Fig. 8M), or strongly developed (Fig. 8I). However, this does not appear to reflect monognathic heterodonty or ontogeny. Rather, it is variation among individual teeth in each file, as a particular serration size or density (or lack thereof) is not indicative of any specific jaw position, and small teeth (juveniles) exhibit the same variation as large (adult) teeth.

The teeth described above fall within the size range of *Carcharhinus elongatus* (Leriche, 1910) and *C. gibbesii* (Woodward, 1889) (see Reinecke *et al.* 2014), species that have been reported from the Oligocene of North America and Europe (Reinecke *et al.* 2001, 2005; Cicimurri & Knight 2009; Cicimurri *et al.* 2022). However, the teeth of *C. gibbesii* appear to have coarse and uniformly serrated lateral heels, whereas the heels of *C. elongatus* are irregularly serrated (similar to the condition in *Physogaleus*) or even smooth. We identify the Catahoula Formation teeth as *C. elongatus* because the serrations are much weaker (or altogether absent) compared to *C. gibbesii*. Reinecke *et al.* (2014) indicated that some Oligocene teeth represent a transitional species between *C. elongatus* and *C. gibbesii*, although this intermediate species has yet to be determined. Müller (1999) reported *C. elongatus* from the Oligocene Old Church Formation of Virginia, but we concur with Cicimurri *et al.* (2022) that the coarse serration pattern of the teeth he illustrated (pl. 6 figs 5–9) is more like that of *C. gibbesii*. Müller (1999) also reported *C. elongatus* and *C. gibbesii* from the Ashley Formation of South Carolina, but he did not illustrate any specimens, and we could not verify their identity.

Family Triakidae Gray, 1851

Genus ***Galeorhinus*** de Blainville, 1816

Type species

Squalus galeus Linnaeus, 1758, Extant.

Galeorhinus sp.
Fig. 9A–B

Material examined

UNITED STATES OF AMERICA – **Mississippi •** 1 isolated tooth; Catahoula Formation; SC2013.28.114 (Fig. 9A–B).

Description

SC2013.28.114 is an incomplete tooth having a crown width measuring 2.5 mm and crown height of approximately 1.2 mm. The mesial edge of each tooth is smooth, elongated, and convex basally but otherwise straight. This edge is strongly inclined distally, and a smooth cutting edge is only obvious along its lower one-half. The distal cutting edge is short and lingually inclined, and it intersects apically with the mesial margin to form a small distally inclined cusp. A short, oblique distal heel bears a series of three denticles that decrease in size basally (Fig. 9B). The labial face is weakly convex and

appears to have been thickened at the base (Fig. 9A). The lingual face is more strongly convex. Crown ornamentation is not obvious, but the specimen is ablated. The root is not preserved.

Remarks

We tentatively identify specimen SC2013.28.114 (Fig. 9A–B) as *Galeorhinus* due to its small size and apparently thickened labial crown foot (Fig. 9A). The tooth differs from superficially similar teeth of Sphyrnidae (see below) and other Carcharhinidae from the Jones Branch locality by having a high and oblique distal heel that bears numerous well-defined denticles. It also differs from *Carcharhinus elongatus* and *Physogaleus* spp. by being unserrated and lacking denticles on the mesial cutting edge. Additionally, the labial crown foot of *Carcharhinus* spp. and *Physogaleus* spp. is flat and not thickened to overhang the root. The unserrated cutting edges easily separate the two teeth from those of *Galeocerdo* (see below).

Ebersole *et al.* (2019) identified three Eocene *Galeorhinus* species from Gulf Coastal Plain deposits in Alabama, namely *Galeorhinus* aff. *G. duchaussoisi* Adnet & Cappetta, 2008, *G. louisi* Adnet & Cappetta, 2008, and *G. ypresiensis* (Casier, 1946). However, none of these species are known to persist into the Oligocene (Adnet & Cappetta 2008). The Catahoula Formation specimens are similar to a lateral tooth identified by Cicimurri & Knight (2009) from the Chattian Chandler Bridge Formation of South Carolina, and Müller (1999) noted a specimen from the Rupelian Old Church Formation of Virginia that is comparable to SC2013.28.114. Reinecke *et al.* (2005) and Haye *et al.* (2008) documented several Oligocene *Galeorhinus* sp. from the late Oligocene (late Chattian) of Germany, and the Catahoula

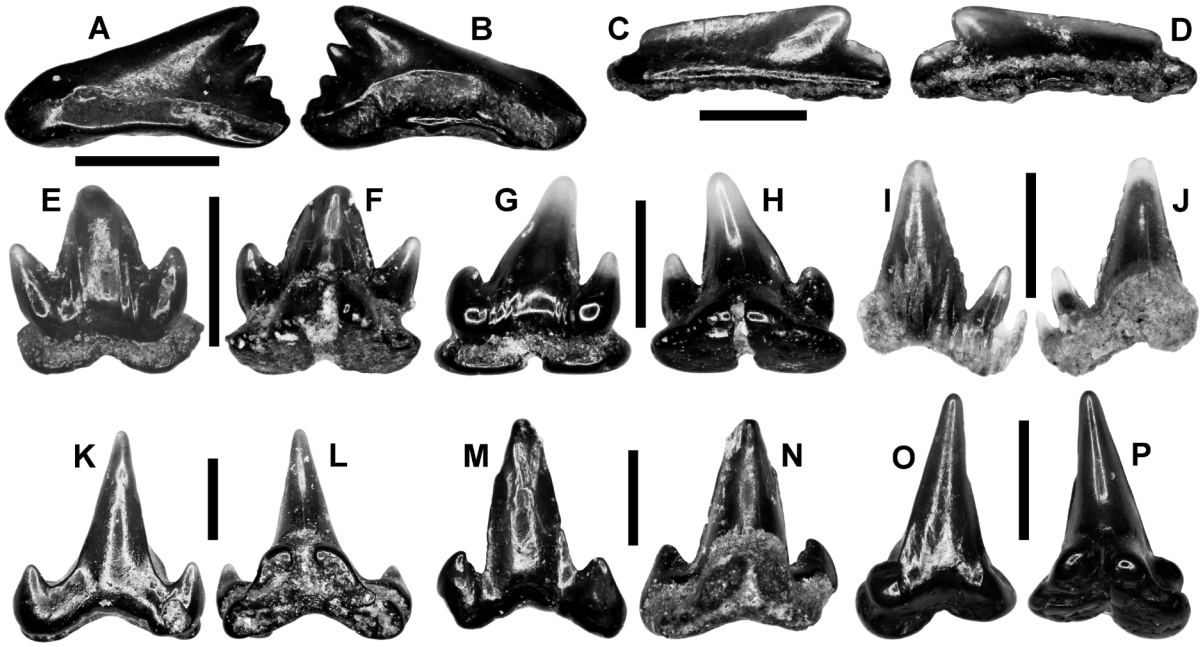

Fig. 9. *Galeorhinus* sp. (A–B), Euselachii fam., gen. et sp. indet. (C–D), *Pachyscyllium distans* (Probst, 1879) (E–J), and *Pachyscyllium* sp. (K–P), teeth. **A–B**. SC2013.28.114, *Galeorhinus* sp., lateral tooth. **A**. Labial view. **B**. Lingual view. **C–D**. SC2013.28.115, Euselachii fam., gen. et sp. indet., posterior tooth. **C.** Labial view. **D**. Lingual view. **E–F**. SC2013.28.117, *Pachyscyllium distans*, anterior tooth. **E**. Labial view. **F**. Lingual view. **G–H**. SC2013.28.116, *P. distans*, lateral tooth. **G**. Labial view. **H**. Lingual view. **I–J**. SC2013.28.125, *P. distans*, tooth. **I**. Labial view. **J**. Lingual view. **K–L**. SC2013.28.126, *Pachyscyllium* sp., anterolateral tooth. **K**. Labial view. **L**. Lingual view. **M–N**. SC2013.28.127, *Pachyscyllium* sp., anterior tooth. **M**. Labial view. **N**. Lingual view. **O–P**. MMNS VP-8796, *Pachyscyllium* sp., lateral tooth. **O**. Labial view. **P**. Lingual view. Scale bars = 1 mm.

Formation material differs from some of those specimens by the lack of labial ornamentation (Reinecke *et al.* 2005). Unfortunately, the poor preservation of the singular Catahoula Formation specimen available to us inhibits our ability to effectively identify the taxon to species.

Family Scyliorhinidae Gill, 1862

Genus ***Pachyscyllium*** Reinecke *et al.*, 2005

Type species

Pachyscyllium albigensis Reinecke *et al.*, 2005, Rupelian, Mainz Basin, western Germany.

Pachyscyllium distans (Probst, 1879)
Fig. 9E–J

Scyllium distans Probst, 1879: 170–171.

Material examined

UNITED STATES OF AMERICA – **Mississippi** • 11 isolated teeth; Catahoula Formation; MMNS VP-12048, SC2013.28.116 (Fig. 9G–H), SC2013.28.117 (Fig. 9E–F), SC2013.28.118 to 28.124, SC2013.28.125 (Fig. 9I–J).

Description

Very small teeth measuring up to 2 mm in total height and 1.5 mm in crown width. The crown consists of a main cusp that is typically flanked by a single pair of lateral cusplets. The main cusp ranges from narrow, tall, and vertical to broad, low, and distally inclined (depending on jaw position). The labial face of the main cusp is convex, and the crown foot is thickened such that it weakly overhangs the root. Additionally, the crown foot may be straight or weakly concave. The lingual face of the main cusp and lateral cusplets is also convex. The labial face bears vertical ridges that may extend to one-half the crown height (Fig. 9I); these ridges may occur across the entire labial face or may be restricted to the region below the lateral cusplets. The lingual face is generally smooth, but faint ridges may occur on the lateral cusplets. The lateral cusplets may be needle-like and extend up to one-third of the total crown height, or they may be low and broadly triangular. Smooth mesial and distal cutting edges extend along the main cusp and lateral cusplets. The bilobate root appears higher lingually than is apparent in labial view. Root lobes are very short and divergent, separated by a shallow and narrow interlobe area. The root is divided into very short, sub-triangular to teardrop-shaped lobes by an elongated nutritive groove (Fig. 9F, H).

Remarks

The available sample indicates that monognathic heterodonty was developed in this taxon. Anterior teeth have a rather narrow, tall, sharply pointed main cusp, and lateral cusplets are also tall and needle-like. Teeth believed to be from lateral files have a comparatively lower and broader main cusp that is distally inclined, and lateral cusplets are also shorter and broader (Fig. 9G–H). The main cusp appears to become more inclined the closer a tooth was located to the commissure. Most of the teeth in our sample exhibit one pair of lateral cusplets, but one specimen exhibits two cusplets on the mesial side (Fig. 9I–J).

These diminutive teeth will not be confused with most other similarly shaped shark teeth found in the Catahoula Formation. The lone exception is another *Pachyscyllium* morphotype (see below), which differs from *P. distans* in several ways, the most conspicuous being the absence of crown ornamentation. Case (1980) documented *P. distans* from the Oligocene River Bend Formation of North Carolina. The

species was apparently geographically widespread and temporally long-ranging, occurring in strata of Oligocene to Pliocene age in Europe (Reinecke *et al.* 2001, 2005, 2011, 2014; Collareta *et al.* 2020; Villafaña *et al.* 2020; Szabó *et al.* 2022).

Pachyscyllium sp.
Fig. 9K–P

Material examined

UNITED STATES OF AMERICA – **Mississippi •** 19 isolated teeth; Catahoula Formation; MMNS VP-8746 (6 teeth), MMNS VP-8796 (Fig. 9O–P), SC2013.28.126 (Fig. 9K–L), SC2013.28.127 (Fig. 9M–N), SC2013.28.128 to 28.131, SC2013.28.132 (2 teeth), SC2013.28.133 (4 teeth).

Description

All but one of the specimens are broken, but these are morphologically comparable to the complete tooth, SC2013.28.126 (Fig. 9K–L). This specimen measures 2.5 mm in crown width and just under 3 mm in total height. The crown consists of a main cusp that is slightly distally inclined, and a single pair of large lateral cusplets. The main cusp is tall, triangular, rather narrow, sharply pointed, and its labial and lingual faces are convex. The lateral cusplets are broad, short, pointed, located very low on the crown, and well separated from the main cusp (Fig. 9K). Smooth cutting edges extend along the main cusp and lateral cusplets. In apical view, the lateral cusplets appear to be located anterior to the labial face of the main cusp. The labial crown foot is thickened, concave, and conspicuously overhangs the root. The crown enameloid lacks ornamentation. The root is low (in labial view) and bilobate with lobes extending laterally just beyond the crown margin. The root lobes are very widely diverging and separated by a broad and shallow U-shaped interlobe area. The lingual attachment surface is flat and rather thin on the lobes, but a large medial boss is bisected by a thin, deep nutritive groove (Fig. 9L).

Remarks

As noted above, the additional incomplete teeth in the sample are morphologically similar to the complete tooth represented by SC2013.28.126. However, we did note some slight differences amongst the teeth, namely the width, robustness, and inclination of the main cusp, as well as the height of the lateral cusplets. Several specimens have a vertical main cusp and symmetrical crowns (Fig. 9M–N), whereas those like SC2013.28.126 have a slightly distally inclined cusp (Fig. 9K, O). We believe that these differences represent monognathic heterodonty within the same taxon, where anterior teeth are symmetrical and lateral teeth have distally inclined main cusps. Variations in tooth robustness (i.e., some specimens are more gracile than others) could reflect dignathic, ontogenetic, or even gynandric heterodonty, the latter of which has been documented in other scyliorhinid sharks (Soares & de Carvalho 2019). Cicimurri *et al.* (2022) reported an incomplete *Pachyscyllium* sp. specimen from the Rupelian (NP24) Ashley Formation of South Carolina, but that tooth exhibits short longitudinal ridges that are not present on these Catahoula Formation specimens. Ebersole *et al.* (2021) reported a single *Pachyscyllium* sp. tooth from the Rupelian (NP23) Glendon Limestone Member of the Byram Formation of Alabama, and Ebersole & Cicimurri (in press) also reported a similar *Pachyscyllium* sp. tooth from the Rupelian Rosefield Formation in Louisiana. Although these teeth are comparable to those described above, additional material from these lithostratigraphic units are needed to ascertain whether the morphologies are conspecific.

The gross morphology of the Catahoula Formation teeth is comparable to that of various Oligo-Miocene *Pachyscyllium* species that have been described, but there are some apparent differences. The Catahoula Formation *Pachyscyllium* sp. teeth have smooth enameloid, whereas those of *P. distans* possess distinct

vertical ridges on the lower portion of the labial face and often on the lingual face of the lateral cusplets. The Catahoula Formation specimens appear to differ from those of *P. dachiardii* (Lawley, 1876) by having consistently shorter lateral cusplets, and from *P. albigensis* Reinecke *et al.*, 2005 by their larger overall size (Reinecke *et al.* 2005; Reinecke & Radwański 2015). Although there is some morphological overlap with *P. braaschi* Reinecke *et al.*, 2005, the few Catahoula Formation specimens available to us appear to have shorter and less divergent lateral cusplets (Reinecke *et al.* 2005, 2014; Haye *et al.* 2008).

Family Sphyrnidae Bonaparte, 1840

Genus ***Sphyrna*** Rafinesque, 1810

Type species

Squalus zygaena Linnaeus, 1758, Extant.

"*Sphyrna*" *gracile* sp. nov.
urn:lsid:zoobank.org:act:4B859E67-6145-4422-98B6-251EB701F01E
Fig. 10

Diagnosis

Mesio-distally wide teeth consisting of a large main cusp and a distal heel. The main cusp is broadly triangular and distally inclined to varying degrees. The mesial cutting edge is straight to weakly convex on the main cusp, but it extends to the end of the mesial root lobe generally through a sloping transition at the base of the cusp. The distal cutting edge is shorter and straight to weakly convex. The distal heel is elongated, low, straight to weakly convex, and differentiated from the distal cutting edge by a shallow notch. All cutting edges are smooth. The root is bilobate with short, sub-rectangular lobes that are highly diverging. The basal margin is straight to weakly concave. The lingual root face is thick, and there is a distinctive medially located nutritive groove. These teeth differ from fossil species reported in the literature, like those of the Miocene *Sphyrna arambourgi* Cappetta, 1970, by having a wider main cusp and weakly sinuous (as opposed to straight) mesial cutting edge. Additionally, "*S.*" *gracile* sp. nov. teeth can be separated from those of both *S. arambourgi* and *S. integra* (Probst, 1878) by having an elongated and straight to weakly convex distal heel (as opposed to being rather short and occasionally cuspidate in the latter taxa). Furthermore, the lower teeth of the former taxon have an angular mesial cutting edge, whereas this edge is curved in the latter taxa. "*Sphyrna*" *gracile* teeth differ from those of the Miocene *S. laevissima* (Cope, 1867) by being less robust and by being smaller in mesio-distal width (up to 6 mm for "*S.*" *gracile* vs 1 cm for *S. laevissima*).

Etymology

The species name alludes to the small size and delicate appearance of the teeth.

Material examined

Holotype

UNITED STATES OF AMERICA – **Mississippi** • upper right lateral tooth; Catahoula Formation; SC2013.28.158 (Fig. 10O–Q).

Paratypes

UNITED STATES OF AMERICA – **Mississippi** • lower left anterior tooth; Catahoula Formation; SC2013.28.155 (Fig. 10A–C) • lower left lateral tooth; Catahoula Formation; SC2013.28.162 (Fig. 10L–N).

Other material

UNITED STATES OF AMERICA – **Mississippi** • 28 isolated teeth; Catahoula Formation; SC2013.28.154, SC2013.28.156 (Fig. 10J–K), SC2013.28.157 (Fig. 10R–S), SC2013.28.158 to 28.160, SC2013.28.161 (Fig.10T–U), SC2013.28.162, SC2013.28.163 (7 teeth), SC2013.28.164 (10 teeth), SC2013.28.912 (Fig. 10F–G), SC2013.28.913 (Fig. 10D–E), SC2013.28.914 (Fig. 10H–I).

Stratum typicum

Shelly, argillaceous sand of the Jones Branch fossil horizon, lower Catahoula Formation, Chattian Stage (horizon no longer accessible).

Locus typicus

Site MS.77.011, Jones Branch, tributary flowing into the Chickasawhay River, south of Waynesboro, Wayne County, Mississippi, USA.

Description

These small teeth measure up to 6 mm in mesio-distal width and slightly over 5 mm in overall height (apico-basal). The crown consists of a conspicuous cusp and a distal heel. The mesial cutting edge is sharp, smooth, and weakly to strongly concave. The mesial cutting edge exhibits a basal heel that may be short or elongated, poorly or conspicuously differentiated from the cusp, and oblique to nearly perpendicular to the cusp. The distal cutting edge is smooth and sharp, straight to convex, may be nearly vertical to moderately distally inclined, and is shorter than the mesial edge. The mesial and distal cutting edges intersect apically to form the cusp, which itself is rather narrow but sharply pointed. An elongated distal heel is very low, weakly convex to angular, and the edge is smooth. A conspicuous notch is located at the junction of the heel and the distal cutting edge, and the apex of the heel is located just distal to the notch. The bilobate root has elongated, widely diverging, sub-rectangular lobes with rounded ends. The

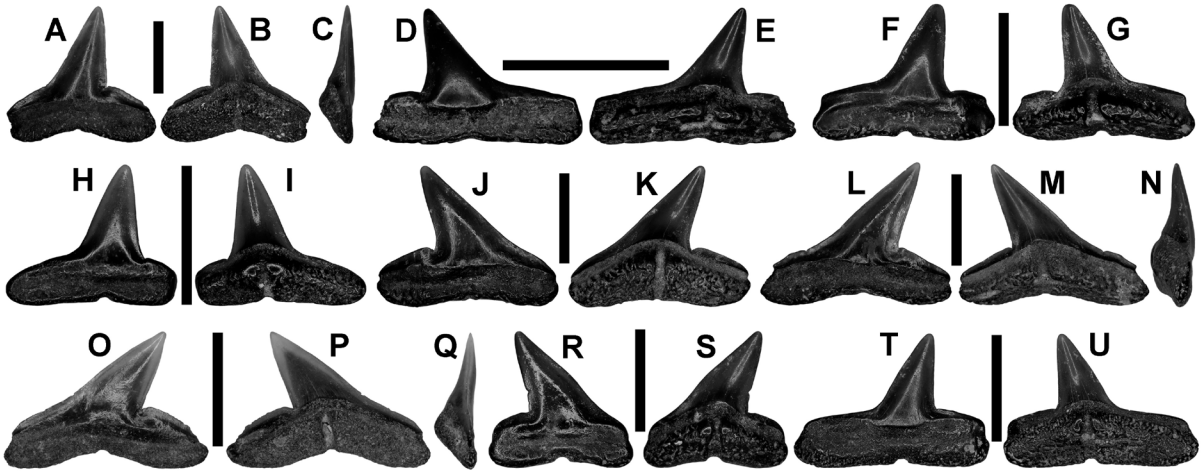

Fig. 10. "*Sphyrna*" *gracile* sp. nov., teeth. **A–C**. SC2013.28.155 (paratype), lower left anterior tooth. **A**. Labial view. **B**. Lingual view. **C**. Mesial view. **D–E**. SC2013.28.913, lower right lateral tooth. **D**. Labial view. **E**. Lingual view. **F–G**. SC2013.28.912, lower left lateral tooth. **F**. Labial view. **G**. Lingual view. **H–I**. SC2013.28.914, lower left lateral tooth. **H**. Labial view. **I**. Lingual view. **J–K**. SC2013.28.156, upper left lateral tooth. **J**. Labial view. **K**. Lingual view. **L–N**. SC2013.28.162 (paratype), lower left lateral tooth. **L**. Labial view. **M**. Lingual view. **N**. Mesial view. **O–Q**. SC2013.28.158 (holotype), upper right lateral tooth. **O**. Labial view. **P**. Lingual view. **Q**. Mesial view. **R–S**. SC2013.28.157, upper left anterior tooth. **R**. Labial view. **S**. Lingual view. **T–U**. SC2013.28.161, upper right lateral tooth. **T**. Labial view. **U**. Lingual view. Scale bars = 3 mm.

interlobe area is low and broadly U-shaped or may be absent (straight basal margin). The lingual root face is bisected by a short but deep nutritive groove.

Remarks

Although the teeth described above share morphological features that occur on teeth of extant Sphyrnidae, there are differences among the various taxa (see below). Assigning the fossils to the extant genus *Sphyrna* is problematic based on molecular divergence work by Lim *et al*. (2010), which indicates that the genera *Eusphyra* and *Sphyrna* did not diverge from their most recent common ancestor until the Early-to-Middle Miocene, four to seven million years after deposition of the Catahoula Formation fossil bed. For the purposes of this report, we follow Ebersole *et al.* (2024a) in placing the generic name *Sphyrna* within quotations, acknowledging dental similarities between the Oligocene and extant species, and taking into account divergence estimates that may result in future placement of the fossil species in a new genus.

To aid our evaluation of the Catahoula Formation sphyrnid sample, we examined the jaws of several extant *Sphyrna* species, including *S. lewini* (Griffith & Smith, 1834) (SC2001.7.1), *S. mokarran* (Rüppell, 1837) (SC2000.120.2), *S. tiburo* (Linnaeus, 1758) (SC96.77.3), and *S. zygaena* (Linnaeus, 1758) (MSC 42600). Additionally, we utilized the illustrated dentitions of *S. media* Springer, 1940 and *S. tudes* (Valenciennes, 1822) provided by Gilbert (1967: figs 14 and 19, respectively). "*Sphyrna*" *gracile* sp. nov. teeth are much smaller in overall size and less stout compared to the teeth of presumed extant relatives *Sphyrna mokarran* and *S. zygaena*, which are also serrated to varying degrees. The upper teeth of "*Sphyrna*" *gracile* differ from those of *S. lewini* by having a less elongated mesial crown foot and a less convex medial portion of the mesial cutting edge. Additionally, the mesial cutting edge on the lower teeth of the former taxon has an angular appearance, whereas this edge on the lower teeth of the latter taxon appears strongly curved. The upper teeth of extant *S. media* have more convex distal cutting edges, a more medially convex portion of the mesial edge, and a shorter distal heel compared to "*Sphyrna*" *gracile*. Furthermore, the lower teeth of the former taxon have a narrower, taller and strongly curved cusp compared to the lower teeth of the latter taxon. and the distal heel of the former taxon is comparatively shorter than that of the latter taxon. The upper teeth of "*Sphyrna*" *gracile* have a somewhat wider and more distally inclined main cusp compared to the upper teeth of extant *S. tudes*. The lower teeth of the latter taxon are also narrower and more erect compared to those of the former taxon.

Numerous Neogene fossil species have been assigned to *Sphyrna*, but our evaluation of the published illustrations of the type or referred specimens leads us to conclude that most of them do not belong to Sphyrnidae, let alone *Sphyrna*. For example, teeth identified as *S. magna* Cope, 1867, *S. americana* Leriche, 1942, and *S. lata* Agassiz, 1843, among many others, are more appropriately identified as *Carcharhinus*. Other examples include *S. gilmorei* Leriche, 1942, which has been placed in *Negaprion* (i.e., Ebersole *et al*. 2019), and *S. tortillis* White, 1926 should be identified as *Physogaleus*.

Of the remaining Neogene species, *Sphyrna arambourgi* Cappetta, 1970, *S. integra* (Probst, 1878), and *S. laevissima* (Cope, 1867) appear to be correctly identified as sphyrnids. The Lower Miocene *S. integra* is based on one complete tooth and one partial tooth (see Pollerspöck & Unger 2023: pl. 11 figs 3–4), but Cappetta (1970: pl. 19 figs 1–18) utilized a larger suite of Middle Miocene specimens to diagnose *S. arambourgi*. Although the complete *S. integra* specimen shown by Pollerspock & Unger (2023: pl. 11 fig. 3) appears to be a lower tooth with a clear separation of a mesial heel compared to the contiguous convex mesial edge on *S. arambourgi* teeth, the latter taxon was synonymized with *S. integra* (Barthelt *et al.* 1991). The teeth of "*Sphyrna*" *gracile* sp. nov. are like those of *S. arambourgi* and *S. integra*, as illustrated by Cappetta (1970: pl. 19 figs 1–18) and Reinecke *et al.* (2011: pls 81–85), but there are differences between the Catahoula material and the two European taxa. For one, the main cusp of *S. arambourgi* is somewhat narrower than that of "*Sphyrna*" *gracile*, particularly on lower teeth.

Additionally, the mesial cutting edge on the upper teeth of *S. arambourgi* is straighter than that on the Catahoula Formation teeth, which are weakly sinuous. Furthermore, the distal heel in *S. arambourgi* and *S. integra* is short and sometimes weakly cuspidate, whereas in "*Sphyrna*" *gracile* sp. nov. the distal heel is elongated and straight to weakly convex. Additionally, the mesial cutting edge of "*Sphyrna*" *gracile* lower teeth has an angular appearance, whereas this edge is curved on comparable teeth of *S. arambourgi*/*S. integra* (albeit sharply curved on the latter). Purdy *et al*. (2001) indicated that the *S. arambourgi* morphology was similar to Mio-Pliocene teeth they referred to *S. media*, but they did not specifically synonymize the former with the latter.

Unfortunately, Cope (1867) did not include illustrations of teeth when he named the *Galeocerdo laevissimus* morphology, but Leriche (1942) later assigned the morphology to *Sphyrna*. Purdy *et al*. (2001: fig. 60) figured Cope's *G. laevissimus* type suite (Cope 1867), which shows that these teeth are much larger in overall size (greater than 1 cm in mesio-distal width) and much more robust compared to those of *"Sphyrna*" *gracile* sp. nov. Additionally, the very wide main cusp of the former species has very convex mesial and distal cutting edges. The *S. laevissima* morphology is discussed further below.

Cicimurri & Knight (2009) reported a similar small and gracile hammerhead-like tooth morphology from the Chandler Bridge Formation (Chattian) of South Carolina, which they assigned to *Sphyrna* cf. *media* (following the observations of Purdy *et al.* 2001). Cicimurri *et al.* (2022) later identified comparable teeth from the Ashley Formation (Rupelian) of South Carolina simply as Sphyrnidae gen. et sp. indet. Examination of specimens from the Ashley (accession SC2007.36) and Chandler Bridge (accession SC2005.2) formations indicate that the teeth are conspecific with *"Sphyrna*" *gracile* sp. nov. Ebersole *et al.* (2024a) later described an isolated tooth as "*Sphyrna*" sp. that was derived from the Rupelian Red Bluff Clay in Alabama. This tooth has a shorter and wider main cusp and more convex mesial edge than those of *"Sphyrna*" *gracile*.

Based on our evaluation of extant *Sphyrna* spp. dentitions, monognathic and dignathic heterodonty are evident in our "*Sphyrna*" *gracile* sp. nov. sample. Teeth from anterior files are rather narrow and have a more vertically directed cusp apex (Fig. 10A–B). In contrast, lateral teeth are wider and have more distally inclined cusps (Fig. 10D–E). Additionally, in progressively more distal tooth files, cusp inclination increases but overall cusp height decreases towards the commissure (compare Fig. 10J, H, D). Dignathic heterodonty is reflected in cusp width and the nature of the mesial cutting edge. Upper teeth generally have a wider main cusp with a convex medial portion of the mesial cutting edge compared to lower teeth (i.e., Fig. 10R vs A). In addition, the elongated mesial cutting edge of upper teeth may only be slightly concave basally (Fig. 10O, L), but on lower teeth the basal one-half of the mesial edge is clearly distinguished as an elongated, roughly horizontal heel (Fig. 10G, U).

The teeth of "*Sphyrna*" *gracile* sp. nov. differ from those of superficially similar carcharhiniform genera within the Catahoula Formation, including *Hemipristis*, *Galeorhinus*, *Physogaleus*, and *Galeocerdo*, by the lack of serrations and/or denticulations on the mesial and distal cutting edges. Although upper teeth of *Carcharhinus elongatus* can be identified by the shallow notch on the mesial and distal sides of the crown, only a distal notch occurs on the teeth of "*Sphyrna*" *gracile*. Lower teeth of "*Sphyrna*" *gracile* have a conspicuously elongated mesial heel and root lobe, whereas the mesial and distal heels of *C. elongatus* lower teeth are roughly equal in length.

"*Sphyrna*" *robustum* sp. nov.
urn:lsid:zoobank.org:act:36D0CA1E-07C4-4FF9-985D-8DC88A9280EB
Fig. 11

Diagnosis

"*Sphyrna*" *robustum* sp. nov. teeth differ from those of coeval "*Sphryna*" *gracile* sp. nov. (see above) by their greater stoutness, larger overall size, lower cusp height with respect to tooth size, and differing

shapes of the mesial cutting edge. These features also serve to distinguish "*S.*" *robustum* from the extinct *S. integra* and *S. arambourgi* (see Cappetta 1970; Reinecke *et al.* 2011). Although morphologically similar to "*S.*" *robustum*, fossil *S. laevissima* teeth have a more biconvex cusp and the mesial cutting edge is conspicuously sinuous (Purdy *et al.* 2001: fig. 60). Of presumed extant descendant species, the teeth of *S. mokarran* and *S. zygaena* are comparable to those of "*S.*" *robustum*. However, the mesial cutting edges of the new Oligocene species are less convex and lack serrations.

Etymology

The species name alludes to the stout appearance of the teeth.

Material examined

Holotype

UNITED STATES OF AMERICA – **Mississippi** • upper right lateral tooth; Catahoula Formation; SC2013.28.171 (Fig. 11Q–S).

Paratypes

UNITED STATES OF AMERICA – **Mississippi** • lower right antero-lateral tooth; Catahoula Formation; SC2013.28.169 (Fig. 11J–L) • lower right lateral tooth; Catahoula Formation; SC2013.28.167 (Fig. 11C–E).

Other material

UNITED STATES OF AMERICA – **Mississippi** • 82 isolated teeth; Catahoula Formation; SC2013.28.165 (22 teeth), SC2013.28.166 (Fig. 11A–B), SC2013.28.168, SC2013.28.170 (Fig. 11F–G), SC2013.28.172 (Fig. 11M–N), SC2013.28.173 to 28.176, SC2013.28.178, SC2013.28.179, SC2013.28.180 (Fig. 11O–P), SC2013.28.181 (Fig. 11H–I), SC2013.28.182 (Fig. 11T–U), SC2013.28.183 (34 teeth), SC2013.28.184 (10 teeth), SC2013.28.915 (Fig. 11V–W), SC2013.28.916 (Fig. 11X–Y), SC2013.28.917 (Fig. 11Z–AA).

Stratum typicum

Shelly, argillaceous sand of the Jones Branch fossil horizon, lower Catahoula Formation, Chattian Stage (horizon no longer accessible).

Locus typicus

Site MS.77.011, Jones Branch, tributary flowing into the Chickasawhay River, south of Waynesboro, Wayne County, Mississippi, USA.

Description

The teeth are mesio-distally wider than high (apico-basally) in all jaw positions available, with specimens measuring up to 12 mm in width but only a maximum of 8 mm in height. All teeth consist of a large cusp and a distal heel. The mesial cutting edge can be straight, weakly sinuous, or concave, but it is always smooth. On teeth with a sinuous cutting edge, the basal portion is concave, and the apical portion is convex. The mesial edge of other teeth is uniformly concave, and the cusp apex is more vertically directed. The distal cutting edge is much shorter than the mesial edge but is always smooth. This edge is most often straight but may be weakly convex, and its orientation may be vertical or distally inclined. The distal heel is low, elongated, and usually oblique, but may be horizontal. The cutting edge on the distal heel is smooth and varies in convexity. This heel is usually separated from the distal cutting edge by an indistinct notch. The root is bilobate, with the elongated lobes being widely divergent and their lateral ends rounded. The basal margin of the root varies from slightly concave to virtually straight. A thickened lingual root face is bisected by a deep nutritive groove.

Remarks

The teeth of "*Sphyrna*" *robustum* sp. nov. differ from those of superficially similar carcharhiniform genera within the Catahoula Formation, including *Hemipristis*, *Galeorhinus*, *Physogaleus*, and *Galeocerdo*, by the lack of serrations and/or denticulations on the mesial and distal cutting edges. Although the upper teeth of *Carcharhinus elongatus* have mesial and distal shoulders that may be weakly to moderately serrated, these heels are distinctly separated from the main cusp by a shallow notch (only a distal notch occurs in "*Sphyrna*" *robustum*). With respect to *Rhizoprionodon*, the teeth of "*Sphyrna*" *robustum* achieve a much larger overall size and have a broader cusp.

"*Sphyrna*" *robustum* sp. nov. teeth differ from those of the coeval "*Sphyrna*" *gracile* sp. nov. by their greater stoutness, larger overall size, lower cusp height with respect to tooth size, and differing shapes of the mesial cutting edge. Most of these features also serve to distinguish the species from presumed extant relatives, including *Sphyrna lewini* (SC2001.7.1), *S. media* (see Gilbert 1967), and *S. tudes* (see Gilbert 1967). The teeth of "*Sphyrna*" *robustum* bear similarities to those in the jaws of extant *Sphyrna mokarran* (SC2000.120.2) and *S. zygaena* (MSC 42600) that we examined, but on the Oligocene specimens the mesial cutting edge of lower teeth is more concave than it is on upper teeth, and the cutting edges are completely smooth on all specimens.

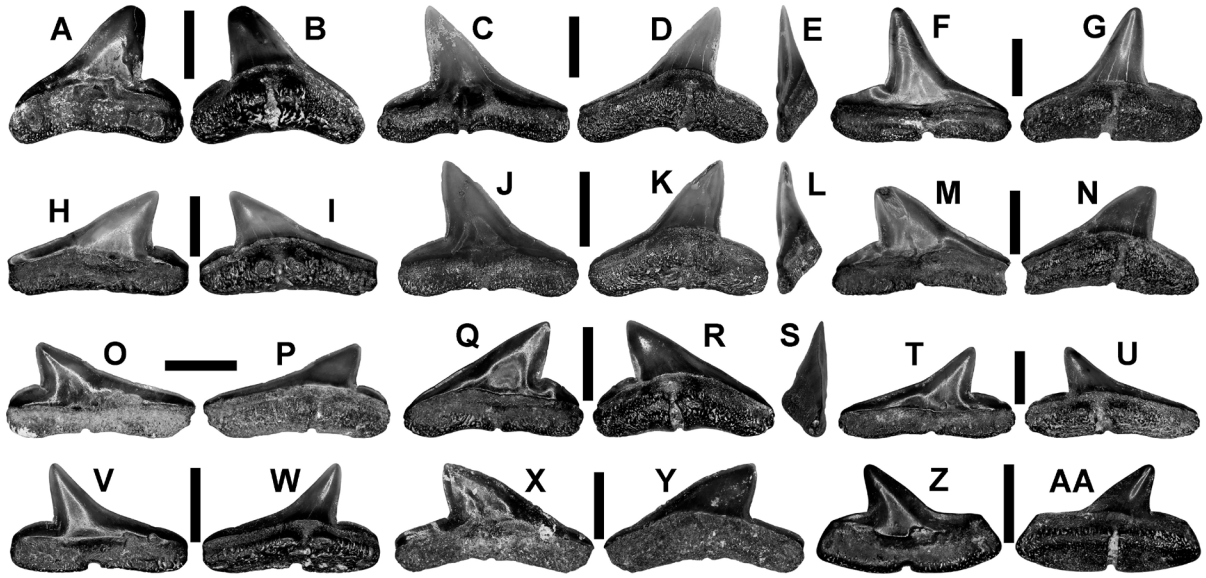

Fig. 11. "*Sphyrna*" *robustum* sp. nov., teeth. **A–B**. SC2013.28.166, upper right anterior tooth. **A**. Labial view. **B**. Lingual view. **C–E**. SC2013.28.167 (paratype), lower right lateral tooth. **C**. Labial view. **D**. Lingual view. **E**. Mesial view. **F–G**. SC2013.28.170, lower right anterior tooth. **F**. Labial view. **G**. Lingual view. **H–I**. SC2013.28.181, upper right lateral tooth. **H**. Labial view. **I**. Lingual view. **J–L**. SC2013.28.169, lower right antero-lateral tooth (paratype). **J**. Labial view. **K**. Lingual view. **L**. Mesial view. **M–N**. SC2013.28.172, upper left lateral tooth. **M**. Labial view. **N**. Lingual view. **O–P**. SC2013.28.180, upper left postero-lateral tooth. **O**. Labial view. **P**. Lingual view. **Q–S**. SC2013.28.171 (holotype), upper right lateral tooth. **Q**. Labial view. **R**. Lingual view. **S**. Mesial view. **T–U**. SC2013.28.182, lower left lateral tooth. **T**. Labial view. **U**. Lingual view. **V–W**. SC2013.28.915, lower right lateral tooth. **V**. Labial view. **W**. Lingual view. **X–Y**. SC2013.28.916, upper left lateral tooth. **X**. Labial view. **Y**. Lingual view. **Z–AA**. SC2013.28.917, lower right postero-lateral tooth. **Z**. Labial view. **AA**. Lingual view. Scale bars = 3 mm.

The Catahoula Formation "*Sphyrna*" *robustum* sp. nov. teeth are comparable to the material that Cope (1867) originally named as *Galeocerdo laevissimus* from the Miocene of Maryland. Leriche (1942) later illustrated its morphology and placed it within *Sphyrna* (i.e., *S. laevissima*). Purdy *et al.* (2001: fig. 60) figured all the teeth within Cope's *G. laevissimus* type suite and synonymized the taxon with extant *S. zygaena*, citing similarities in gross morphology. Although Cope (1867) specifically stated that the cutting edges of the teeth he examined were smooth, Purdy *et al*. (2001) noted that tooth serrations on fossil specimens became more prominent from the Miocene to the Pliocene, indicating phyletic change within the taxon. However, Reinecke *et al.* (2011) later provided quantitative data separating the *laevissima* morphology from that of *S. zygaena*. In any case, the "*Sphyrna*" *robustum* sp. nov. teeth differ from both *S. laevissima* and *S. zygaena* by having narrower cusps and much less convex cutting edges that are completely smooth. Ebersole *et al*. (2024a) reported an isolated tooth derived from the Rupelian Red Bluff Clay in Alabama that they conservatively assigned to "*Sphyrna*" sp.

Our evaluation of the dentitions of *Sphyrna mokarran* (SC2000.120.2) and *S. zygaena* (MSC 42600) provides support for our conclusion that monognathic and dignathic heterodonty was developed in the Catahoula Formation taxon. Anterior teeth have a rather narrow (mesio-distal) crown and somewhat erect cusp (Fig. 11A), whereas teeth from more lateral positions are wider and have a more distally inclined cusp (Fig. 11Q). The degree of distal inclination appears to have increased towards the commissure, and at the same time overall tooth height decreased (Fig. 11O). Dignathic heterodonty is reflected in the narrowness of the tooth cusp, with upper teeth having a wider cusp (Fig. 11X) compared to lower teeth (Fig. 11C). The variations in tooth shape and development of monognathic and dignathic heterodonty would seem to provide a clear distinction between "*Sphyrna*" *robustum* sp. nov. and "*S*." *gracile* sp. nov. However, we also note that robust and gracile *Sphyrna* or *Sphyrna*-like tooth morphologies have consistently been documented together within Oligo-Miocene strata. For example, following Purdy *et al*. (2001), Cicimurri & Knight (2009) reported teeth of *Sphyrna* cf. *media* (small, narrow-cusped) and *S. zygaena* (large, broad-cusped) from the Chattian Chandler Bridge Formation of South Carolina. Later, Cicimurri *et al.* (2022) documented a small, narrow-cusped and a larger, broad-cusped *Sphyrna*-like morphology for teeth from the Ashley Formation (Rupelian) of South Carolina that they simply referred to Sphyrnidae gen. et sp. indet. based on the work of Lim *et al.* (2010) (see also Cappetta 1970; Purdy *et al.* 2001; Carrillo-Briceño *et al.* 2016, 2019). Although these morphologies have been treated as separate taxa (including herein), it could be interpreted that these morphologies actually represent other forms of heterodonty within a single taxon.

As part of our analysis of these teeth, we considered the possibility that the "*Sphyrna*" *gracile* sp. nov. (small, narrow-cusped) morphology represents ontogenetic and/or gynandric heterodonty within *S. robustum* sp. nov. With respect to ontogenetic heterodonty, studies have demonstrated dietary shifts in extant *Sphyrna* spp. from juvenile to adult growth stages (i.e., Gonzalez-Pestana *et al.* 2017). However, little has been said about the changes, if any, in tooth shape during that shift. Mello & Brito (2013) stated that ontogenetic heterodonty was "weak among sphyrnids" (p. 467). These authors examined the embryonic teeth of *Sphyrna tiburo* (Linnaeus, 1758), *S. tudes* (Valenciennes, 1822), and *Eusphyra blochii* (Cuvier, 1816) and found that there is an ontogenetic change in the anterior tooth files of these taxa, but that lateral and posterior tooth files remain stable. Purdy *et al*. (2001) noted that the teeth of juvenile/young adult *S. zygaena* have smooth cutting edges, whereas serrations occur on the teeth of "large" individuals. This latter form of ontogenetic heterodonty is comparable to that documented in *Rhizoprionodon terraenovae*, where tooth shape remains relatively constant from birth to adulthood, but serrations develop on the teeth as the shark matures (Ebersole *et al*. 2023).

We examined the jaws of a juvenile and an adult *Sphyrna lewini* to determine whether ontogenetic heterodonty occurs in this taxon. We found that tooth size in the upper files increases with age, but a more conspicuous change is the orientation of the main cusp. For example, the fourth upper anterior

tooth of a juvenile *S. lewini* (MSC 50182) measures 6 mm in width and has a cusp that is 4 mm high and 3 mm wide, whereas the same adult tooth in MSC 42605 is 9 mm wide with a cusp that is 5 mm high and 4 mm wide. More telling, the distal cusp inclination of the juvenile tooth is 50° and on the adult tooth it is 63°. These same changes are true for the seventh upper tooth file, with the tooth width of the juvenile measuring 7.5 mm, cusp height 4 mm, cusp width 3.5 mm, and cusp inclination 44°. In contrast, the same adult tooth is 11 mm wide with a cusp measuring 5 mm high and 4 mm wide, and cusp inclination is 58°. Additionally, teeth in the first upper file of both the juvenile and adult dentitions are comparable (roughly symmetrical with a vertical cusp and well-differentiated lateral heels), but the juvenile second tooth is more similar to those of the succeeding files (distally inclined). In the adult dentition, the upper second tooth is comparable to the tooth in the first file. Our observations show that although there is an increase in tooth size from juvenile to adult growth stages, a more significant change is that the tooth cusps become much more upright into adulthood. Considering our observations of dentitions of juvenile and adult *Sphyrna lewini*, we believe that the morphological differences between "*Sphyrna*" *gracile* sp. nov. and "*S.*" *robustum* sp. nov. are too great for the morphologies to represent ontogenetic heterodonty.

Concerning gynandric heterodonty, Mello & Brito (2013) stated that "sexual heterodonty is hardly developed" in Sphyrnidae. Although differences in growth rates, age at maturity, and dietary preference between male and female hammerhead sharks have been documented (Klimley 1987), to our knowledge there is no published detailed description of gynandric variation within a given species. We herein treat the two Catahoula Formation "*Sphyrna*" spp. morphologies as taxonomically distinct because our samples do not appear to exhibit any morphological overlap in overall size, main cusp width, cutting edge shape, or presence/absence of serrations.

Family Galeocerdonidae Poey, 1875

Genus ***Galeocerdo*** Müller & Henle, 1837

Type species

Squalus cuvier Péron & Lesueur in Lesueur, 1822, Extant.

Galeocerdo platycuspidatum sp. nov.
urn:lsid:zoobank.org:act:AA878AB5-B515-4297-97B0-2902357D5FEC
Fig. 12

Diagnosis

The teeth of the new Oligocene species are distinguished by the combination of a very wide cusp with respect to crown width (cusp width comprises an average of 51% of total tooth width), a highly convex mesial cutting edge, a convex distal cutting edge, an obtuse distal angle (formed by the intersection of the distal cutting edge and distal heel), and a high distal heel (in lingual view) that is straight to only weakly concave. Of the six fossil species currently recognized, the teeth of the new taxon differ from the teeth of the Neogene *Galeocerdo aduncus* (Agassiz, 1843) by attaining larger overall sizes, having greater overall crown height and a comparatively smaller but wider cusp, and by having a more obtuse angle between the distal cutting edge and distal heel. *Galeocerdo platycuspidatum* sp. nov. teeth differ from those of the Neogene *Galeocerdo capellini* Lawley, 1876 by having a mesio-distally wider cusp, a more convex mesial cutting edge, and a distal angle of 90°. These teeth differ from the Eocene *G. clarkensis* White, 1956 by having a mesial swelling on the cutting edge (as opposed to being evenly convex), coarser serrations, and a wider distal angle (which is less than 90° in *G. clarkensis*). *Galeocerdo platycuspidatum* teeth are superficially similar to those of the Eocene *G. eaglesomei* White, 1955 but are easily separated by having compound (as opposed to simple) serrations. Finally, *Galeocerdo*

platycuspidatum teeth can be differentiated from those of the Miocene *G. mayumbensis* Dartevelle & Casier, 1943 by having a wider cusp, a (generally) more convex mesial cutting edge, and a higher and less concave distal cutting edge.

Etymology

The species name alludes to the mesio-distally wide cusp with a rather flat labial face.

Material examined

Holotype

UNITED STATES OF AMERICA – **Mississippi** • antero-lateral tooth; Catahoula Formation; MMNS VP-6622.2 (Fig. 12H–J).

Paratypes

UNITED STATES OF AMERICA – **Mississippi** • anterior tooth; Catahoula Formation; MMNS VP-6622.1 (Fig. 12A–C) • postero-lateral tooth; Catahoula Formation; MMNS VP-12050 (Fig. 12Y–AA).

Other material

UNITED STATES OF AMERICA – **Mississippi** • 43 isolated teeth; Catahoula Formation; MMNS VP-6622 (29 teeth), MMNS VP-6622.3 (Fig. 12K–L), MMNS VP-6622.4 (Fig. 12O–P), MMNS VP-6622.5 (Fig. 12W–X), MMNS VP-6622.6 (Fig. 12U–V), MMNS VP-6622.7 (Fig. 12Q–R), MMNS VP-6622.8 (Fig. 12M–N), MMNS VP-12049 (Fig. 12F–G), MMNS VP-12051 (Fig. 12S–T), MMNS VP-12052 (Fig. 12D–E), SC2013.28.109 to 28.113.

Stratum typicum

Shelly, argillaceous sand of the Jones Branch fossil horizon, lower Catahoula Formation, Chattian Stage (horizon no longer accessible).

Locus typicus

Site MS.77.011, Jones Branch, tributary flowing into the Chickasawhay River, south of Waynesboro, Wayne County, Mississippi, USA.

Description

The teeth are broad-based and vary in overall height, with the largest specimens measuring up to 23 mm in mesio-distal width and 25 mm in apico-basal height. The labial crown face is virtually flat, but the lingual face is convex, and enameloid on both faces is smooth. In mesial view, the crown has a slight labial curvature. The basal one-half of the elongated mesial cutting edge can be convex (Fig. 12A), slightly concave (Fig. 12H), or nearly straight (Fig. 12F). However, the upper one-half to one-third of the mesial cutting edge is strongly convex and forms a conspicuous medial swelling (Figs 12O). This cutting edge is serrated, and the serrations are typically very coarse along the lower three-quarters of the cutting edges but become finer towards the crown apex (Fig. 12K). The distal cutting edge is much shorter, weakly convex but may be straight, usually lingually inclined but may be vertical, and serrated. The distal edge serrations are of the same size as or slightly smaller than those occurring on the apical portion of the mesial edge. The mesial and distal cutting edges converge apically to form a very broad, pointed cusp that is distally inclined to varying degrees. Serrations of both cutting edges extend virtually to the cusp apex. An elongated distal heel forms an obtuse angle with the distal cutting edge (i.e., Fig. 12I, T). The heel is oblique and can bear more than 12 denticles, which decrease in size towards the distal margin. The cutting edges on the denticles are serrated on the apical portion and often on the basal portion (i.e., Fig. 12D). The root is bilobate with sub-rectangular lobes that vary in length and degree of

divergence. The lobes are separated by a deep V-shaped to shallow U-shaped interlobe area (compare Fig. 12G to R). Root lobe extremities may be rounded or pointed. A low lingual boss bears a long, wide, and shallow nutritive groove (Fig. 12K).

Remarks

Monognathic and ontogenetic heterodonty are evident in our sample based on jaws of extant *Galeocerdo cuvier* (Péron & Lesueur in Lesueur, 1822) that we examined (SC2000.120.10, SC2020.53.4, SC2020.53.18, MSC 42597, MSC 42624). Teeth that are slightly asymmetrical represent symphyseal files (Fig. 12D–E). Specimens that are roughly as high as wide, have a somewhat angular to very convex mesial edge, and have a vertically oriented cusp are considered anterior teeth (Fig. 12A, K). Teeth that are more mesio-distally elongated, have a more convex mesial cutting edge, and have a strongly distally directed cusp are lateral teeth (Fig. 12O, Q). Overall, crown height decreases and cusp inclination increases towards the commissure (compare Fig. 12H, O, W, U). Some of the teeth in our sample (Fig. 12O) are comparable in size to those in the jaws of a 300 kg female of *G. cuvier* represented by SC2000.120.10.

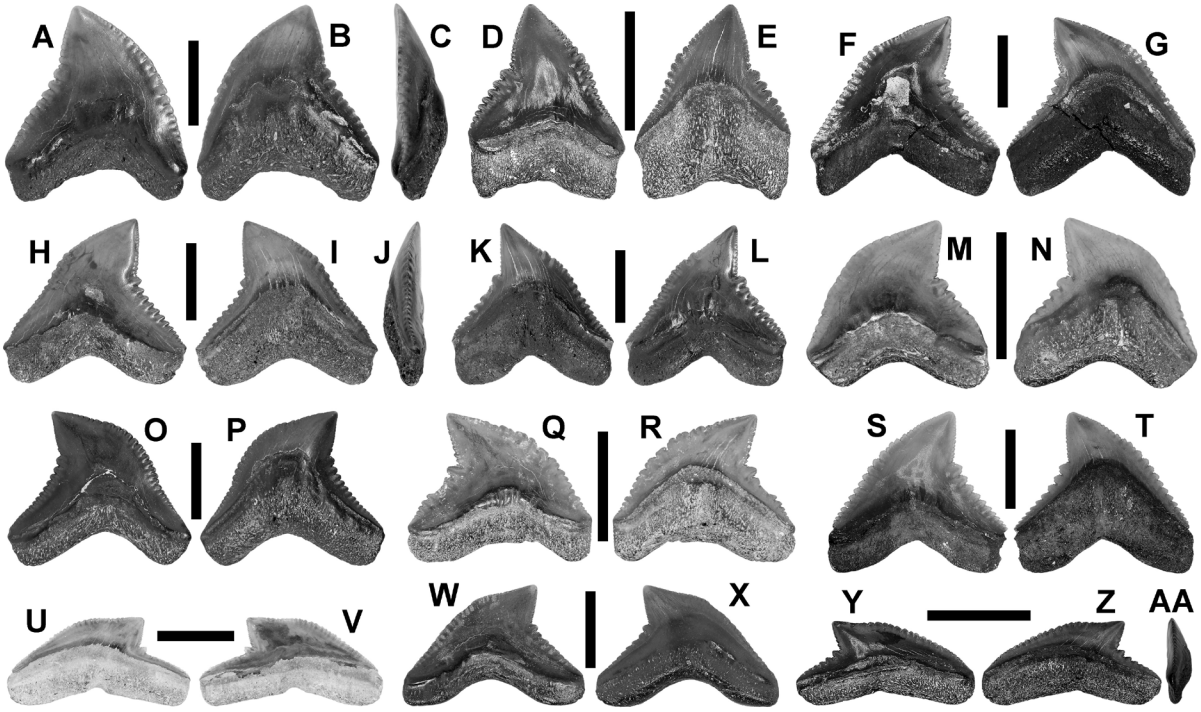

Fig. 12. *Galeocerdo platycuspidatum* sp. nov., teeth. **A–C**. MMNS VP-6622.1 (paratype), anterior tooth. **A**. Labial view. **B**. Lingual view. **C**. Mesial view. **D–E**. MMNS VP-12052, symphyseal tooth. **D**. Labial view. **E**. Lingual view. **F–G**. MMNS VP-12049, anterior tooth. **F**. Labial view. **G**. Lingual view. **H–J**. MMNS VP-6622.2 (holotype), anterior tooth. **H**. Labial view. **I**. Lingual view. **J**. Mesial view. **K–L**. MMNS VP-6622.3, anterior tooth. **K**. Labial view. **L**. Lingual view. **M–N**. MMNS VP-6622.8, anterior tooth. **M**. Labial view. **N**. Lingual view. **O–P**. MMNS VP-6622.4, lateral tooth. **O**. Labial view. **P**. Lingual view. **Q–R**. MMNS VP-6622.7, lateral tooth. **Q**. Labial view. **R**. Lingual view. **S–T**. MMNS VP-12051, anterior tooth. **S**. Labial view. **T**. Lingual view. **U–V**. MMNS VP-6622.6, posterior tooth. **U**. Labial view. **V**. Lingual view. **W–X**. MMNS VP-6622.5, postero-lateral tooth. **W**. Labial view. **X**. Lingual view. **Y–AA**. MMNS VP-12050 (paratype), posterior tooth. **Y**. Labial view. **Z**. Lingual view. **AA**. Mesial view. Scale bars = 1 cm.

Ontogenetic heterodonty is not only expressed as a difference in overall size among the teeth in our sample, but larger teeth of presumed adults have coarser serrations on the mesial cutting edge and more denticles on the distal heel compared to smaller (juvenile) teeth. Additionally, compound serrations are better developed on large teeth, with additional serrae occurring on the apical and basal edges of a serration, as opposed to only on the basal side on small teeth. A similar phenomenon was observed on the distal heel, where denticles of larger teeth bear serrae on the apical and basal edges of a denticle, but serrations are only on one edge of denticles on the smaller teeth. *Galeocerdo* teeth in the Catahoula Formation are characterized by the combination of coarse compound serrations on the mesial and distal cutting edges and a denticulated (with serrations) distal heel, features that are lacking on superficially similar teeth of *Physogaleus*, *Galeorhinus*, *Hemipristis*, and "*Sphyrna*" that occur in the Catahoula Formation.

We also attempted to determine whether dignathic heterodonty was developed in the Catahoula Formation *Galeocerdo*. We observed slight dignathic heterodonty in the extant *G. cuvier* jaws we examined, and "broad-toothed" (upper) and "narrow-toothed" (lower) morphologies have been attributed to extinct *G. aduncus* (Agassiz, 1835) (i.e., Türtscher *et al.* 2021). For *G. cuvier*, we found that cusp width (measured from the base of the distal edge to the opposite side on the mesial edge, parallel to the labial crown foot) did not vary between upper and equivalent lower teeth. However, cusp length (measured along the distal cutting edge) on upper teeth was 1.5 mm to 2 mm longer than their lower counterparts. With respect to the Catahoula Formation *Galeocerdo*, the cusp width and height of all teeth measured varies slightly between 9 and 11 mm, and between 6 and 7 mm, respectively, and this overlap precluded the distinction of isolated upper teeth from lower teeth. However, the medial portion of the mesial cutting edge on extant *G. cuvier* upper anterior teeth is very convex, whereas the mesial edge of lower teeth is more uniformly convex. Our Catahoula Formation sample includes similar morphologies, and we believe that teeth like those shown in Fig. 12H, O, and F are upper teeth, whereas those shown in Fig. 12A, Q, and S are lower teeth.

Six *Galeocerdo* species are recognized in the fossil record (including *G. cuvier*; Türtscher *et al.* 2021), and two of these, *G. eaglesomei* White, 1955 and *G. clarkensis* White, 1956, have been documented from Eocene strata in the Gulf Coastal Plain (Ebersole *et al.* 2019). Teeth of *G. eaglesomei* are superficially similar to those of *Galeocerdo platycuspidatum* sp. nov., but the latter have compound (as opposed to simple) serrations and a larger cusp. Although multiple authors identified other Eocene teeth from Alabama as *G. latidens* (see Tuomey 1858; Westgate 2001; Feldmann & Portell 2007; Clayton *et al.* 2013; Cappetta & Case 2016), this taxon is (at least in part) synonymous with *G. eaglesomei* (Ebersole *et al*. 2019; Türtscher *et al.* 2021).

The mesial cutting edge on *G. clarkensis* teeth is more evenly convex, lacks a conspicuous medial swelling on the mesial cutting edge, and has finer serrations compared to the Catahoula Formation teeth. Additionally, the distal angle on *G. clarkensis* teeth is 90° or less, whereas the angle is obtuse on *G. platycuspidatum* sp. nov. teeth (except on postero-lateral teeth, where it is approximately 90°).

The morphological features of *Galeocerdo platycuspidatum* sp. nov. teeth are like those of the Miocene *G. mayumbensis* Dartevelle & Casier, 1943, but examination of the type specimens originally figured (Darteville & Casier 1943: pl. 12 figs 22–29) indicates that the two are not conspecific. The cusp in *Galeocerdo platycuspidatum* is much wider, the mesial cutting edge is generally more convex, the distal cutting edge is usually convex, and the distal heel is higher but less concave compared to *G. mayumbensis*. Unfortunately, only two of the teeth shown by Dartevelle & Casier (1943: figs 25, 29) are complete and could be measured to determine the proportion of cusp width to tooth width. Those two teeth appear to be similar to those we show in Fig. 12G and I, and when compared to each other the *G. mayumbensis* teeth have a cusp that represents an average of 46% of total tooth width, whereas for *G. platycuspidatum* this proportion is 51%.

The temporal occurrence of the Catahoula Formation specimens is also older than the typically Miocene records of *G. mayumbensis* (see also Perez 2022). The Catahoula Formation teeth are similar to specimens that Müller (1999) identified as a new species, *G. casei*, from the Oligo-Miocene Belgrade Formation of North Carolina. However, this taxon has been placed in synonymy with *G. mayumbensis* (Andrianavalona *et al.* 2015; Türtscher *et al.* 2021). Müller's figured specimens (Müller 1999: pl. 11 figs 1–4) have a mesio-distally narrow cusp closer to that of *G. mayumbensis* as opposed to *G. platycuspidatum* sp. nov. Only three of the four teeth shown by Müller (1999) are complete, and the cusp width of these specimens averages 42% of total tooth width, significantly lower than the average for *G. platycuspidatum* (51%).

Ebersole *et al*. (2024a) identified two teeth from the earliest Oligocene (lowermost Rupelian) Red Bluff Clay in Alabama as *Galeocerdo* sp. These teeth have compound serrations like those of *G. platycuspidatum* sp. nov., but the mesial cutting edge of the former is more evenly (and less) convex than on the latter. Additionally, the distal heel denticles of the Red Bluff Clay specimens are very large considering the relatively small tooth size, and the main cusp is narrower and more elongated compared to that of *G. platycuspidatum*. Ebersole *et al*. (2024a) postulated that the Red Bluff Clay teeth may represent an undescribed earliest Oligocene taxon, which is congruent with the hypothesis that Cenozoic tiger shark diversity is greater than presently recognized (Türtscher *et al.* 2021).

Cicimurri & Knight (2009) and Cicimurri *et al.* (2022) reported teeth of *Galeocerdo aduncus* (Agassiz, 1843) from the Chattian Chandler Bridge Formation and the Rupelian Ashley Formation, respectively, of South Carolina. The Catahoula Formation specimens differ significantly from the South Carolina specimens by attaining larger overall sizes, having greater overall crown height and a comparatively smaller but wider cusp, and the angle formed between the distal cutting edge and distal heel is obtuse. In contrast, this angle is 90º or less in *G. aduncus*, and the distal heel is clearly separated from the distal cutting edge by a distinct notch. Furthermore, the serrations of the Catahoula Formation *Galeocerdo* are larger and more complex compared to the South Carolina Oligocene teeth.

Galeocerdo capellini Lawley, 1876 is based on a single tooth, but if considered valid both this taxon and *G. cuvier* differ from *G. platycuspidatum* sp. nov. by having a mesio-distally narrower cusp, a less convex mesial cutting edge, and the distal angle is 90° or less.

Division Batomorphi Cappetta, 1980b
Order Rhinopristiformes Naylor *et al.*, 2012
Family Rhinidae Müller & Henle, 1841

Genus ***Rhynchobatus*** Müller & Henle, 1837

Type species

Rhinobatus laevis Bloch & Schneider, 1801, Extant.

Rhynchobatus cf. ***pristinus*** (Probst, 1877)
Fig. 13G–L

Xxx pristinus Probst, 1877: 81–82.

Material examined

UNITED STATES OF AMERICA – **Mississippi** • 246 isolated teeth; Catahoula Formation; MMNS VP-7747 (16 teeth), MMNS VP-7754 (33 teeth), MMNS VP-12078, SC2013.28.494, SC2013.28.495,

SC2013.28.496 (Fig. 13G–I), SC2013.28.497 to 28.499, SC2013.28.500 (Fig. 13J–L), SC2013.28.501, SC2013.28.502, SC2013.28.503 (7 teeth), SC2013.28.504 (17 teeth), SC2013.28.505 (7 teeth), SC2013.28.506 (14 teeth), SC2013.28.507 (20 teeth), SC2013.28.508 (42 teeth), SC2013.28.509 (28 teeth), SC2013.28.510 (15 teeth), SC2013.28.511 (36 teeth), SC2013.28.526.

Description

In occlusal view, the main body of the tooth crown is usually wider than long, with larger specimens measuring 4 mm in mesio-distal width. The occlusal outline of these teeth is sub-rectangular, with the labial margin being convex and the sides straight or slightly angled medially (Fig. 13H, K). Some teeth have a circular occlusal outline. The labial and lingual faces are separated by a transverse crest

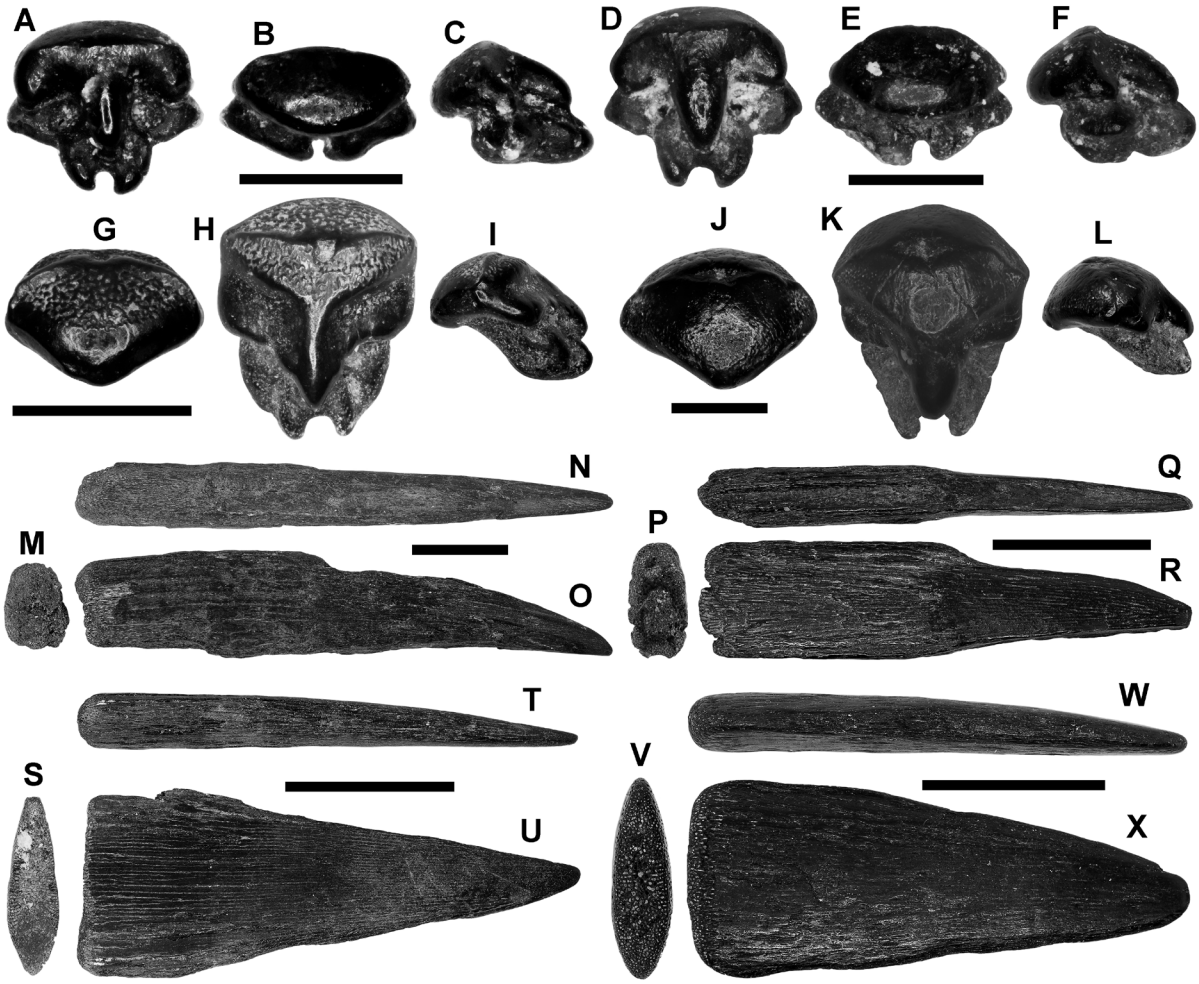

Fig. 13. *Pristis* sp. (A–F, M–R), *Rhynchobatus* cf. *pristinus* (Probst, 1877) (G–L), and *Anoxypristis* sp. (S–X), teeth and rostral spines. **A–C**. SC2013.28.490, *Pristis* sp., tooth. **A**. Oro-lingual view. **B**. Labial view. **C**. Profile view. **D–F**. SC2013.28.486, *Pristis* sp., tooth. **D**. Oro-lingual view. **E**. Labial view. **F**. Profile view. **G–I**. SC2013.28.496, *Rhynchobatus* cf. *pristinus*, tooth. **G**. Labial view. **H**. Occlusal view. **I**. Profile view. **J–L**. SC2013.28.500, *R.* cf. *pristinus*, tooth. **J**. Labial view. **K**. Occlusal view. **L**. Profile view. **M–O**. MMNS VP-12070, *Pristis* sp., right rostral spine. **M**. Basal view. **N**. Posterior view. **O**. Dorsal view. **P–R**. MMNS VP-7787.1, *Pristis* sp., right rostral spine. **P**. Basal view. **Q**. Posterior view. **R**. Dorsal view. **S–U**. MMNS VP-12071, *Anoyxpristis* sp., right rostral spine. **S**. Basal view. **T**. Posterior view. **U**. Dorsal view. **V–X**. MMNS VP-12072.1, *Anoxypristis* sp., right rostral spine. **V**. Basal view. **W**. Posterior view. **X**. Dorsal view. Scale bars: A–F = 1 mm; G–L = 3 mm; M–X = 1 cm.

that varies in size, and the convex labial face is coarsely tuberculated (Fig. 13G–H). These tubercles sometimes appear to coalesce into discontinuous ridges. The apical part of the lingual surface is flat and has a triangular outline, and unworn teeth have a tuberculated appearance. This surface transitions to a smooth, convex portion of the lingual face. The sides of the lingual crown foot are formed into thin, shelf-like projections. There is a pronounced medial uvula that extends onto the root surface. The uvula may be short and wide or narrow and elongated (compare Fig. 13H to K). In profile view, the labial crown foot overhangs the low root, and the root extends slightly beyond the lingual crown foot (Fig. 13I, L). In basal view, the root is obviously bilobate, with the somewhat triangular lobes being separated by a longitudinal nutritive groove. The basal attachment surfaces are flat to weakly convex. In occlusal view, the root bears margino-lingual foramina that flank the crown uvula, and the lingual root projection has a notched appearance.

Remarks

Various tooth sizes and slightly differing morphologies occur in our sample, but we attribute these minor differences to heterodonty. Specimens with a circular occlusal outline may represent symphyseal or anterior positions and those with a more rectangular outline are from lateral files (monognathic heterodonty). Variation in tooth size could reflect ontogenetic heterodonty (i.e., juvenile versus adult individuals) or even dignathic heterodonty, given the unusual configuration of the *Rhynchobatus* dentition (see Dean *et al.* 2017: figs 1–2). Crown ornamentation is difficult to discern on many specimens, which in part is the result of post mortem ablation (i.e., current transport) but also in vivo wear (which is particularly evident at the crown apex).

These teeth are significantly larger and more robust than those of *Pristis* sp., described below, and they possess labial ornamentation but lack lingual lateral uvulae. Cicimurri & Knight (2009) reported four teeth from the Chattian Chandler Bridge Formation of South Carolina that they tentatively identified as *Rhynchobatus pristinus*, and the species was noted in the Oligocene Old Church Formation of Virginia (Müller 1999) and the Oligo-Miocene Belgrade Formation of North Carolina (Case 1980; Müller 1999). Cicimurri *et al.* (2022) reported a few teeth from the Rupelian Ashley Formation that were identified as *Rhynchobatus* sp. Most of the Catahoula Formation specimens are ablated, but well-preserved teeth fall within the range of variation of *R. pristinus* and are tentatively referred to that species. *Rhynchobatus pristinus* apparently had a wide distribution in the Western Hemisphere (Cappetta 1970; Laurito 1999; Ward & Bonavia 2001; Vialle *et al.* 2011; Fialho *et al.* 2019), but the specimens noted in the aforementioned reports are variable and it remains to be determined whether all of these records are accurately attributed to *R. pristinus*. It is interesting to note that all of the Oligocene records known to us are from the Atlantic Coastal Plain of the USA, and the teeth in our sample represent the first occurrences of fossil *Rhynchobatus* in the Gulf Coastal Plain of the USA.

Family Pristidae Bonaparte, 1838

Genus ***Pristis*** Linck, 1790

Type species

Squalus pristis Linnaeus, 1758, Extant.

Pristis sp.
Fig. 13A–F, M–R

Material examined

UNITED STATES OF AMERICA – **Mississippi •** 12 rostral spines; Catahoula Formation; MMNS VP-7787 (5 specimens), MMNS VP-7787.1 (Fig. 13P–R), MMNS VP-12070 (Fig. 13M–O), SC2013.28.515,

SC2013.28.516, SC2013.28.517 (3 specimens) • 28 isolated teeth; Catahoula Formation; MMNS VP-7748 (4 teeth), MMNS VP-8744 (2 teeth), MMNS VP-9211 (4 teeth), SC2013.28.486 (Fig. 13D–F), SC2013.28.487 to 28.489, SC2013.28.490 (Fig. 13A–C), SC2013.28.491 (4 teeth), SC2013.28.492 (3 teeth), SC2013.28.493 (4 teeth), SC2013.28.512, SC2013.28.527.

Description

The rostral spines are composed entirely of dentine. These spines are elongated, antero-posteriorly narrow, and dorso-ventrally flattened but thick. The anterior and posterior margins are parallel along most of the spine length, but near the distal tip, the anterior margin converges towards the posterior margin to form a sharp point. The anterior margin is rounded except at the distal tip, which is a sharp edge. The posterior margin bears a furrow along its entire length. The dorsal and ventral surfaces are weakly convex except at the distal tip, where the surfaces are flat. Fine growth lines are visible near the base, and the basal surface has a somewhat D-shaped outline (Fig. 13M, P).

The teeth are tiny, measuring 1 mm in total height. Crown width (mesio-distal) averages 1.2 mm, with the smallest measuring 1.0 mm and the largest 1.8 mm in this dimension. Crown length averages 1.1 mm, with the smallest measuring 0.8 mm and the largest 1.5 mm in this dimension. The teeth are somewhat globular in appearance, with a crown that is convex in labial and profile views (Fig. 13B, E–F). In occlusal view, a transverse crest divides the crown into labial and lingual parts (Fig. 13D). The crest is generally blunt but can be sharp, and it does not reach the foot of the lateral crown. In labial view, the crest can be flat and weakly cuspidate with a pointed apex. The labial crown margin is weakly to strongly convex, and the labial face is convex to varying degrees. The lingual face exhibits an elongate medial protuberance (i.e., uvula) that extends onto the root, and this protuberance varies in width and length. The distal ends of the crown are lingually directed and form a roughly 70º angle with the medial lingual uvula (Fig. 13A, D). The angularity of the lateral crown projections varies from narrow and pointed to wide and rounded. The crown slightly overhangs the root labially, but the root extends beyond the lateral and lingual crown faces (Fig. 13A, C, E). In basal view, the root is bisected by a wide nutritive groove that is perforated (medially) by several small foramina. The root lobes are very short in profile view and have a cleaver-shaped basal outline, with a distinctive narrow process extending lingually. The oral root surface bears a pair of large foramina, one on each side of the medial uvula.

Remarks

Although all the rostral spines are ablated, they compare well to spines in the rostra of extant *Pristis pectinata* Latham, 1794 (MSC 43849, MSC 43850, SC90.80.1) that we examined. Some of the Catahoula Formation spines have a sharp antero-distal margin and oblique striations on the dorsal and ventral surfaces. These features were observed on extant *Pristis* spines and have been reported on Eocene specimens, and they indicate that the Catahoula sawfishes used their spined rostrum to probe the sandy substrate for prey (Cicimurri 2007; Ebersole *et al.* 2019). It is interesting to note that the figured specimens exhibit a distinct transition from sub-parallel margins to gently apically converging (Fig. 13O, R). Some rostral spines exhibiting this morphology reported from elsewhere have been assigned to *Pristis brayi* Casier, 1949 (see Hovestadt & Steurbaut 2023: 88). However, our examination of several extant *Pristis* spp. rostra demonstrates that the beginning of this constriction represents the point where the spine was exposed from the rostrum, with the proximal end set within a deep alveolus of the rostral cartilage (the distal end is exposed to wear). Ebersole *et al.* (2019) discussed the taxonomic uncertainty involved with the speciation of isolated Paleogene *Pristis* spines, and we herein follow these authors by leaving the Catahoula Formation specimens within open nomenclature. It cannot be ascertained whether similar rostral spines reported from middle Eocene deposits in Alabama (Cappetta & Case 2016; Ebersole *et al*. 2019) are conspecific with the Catahoula Formation taxon, or if multiple Paleogene taxa are present.

The familial/generic assignment of teeth like those described above has been debated over the past several years, with alternating assignments to Rhinobatidae/*Rhinobatos* and Pristidae/*Pristis* (i.e., Cappetta & Case 2016; Ebersole *et al.* 2019; Adnet *et al.* 2020), but all sources agree that the morphology is assignable to Rhinopristiformes. Reinecke *et al.* (2023) provided a monograph that helped us make a more informed identification of these fossil teeth. The Catahoula Formation teeth are wider (mesio-distally) than long (labio-lingually). Additionally, the transverse crest, which ranges from low and rounded to sharp and cuspidate, has a straight to sinuous appearance (in occlusal view). Although the lateral crown margins are lingually directed and extend beyond the lingual medial uvula, we do not view these structures as lateral uvulae (sensu Cappetta 2012). Furthermore, in profile view the oral surface of the lingual medial uvula has a weakly to strongly sinuous outline, depending on the height of the transverse crest and the convexity of the uvula itself.

The features we observed on the Catahoula Formation teeth described above are consistent with those of fossil and extant representatives of *Pristis* (Cappetta 2012; Carrillo-Briceño *et al.* 2015, 2016; Reinecke *et al.* 2023). These features include a sinuous transverse crest and a lack of lateral uvulae (in occlusal view), as well as the sinuous oral margin of the medial lingual uvula and slight labial overhang of the root (in profile view). Additionally, the basal root surface is cleaver-shaped with a distinctively lingually elongated projection.

In contrast, teeth of the extant rhinobatids *Pseudobatos horkelii* (Müller & Henle, 1841) and *Glaucostegus cemiculus* (Geoffroy Saint-Hilaire, 1817) have distinctive labial and lingual portions of the crown (see Reinecke *et al.* 2023: pls 13, 17) like the fossil teeth of *Rhynchobatus* we observed (see above). Although teeth of the extant *Rhinobatos annandalei* Norman, 1926 and *Acroteriobatus annulatus* (Smith in Müller & Henle, 1841) are similar to our Catahoula Formation specimens, they differ by having a straight transverse crest (occlusal view), a generally convex oro-lingual margin and a shorter, more oblique medial lingual uvula (profile view), a greater labial overhang of the root (profile view), and a shorter lingual projection of the root (basal view). These differences can be observed among the teeth shown by Reinecke *et al.* (2023: pls 1–4, 9–10, 5–16).

There are slight variations in tooth morphology within our Catahoula Formation sample that likely reflect some form of heterodonty. Narrow teeth with sharp and generally cuspidate transverse crests may represent anterior jaw positions, whereas teeth that are conspicuously wider than long with a low and rounded transverse crest may have been from lateral files.

Genus ***Anoxypristis*** White & Moy-Thomas, 1941

Type species

Pristis cuspidatus Latham, 1794, Extant.

Anoxypristis sp.
Fig. 13S–X

Material examined

UNITED STATES OF AMERICA – **Mississippi** • 10 rostral spines; Catahoula Formation; MMNS VP-12071 (Fig. 13S–U), MMNS VP-12072 (7 specimens), MMNS VP-12072.1 (Fig. 13V–X), SC2013.28.514.

Description

The spines are elongated, very thin dorso-ventrally (Fig. 13T, W), with a triangular dorsal outline. The anterior and posterior faces are thin and converge distally to form a medially located point (Fig. 13U, X). The basal surface may have an elliptical or teardrop-shaped (rounded anterior margin but tapering posteriorly) outline (Fig. 13S, V).

Remarks

These spines are comparable to those occurring on a rostrum of extant *Anoxypristis* sp. that we examined (SC86.214.1). They differ from the spines of the Catahoula Formation *Pristis* sp. (see above) and those of extant *Pristis* (i.e., MSC 43849, MSC 43850, SC90.80.1) by being much thinner dorso-ventrally (although *Pristis* spines are very thin at the pointed distal end), having rather thin anterior and posterior faces, and having an elliptical to teardrop-shaped basal outline. In contrast, the fossil *Pristis* sp. spines are comparably thicker, very elongated but narrow antero-posteriorly, the posterior surface is concave, and the basal outline is "D" shaped. Although Cicimurri & Knight (2009) observed an *Anoxypristis* sp. rostral spine from the Chandler Bridge Formation (Chattian, NP25) of South Carolina that was housed in a private collection, sawfish specimens have yet to be formally described from the South Carolina Oligocene. *Anoxypristis* spines of similar morphology to those from the Catahoula Formation have been confirmed from middle Eocene deposits in Alabama (Cappetta & Case 2016; Ebersole *et al*. 2019), but we cannot determine whether they are conspecific.

Order Myliobatiformes Compagno, 1973
Suborder Myliobatoidei Compagno, 1973
Family Dasyatidae Jordan & Gilbert, 1879

Genus ***Hypanus*** Rafinesque, 1818

Type species

Raja say Lesueur, 1817, Extant.

Hypanus? ***heterodontus*** sp. nov.
urn:lsid:zoobank.org:act:DECAA150-D2AE-4591-BC8B-2EE90BF5D560
Figs 14–17, 18A–J

Diagnosis

Low-crowned teeth and high-crowned teeth are represented for this taxon. Low-crowned teeth generally have a convex labial face (amount of convexity varies) with a transversely depressed area near the apex. The labial face bears highly irregular ridges that are weakly to strongly developed and extend onto a wide transverse crest. The lingual face is smooth and bears a medial longitudinal crest flanked by lateral depressed areas. The bilobate root is low, located closer to, and extending beyond, the lingual crown margin. High-crowned teeth are cuspidate, with cusp height and degree of distal and lingual inclination varying. A thin transverse crest subdivides the crown into a large lingual face and much smaller labial face. The labial face may be virtually smooth but is usually ornamented with irregular and disconnected vertical ridges, sometimes forming a reticulated network. The lingual face is smooth and exhibits a medial longitudinal crest of varying width.

New fossil species of *Hypanus* have yet to be named, but fossil teeth of several extant species (formerly placed in *Dasyatis*) have been reported. A small male tooth identified as *H. americanus* (Hildebrand & Schroeder, 1928) from the lower Miocene Pungo River Formation of North Carolina has a much more

concave labial face and the lingual crown curvature is more pronounced apically than on *Hypanus*? *heterodontus* sp. nov. teeth of similar stature (Purdy *et al.* 2001). However, this comparison may be irrelevant, as we believe the Miocene tooth is that of a mobulid ray. Fitch (1966, 1970) reported a total of 12 *H. dipterurus* (Jordan & Gilbert, 1880) teeth from Pleistocene deposits of California, but he did not describe or illustrate them. Deynat & Brito (1994) reported caudal spines of *H. guttatus* (Bloch & Schneider, 1801) from the Miocene of central South America, but no teeth were noted. Pliocene teeth from the Yorktown Formation of North Carolina identified as *H. say* (Lesueur, 1817) by Purdy *et al.* (2001) are smaller in overall size and more strongly ornamented compared to *H*.? *heterodontus*. However, high-crowned teeth of living *H. say* have a more concave labial face and more strongly lingually curved crown compared to *H*.? *heterodontus*, and the ornamentation on low-crowned teeth of the former species does not extend onto the transverse crest as it does on teeth of the latter species (see Reinecke *et al.* 2023: pls 64–67).

Etymology

The species name refers to the variation in gross crown morphology and ornamentation.

Material examined

Holotype

UNITED STATES OF AMERICA – **Mississippi** • low-crowned tooth (Fig. 14P–T); Catahoula Formation; SC2013.28.449.

Paratypes

UNITED STATES OF AMERICA – **Mississippi** • high-crowned tooth (Fig. 14F–J); Catahoula Formation; SC2013.28.406 • high-crowned tooth (Fig. 14K–O); Catahoula Formation; SC2013.28.409 • low-crowned tooth (Fig. 14A–E); Catahoula Formation; SC2013.28.444.

Other material

UNITED STATES OF AMERICA – **Mississippi** • 574 isolated teeth; Catahoula Formation; MMNS VP-7530 (16 teeth), MMNS VP-7749 (60 teeth), MMNS VP-7912, MMNS VP-8742, MMNS VP-12068, MMNS VP- 12069, SC2013.28.407 (Fig. 17K–O), SC2013.28.408 (Fig. 16K–O), SC2013.28.410, SC2013.28.411, SC2013.28.412 (Fig. 16F–J), SC2013.28.413 (Fig. 16P–T), SC2013.28.414 to 28.420, SC2013.28.421 (Fig. 17P–T), SC2013.28.422 (Fig. 16U–Y), SC2013.28.423 (Fig. 17U–Y), SC2013.28.424 (Fig. 16A–E), SC2013.28.425 to 28.427, SC2013.28.428 (Fig. 16Z–DD), SC2013.28.431 (19 teeth), SC2013.28.432 (5 teeth), SC2013.28.433 (8 teeth), SC2013.28.434 (5 teeth), SC2013.28.435 (6 teeth), SC2013.28.436 (15 teeth), SC2013.28.437 (Fig. 15F–J), SC2013.28.438, SC2013.28.439, SC2013.28.440 (Fig. 15K–O), SC2013.28.441 (5 teeth), SC2013.28.442 (7 teeth), SC2013.28.443, SC2013.28.445 (Fig. 15P–T), SC2013.28.446 (19 teeth), SC2013.28.447 (15 teeth), SC2013.28.448, SC2013.28.450 (Fig. 15Z–DD), SC2013.28.451 to 28.454, SC2013.28.455 (Fig. 15U–Y), SC2013.28.456, SC2013.28.457, SC2013.28.458 (19 teeth), SC2013.28.459 (22 teeth), SC2013.28.460, SC2013.28.461 (Fig. 15A–E), SC2013.28.462, SC2013.28.463, SC2013.28.464 (5 teeth), SC2013.28.465, SC2013.28.466 (Fig. 17A–E), SC2013.28.467 (6 teeth), SC2013.28.468 (11 teeth), SC2013.28.469, SC2013.28.470 (Fig. 17F–J), SC2013.28.471 to 28.473, SC2013.28.474 (4 teeth), SC2013.28.475 (Fig.18A–E), SC2013.28.476 (Fig. 18F–J), SC2013.28.477 (195 teeth) SC2013.28.478 (55 teeth), SC2013.28.513, SC2013.28.523 (3 teeth), SC2013.28.524 (5 teeth), SC2013.28.525 (15 teeth).

Stratum typicum

Shelly, argillaceous sand of the Jones Branch fossil horizon, lower Catahoula Formation, Chattian Stage (horizon no longer accessible).

Locus typicus

Site MS.77.011, Jones Branch, tributary flowing into the Chickasawhay River, south of Waynesboro, Wayne County, Mississippi, USA.

Description

Two morphotypes are represented in the sample, namely low-crowned and high-crowned. Most of the specimens of both morphotypes measure 1.5 mm or less in greatest width (mesio-distal), but a handful of larger specimens (n = 11) measure between 2 mm and 3.2 mm in width.

The low-crowned morphotype has a somewhat six-sided occlusal outline but can appear to be diamond-shaped. The crown width is slightly greater than the length. The mesial and distal ends of the crown are angular (with the angles located somewhat labially), whereas the labial and lingual margins are generally broader and have rounded to straight margins. In labial view, the crown base may be uniformly convex (broadly or narrowly) or can be straight medially (compare Figs 15A, F, 17A). In profile view, the labial face ranges from weakly to strongly convex, and a weak depression typically occurs within the apical one-half of the crown (Figs 15E, J, 17E). The lingual margin may be straight but sloping from the apex to the crown foot (Fig. 15DD), but most often it is sub-angular, such that there is a more vertical portion transitioning basally to an elongated heel (Fig. 17J). There is a thick transverse crest extending nearly to the crown foot of the mesial and distal sides (Figs 15H, 17J). The labial crown face is ornamented to varying degrees, with the ornament ranging from occasional discontinuous and irregular interconnected ridges (Fig. 15U) to extensive similar ornamentation forming a reticulated network (Fig. 15A). The ornamentation does not reach the base of the crown foot (Fig. 15A, E), but it does extend onto the apical surface on the lingual side of the transverse crest (Fig. 15C, G, M, Q). The lingual crown face is otherwise smooth. The transverse crest is intersected by a lingual crest that ranges from strong to inconspicuous (compare Fig. 15H to W). In profile view, the crown base is generally straight (Fig. 15O), but the labial margin may extend basally beyond the origin of the root (Fig. 15DD). In basal view, the enameloid extends to the aboral surface of the crown, and the root appears to emanate from a basin framed by the enameloid (Figs 15D, 17I). The bilobate root is large, rather low, and located at the lingual one-half of the tooth (Figs 15J, Y, 17E). The root lobes are separated by a wide and deep nutritive groove, and the basal attachment surface is sub-triangular and flat to weakly convex (Fig. 15I, N). Well-preserved specimens show that the lobes extend beyond the lingual crown margin (Fig. 15J).

The high-crowned specimens measure up to 1.7 mm in crown height, and they have a sub-triangular outline in occlusal view (Figs 16G, 17L). In this view, the lingual face is more extensive than the labial face (Figs 16L, 17Q). The mesial and distal ends of the crown may be sharply angular or rounded (compare Fig. 16G to AA), and these lateral angles are located closer to the labial margin (Fig. 16V). The lingual margin is generally strongly and uniformly convex, but some specimens are embayed laterally. The labial margin ranges from nearly straight to strongly convex (compare Figs 16L and 17V). In profile view, the labial margin is convex to varying degrees (Figs 16J, 17T, Y). The cusp is conspicuous, and on some specimens, it is strongly lingually inclined, such that the labial margin appears to be somewhat angular (Fig. 17O). The lingual face is expansive and generally convex, although there are depressed areas on both sides of the crown. The crown foot is extended into a short, straight to sloping shelf-like structure, and the transition from cusp apex to lingual crown foot is strongly concave (Fig. 16E, Y). The crown base may be straight, or the labial margin may extend somewhat basally beyond the origin of the root (compare Fig. 16T to 17O). In occlusal (and profile) view, there is a thin transverse crest (close to the labial margin) that extends the entire height of the cusp but does not reach the crown foot (Fig. 14G, J). This crest forms the border of the labial face, which itself ranges from very weakly convex to slightly concave (compare Fig. 16U to 17K). Additionally, the labial face is ornamented to varying degrees, ranging from a few incomplete, sinuous vertical ridges (Fig. 17P) to more extensive and interconnected ridges (Fig. 14K), and sometimes heavy ornamentation consisting of a weakly reticulated network of ridges (Fig. 17U). The ornamentation never reaches the crown foot, which is formed by a rim of smooth

enameloid (Fig. 16K, Z). In labial view, the crown has a sub-triangular outline with the basal margin being uniformly convex to varying degrees (compare Fig. 14K to 16Z) and the cusp being vertical to distally inclined to varying degrees (compare Figs 14F, 16P, and 17P). Additionally, the mesial and distal sides may be straight (Fig. 14F), slightly convex (Fig. 16F), concave (Fig. 17K), or evenly convex on the mesial side but concave on the distal side (Fig. 17P). The transverse crest is intersected on the lingual side by a broad longitudinal crest that does not reach the crown foot (Figs 14H, 16H, 17M). In basal view, the enameloid extends to the aboral surface of the crown, and the root emanates from a basin within the enameloid (Figs 16CC, 17N). The bilobate root is large and located at the distal one-half of the tooth (Figs 14O, 16E). The lobes are separated by a wide and deep nutritive groove, and the basal attachment surface is sub-triangular and flat to weakly convex (Fig. 16N, S). Well-preserved specimens show that the lobes extend beyond the lingual crown margin (Fig. 16O, T).

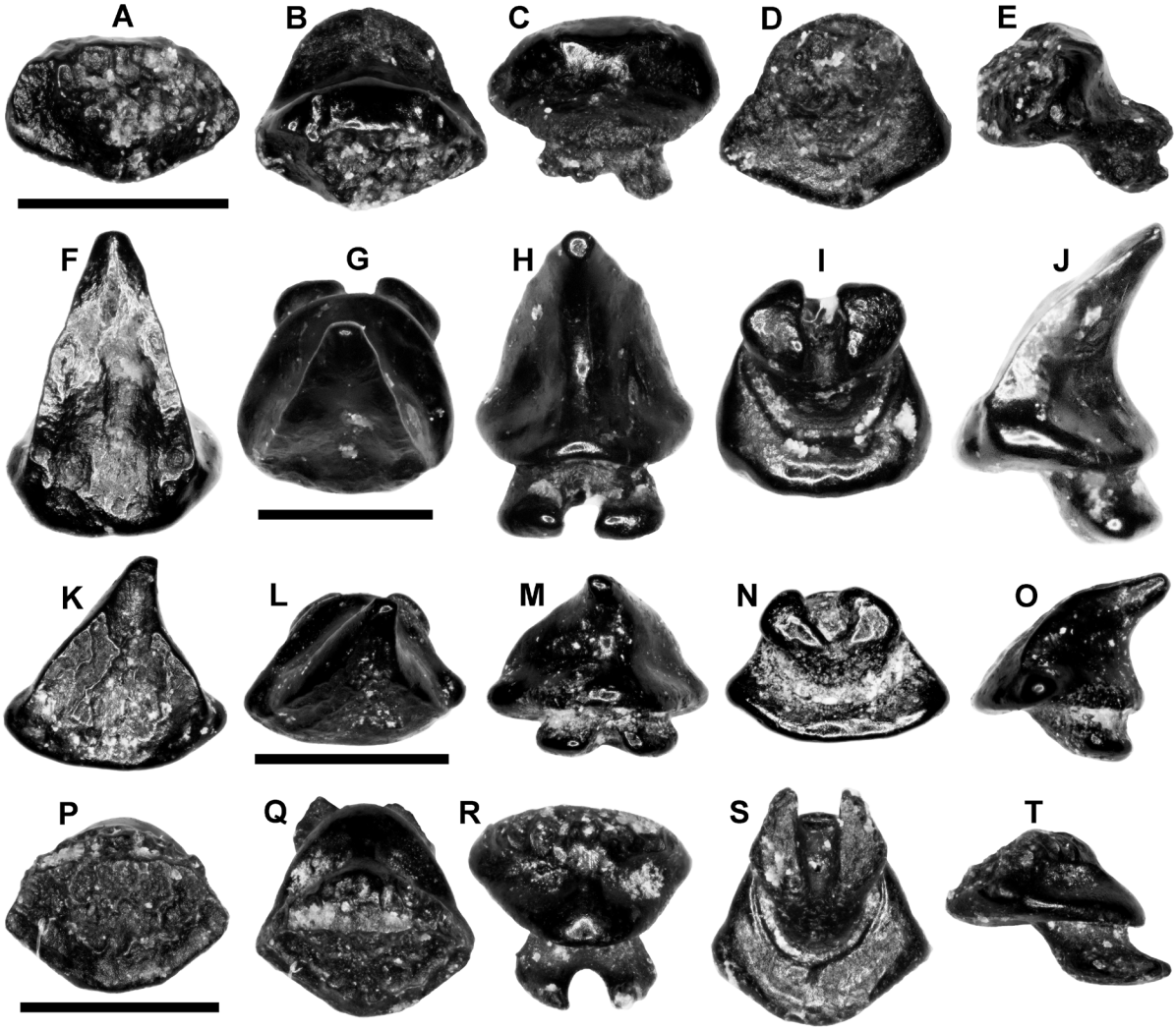

Fig. 14. *Hypanus*? *heterodontus* sp. nov., teeth (type specimens). **A–E**. SC2013.28.444 (paratype), low-crowned tooth. **A**. Labial view. **B**. Occlusal view. **C**. Lingual view. **D**. Basal view. **E**. Profile view. **F–J**. SC2013.28.406 (paratype), high-crowned tooth. **F**. Labial view. **G**. Occlusal view. **H**. Lingual view. **I**. Basal view. **J**. Profile view. **K–O**. SC2013.28.409 (paratype), high-crowned tooth. **K**. Labial view. **L**. Occlusal view. **M**. Lingual view. **N**. Basal view. **O**. Distal view. **P–T**. SC2013.28.449 (holotype), low-crowned tooth. **P**. Labial view. **Q**. Occlusal view. **R**. Oro-lingual view. **S**. Basal view. **T**. Profile view. Scale bars = 1 mm.

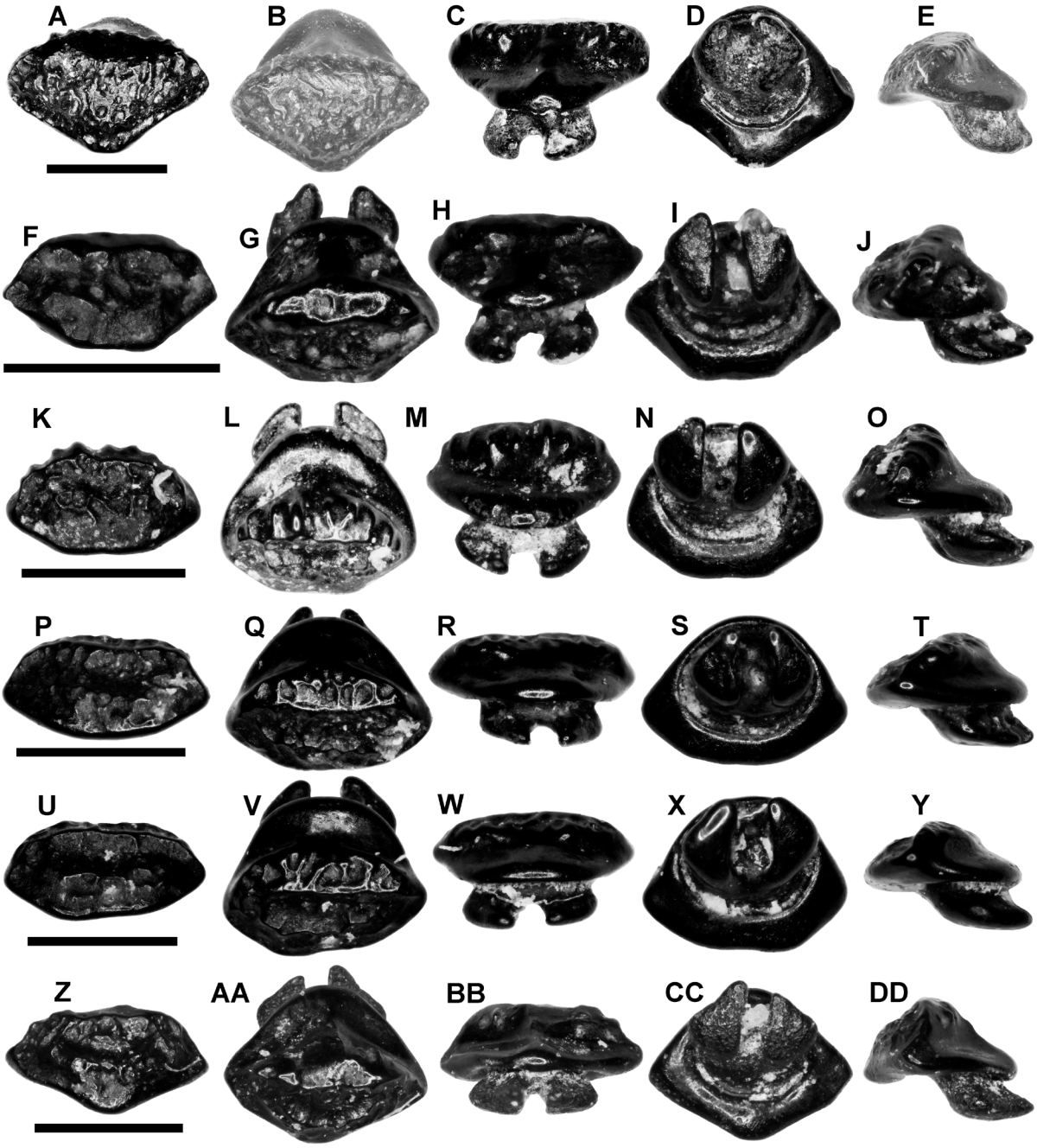

Fig. 15. *Hypanus*? *heterodontus* sp. nov., low-crowned teeth. **A–E**. SC2013.28.461. **A**. Labial view. **B**. Occlusal view. **C**. Lingual view. **D**. Basal view. **E**. Profile view. **F–J**. SC2013.28.437. **F**. Labial view. **G**. Occlusal view. **H**. Lingual view. **I**. Basal view. **J**. Profile view. **K–O**. SC2013.28.440. **K**. Labial view. **L**. Occlusal view. **M**. Lingual view. **N**. Basal view. **O**. Profile view. **P–T**. SC2013.28.445. **P**. Labial view. **Q**. Occlusal view. **R**. Lingual view. **S**. Basal view. **T**. Profile view. **U–Y**. SC2013.28.455. **U**. Labial view. **V**. Occlusal view. **W**. Lingual view. **X**. Basal view. **Y**. Profile view. **Z–DD**. SC2013.28.450. **Z**. Labial view. **AA**. Occlusal view. **BB**. Lingual view. **CC**. Basal view. **DD**. Profile view. Scale bars = 1 mm.

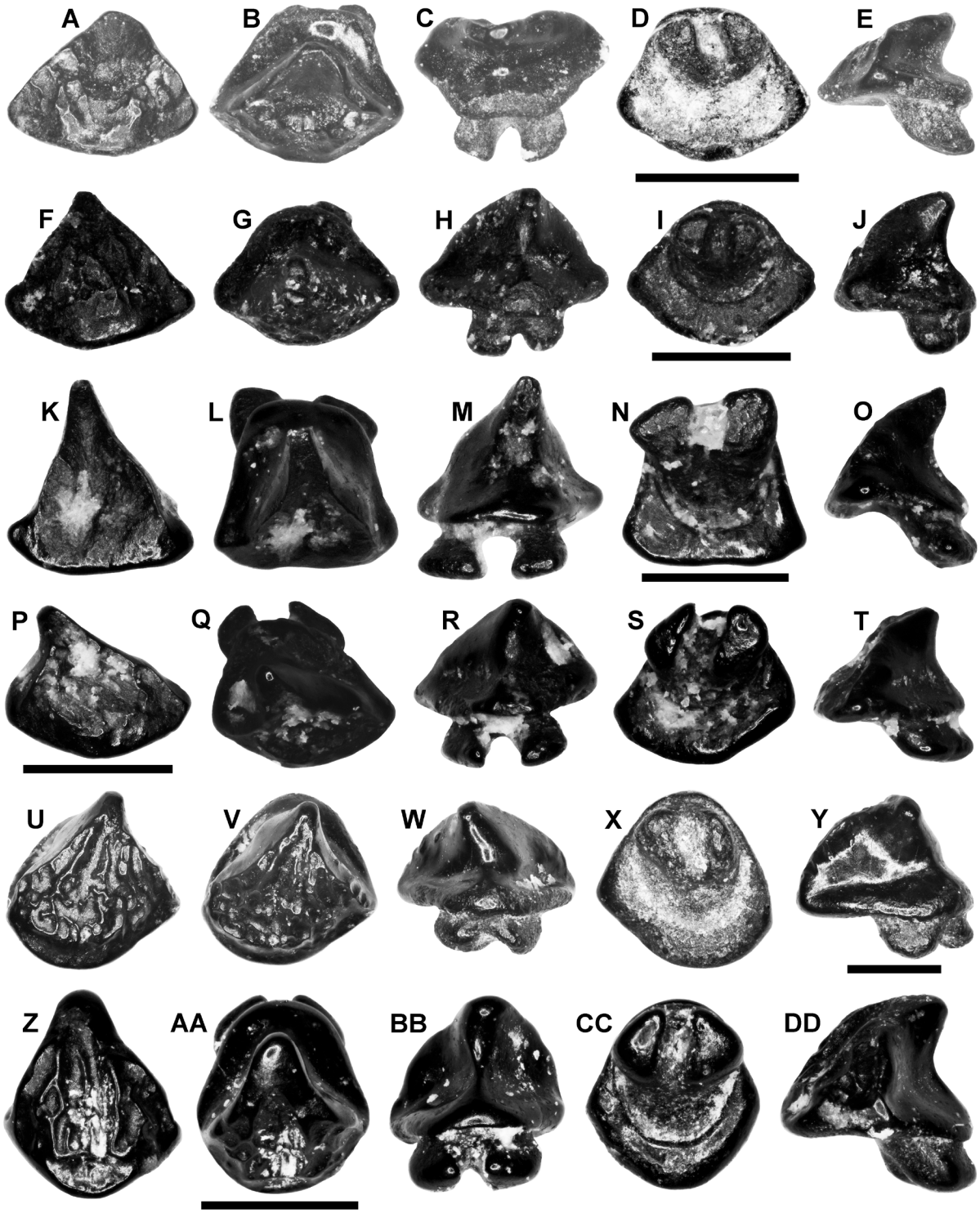

Fig. 16. *Hypanus*? *heterodontus* sp. nov., high-crowned teeth. **A–E**. SC 2013.28.424. **A**. Labial view. **B**. Occlusal view. **C**. Lingual view. **D**. Basal view. **E**. Profile view. **F–J**. SC2013.28.412. **F**. Labial view. **G**. Occlusal view. **H**. Lingual view. **I**. Basal view. **J**. Profile view. **K–O**. SC2013.28.408. **K**. Labial view. **L**. Occlusal view. **M**. Lingual view. **N**. Basal view. **O**. Profile view. **P–T**. SC2013.28.413. **P**. Labial view. **Q**. Occlusal view. **R**. Lingual view. **S**. Basal view. **T**. Profile view. **U–Y**. SC2013.28.422. **U**. Labial view. **V**. Occlusal view. **W**. Lingual view. **X**. Basal view. **Y**. Profile view. **Z–DD**. SC2013.28.428. **Z**. Labial view. **AA**. Occlusal view. **BB**. Lingual view. **CC**. Basal view. **DD**. Profile view. Scale bars = 1 mm.

Remarks

The low-crowned dasyatid teeth described above are easily distinguished from those of Catahoula Formation rhinopristiform rays (see above) by their roughly six-sided outline, extensive pitted crown ornamentation, lack of lingual lateral protuberances (i.e., uvulae), and the overall morphology of the root. There is extensive morphological variation within our sample of Catahoula Formation dasyatid teeth, which we believe reflects heterodonty within a single species. Extant dasyatid rays exhibit gynandric heterodonty, where female and juvenile male teeth are low-crowned, but teeth of mature males are high-crowned and cuspidate (Reinecke *et al.* 2023). The male high-crowned morphology develops during the breeding season, when the pointed teeth are utilized to grasp onto a female during copulation (Kajiura & Tricas 1996). Although the low- and high-crowned Catahoula Formation morphologies appear to be disparate, the high-crowned teeth bear similar, although much reduced, ornamentation as occurs on low-crowned specimens. Reinecke *et al.* (2023) provided excellent illustrations of dentitions of numerous extant dasyatid taxa that demonstrate this phenomenon (i.e., compare their pls 70–72, 74), which is also observed in the Catahoula Formation sample we examined. We therefore conclude that the high-crowned morphology represents breeding teeth of mature males, whereas low-crowned teeth represent immature or non-breeding male individuals or females.

With respect to the male cuspidate morphology, there is obvious variation in crown morphology that indicates at least monognathic heterodonty. One specimen (Fig. 14F–J) has a tall, broad, and symmetrical cusp that indicates it occupied a file close to the symphysis. Another specimen (Fig. 17K–O) has a tall, narrow, and symmetrical crown that may reflect an anterior tooth file. Most specimens have a relatively short and distally inclined cusp, and we believe that they represent lateral tooth files. The tooth height decreases, but cusp inclination increases towards the commissure (compare Figs 16K, P, 17P). This interpretation is consistent with the morphological variation within extant dasyatid dentitions as shown by Reinecke *et al.* (2023).

It is also possible that the Catahoula Formation sample reflects dignathic heterodonty. For example, tall and symmetrical cuspidate teeth may have been from the anterior portion of the lower dentition (Fig. 16K), but asymmetrical teeth with relatively short cusps may have been from the upper symphyseal region (Fig. 16U). With respect to crown width (mesio-distal) versus length (labio-lingual), upper teeth may be broader than their lower jaw counterparts (i.e., compare Fig. 16H to 17L). Low-crowned teeth of extant *Hypanus say* bearing a transverse apical depression on the labial face occur in the jaws of both male and female individuals (i.e., Reinecke *et al*. 2023: pls 64–65), so this feature does not provide clarity with respect to distinguishing upper from lower teeth of the Catahoula Formation species. However, crown ornamentation within the upper dentition may be weaker than that of the lower dentition (compare Fig. 15U to A).

The sample of *Hypanus*? *heterodontus* sp. nov. available to us includes small and large versions of low-crowned teeth, all of comparable morphology, that we interpret as an ontogenetic increase in tooth size within the new species. Most of the low-crowned teeth measure less than 1.6 mm in greatest width, but some of the largest specimens measure 3.2 mm in this dimension. In occlusal view, these large teeth have a diamond-shaped outline (Fig. 18A, F) and in profile view the labial face is convex to varying degrees with an apically depressed area (Fig. 18D, I). Additionally, the labial ornamentation of the larger teeth can consist of irregular interconnected ridges like that occurring on small low-crowned teeth (compare Fig. 18B to 15A). Lastly, the crown ornamentation on large teeth extends onto the apical part of the lingual side of the transverse crest (Fig. 18C, H). All the features of the large teeth can also be observed on the smaller teeth (i.e., compare Fig. 18A–J to specimens in Fig. 15), and we therefore consider the specimens to be conspecific.

The overall crown shapes of the low- and high-crowned teeth, as well as the morphological variation we observed within the Catahoula Formation sample, are consistent with extant *Hypanus say* as shown by Reinecke *et al.* (2023). The various forms of heterodonty expressed in *H. say* also appear to provide the best model with which to compare the Catahoula Formation species. We tentatively assign the new species to *Hypanus* Rafinesque, 1818, to indicate close similarities to extant *Hypanus* teeth and take

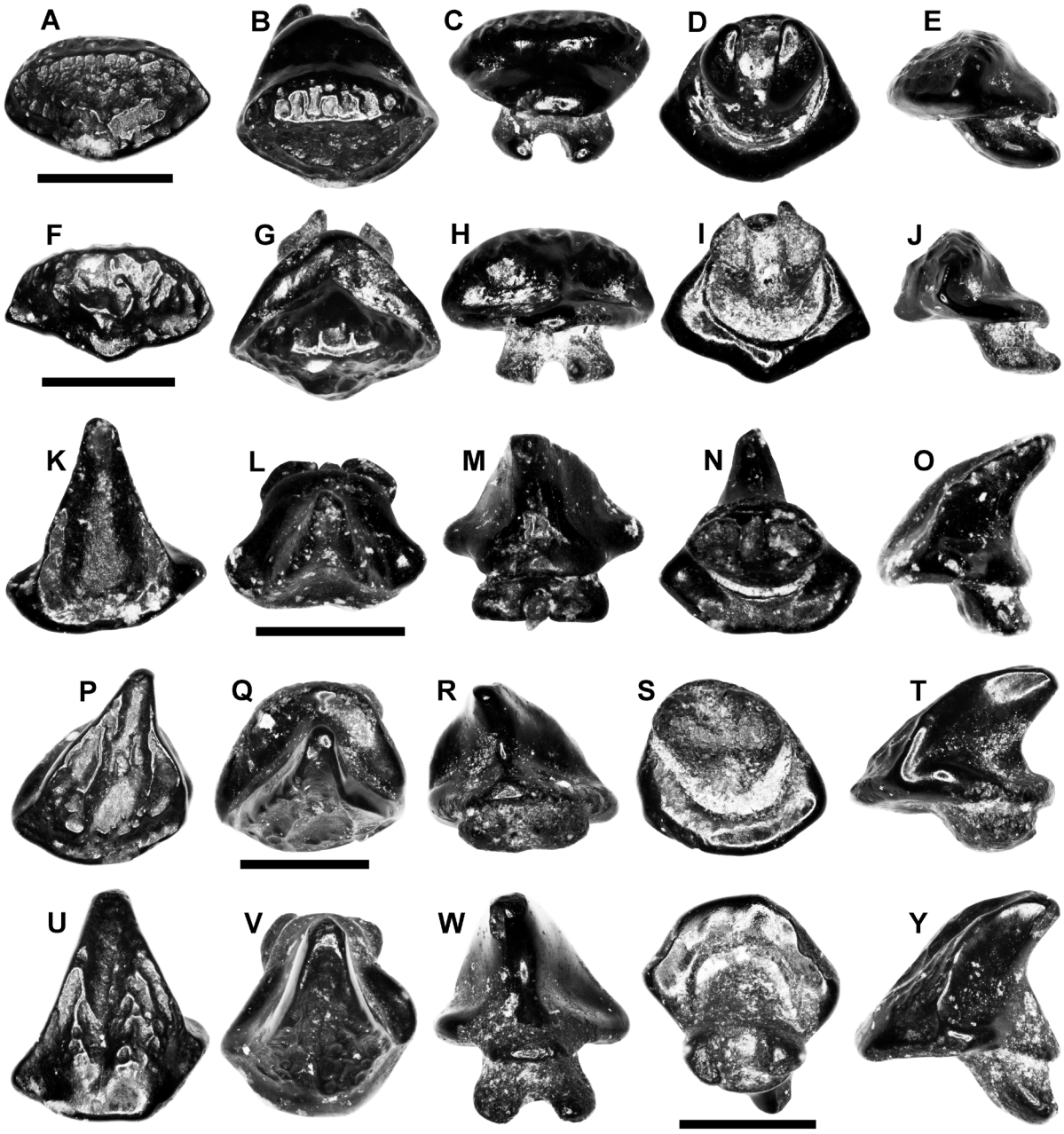

Fig. 17. *Hypanus*? *heterodontus* sp. nov., teeth. **A–E**. SC2013.28.466, low-crowned tooth. **A**. Labial view. **B**. Occlusal view. **C**. Lingual view. **D**. Basal view. **E**. Profile view. **F–J**. SC2013.28.470, low-crowned tooth. **F**. Labial view. **G**. Occlusal view. **H**. Lingual view. **I**. Basal view. **J**. Profile view. **K–O**. SC2013.28.407, high-crowned tooth. **K**. Labial view. **L**. Occlusal view. **M**. Lingual view. **N**. Basal view. **O**. Profile view. **P–T**. SC2013.28.421, high-crowned tooth. **P**. Labial view. **Q**. Occlusal view. **R**. Lingual view. **S**. Basal view. **T**. Profile view. **U–Y**. SC2013.28.423, high-crowned tooth. **U**. Labial view. **V**. Occlusal view. **W**. Lingual view. **X**. Basal view. **Y**. Profile view. Scale bars = 1 mm.

into consideration the possibility that the extinct species belongs to an unrecognized genus within the *Hypanus* lineage. Although *Hypanus* was not included in their study of batoid diversification, Puckridge *et al.* (2013) indicated that diversification within Dasyatidae began well before the Oligocene. In their recent study of *Hypanus* diversity, Petean *et al.* (2024) did not discuss the timing of diversification but recognized three clades within *Hypanus*. Two of these clades, including the *H. americanus* and *H. say* complexes, have representatives living within the present-day Gulf of Mexico (Hoese & Moore 1998).

Two dasyatid taxa were reported from the Rupelian Ashley Formation of South Carolina by Cicimurri *et al.* (2022), including "*Taeniurops*" *cavernosus* (Probst, 1877) and "*Dasyatis*" sp. The low-crowned morphotype of the former taxon is comparable to the low-crowned teeth from the Catahoula Formation. However, the high-crowned morphology shown by Cicimurri *et al*. (2022: fig. 7o, u) has more extensive labial ornamentation and a more vertically oriented cusp compared to the Catahoula Formation high-crowned morphotype (compare to Fig. 16J, T). With respect to low-crowned Miocene teeth assigned to *T. cavernosus*, these have in common with the Ashley Formation "*T*." *cavernosus* specimens a deeper apical depression on the labial face that is framed basally by a more conspicuous transverse ridge-like structure (i.e., Cappetta 1970; Villafaña *et al.* 2020). This morphology is particularly evident on extant *T. grabatus* (Geoffroy Saint-Hilaire, 1817) teeth (see Reinecke *et al.* 2023) and is unlike that of *Hypanus*? *heterodontus* sp. nov. teeth.

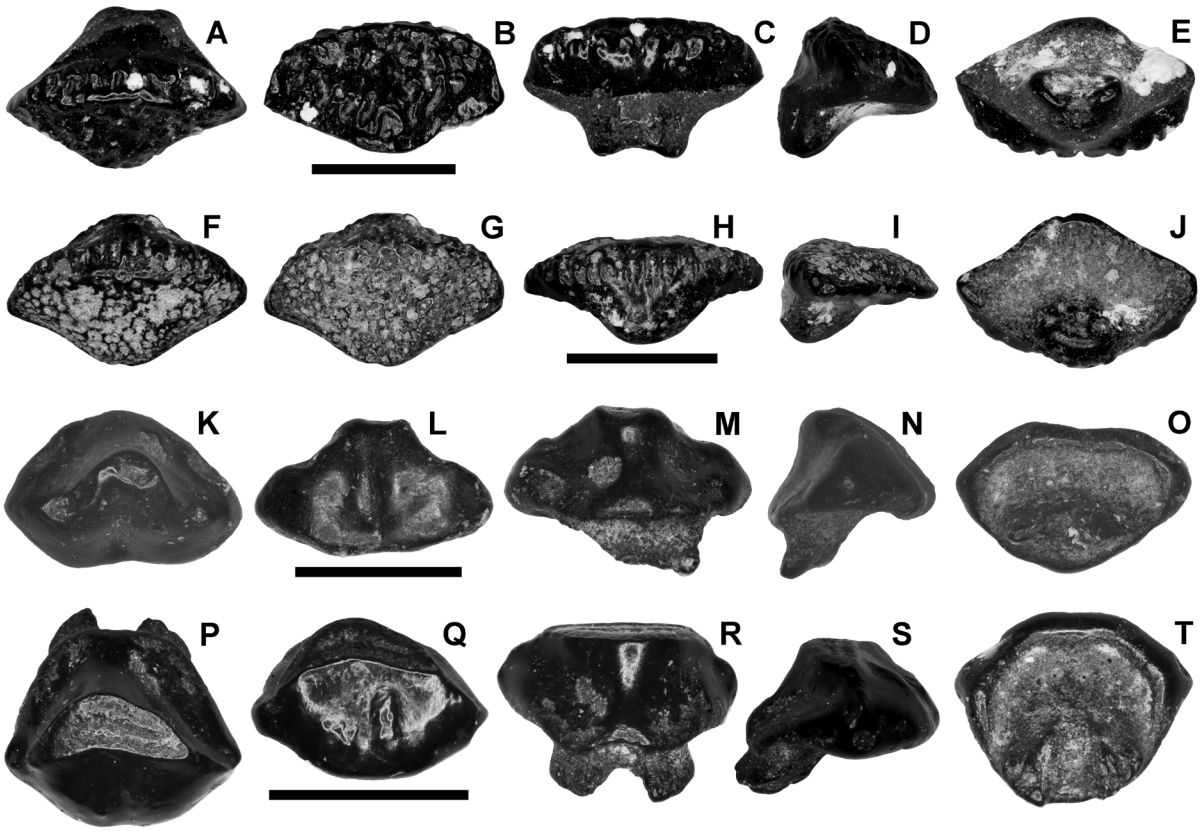

Fig. 18. *Hypanus*? *heterodontus* sp. nov. (A–J) and Dasyatidae gen. et sp. indet. (K–T), teeth. **A–E**. SC2013.28.475, *Hypanus*? *heterodontus*, tooth. **A**. Occlusal view. **B**. Labial view. **C**. Lingual view. **D**. Profile view. **E**. Basal view. **F–J**. SC2013.28.470, *Hypanus*? *heterodontus*, tooth. **F**. Occlusal view. **G**. Labial view. **H**. Lingual view. **I**. Profile view. **J**. Basal view. **K–O**. SC2013.28.429, Dasyatidae gen. et sp. indet., tooth. **K**. Occlusal view. **L**. Labial view. **M**. Lingual view. **N**. Profile view. **O**. Basal view. **P–T**. SC2013.28.430, Dasyatidae gen. et sp. indet., tooth. **P**. Occlusal view. **Q**. Labial view. **R**. Oro-lingual view. **S**. Profile view. **T**. Basal view. Scale bars = 2 mm.

Cicimurri & Knight (2009) reported two dasyatid morphotypes from the Chattian Chandler Bridge Formation that are similar to "*Hypanus*" specimens from the Catahoula Formation. Both morphotypes are slightly larger than the Catahoula specimens, and material identified as *Dasyatis cavernosa* (Probst, 1877) by Cicimurri & Knight (2009: fig. 8a) has a narrower transverse crest and more extensive labial ornamentation compared to *Hypanus*? *heterodontus* sp. nov. A tooth referred to *D. rugosa* (Probst, 1877) by Cicimurri & Knight (2009: fig. 8c) is also comparable to certain Catahoula Formation specimens, but the ornamentation on the South Carolina taxon appears to consist of indistinct rugosities rather than interconnected ridges. Gynandric heterodonty was also documented in the Chandler Bridge sample, as a male tooth attributed to *D. cavernosa* (Probst, 1877) by Cicimurri & Knight (2009: fig. 8b) is quite similar to male teeth of *Hypanus*? *heterodontus* from the Catahoula Formation (Fig. 17K).

The low-crowned teeth of *Hypanus*? *heterodontus* sp. nov. appear to have a more consistently developed apical labial depression and less organized reticulated ornamentation compared to equivalent teeth from the Oligo-Miocene of Germany identified as *Dasyatis delfortriei* Cappetta, 1970 (Reinecke *et al.* 2005; Haye *et al.* 2008). The high-crowned (male) teeth of the latter taxon also have a distinctive reticulated labial crown ornamentation compared to similarly shaped teeth of the former taxon (see also Reinecke *et al.* 2023: text-fig. 1). Low-crowned teeth of the Oligocene *Dasyatis rugosa* from Germany appear to have a more convex basal portion of the labial face as well as more extensive ornamentation compared to the Catahoula Formation specimens, and high-crowned teeth of the former are also more extensively ornamented compared to *Hypanus*? *heterodontus* (Haye *et al.* 2008; Reinecke *et al.* 2008). Low-crowned teeth of *Dasyatis strangulata* (Probst, 1877) from the Oligo-Miocene of Germany (Reinecke *et al.* 2008, 2014; also Reinecke & Radwański 2015) lack an apical labial depression, as typically occurs on the Catahoula Formation low-crowned specimens. Additionally, low-crowned teeth of *Dasyatis* sp. from the Thalberg Beds have more strongly developed crown ornamentation compared to the Catahoula Formation specimens, and the ornamentation on male teeth extends onto the transverse crest of the former but not on the latter (Reinecke *et al.* 2014). Low-crowned teeth of *T. cavernosus* from Miocene strata appear to have a more concave labial face framed by a conspicuous transverse ridge-like structure, a morphology quite obvious on extant *Taeniurops grabatus* (Villafaña *et al*. 2020; Reinecke *et al.* 2023).

Dasyatidae gen. et sp. indet.
18K–T

Material examined

UNITED STATES OF AMERICA – **Mississippi •** 3 isolated teeth; Catahoula Formation; SC2013.28.429 (Fig. 18K–O), SC2013.28.430 (Fig. 18P–T), SC2013.28.479.

Description

The large dasyatid teeth are wider (mesio-distally) than long (labio-lingually). Specimen SC2013.28.429 measures 4 mm wide and 3 mm long, and SC2013.28.430 measures 3 mm and 2.5 mm, respectively, in these dimensions. In occlusal view, the crown is divided into labial and lingual parts by a sharp transverse crest (Fig. 18K, P) that does not reach the mesial and distal base of the crown (Fig. 18N, S). The lingual side of the crown is more expansive, and its margin is strongly convex but may be somewhat squared. The labial margin is weakly to moderately convex. The labial face of S2013.28.429 is concave medially but otherwise weakly convex mesio-distally, whereas SC2013.28.430 has a more uniformly convex labial face. In profile view, the labial crown foot is highly convex, but apically the surface is relatively flat. Both specimens have a broad but low, medially located, and rounded ridge that divides the lingual face into concave mesial and distal parts (Fig. 18M, R). This ridge intersects with the cusp apex, which is flat on both specimens due to in vivo wear. The worn occlusal surface of both specimens exhibits an elliptical to D-shaped outline and the internal dentine is visible (Fig. 18K, P). In labial view, the cusp on SC2013.28.429 is more clearly distinguished (Fig. 18L), and in profile view it appears to

be distally curved (Fig. 18N). The crown of SC2013.28.430 is more extensively worn and the nature of the cusp is unknown. The crown enameloid is smooth, although SC2013.28.430 exhibits two unusual, indistinct node-like features on the labial face. The crown extends well beyond the root labially and laterally (Fig. 18R–S). The root of both specimens is ablated, but that on SC2013.28.430 is low and completely divided into two lobes by a nutritive groove (Fig. 18T). In basal view, a foramen is located within the groove, and root lobes have a crescent-shaped outline. The basal view also makes evident how small the root is compared to the size of the crown, that enameloid extends onto the underside of the crown (especially labially), and the root lobes extend beyond the lingual crown margin (Fig. 18O, T).

Remarks

Specimens SC2013.28.429 and SC2013.28.430 are of large size and have unornamented enameloid, which clearly distinguishes them from the teeth of *Hypanus*? *heterodontus* sp. nov. that also occur in the Catahoula Formation (see above). Specimen SC2013.28.429 is highly ablated but is comparable to, although smaller than, SC2013.28.430. Cicimurri & Knight (2009) reported a similarly large and smooth-crowned dasyatoid tooth morphology from the Chattian Chandler Bridge Formation of South Carolina, which Reinecke *et al.* (2014) proposed as a possible representative of *Taeniurops*. However, teeth of extant *Taeniurops grabatus* exhibit a conspicuous labial depression not observed on the U.S. Oligocene specimens. Additionally, teeth of extant *Dasyatis pastinaca* (Linnaeus, 1758) and *Neotrygon orientalis* Last, White & Séret, 2016 have smooth crowns and superficially similar tooth shapes, further complicating our ability to accurately identify the Catahoula Formation specimens (see Reinecke *et al.* 2023). Specimens SC2013.28.429 and SC2013.28.430 are reminiscent of Middle Miocene specimens from France that Cappetta named *Dasyatis serralheiroi* (Cappetta 1970: 92–95, pl. 20 figs 1–16. However, we hesitate to identify the material beyond the family level due to the limited comparative material available to us.

Family Myliobatidae Bonaparte, 1840a

Genus ***Myliobatis*** Cuvier, 1816

Type species

Raja aquila Linnaeus, 1758, Extant.

"*Myliobatis*" sp.
Fig. 19A–L

Material examined

UNITED STATES OF AMERICA – **Mississippi** • 170 isolated teeth; Catahoula Formation; MMNS VP-12061 (21 teeth), MMNS VP-12062 (Fig. 19A–C), SC2013.28.363 (Fig. 19D–F), SC2013.28.364 (Fig. 19G–I), SC2013.28.365 to 28.370, SC2013.28.371 (3 teeth), SC2013.28.372 (2 teeth), SC2013.28.373 (3 teeth), SC2013.28.374 (2 teeth), SC2013.28.375, SC2013.28.376, SC2013.28.377 (13 teeth), SC2013.28.378, SC2013.28.379, SC2013.28.380 (18 teeth), SC2013.28.381 (40 teeth), SC2013.28.382 (54 teeth) • 1 dentition; Catahoula Formation; MMNS VP-12063 (Fig. 19J–L).

Description

This sample contains teeth that are much wider (mesio-distally) than long (labio-lingually). In occlusal view, the crown is six-sided, with somewhat rounded lateral angles that are located closer to the labial margin, and the overall shape ranges from arcuate (i.e., the labial margin concave and lingual margin convex) to straight (Fig. 19A, D, G). Other teeth have a four-sided, squared appearance in occlusal view due to the significantly reduced area of the labial and lingual crown faces. Width and length dimensions of these latter teeth are roughly equal. In profile view, the labial and lingual faces of all teeth

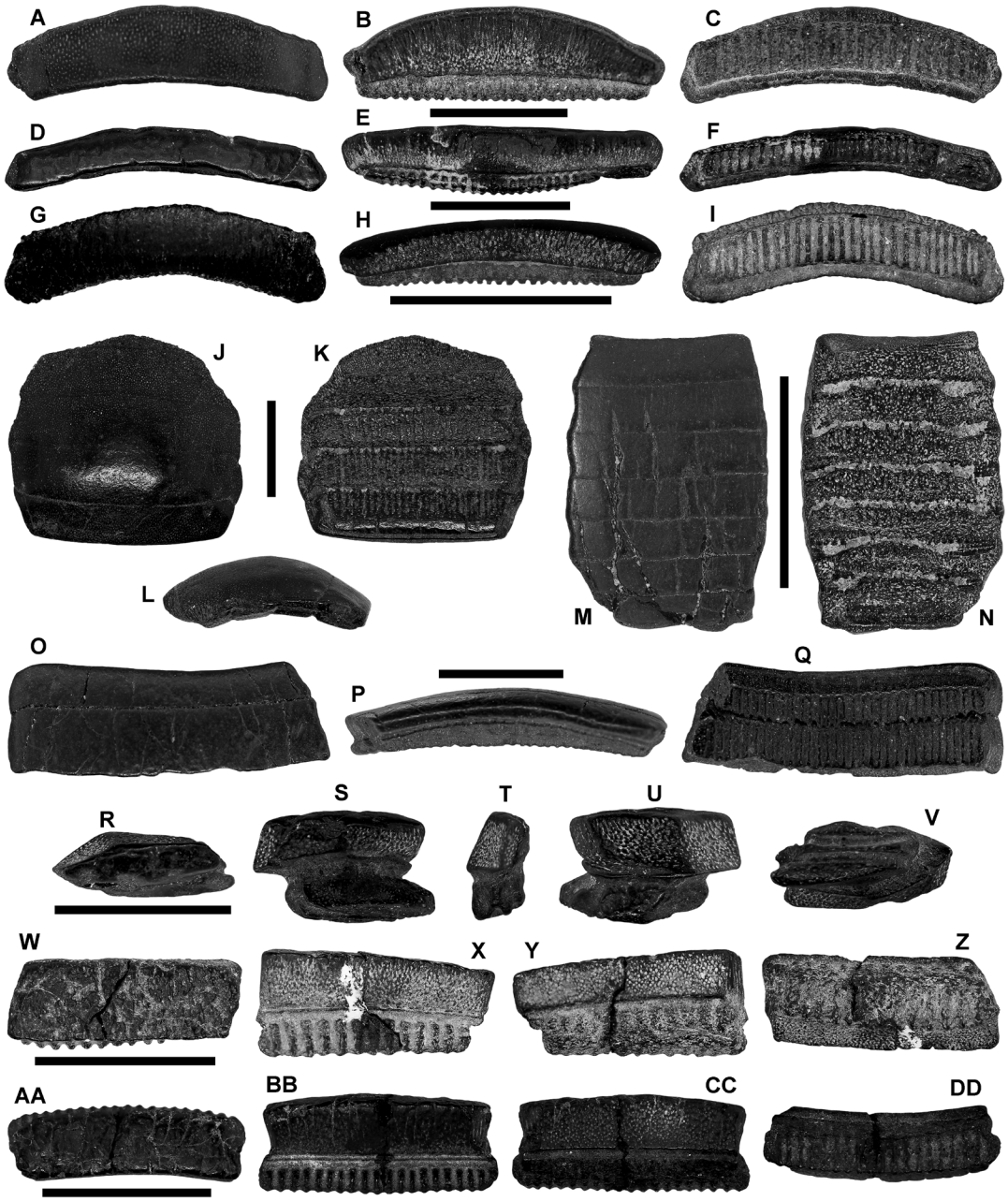

Fig. 19. "*Myliobatis*" sp. (A–L) and "*Aetomylaeus*" sp. (M–DD), teeth. **A–C**. MMNS VP-12062, "*Myliobatis*" sp., upper symphyseal tooth. **A**. Occlusal view. **B**. Labial view. **C**. Basal view. **D–F**. SC2013.28.363, "*Myliobatis*" sp., lower symphyseal tooth. **D**. Occlusal view. **E**. Labial view. **F**. Basal view. **G–I**. SC2013.28.364, "*Myliobatis*" sp., upper symphyseal tooth. **G**. Occlusal view. **H**. Labial view. **I**. Basal view. **J–L**. MMNS VP-12063, "*Myliobatis*" sp., upper tooth plate. **J**. Occlusal view. **K**. Basal view. **L**. Left profile view. **M–N**. MMNS VP-12064.1, "*Aetomylaeus*" sp., lower tooth plate. **M**. Occlusal view. **N**. Basal view. **O–Q**. MMNS VP-12065, "*Aetomylaeus*" sp., fragmentary upper tooth plate. **O**. Occlusal view. **P**. Labial view. **Q**. Basal view. **R–V**. MMNS VP-12066, "*Aetomylaeus*" sp., lateral tooth. **R**. Occlusal view. **S**. Distal view. **T**. Labial view. **U**. Mesial view. **V**. Basal view. **W–Z**. SC2013.28.383, "*Aetomylaeus*" sp., partial symphyseal tooth. **W**. Occlusal view. **X**. Lingual view. **Y**. Labial view. **Z**. Basal view. **AA–DD**. SC2013.28.384, "*Aetomylaeus*" sp., partial symphyseal tooth. **AA**. Occlusal view. **BB**. Lingual view. **CC**. Labial view. **DD**. Basal view. Scale bars: A–L, O–DD = 1 cm; M–N = 2 cm.

are lingually inclined, although one large specimen demonstrates a very thick crown with a concave labial (and convex lingual) crown foot transitioning to a more vertical face. The labial face of relatively unworn crowns bears a reticulated network of ridges near the crown foot, which transitions to irregular vertical ridges towards the apex (Fig. 19B). The lingual face is tuberculated basally but otherwise exhibits irregular vertical ridges towards the apex. The labial crown foot may be formed into a thin ridge-like projection that overhangs the root. The lingual crown foot bears a thin, shelf-like transverse ridge that further distinguishes the crown from the root. The crown also overhangs the root on the mesial and distal sides, but lingually the root extends a short distance beyond the transverse ridge. The root is low and may have a straight or convex basal attachment surface, depending on tooth position. The labial face of the root is weakly lingually inclined. In basal view, the root is differentiated into numerous thin, closely spaced, parallel lamellae by nutritive grooves (Fig. 19C, F, I).

Remarks

Monognathic, dignathic, and ontogenetic heterodonty are evident in our sample. Monognathic heterodonty is expressed as a drastic transition (disjunct heterodonty) from very wide teeth of symphyseal files to more symmetrical, roughly diamond-shaped teeth in lateral files, the exact number of which in the dentition of this ray is unknown. Upper symphyseal teeth can be identified by their convex occlusal outline and straight basal attachment surface (Fig. 19B, H). In contrast, lower symphyseal teeth have a straight occlusal outline and convex basal attachment surface (Fig. 19E). We could not identify a feature among the fossil specimens that would allow the upper lateral teeth to be differentiated from those in the lower files. Ontogenetic variation is apparent based on the morphological criteria noted for "*Rhinoptera*" sp. (see below). MMNS VP-12063 (Fig. 19J–L) is an ablated upper dentition consisting of fused symphyseal and lateral teeth. The specimen shows that the upper dentition was convex both labio-lingually and mesio-distally.

The teeth we identify as "*Myliobatis*" sp. differ from those of "*Rhinoptera*" sp. by their basally reticulated to apically ridged labial crown faces, basally tuberculated to apically ridged lingual crown faces, lateral angles that are located closer to the labial crown margin, thin and shelf-like lingual transverse ridge at the crown foot, and root lamellae that extend beyond the lingual crown foot. Although these teeth exhibit morphological similarities to those of extant *Myliobatis*, molecular divergence estimates indicate that most extant myliobatid genera diverged from one another at sometime during the Early-to-Middle Miocene (Villalobos-Segura & Underwood 2020). This, in turn, indicates that the early Chattian teeth in our sample likely belong to a genus that is ancestral to extant *Myliobatis*. Therefore, herein we refer these teeth to "*Myliobatis*" with the understanding that future studies may assign this morphology to a new stem genus within the *Myliobatis* lineage.

Genus ***Aetomylaeus*** Garman, 1908

Type species

Myliobatus maculatus Gray 1834, Extant.

"*Aetomylaeus*" sp.
Fig. 19M–DD

Material examined

UNITED STATES OF AMERICA – **Mississippi** • 49 isolated teeth; Catahoula Formation; MMNS VP-12064 (3 teeth), MMNS VP-12065 (4 teeth), MMNS VP-12066 (Fig. 19R–V), SC2013.28.383 (Fig. 19W–Z), SC2013.28.384 (Fig. 19AA–DD), SC2013.28.385 to 28.388, SC2013.28.389 (8 teeth), SC2013.28.390, SC2013.28.391 (3 teeth), SC2013.28.392 (3 teeth), SC2013.28.393 (20 teeth) • 2 dentitions; Catahoula Formation; MMNS VP-12064.1 (Fig.19M–N), MMNS VP-12065.1 (Fig. 19O–Q).

Description

Teeth in the sample are generally mesio-distally much wider than long (labio-lingually). In occlusal view, the six-sided crown exhibits obtuse lateral angles that are located closer to the lingual margin, and the occlusal outline ranges from straight to slightly arcuate. Other teeth have a four-sided appearance in occlusal view due to the diminutive area of the labial and lingual faces. These teeth are much longer (labio-lingually) than wide (mesio-distally) and have an elongated diamond-shaped outline (Fig. 19R). In profile view, the labial and lingual faces of all teeth are lingually inclined (Fig. 19U). Well-preserved teeth show that the labial face bears a reticulated network of ridges that may transition to vertical ridges near the apex (Fig. 19Y, CC). The lingual face is largely tuberculated but bears irregular vertical ridges near the apex (Fig. 19X, BB). The labial crown foot overhangs the root, and the basal surface exhibits a longitudinal furrow. A very thin and sharp transverse ridge occurring at the lingual crown foot is inconspicuous. The crown also overhangs the root on the mesial and distal sides, but lingually the root extends well beyond the crown foot. The root is low and may have a straight or convex basal attachment surface, depending on tooth position. In basal view, the root is differentiated into numerous thin, closely spaced, parallel lamellae by nutritive grooves (Fig. 19Z, DD).

Remarks

Monognathic, dignathic, and ontogenetic heterodonty in our sample was determined based on the morphological criteria described above for "*Myliobatis*" sp. Specimens MMNS VP-12064.1 (Fig. 19M–N) and 12065.1 (Fig. 19O–Q) show that the lower dentition was flat labio-lingually and mesio-distally. Symphyseal teeth of "*Aetomylaeus*" sp. can be separated from "*Myliobatis*" sp. and "*Rhinoptera*" sp. (see below) by the more uniformly reticulated ornamentation on the labial and lingual faces, lateral angles that are located closer to the lingual crown margin, the very thin and inconspicuous transverse ridge at the lingual crown foot, and a root that extends well beyond the lingual crown foot. Lateral teeth of "*Aetomylaeus*" sp. (Fig. 19R–V) also differ from those of "*Myliobatis*" sp. by their being labio-lingually longer than mesio-distally wide (whereas they are roughly equal in these dimensions in the latter taxon). Except for the ultimate lateral file, lateral teeth of "*Rhinoptera*" sp. are all six-sided. Those from medial lateral positions are roughly hexagonal, whereas the ultimate lateral tooth has a pentagonal occlusal outline. We note that specimens are often worn through in vivo use down to the crown foot. However, even highly worn specimens can be accurately identified based on the nature of the lingual transverse ridge and lingual elongation of the root.

It is difficult to determine the Oligocene geographic and stratigraphic distribution of "*Aetomylaeus*" because: 1) Oligocene fish faunas in the USA are relatively uncommon and 2) Paleogene Myliobatidae teeth generally appear to be (mis)identified as *Myliobatis* or *Rhinoptera* simply based on overall shape (see discussion in Ebersole *et al.* 2019). Cicimurri & Knight (2009) reported a tooth from the Chattian Chandler Bridge Formation of South Carolina (as Myliobatidae gen. indet.) that compares favorably to the Catahoula Formation "*Aetomylaeus*" sp. Ebersole *et al.* (2021) recently reported similar teeth derived from the Rupelian (NP23) Byram Formation of Alabama that they identified as "*Aetomylaeus*" sp. As with "*Myliobatis*" sp., the teeth in our sample likely represent an undescribed Oligocene member of the extant *Aetomylaeus* lineage and are therefore referred to herein as "*Aetomylaeus*" sp.

Family Rhinopteridae? Jordan & Evermann, 1896

Genus ***Rhinoptera*** Cuvier, 1829

Type species

Myliobatis marginata Geoffroy Saint-Hilaire, 1817, Extant.

"*Rhinoptera*" sp.
Fig. 20

Material examined

UNITED STATES OF AMERICA – **Mississippi •** 110 isolated teeth; Catahoula Formation; MMNS VP-12059 (Fig. 20E–H), MMNS VP-12060 (Fig. 20I–L), SC2013.28.336 to 28.343, SC2013.28.344 (Fig. 20A–D), SC2013.28.345, SC2013.28.346, SC2013.28.347 (Fig. 20M–Q), SC2013.28.348 to 28.353, SC2013.28.354 (4 teeth), SC2013.28.355 (3 teeth), SC2013.28.356 (4 teeth), SC2013.28.357 (10 teeth), SC2013.28.358 (11 teeth), SC2013.28.359 (4 teeth), SC2013.28.360 (4 teeth), SC2013.28.361 (12 teeth), SC2013.28.362 (38 teeth).

Description

Teeth vary in width, and relatively unworn specimens exhibit a thick crown. In occlusal view, the crown is six-sided with sharp and centrally located lateral angles that are acute to roughly 90º. The overall shape is variable (straight, sinuous, or weakly convex). In profile view, the labial and lingual faces are vertical to slightly lingually inclined. The labial and lingual faces are generally heavily corrugated with vertical ridges, which are overprinted with finer vertical ridges (Fig. 20J–K). The ornamentation on the lingual face is usually less developed than on the labial face, and ornament appears to become obsolete apically. Some specimens show that lingual ornamentation can consist of short basal vertical ridges that transition apically to beaded ridges. The labial crown face overhangs the root, and the basal surface of the crown base bears a shallow transverse furrow. The lingual crown foot is marked by a very thick and rounded, shelf-like transverse ridge. The root is low with nearly vertical labial and lingual faces. In basal view, the root is subdivided into numerous thin, parallel lamellae by nutritive grooves. The lamellae are perpendicular or oblique to the tooth width (Fig. 20H). The lingual face of the root does not extend beyond the crown foot.

Lateral teeth vary in mesio-distal width but are generally six-sided and similar to the symphyseal teeth in all other aspects. The ultimate lateral tooth, the last tooth at the margin of the dentition, has a five-sided occlusal outline. The mesial side has a sharply angular margin, whereas the distal side is a straight edge that parallels the length of the dentition. The crown of lateral teeth is higher on the mesial side than on the distal side (Fig. 20C, J). Root lamellae are oblique to crown width (Fig. 20D, L).

Remarks

Monognathic and ontogenetic heterodonty are evident in our sample. Monognathic heterodonty is expressed as a transition from a very wide symphyseal file to lateral files that become progressively less wide (gradient heterodonty) towards the commissure. From the symphysis (Fig. 20E–H), the mesio-distal tooth width in succeeding lateral files progressively decreases from roughly three times as wide as long (Fig. 20I–L) to two times as wide as long (Fig. 20M–Q), to symmetrically hexagonal. The exact number of files of each morphology is unknown, as our sample does not include complete tooth plates. The margin of the dentition was formed of teeth with a pentagonal outline, where the mesial margin is angular and the distal margin straight. Dignathic heterodonty is difficult to discern based on the sample, but transversely convex specimens (Fig. 20G) may have comprised the upper dentition. Overall, these teeth are arched, but there is a medial region where the crown is worn flat. In contrast, relatively flat teeth with roughly uniformly worn crowns were likely part of the lower dentition. Ontogenetic heterodonty is identified based on the variation in tooth size within the sample available to us, which presumably reflects juvenile (i.e., smaller teeth) and adult specimens.

Cicimurri *et al.* (2022) reported "*Rhinoptera*" sp. teeth from the Rupelian Ashley Formation, and Cicimurri & Knight (2009) identified *Rhinoptera* cf. *studeri* (Agassiz, 1843) from the Chattian Chandler Bridge Formation of South Carolina. These identifications were based on very limited and fragmentary

specimens, and it is difficult to make accurate comparisons between that material and the Catahoula Formation sample. Müller (1999) identified *R*. aff. *brasiliensis* Müller, 1836 and *R*. aff. *bonasus* Mitchill, 1815 in his sample of teeth from the Oligo-Miocene Belgrade Formation of North Carolina. That material does appear to be similar to the Catahoula Formation sample in terms of gross morphology and crown ornamentation on the vertical faces. However, it is unlikely that the fossil specimens represent extant taxa, particularly considering that the genus *Rhinoptera* apparently did not diverge from Myliobatidae until the Miocene (Naylor *et al.* 2012; Villalobos-Segura & Underwood 2020). Additionally, the variation we observed in the Catahoula Formation sample, which is also reflected in the sample reported by Müller (1999), is attributed herein to intraspecific variation (heterodonty) rather than the presence of multiple species. This interpretation is supported by the work of Hovestadt & Hovestadt-Euler (2013), who documented variation within dentitions of extant myliobatiform species. We follow other authors in placing the generic name *Rhinoptera* in quotation marks to acknowledge the dental similarities between the Oligocene taxon and extant *Rhinoptera*, and to address the temporal separation of the occurrences (Ebersole *et al.* 2019; Cicimurri *et al.* 2022).

We place the Catahoula Formation taxon within Rhinopteridae following the conclusions of phylogenetic studies for extant *Rhinoptera* (i.e., Palacios-Barreto *et al*. 2023) and the very close similarity of the fossil teeth to those of extant members of this genus. However, this assignment is tentative if *Rhinoptera*/Rhinopteridae diverged from Myliobatidae during the Miocene. Ebersole *et al.* (2019) reported "*Rhinoptera*" sp. teeth from Ypresian, Lutetian, and Bartonian strata of Alabama that were all comparable to each other in terms of overall shape and crown ornamentation. Those authors therefore

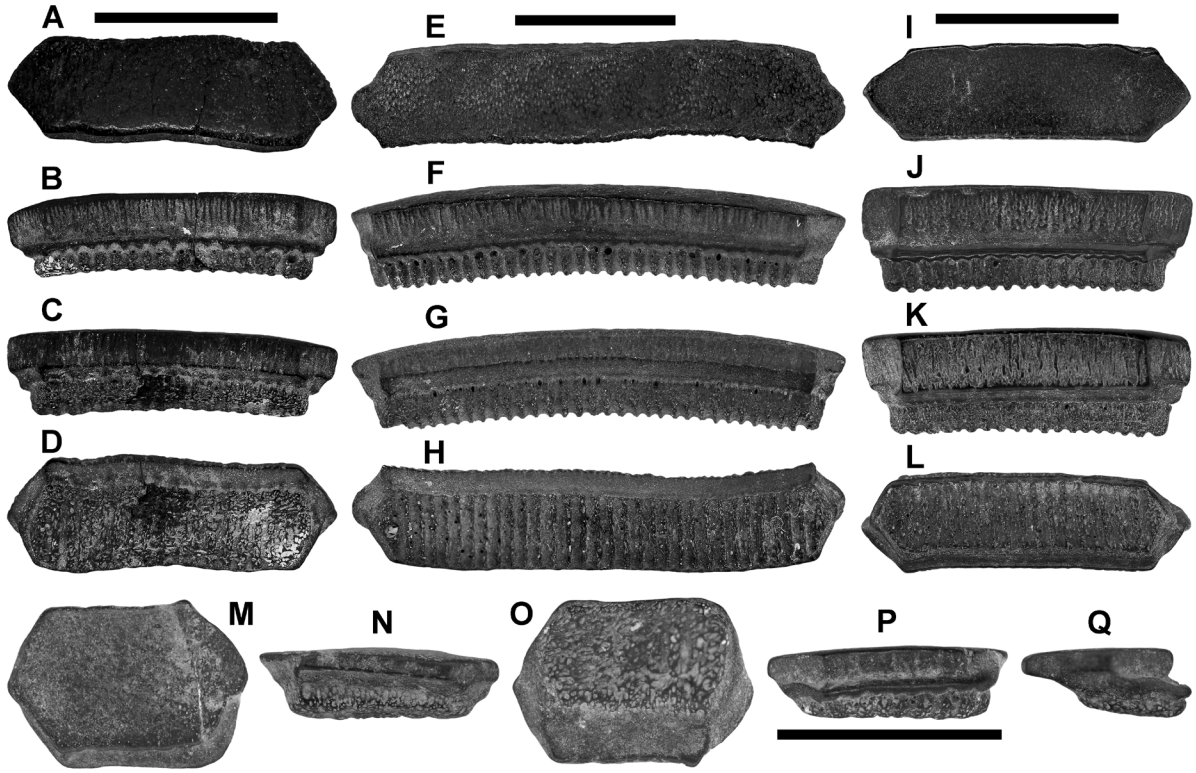

Fig. 20. "*Rhinoptera*" sp., teeth. **A–D**. SC2013.28.344, proximal lateral tooth. **A**. Occlusal view. **B**. Lingual view. **C**. Labial view. **D**. Basal view. **E–H**. MMNS VP-12059, upper symphyseal tooth. **E**. Occlusal view. **F**. Lingual view. **G**. Labial view. **H**. Basal view. **I–L**. MMNS VP-12060, proximal lateral tooth. **I**. Occlusal view. **J**. Lingual view. **K**. Labial view. **L**. Basal view. **M–Q**. SC2013.28.347, distal lateral tooth. **M**. Occlusal view. **N**. Labial view. **O**. Basal view. **P**. Lingual view. **Q**. Profile view. Scale bars = 1 cm.

could not determine, based on tooth shape alone, whether one or more species were represented in their temporally wide-ranging sample. The Catahoula Formation "*Rhinoptera*" sp. specimens exhibit features comparable to those Eocene examples (i.e., vertical ridges sometimes transitioning to apical beaded ridges, wide lingual transverse ridge), and we therefore refrain from making a more specific determination without the aid of more complete (i.e., skeletal) material.

Family Mobulidae Gill, 1893?

Genus ***Plinthicus*** Cope, 1869

Type species

Plinthicus stenodon Cope, 1869, Oligocene (Rupelian), New Jersey, USA.

Plinthicus sp.
Fig. 21A–D

Material examined

UNITED STATES OF AMERICA – **Mississippi** • 1 isolated tooth; Catahoula Formation; SC2013.28.522.

Description

The tooth is wider than long (4.5 mm and 2.5 mm in these dimensions), and the crown measures 2 mm in height. In occlusal view, the crown has a roughly oval outline, and the occlusal surface is concave. The labial margin is thickened and forms a conspicuous rim around the depressed oral surface, but the lingual margin is thin and developed into a thin, lingually directed, shelf-like projection. In profile view, the labial and lingual faces are highly inclined (Fig. 21D), and the surfaces bear numerous robust, irregular vertical ridges. The labial crown foot is formed into a sharp projection that overhangs the root (Fig. 21C), whereas there is a thick and rounded transverse ridge at the lingual crown foot (Fig. 21A). The root is not well preserved but appears to have been smaller in area than the crown.

Remarks

Specimen SC2013.28.522 is easily distinguished from the superficially similar myliobatiform teeth described above by its concave occlusal surface, thinner profile, and coarse vertical ridges on the labial and lingual faces. *Plinthicus* has been reported from Oligocene strata of South Carolina (Cicimurri & Knight 2009; Cicimurri *et al.* 2022), but it is difficult to accurately compare the ablated Catahoula Formation specimen to the South Carolina material. However, Cicimurri *et al.* (2022) indicated that the Ashley Formation specimens (ca 28.5 Ma) differed from Mio-Pliocene *P. stenodon* Cope, 1869 and could represent a new species. The Catahoula Formation tooth clearly differs from *P. kruibekensis* Bor, 1990 from the Rupelian Boom Clay Formation of Belgium by its inclined labial and lingual faces that bear coarse but few vertical ridges. In contrast, the Belgian taxon has a convex labial and concave lingual face that bears finer and more numerous vertical ridges. Although recent taxonomic rankings place extant filter-feeding "devil rays" within Mobulidae (i.e., Notabartolo di Sciara 2020), it may not be correct to include all extinct mobulid-like taxa within this family. Villalobos-Segura & Underwood (2020) presented molecular divergence times for various batoid taxa that indicate that the clade containing Mobulidae did not diverge from its common ancestor until the Early Miocene. Therefore, it does not appear to be prudent to refer Paleogene mobulid-like teeth of presumed planktivorous rays to Mobulidae. However, for the purposes of this report we tentatively follow convention for familial assignment of this genus.

Genus ***Paramobula*** Pfeil, 1981

Type species

Manta fragilis Cappetta, 1970, Middle Miocene, southern France.

Paramobula fragilis (Cappetta, 1970)
Fig. 21E–N

Mantra fragilis Cappetta, 1970: 112–113.

Material examined

UNITED STATES OF AMERICA – **Mississippi** • 2 isolated teeth; Catahoula Formation; MMNS VP-8429 (Fig. 21E–I), MMNS VP-11678 (Fig. 21J–N).

Description

The crown is wider than long and labio-lingually thin. MMNS VP-8429 measures 4.2 mm in mesio-distal width and 2.2 mm in total apico-basal height, whereas MMNS VP-11678 is 3.5 mm and 3 mm in these dimensions. The labial and lingual faces are lingually inclined and heavily ornamented with longitudinal ridges. These ridges may be wide and widely separated, or thin and closely spaced, or some combination of both (compare Fig. 21E to J). The ornamentation on the lingual face (Fig. 21G, L) is somewhat less extensive than that on the labial face. The labial crown foot of MMNS VP-11687 is somewhat ridge-like and the lingual crown foot is formed into a shelf-like projection. The crown base of MMNS VP-8429 is

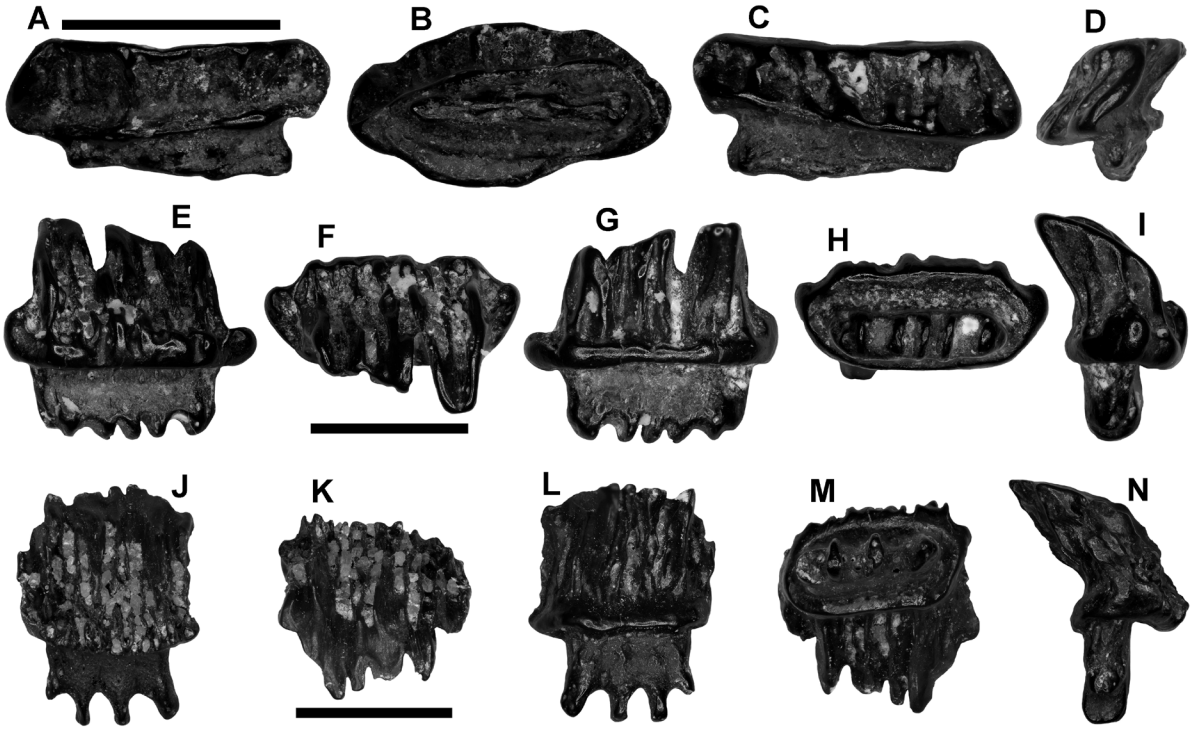

Fig. 21. *Plinthicus* sp. (A–D) and *Paramobula fragilis* (Cappetta, 1970) (E–N), teeth. **A–D**. SC2013.28.522, *Plinthicus* sp., lateral tooth. **A**. Lingual view. **B**. Basal view. **C**. Labial view. **D**. Profile view. **E–I**. MMNS VP-8429, *Paramobula fragilis*, tooth. **E**. Labial view. **F**. Occlusal view. **G**. Lingual view. **H**. Basal view. **I**. Distal view. **J–N**. MMNS VP-11678, *P. fragilis*, tooth. **J**. Labial view. **K**. Occlusal view. **L**. Lingual view. **M**. Basal view. **N**. Distal view. Scale bars = 3 mm.

formed into a robust cingulum that extends around the entire perimeter. The complex occlusal surface is flat to weakly depressed and has very irregular labial and lingual margins (Fig. 21F, K). Additionally, in profile view, the occlusal surface is lingually inclined and rather straight (Fig. 21I). The root is high but labio-lingually thin, and it is located close to the lingual crown margin (Fig. 21N). The basal surface is subdivided into four or five thin lamellae by wide and shallow nutritive grooves (Fig. 21H, M).

Remarks

These two teeth clearly differ from that of *Plinthicus* sp. (see above) by the much coarser labial and lingual ornamentation and by the flat occlusal surface that has a highly irregular outline. In contrast, the *Plinthicus* sp. tooth in our sample (SC2013.28.522) has a distinctively concave occlusal surface.

Specimens MMNS VP-8429 and MMNS VP-11678 are comparable to teeth that Cicimurri & Knight (2009) identified as *Paramobula fragilis* (Cappetta, 1970) from the Chandler Bridge Formation of South Carolina. Comparison of the Catahoula Formation teeth to a small sample from the Chandler Bridge Formation (SC2005.2) indicates that the material is conspecific. The taxon *Manta fragilis* was named by Cappetta (1970) based on teeth from the Middle Miocene (Langhian) of France (Cappetta 1970: pl. 28 fig. 10) that have a high, labio-lingually narrow crown that bears significant vertical ridges on the labial and lingual faces. Pfeil (1981) later erected the name *Paramobula* for this morphology, but Cappetta & Stringer (2002) and Cappetta (2012) synonymized the genus with *Mobula*. However, the *fragilis* morphology is significantly different from teeth of extant *Mobula* species (see Notabartolo di Sciara 1987) and fossil species like *M. loupianensis* Cappetta, 1970. We therefore resurrect *Paramobula* Pfeil, 1981 to accommodate the more *Plinthicus*-like nature of the *fragilis* morphotype.

Batomorphi fam., gen. et sp. indet.
Fig. 22A–L

Material examined

UNITED STATES OF AMERICA – **Mississippi** • 326 poorly preserved isolated teeth; Catahoula Formation; SC2013.28.394 to 28.398, SC2013.28.399 (2 specimens), SC2013.28.400 (49 specimens), SC2013.28.401 (19 specimens), SC2013.28.402 (16 specimens), SC2013.28.403 (17 specimens), SC2013.28.404 (218 specimens) • 9 dermal thorns; Catahoula Formation; MMNS VP-6650.1 (Fig. 22G–I), MMNS VP-6650.2 (Fig. 22D–F), MMNS VP-8066.1 (Fig. 22J–L), MMNS VP-8066.2, SC2013.28.405, SC2013.28.518, SC2013.28.520, SC2013.28.521, SC2013.28.528 • 43 caudal spines; Catahoula Formation; MMNS VP-7035 (13 specimens), MMNS VP-7035.1 (Fig. 22A–C), SC2013.28.480, SC2013.28.481, SC2013.28.482, SC2013.28.483 (16 specimens), SC2013.28.484, SC2013.28.485 (9 specimens).

Description

Several thorn-like denticles measuring up to 3.5 mm in antero-postero length and 2.5 mm in medio-lateral width consist of a rather small crown atop a taller and wider base. The crown is small, conical, and covered with smooth enameloid. Some of these denticles (i.e., Fig. 22D–F) have a high conical base that bears numerous widely spaced radiating furrows. Although the furrows reach the crown foot, they do not extend to the base of the crown. Other similar denticles (Fig. 22G–I) are laterally compressed with broad and nearly vertical sides that bear fine vertical striations. Both types of denticles have a circular to sub-rectangular basal outline (Fig. 22E, H), and the basal surface is weakly convex (Fig. 22D, G). An additional denticle morphotype is comprised of a triangular, highly distally inclined crown and very thin base (Fig. 22J–L). Smooth enameloid is limited to the dorsal surface of the crown. The base is flared outward from the crown, has a roughly triangular outline, and the basal surface is weakly concave.

The caudal spines in our sample are elongated, distally tapering, and dorso-ventrally flattened (Fig. 22A–C). The dorsal surface is covered by enameloid except for the distal end, where the element was embedded in soft tissue. The proximal end is also wide and spatulate, whereas the distal tip is

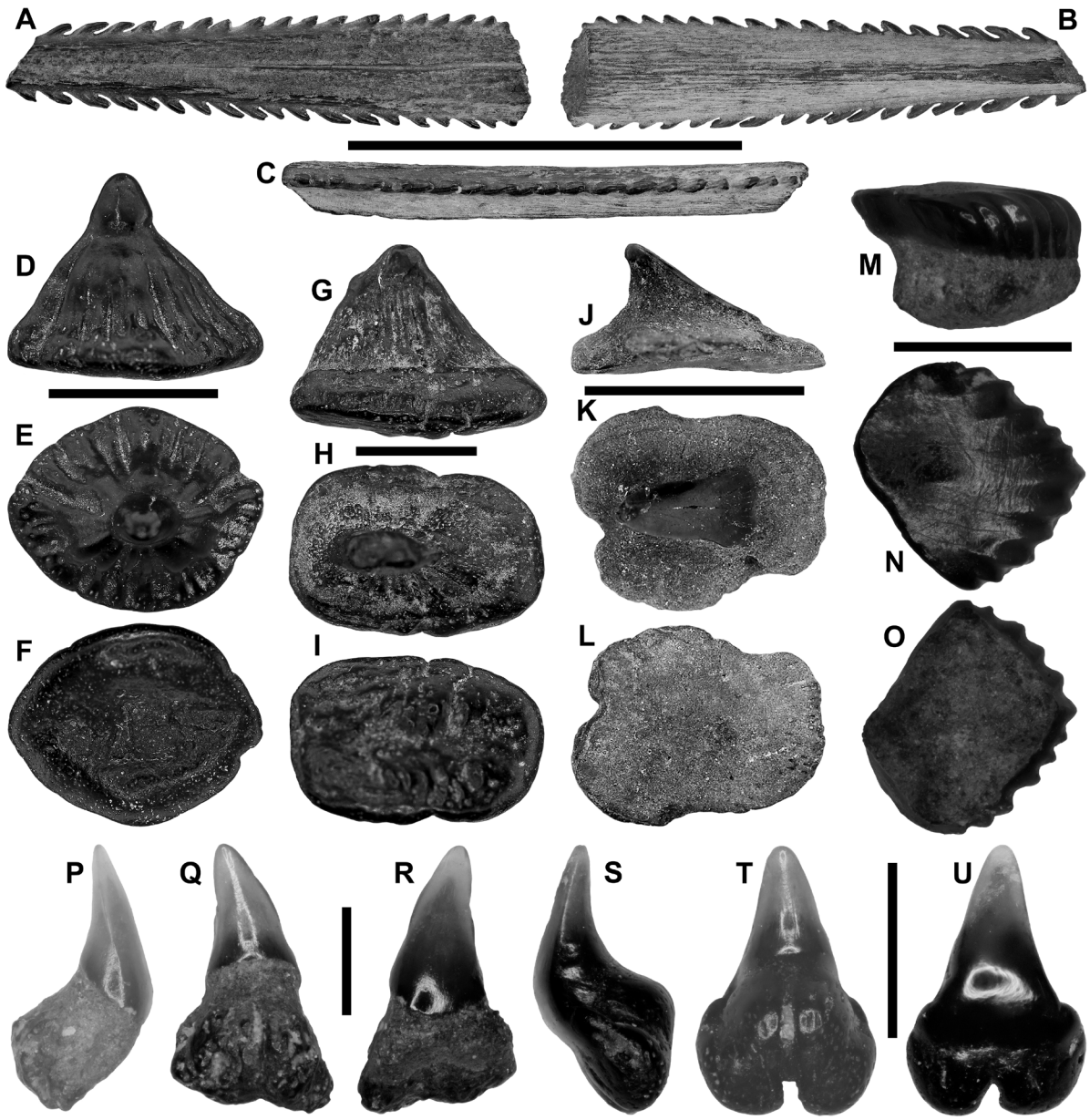

Fig. 22. Elasmobranchii indet., remains: Myliobatiformes gen. et sp. indet. (A–C), Batomorphi fam., gen. et sp. indet. (D–L), and Galeomorphii fam., gen. et sp. indet. (M–U). **A–C**. MMNS VP-7035.1, Myliobatiformes gen. et sp. indet., caudal spine. **A**. Dorsal view. **B**. Ventral view. **C**. Right profile view. **D–F**. MMNS VP-6650.2, Batomorphi fam., gen. et sp. indet., dermal denticle. **D**. Profile view. **E**. Apical view. **F**. Basal view. **G–I**. MMNS VP-6650.1, Batomorphi fam., gen. et sp. indet., dermal denticle. **G**. Profile view. **H**. Apical view. **I**. Basal view. **J–L**. MMNS VP-8066.1, Batomorphi fam., gen. et sp. indet., dermal denticle. **J**. Profile view. **K**. Apical view. **L**. Basal view. **M–O**. MMNS VP-7750, Galeomorphii fam., gen. et sp. indet., placoid scale. **M**. Profile view. **N**. Apical view. **O**. Basal view. **P–R**. MMNS VP-7753, Galeomorphii fam., gen. et sp. indet., symphyseal tooth. **P**. Distal view. **Q**. Lingual view. **R**. Labial view. **S–U**. MMNS VP-8741.1, Galeomorphii fam., gen. et sp. indet., symphyseal tooth. **S**. Distal view. **T**. Lingual view. **U**. Labial view. Scale bars: A–C = 2 cm; D–L = 5 mm; M–U = 1 mm.

sharply pointed. The ventral surface lacks enameloid and has a single robust, rounded medial ridge that parallels the spine length (Fig. 22B). The right and left lateral surfaces bear a single row of denticles. The closely spaced denticles are enameloid-covered, sharply angled proximally, and sharply pointed (Fig. 22A). Denticle size is consistent except for the distal tip, where they quickly decrease in size.

Remarks

The 326 highly worn symphyseal and lateral teeth represent elements from durophagous ray dentitions. These include complete and broken specimens with tooth crowns that have been worn through in vivo use down to, and beyond, the lingual transverse ridge. Many specimens have also been modified through post mortem transport, as they are polished and have rounded edges and corners. Thus, their taxonomically significant features, like crown ornamentation, shape of the lingual transverse ridge, and nature of the root lobes, are not preserved. We could therefore not determine whether the specimens represent "*Rhinoptera*" sp., "*Myliobatis*" sp., or "*Aetomylaeus*" sp., but they are included here for completeness and to document the overall abundance of durophagous ray teeth.

One thorn-like denticle morphology (not shown), represented by SC2013.28.405, is comparable to a denticle from the Chattian Chandler Bridge Formation of South Carolina that Cicimurri & Knight (2009) assigned to Dasyatidae (see their fig. 8e). MMNS VP-8066 (Fig. 22J–L) is reminiscent of dermal thorns referred to *Bathytoshia centroura* (Mitchill, 1815) by Purdy *et al.* (2001). Other denticles like those shown in Fig. 22D–F and G–I (also including SC2013.28.520, SC2013.28.521 and SC2013.28.528) are similar to each other and are believed to represent the same taxon. It is possible these represent one of the rhinopristiform fishes we identified by teeth (i.e., *Rhynchobatus*).

Although there is slight variation in the gross morphology of the caudal spines, the shape of the lateral denticles is consistent, and the specimens could represent the same taxon. Unfortunately, we cannot say with certainty to which species they belong, but it is likely they represent one (or more) of the taxa within Dasyatidae or Myliobatidae we identified by their teeth.

Euselachii fam., gen. et sp. indet.
Fig. 9C–D, 22M–U

Material examined

UNITED STATES OF AMERICA – **Mississippi •** 10 placoid scales; Catahoula Formation; MMNS VP-7750 (Fig. 22M–O), SC2013.28.330, SC2013.28.331 (2 specimens), SC2013.28.332, SC2013.28.333 (2 specimens), SC2013.28.334 (2 specimens), SC2013.28.529, SC2013.28.530 • 10 teeth; Catahoula Formation; MMNS VP-7753 (Fig. 22P–R), MMNS VP-8736, MMNS VP-8741.1 (Fig. 5–U), MMNS VP-8741.2, SC2013.28.115 (Fig. 9C–D), SC2013.28.264 (2 specimens), SC2013.28.265 (2 specimens), SC2013.28.268.

Description

Specimens assigned only to Euselachii indet. include teeth and placoid scales. Several small teeth consist of a simple triangular main cusp and bilobate root (Fig. 22P–U). The crown has smooth to weakly serrated cutting edges that may not extend to the apex or crown foot. The labial face is nearly flat, but the lingual face is convex, and both faces have smooth enameloid. The root is robust for the size of the tooth, and very short root lobes are separated by a well-developed lingual nutritive groove.

Placoid scales consist of an enameloid-covered crown and dentine base (Fig. 22M–O). The crown on each specimen is apico-basally flattened, and the apical surface may be weakly convex or flat. The apical outline is oval or rhomboidal. Several specimens have smooth enameloid, but others exhibit a series of

parallel ridges along the anterior margin (Fig. 22N). These ridges do not extend to the posterior margin. The base has a somewhat triangular outline in profile, and the basal surface is flat.

Remarks

Teeth like those shown in Fig. 22P and S probably belong to a member of Carcharhiniformes, as they are similar to the symphyseal and parasymphyseal teeth that occur in the jaws of extant *Carcharhinus* spp. that we examined. It is possible that specimens with serrated cutting edges are from the upper dentition, whereas those with smooth cutting edges are from the lower dentition. Several other shark teeth are too broken or abraded to be confidently identified beyond Euselachii. For example, SC2013.28.115 (Fig. 9C–D) is an ablated posterior tooth that bears similarity to the teeth of *Galeorhinus* (i.e., Fig. 9A–B), *Physogaleus* (i.e., Fig. 7EE–JJ), and *Rhizoprionodon* (i.e., Fig. 8A–D). The labial crown foot appears to be thickened as on *Galeorhinus* teeth, but this may be an artifact of preservation, as the root is abraded. Additionally, the distal heel is not as clearly separated from the cusp as it is in *Galeorhinus* (Fig. 9A; also see Herman *et al.* 2003). The short and somewhat pointed distal heel is reminiscent of *Physogaleus* (Reinecke *et al.* 2005; Haye *et al.* 2008) and even *Rhizoprionodon* (see Ebersole *et al.* 2023).

Isolated scales are rare in the elasmobranch component of the Catahoula Formation compared to isolated teeth. This phenomenon could be related to a collecting bias, but it may be an artifact of winnowing (removal of very small items through current action). At least two scale morphotypes are represented, including those with anterior ridges and those that are smooth. We cannot confidently assign these specimens to any particular elasmobranch genus that we identified by its teeth, nor can we determine whether more than one taxon is represented. However, specimens SC2013.28.334 and MMNS VP-7750 are similar to scales that Dillon *et al.* (2017) identified as ridged abrasion strength morphotypes (i.e., with a protective function), potentially of Ginglymostomatidae.

We include here for completeness nine isolated calcified cartilage tesserae (SC2013.28.335). These have a columnar appearance when viewed perpendicular to their length, and the surface is roughened. The outline is six-sided. We cannot determine what skeletal element (probably cranial) nor the species the tesserae represent.

Class Osteichthyes Huxley, 1880
Subclass Actinopterygii (sensu Goodrich 1930)
Unranked Neopterygii Regan, 1923
Infraclass Holostei Müller, 1845
Division Ginglymodi Cope, 1871
Order Lepisosteiformes Hay, 1929
Family Lepisosteidae Cuvier, 1825

Lepisosteidae gen. et sp. indet.
Fig. 23A–H

Material examined

UNITED STATES OF AMERICA – **Mississippi** • 109 isolated teeth; Catahoula Formation; MMNS VP-7685 (7 teeth), SC2013.28.627 to 28.629, SC2013.28.630 (Fig. 23G–H), SC2013.28.631, SC2013.28.632, SC2013.28.633 (9 teeth), SC2013.28.634 (25 teeth), SC2013.28.635 (12 teeth), SC2013.28.636 (15 teeth), SC2013.28.637 (12 teeth), SC2013.28.638 (19 teeth), SC2013.28.639 to 28.642 • 64 isolated scales; Catahoula Formation; SC2013.28.609 to 28.617, SC2013.28.618 (Fig. 23A–C), SC2013.28.619 (Fig. 23D–F), SC2013.28.620 to 28.622, SC2013.28.623 (2 specimens), SC2013.28.624 (2 specimens), SC2013.28.625 (4 specimens), SC2013.28.626 (42 specimens).

Description

Numerous isolated teeth are included in our Lepisosteidae sample. These teeth vary in size and overall height, but all consist of a cylindrical base and enameloid crown (Fig. 23G). In anterior/posterior view, teeth are straight to slightly lingually curved. The basal portion of the tooth is striated, and the basal outline is circular with a deep pulp cavity (Fig. 23H). The crown is formed of translucent enameloid having smooth exterior surfaces. The crown shape of large teeth varies from short and conical to slightly antero-posteriorly compressed, and those with conical crowns lack cutting edges, whereas compressed specimens are bicarinate with smooth labio-lingually oriented cutting edges. Small specimens exhibit a taller, needle-like crown that is conspicuously antero-posteriorly compressed. The crowns of these teeth exhibit sharp and elongated anterior and posterior cutting edges that do not reach the tooth base.

Two scale morphologies have been identified, both of which are generally rhomboidal in outline but may also be somewhat teardrop-shaped. The external surface may or may not have a thick ganoine covering. Those with ganoine may have a smooth texture (Fig. 23A), but specimens with deeply pitted ganoine or ganoine with highly irregular margins occur (Fig. 23F). The inner surface is smooth (Fig. 23C–D) and often convex (Fig. 23B, E). A posterior projection from the main body of the scale varies from short to very elongated. Some specimens exhibit concentric growth lines on the external surface.

Remarks

Of the teeth in our sample, large specimens are comparable to those occurring in furrows along the maxillae and dentaries of extant *Lepisosteus osseus* (Linnaeus, 1758) specimens that we examined (MSC 42585, MSC 49487). The small, more needle-like specimens in our sample are similar to teeth we observed along the labial jaw margins of those *L. osseus* specimens. The largest scales in our sample (i.e., SC2013.28.619) have pitted ganoine or ganoine with irregular outlines and are reminiscent of scales referred to *Atractosteus*.

Although Grande (2010) identified four Paleogene gar taxa, he indicated that isolated teeth and scales lacked taxonomically significant features allowing for identification beyond the family level. In lieu of cranial material, we follow Ebersole *et al.* (2019) and refrain from assigning the Catahoula Formation gar material to any particular genus. Additionally, we cannot be certain whether differences in scale morphology within our sample represent inter- or intraspecific variation (among species versus along the body of an individual fish). Gar fossils have been documented from Eocene strata within the Gulf Coastal Plain (i.e., Breard & Stringer 1999; Westgate 2001; Ebersole *et al.* 2019), but none have been previously reported from the Oligocene.

Division Teleosteomorpha Arratia *et al.*, 2004
Subdivision Teleostei Müller, 1845
Supercohort Teleocephala de Pinna, 1996
Cohort Elopomorpha Greenwood *et al.*, 1966
Order Albuliformes Greenwood *et al*., 1966
Family Albulidae Bleeker, 1859

Albulidae gen. et sp. indet.
Fig. 23I–S

Material examined

UNITED STATES OF AMERICA – **Mississippi** • 6 isolated pharyngeal bones; Catahoula Formation; MMNS VP-6578 (Fig. 23I–K), MMNS VP-6967 (3 specimens), SC2013.28.692, SC2013.28.693 • 48 isolated teeth; Catahoula Formation; SC2013.28.594 (Fig. 23L–N), SC2013.28.595 (46 teeth),

SC2013.28.840 (Fig. 23O–Q) • 9 sagittae; Catahoula Formation; MMNS VP-7454, SC2013.28.802, SC2013.28.803, SC2013.28.804 (2 specimens), SC2013.28.911 (Fig. 23R–S), GLS otolith comparative collection (3 specimens).

Description

Our sample includes ablated pharyngeal bones, isolated teeth, and otoliths (sagittae). The pharyngeal bones are ablated, but each specimen exhibits a very flattened and slightly polished oral surface and more convex, roughened aboral surface. A probable basibranchial (MMNS VP-6578) is antero-posteriorly elongated but narrow. The oral surface of each specimen includes several scattered teeth (Fig. 23I), which are only visible in outline because of their in vivo wear down to the level of the bone surface. Numerous openings within the oral surface are interpreted to represent alveoli for missing teeth. Enameloid crowns of replacement teeth are visible in profile (Fig. 23J) and aboral views (Fig. 23K).

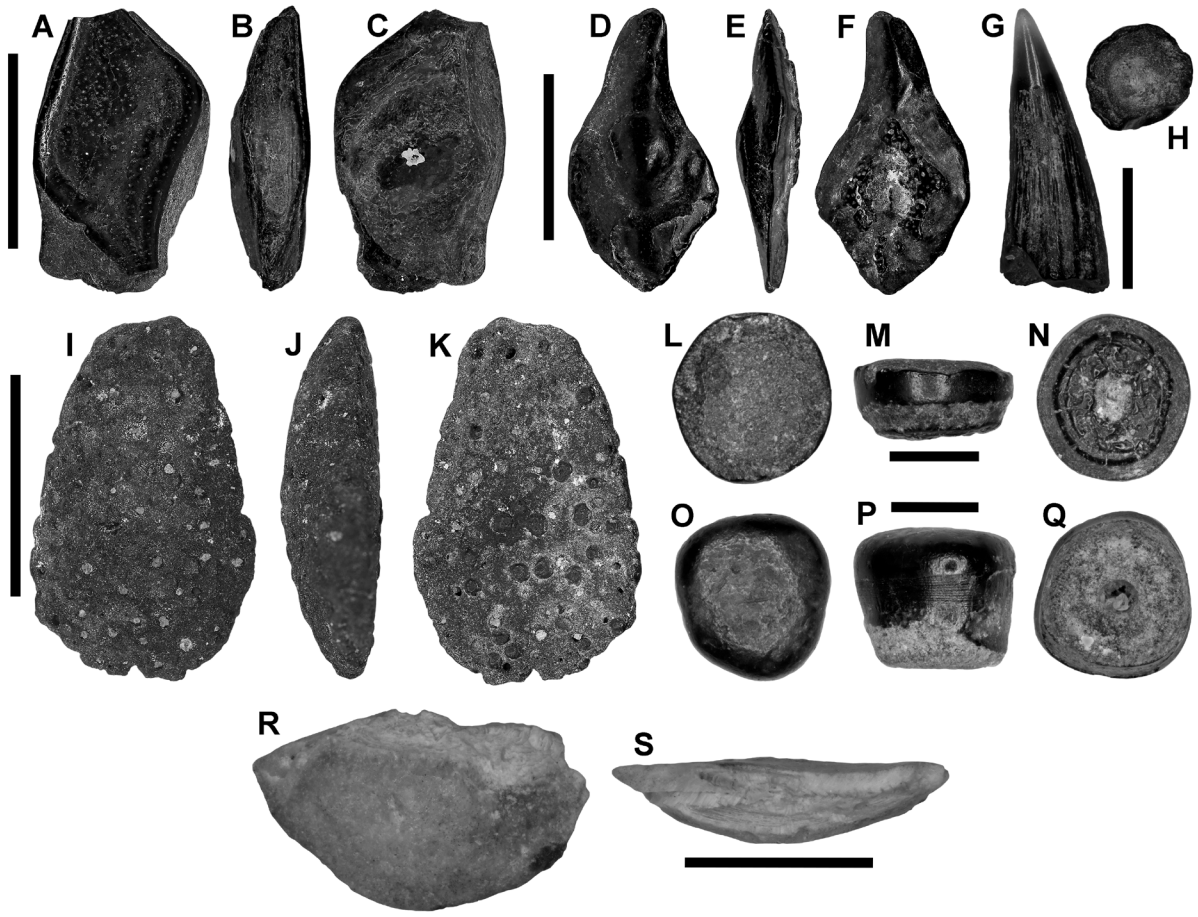

Fig. 23. Lepisosteidae gen. et sp. indet. (A–H) and Albulidae gen. et sp. indet. (I–S), remains. **A–C**. SC2013.28.618, Lepisosteidae gen. et sp. indet., scale. **A**. Outer view. **B**. Profile view. **C**. Inner view. **D–F**. SC2013.28.619, Lepisosteidae gen. et sp. indet., scale. **D**. Outer view. **E**. Profile view. **F**. Inner view. **G–H**. SC2013.28.630, Lepisosteidae gen. et sp. indet., tooth. **G**. Profile view. **H**. Basal view. **I–K**. MMNS VP-6578, Albulidae gen. et sp. indet., pharyngeal plate. **I**. Oral view. **J**. Profile view. **K**. Aboral view. **L–N**. SC2013.28.594, Albulidae gen. et sp. indet., tooth. **L**. Occlusal view. **M**. Profile view. **N**. Basal view. **O–Q**. SC2013.28.840, Albulidae gen. et sp. indet., tooth. **O**. Occlusal view. **P**. Profile view. **Q**. Basal view. **R–S**. SC2013.28.911, Albulidae gen. et sp. indet., left sagitta (reversed). **R**. Inner view. **S**. Dorsal view. Scale bars: A–F = 5 mm; G–H = 3 mm; I–S = 1 mm.

Nearly all the isolated teeth are highly worn through in vivo use, and the remaining portion of these specimens consists of the crown and a short basal area. In profile view, the crowns are high and basally tapering (Fig. 23M, P), but their original unworn height is unknown. The crown is covered with a thin layer of smooth enameloid that does not reach the tooth base. In occlusal view, the crown has a circular outline, and the triturating surface largely consists of exposed dentine framed by thin enameloid (Fig. 23L, O). In basal view, the circular pulp cavity is framed by a thick wall of dentine (Fig. 23N, Q).

The sagittae (Fig. 23R–S) are very small, with only a few exceeding 4 mm. They have a somewhat oblong to elliptic outline (sensu Smale *et al.* 1995), and the margins are generally smooth. The inner face is conspicuously convex and twisted, and a prominent long sulcus occurs primarily in the dorsal and posterior regions. The sulcus has a wide, anterodorsally opening ostium that is filled with colliculum. The caudal area has an anterior sub-horizontal portion and a posterior downturned portion that is usually deeply excavated. A caudal keel is present on well-preserved specimens. The outer face is concave, twisted (especially in adults), thickest postero-dorsally but thinning toward the anterior, and annual growth rings are often visible to the naked eye.

Remarks

Albulid pharyngeal bones, isolated teeth, and otoliths are represented in our sample. These fossils cannot be confidently assigned to any particular genus, and we cannot ascertain whether the remains represent more than one taxon. A single tooth recovered from the Glendon Limestone Member of the Byram Formation of southwestern Alabama was identified as *Albula* sp. by Ebersole *et al.* (2021), and several isolated teeth were reported from the late Rupelian Ashley Formation of South Carolina (Cicimurri *et al.* 2022). Cicimurri & Knight (2009) also mentioned the occurrence of albulid teeth in the Chattian Chandler Bridge Formation of South Carolina. Albulid otoliths have been reported from the Rupelian Rosefield Formation in Louisiana (Stringer *et al*. 2001).

The small overall size of the Catahoula Formation otoliths is in stark contrast to those of Eocene albulids, which approach 20 mm in length (Ebersole *et al.* 2019). Otoliths can attain even larger sizes, as a specimen from the Eocene Clinchfield Formation of Georgia measures 21.48 mm (Stringer *et al.* 2022a). Although albulid otoliths occur within numerous Paleogene lithostratigraphic units within the Gulf Coastal Plain, they are typically not abundant (Breard & Stringer 1995, 1999; Stringer & Breard 1997; Stringer & Miller 2001; Schweitzer *et al*. 2014). Nolf & Stringer (2003) reported only five specimens of *Albula* sp. among the 5559 otoliths (0.09% of total sample) from the upper Eocene (primarily Priabonian) Yazoo Clay in Louisiana, and albulid otoliths represented a slightly higher 1.33% of the total sample (n = 20) from the Clinchfield Formation (Stringer *et al.* 2022a). Far fewer otolith specimens were obtained from the Catahoula Formation, but those of albulids constitute 2.47% of the sample.

Order Anguilliformes (sensu Inoue *et al.* 2010)
Suborder Congroidei Kaup, 1856
Family Congridae Kaup, 1856
Subfamily Bathymyrinae Böhlke, 1949

Genus ***Protanago*** Schwarzhans, Stringer & Takeuchi, 2024

Type species

Otolithus (*Platessae*) *sector* Koken, 1888

Protanago nonsector (Nolf & Stringer, 2003)
Fig. 24A–D

Ariosoma nonsector Nolf & Stringer, 2003: 7.

Material examined

UNITED STATES OF AMERICA – **Mississippi •** 2 sagittae; Catahoula Formation; MMNS VP-8200.3 (Fig. 24A–B), MMNS VP-8713 (Fig. 24C–D).

Description

The sagitta outline is primarily oval (sensu Smale *et al.* 1995; also Nolf & Stringer 2003) due to the presence of a prominent dorsal dome (Fig. 24A, C), which increases the height of the otolith relative to its length. Height/length ratios are commonly 0.85. The margins are smooth and a posterodorsal concavity is common. The inner face is generally smooth and evenly convex, although some irregular depressions occur within the upper portion of the dorsal area. The sulcus is wide, slightly incised, and undivided, with no clearly defined ostium and cauda (Fig. 24C). The sulcus begins very near the anterior margin and extends approximately 85% the length of the inner face (Fig. 24A). The sulcus is filled with colliculum except for the backward curving ostial channel. No ventral furrow is present. The outer face is relatively smooth and convex (Fig. 24B, D), with the exception of an area near the posterior end, where a shallow and dorsoventrally oriented depression occurs.

Remarks

Protanago nonsector otoliths from the Catahoula Formation have several characteristics in common with *Ariosoma* as illustrated in Schwarzhans (2019a), but it differs in the lack of an S-shaped sulcus, which is considered to be a diagnostic and autapomorphic characteristic of *Ariosoma* (Schwarzhans *et al.* 2024). *Protanago nonsector* (previously reported as *Ariosoma nonsector*) otoliths are widely distributed across Paleogene sediments in the Gulf Coastal Plain, from Louisiana eastward into Georgia (Breard & Stringer 1995; Nolf 2013; Ebersole *et al.* 2019; Stringer *et al.* 2022a). This species was abundant in the upper Eocene (primarily Priabonian) Yazoo Clay in Louisiana, where it constituted 10.9% of the

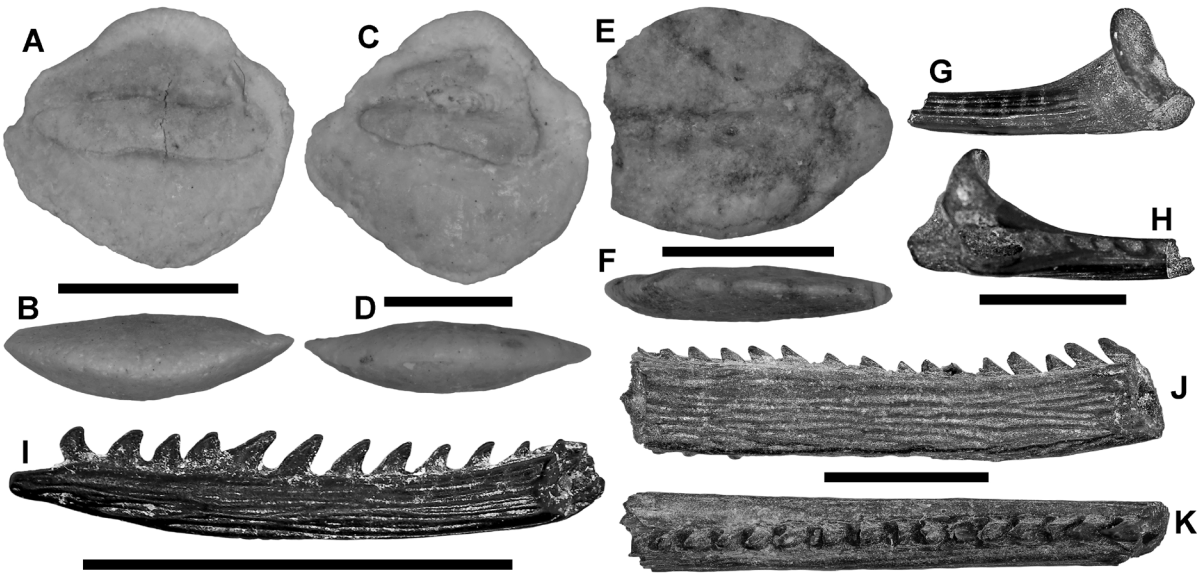

Fig. 24. *Protanago nonsector* (Nolf & Stringer, 2003) (A–D), Congridae gen. et sp. indet. (E–F), and Siluriformes indet. (G–K), remains. **A–B**. MMNS VP-8200.3, *Protanago nonsector*, right sagitta. **A**. Inner view. **B**. Dorsal view. **C–D**. MMNS VP-8713, *P. nonsector*, left sagitta (reversed). **C**. Inner view. **D**. Dorsal view. **E–F**. MMNS VP-12073, Congridae gen. et sp. indet., sagitta. **E**. Inner view. **F**. Dorsal view. **G–H**. SC2013.28.750, Siluriformes indet., pectoral spine. **G**. Ventral view. **H**. Dorsal view. **I**. MMNS VP-6651, Siluriformes indet., pectoral spine, ventral view. **J–K**. MMNS VP-7560, Siluriformes indet., pectoral spine. **J**. Dorsal view. **K**. Posterior view. Scale bars: A–B, E–F = 2 mm; C–D, I–K = 1 mm; G–H = 5 mm.

5599 specimens available (Nolf & Stringer 2003), and it has also been identified in small numbers in the Eocene and Oligocene of Alabama (Ebersole *et al.* 2019, 2021). *Protanago nonsector* appears to be the only species of this genus recorded outside of North America, as it has been documented in Italy (Schwarzhans *et al.* 2024). Schwarzhans' work on extant species of the family Congridae (Schwarzhans 2019b) indicates that careful review of Paleogene congrid otoliths is warranted.

One additional Catahoula Formation specimen (MMNS VP-8713) exhibits the salient features of *Protanago* sp., but we cannot make a more accurate determination due to its poor preservation and small size (juvenile). It is possible that the otolith represents *P. nonsector*, but we cannot rule out the possibility that it belongs to a different, but closely related, species. The otolith is mentioned here for completeness.

Congridae gen. et sp. indet.
Fig. 24E–F

Material examined

UNITED STATES OF AMERICA – **Mississippi •** 1 sagitta; Catahoula Formation; MMNS VP-12073.

Description

The sagitta is oval to somewhat elliptic in outline (sensu Smale *et al.* 1995) and the margins are rather smooth. The height/length ratio is 0.55. The inner face varies from nearly flat to very slightly convex. The sulcus is undivided, slants very slightly in the posteroventral direction, and extends across approximately 75% of the inner face. The sulcus tapers at the anterior and the posterior, and it appears to reach the anterior margin, possibly through a shallow ostial channel. There is a conspicuous depressed area, somewhat rectangular in shape, above the sulcus. The outer face is only slightly more convex than the inner face.

Remarks

The otolith described above exhibits the typical congrid feature of having an undivided sulcus (Fig. 24E). MMNS VP-12073 differs significantly from specimens of *Protanago nonsector* (see above) by having much less convex dorsal and ventral margins, with a H/L ratio of 0.55 vs 0.85 for the latter taxon (compare to Fig. 24A, C). Specimen MMNS VP-12073 is similar to *Protoanguilla*?, a species reported as *Pseudophichthys glaber* from middle Eocene to lower Oligocene deposits in Louisiana and Mississippi (Nolf & Stringer 2003; Nolf 2013; Stringer *et al.* 2020c). Unfortunately, the anterior one-quarter of the otolith is lacking and definitive identification to *Protoanguilla*? is not possible without additional specimens. Schwarzhans *et al.* (2024) indicated that *Pseudophichthys glaber* differed from the extant *Pseudophichthys* and erected the otolith-based genus *Protoanguilla*? for the taxon.

Unranked Clupeocephala Patterson & Rosen, 1977
Cohort Otocephala (sensu Nelson *et al*. 2016)
Superorder Ostariophysi (sensu Nelson *et al*. 2016)
Series Otophysi (sensu Fink & Fink 1981)
Subseries Siluriphysi Fink & Fink, 1996
Order Siluriformes Cuvier, 1816

Siluriformes fam., gen. et sp. indet.
Fig. 24G–K

Material examined

UNITED STATES OF AMERICA – **Mississippi •** 8 isolated fin spines; Catahoula Formation; MMNS VP-6651 (Fig. 24I), MMNS VP-7560 (Fig. 24J–K), SC2013.28.750 (Fig. 24G–H), SC2013.28.751 to 28.755.

Description

The sample includes incomplete pectoral fin spines potentially representing two morphologies. Three specimens are the proximal end of right spines (i.e., Fig. 24G–H). These have a flared, shelf-like dorsal process at the base, and this structure is roughly perpendicular to the spine length. The spine itself was elongated, curving towards the posterior, distally tapering, and dorso-ventrally flattened. The anterior margin is convex, whereas the posterior margin is lined with small circular depressions. The dorsal and ventral surfaces of the spine are convex and bear fine longitudinal striations. There is a triangular, antero-ventrally located fossa at the spine base.

The remaining specimens are incomplete spines and ablated spine fragments. Specimens MMNS VP-6651 (Fig. 24I) and MMNS VP-7560 (Fig. 24J–K) are large incomplete spines where MMNS VP-6651 lacks its base and MMNS VP-7560 lacks its base and distal tip. Both specimens are elongated, narrow and thin, and curving along their length. Additionally, MMNS VP-6651 preserves a bluntly pointed distal tip. Both specimens exhibit numerous dorsal and ventral parallel ridges along their entire preserved length. Furthermore, the anterior margin is rounded, whereas the posterior margin bears a single row of basally directed, triangular denticles (Fig. 22J–K). Both specimens also show that these denticles increase in size distally (Fig. 24I). The other ablated spine fragments exhibit a comparable morphology.

Remarks

There are several extant catfish species within Ictaluridae and Ariidae that have ornamented fin spines, and we cannot confidently identify our fragmentary specimens beyond the ordinal level. However, two taxa may be represented based on the morphological variation we observed in the Catahoula Formation sample, with one having a dimpled posterior margin and the other barbed. It is possible that the morphologies represent the same spine, where the barbed section was located distal to the preserved portions of the spines in our sample. Ariidae fin spines have been reported from Eocene strata (Ebersole *et al.* 2019) and Ictaluridae spines from the Late Miocene (Ebersole & Jacquemin 2018) and Pleistocene (Jacquemin *et al.* 2016) of Alabama, but to our knowledge, the Catahoula Formation specimens represent the first North American Oligocene record of catfishes. These fishes were not identified in the Oligocene marine paleofaunas of North and South Carolina (Case 1980; Müller 1999; Cicimurri & Knight 2009; Cicimurri *et al.* 2022).

Barbed fin spines could be confused with myliobatiform caudal spines, as both exhibit barbed margins. However, myliobatiform caudal spines are barbed on their right and left lateral margins (as opposed to only the posterior margin on our specimens), the dorsal surface is covered with enameloid (which is lacking on catfish spines), and they are symmetrical in dorsal view.

Cohort Euteleostei Rosen, 1985
Superorder Acanthopterygii Greenwood *et al*., 1966
Series Percomorpha (sensu Nelson *et al*. 2016)
Subseries Ovalentaria Smith & Near in Wainwright *et al*., 2012
Order Istiophoriformes Betancur-R *et al.*, 2013
Family Sphyraenidae Rafinesque, 1815

Genus ***Sphyraena*** Artedi in Röse, 1793

Type species

Esox sphyraena Linnaeus, 1758, Extant, Mediterranean Sea.

Sphyraena sp.
Fig. 25A–F

Material examined

UNITED STATES OF AMERICA – **Mississippi •** 609 isolated teeth; Catahoula Formation; MMNS VP-9048, SC2013.28.531 to 28.536, SC2013.28.537 (50 teeth), SC2013.28.538 (8 teeth), SC2013.28.539 (15 teeth), SC2013.28.540 (7 teeth), SC2013.28.541 to 28.544, SC2013.28.545 (Fig. 25A–C), SC2013.28.546 (20 teeth), SC2013.28.547 (5 teeth), SC2013.28.548 (2 teeth), SC2013.28.549 (109 teeth), SC2013.28.550 to 28.557, SC2013.28.558 (Fig. 25D–F), SC2013.28.559 (79 teeth), SC2013.28.560 (35 teeth), SC2013.28.561 (10 teeth), SC2013.28.562 (12 teeth), SC2013.28.563 (10 teeth), SC2013.28.564 (226 teeth).

Description

Two tooth morphologies are represented in our sample. The first includes tall teeth measuring up to 12 mm in height. These teeth have a sinuous profile, with the labial margin formed into a sharp, smooth carina that extends from the tooth base to the crown apex (Fig. 25A). This carina is more convex along the basal one-half, after which it is posteriorly directed and may or may not have a slight vertical rise to the apex. The posterior margin is convex and thickest basally, but it thins apically. In profile this margin is straight to concave along the lower two-thirds, but apically it can be straight to weakly convex. The apex bears a diminutive posterior barb, and on some teeth this barb is represented only by a short anterior carina. Relatively pristine specimens exhibit vertical striations or wrinkling at the postero-basal surface. In anterior/posterior view, the tooth is straight to slightly medially curved (Fig. 25B). The basal attachment surface is weakly concave, and its outline is generally teardrop-shaped on smaller specimens and oval on larger specimens (Fig. 25C).

Teeth of the second morphology are lanceolate and highly labio-lingually compressed (Fig. 25D). In anterior/posterior view, the crown is straight to weakly medially curved (Fig. 25E). The anterior and posterior margins are formed into sharp and smooth carinae that extend from the base to the apex. Well-preserved teeth show that the crown is covered with thin enameloid that can be striated basally, but enameloid largely remains only at the anterior and posterior carinae. The labial and lingual crown faces are weakly convex, but the basal portion of the lingual face is somewhat more convex. In basal view, the attachment surface is concave, and the outline is elliptical (Fig. 25F). There are two slightly differing morphotypes, with one being taller and antero-posteriorly narrower than the other. The taller teeth are more often medially curved, whereas the shorter teeth are rather straight. Additionally, the cutting edges of taller teeth are proportionally longer and the apex more pointed compared to the shorter and wider teeth.

Remarks

Based on extant specimens of *Sphyraena barracuda* (Walbaum, 1792) that we examined (SC2018.3.1; MSC 43215), the tall teeth with an anterior carina and posterior apical barb are laniary teeth that were located at the anterior end of the premaxilla or dentary. The lanceolate specimens occurred within the cheek regions of the palatine or dentary. Ebersole *et al.* (2019) and Ballen (2020) have indicated that tooth morphologies among extant Sphyraenidae are taxonomically distinctive, but intraspecific variation is not well documented. There is no evidence contradicting our conclusion that various Catahoula Formation *Sphyraena* morphologies are conspecific. Regarding the laniary teeth, all the well-preserved specimens, from the smallest (3 mm in height) to the largest (12 mm) exhibit a smooth anterior cutting edge, diminutive postero-apical barb, and postero-basal vertical striations. Specimen SC2018.3.1 also indicates that somewhat taller and narrower lanceolate specimens from the Catahoula Formation were from the anterior dentary, whereas the slightly shorter and wider teeth were located on the palatine. The Catahoula Formation sample includes teeth with and without striations and ridges, and we observed this

phenomenon in the jaws of the extant *Sphyraena* spp. that we examined. Crown ornamentation therefore does not appear to be taxonomically significant.

Santini *et al.* (2015) demonstrated the existence of three *Sphyraena* lineages by the late Eocene, and the age of the Catahoula Formation specimens is close to the timing of radiation of the *S. obtusata* Cuvier, 1829 and *S. sphyraena* (Linnaeus, 1758) species groups (with each group containing several species). Extant representatives of both species groups currently inhabit the Gulf of Mexico (Hoese & Moore 1998). Ballen (2020) presented a listing of fossil *Sphyraena* species, including several from the Oligocene. *Sphyraena intermedia* Bassani, 1889 and *S. pannonica* Weiler, 1938 were based on skeletal material that included crania, but neither author provided tooth descriptions. *Sphyraena tyrolensis* von Meyer, 1863 is known from a dentary and various isolated teeth. Although von Meyer (1863) mentioned the occurrence of basal striations on laniary teeth ("Fangzahn" therein), he did not mention the presence of an apical barb, and the laniary tooth of the figured specimen (pl. 50 figs 7–8) is broken apically. The remainder of the teeth along the ramus of this specimen are otherwise comparable to any species of *Sphyraena*. Ebersole *et al.* (2021) documented similar *Sphyraena* sp. dentary teeth from the Rupelian Byram Formation in Alabama, and Ebersole *et al.* (2024a) identified both laniary and dentary teeth

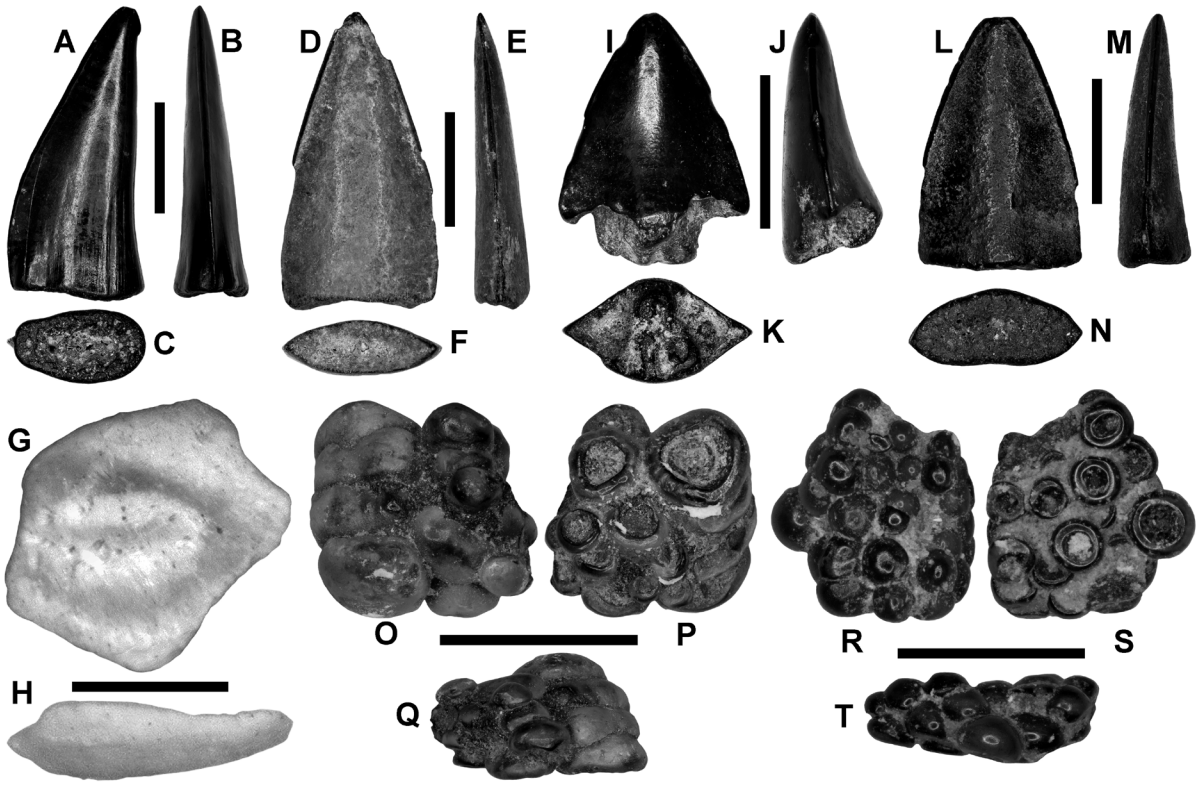

Fig. 25. *Sphyraena* sp. (A–F), *Syacium* sp. (G–H), *Acanthocybium* sp. (I–K), *Scomberomorus* sp. (L–N), and Labridae gen. et sp. indet. (O–T), remains. **A–C**. SC2013.28.545, *Sphyraena* sp., laniary tooth. **A**. Labial view. **B**. Posterior view. **C**. Basal view. **D–F**. SC2013.28.558, *Sphyraena* sp., tooth. **D**. Lingual view. **E**. Carinal view. **F**. Basal view. **G–H**. MMNS VP-12074, *Syacium* sp., left otolith (reversed). **G**. Inner view. **H**. Dorsal view. **I–K**. SC2013.28.579, *Acanthocybium* sp., tooth. **I**. Lingual view. **J**. Carinal view. **K**. Basal view. **L–N**. SC2013.28.572, *Scomberomorus* sp., tooth. **L**. Lingual view. **M**. Carinal view. **N**. Basal view. **O–Q**. SC2013.28.596, Labridae gen. et sp. indet., tooth mass. **O**. Oral view. **P**. Aboral view. **Q**. Profile view. **R–T**. SC2013.28.597, Labridae gen. et sp. indet., tooth mass. **R**. Oral view. **S**. Aboral view. **T**. Profile view. Scale bars: A–F, I–N = 5 mm; G–H = 1 mm; O–Q = 4 mm; R–T = 2 mm.

from the Rupelian Red Bluff Clay in the same state. Leidy (1855) named *S. major* based on specimens recovered from the Ashley River of South Carolina. He did not provide a description of the teeth and only mentioned that the material was collected from the Ashley River. The fossils in question may have been derived from the Ashley Formation (Rupelian), but the source unit could be older or younger (see Albright *et al.* 2018). We refrain from making a species determination, because we cannot accurately compare the Catahoula Formation material to all the other named species due to the lack of described morphological features.

Order Pleuronectiformes Bleeker, 1859
Superfamily Pleuronectoidea Rafinesque, 1815
Family Cyclopsettidae Campbell *et al*., 2019

Genus ***Syacium*** Ranzani, 1842

Type species

Syacium micrurum Ranzani, 1842, Extant.

Syacium sp.
Fig. 25G–H

Material examined

UNITED STATES OF AMERICA – **Mississippi** • 3 sagittae; Catahoula Formation; MMNS VP-12074, GLS otolith comparative collection (2 specimens).

Description

The sagittae have a primarily square outline (sensu Smale *et al*. 1995). The margins are generally smooth but can be variable and irregular. The inner face is slightly convex and smooth (Fig. 25H). A highly specialized, fusiform sulcus slants downward from the posterodorsal margin to almost the anteroventral margin (Fig. 25G). The sulcus is widest just behind its midline but is narrower at the anterior and posterior ends. Although the sulcus extends across approximately 75% of the inner face, it is narrow and represents roughly 20% of the height. The sulcus is divided into ostial and caudal areas. The ostium is located near the lower portion of the anterior and anteroventral margins but does not reach the margins. The ostium is tapered and almost pointed at the anterior end. The cauda is longer and wider than the ostium, and the anterior of the cauda is tapered, whereas the center portion is enlarged. The cauda is excavated slightly deeper than the ostium. The ostium and cauda are conspicuously connected or fused, and the structure is filled with colliculum. A marked circumsulcal depression extends from above the ostium, around the cauda, and ends below the ostium. The circumsulcal depression forms an elevated flattened area for the fusiform sulcus. A ventral furrow is not present. The outer face is fairly flat on the dorsal and ventral areas, but is slightly convex in the center.

Remarks

The *Syacium* sp. otoliths from the Catahoula Formation are very similar to the *Syacium* sp. sagittae from the Rupelian Glendon Limestone Member of the Byram Formation of Alabama (Ebersole *et al.* 2021). This genus appears to be rare in Paleogene strata across the Gulf and Atlantic coastal plains of the USA, but it is somewhat more common (although still rare) during the Neogene (Stringer 1992; Nolf & Stringer 2003; Nolf 2013; Stringer *et al*. 2017; Stringer & Bell 2018; Ebersole *et al*. 2019; Stringer & Shannon 2019; Stringer & Hulbert 2020).

Order Scombriformes Rafinesque, 1810
Suborder Scombroidei Bleeker, 1859
Family Scombridae Rafinesque, 1815
Subfamily Scombrinae Rafinesque, 1815
Tribe Scomberomorini Starks, 1910

Genus ***Acanthocybium*** Gill, 1862

Type species

Cybium solandri Cuvier & Valenciennes, 1832, Extant.

?***Acanthocybium*** sp.
Fig. 25I–K

Material examined

UNITED STATES OF AMERICA – **Mississippi** • 3 isolated teeth; Catahoula Formation; SC2013.28.577, SC2013.28.578, SC2013.28.579 (Fig. 23I–K).

Description

The teeth have a lanceolate profile. The anterior and posterior margins are formed into sharp smooth carinae, each of which extends from the tooth base and coalesces at a rounded apex (Fig. 25I). In anterior and posterior views, the crown is nearly vertical but has a slight lingual curvature, and the carina is located closer to the labial face (Fig. 25J). The lingual face is more convex than the labial face, particularly at the lower one-third. In basal view, the carinae are conspicuously differentiated from the main body of the crown due to the medially convex lingual face, and a deep pulp cavity is visible (Fig. 25K).

Remarks

These specimens differ from the lanceolate *Sphyraena* sp. teeth (see above) and from teeth assigned to *Scomberomorus* sp. (see below) by being much thicker labio-lingually and having much more convex labial and (especially) lingual faces. The Catahoula Formation teeth are comparable to those occurring in *Acanthocybium* premaxillae and a dentary (SC2016.1.14) that we examined from the late Rupelian Ashley Formation of South Carolina. The premaxillary teeth of the Ashley Formation taxon are two to three times larger than those of the dentary, but the dentary teeth are equally convex labially and lingually. Based on these observations, the Catahoula Formation teeth were located in the premaxilla.

The Catahoula Formation teeth are also similar to specimens identified as *Palaeocybium* from the Eocene of Alabama (Ebersole *et al.* 2019), as well as to the Oligocene *Neocybium parvidentatum* Monsch & Bannikov, 2012 of Europe (see also Leriche 1908). However, *Palaeocybium* possesses two rows of teeth in the jaws (Monsch 2005), which cannot be determined from the isolated teeth in our Catahoula Formation sample. To our knowledge, *Palaeocybium* is unknown beyond the Eocene. Jaws of *Neocybium* and the South Carolina *Acanthocybium* have only a single row of teeth, with those of the former perhaps being less convex and more widely separated in the jaws (Monsch & Bannikov 2012). We tentatively assign the Catahoula Formation specimens to *Acanthocybium* due to dental similarities between the Mississippi fossils and the South Carolina Oligocene *Acanthocybium*.

Genus ***Scomberomorus*** Bleeker, 1859

Type species

Scomber regalis Bloch, 1793, Extant.

Scomberomorus sp.
Fig. 25L–N

Material examined

UNITED STATES OF AMERICA – **Mississippi** • 175 isolated teeth; Catahoula Formation; SC2013.28.565 to 28.571, SC2013.28.572 (Fig. 25L–N), SC2013.28.573 (2 teeth), SC2013.28.574 (101 teeth), SC2013.28.575 (50 teeth), SC2013.28.576 (14 teeth).

Description

The teeth are broadly triangular, with larger specimens measuring 11 mm in apico-basal height and 7 mm in width (antero-posterior). The labial and lingual crown faces are convex, but the lingual face, particularly near the base, is more so. In anterior/posterior view, the crown is medially curved but may be straight (Fig. 25M). The anterior and posterior margins are formed into smooth, sharp, convex cutting edges, and in labial view these edges converge to a rounded apex. It appears that enameloid once covered the crown surface, but this is generally only preserved at the cutting edges of the teeth in our sample. In basal view, the tooth has a thin D-shaped outline, and the basal surface is flat to weakly concave (Fig. 25N).

Remarks

The teeth described above are similar to *Sphyraena* sp. non-laniary teeth (see above) but can be differentiated by their thicker crown that is asymmetrical in basal view (compare Fig. 25N to 25F). The lingual face of *Scomberomorus* sp. teeth is much more convex than the labial face, and the crown is more medially curved. In contrast, the *Sphyraena* sp. crown is thinner, straighter (in carinal view), and the labial and lingual crown faces are slightly but equally convex. The teeth of *Scomberomorus* sp. differ from those of ?*Acanthocybium* sp. (see above) by their labio-lingually thinner crown (compare Fig. 25N to K) and primarily flat basal surface. Although two species of *Scomberomorus* have been identified from Eocene deposits in Alabama (see Ebersole *et al.* 2019), the teeth in our sample represent the first occurrence of this taxon within any Oligocene strata in the Gulf Coastal Plain of the USA.

Order Labriformes Kaufman & Liem, 1982
Family Labridae Cuvier, 1816

Labridae gen. et sp. indet.
Fig. 25O–T

Material examined

UNITED STATES OF AMERICA – **Mississippi** • 12 isolated teeth; Catahoula Formation; SC2013.28.603 (12 specimens) • 7 tooth masses; Catahoula Formation; SC2013.28.596 (Fig. 25O–Q), SC2013.28.597 (Fig. 25R–T), SC2013.28.598 to 28.602.

Description

Our sample includes fragments of pharyngeal plates and isolated teeth. The pharyngeal plate fragments consist of tightly packed teeth of differing sizes that form a roughly contiguous surface. In cross section, up to four sets of replacement teeth are visible (Fig. 25Q, T). Teeth were apparently not replaced at a regular rate, as newer (replacement) teeth are intermingled with older functional teeth (Fig. 25O, R). In profile view, individual teeth can be low with a convex occlusal surface or high with a globular appearance. In occlusal/basal view, they have a circular to oval outline. Teeth essentially consist of a very thick enameloid cap with an open pulp cavity free of dentine (Fig. 25P, S).

Remarks

The unusual arrangement of the teeth within the jaw plates, as well as the composition of individual teeth, facilitates separating wrasse specimens from those of other, similar-looking taxa (see below). Fossil occurrences of Labridae are sparse, but Cicimurri *et al.* (2022) reported specimens from the Rupelian Ashley Formation of South Carolina, and Cicimurri & Knight (2009) mentioned their occurrence in the Chattian Chandler Bridge Formation. Labrid molecular divergence times were estimated by Cowman *et al.* (2009), who postulated that the extant lineages within this family largely diverged within the Miocene. This suggests that the labrid elements in our Catahoula Formation sample represent an unrecognized stem-member of the lineage.

Order Perciformes (sensu Nelson *et al*. 2016)
Family Haemulidae Gill, 1885

Genus ***Allomorone*** Dante & Frizzel in Frizzell & Dante, 1965

Type species

Orthopristis duplex Girard, 1858, Extant.

Allomorone sp.
Fig. 26A–B

Material examined

UNITED STATES OF AMERICA – **Mississippi •** 1 sagitta; Catahoula Formation; MMNS VP-12060.

Description

MMNS VP-12060 has an elliptic outline (sensu Smale *et al.* 1995) with a rather prominent, somewhat blunt rostrum with excisura. The inner face is broadly and evenly convex with a conspicuous sulcus (heterosulcoid type). The sulcus extends approximately 80% of the length of the inner face (Fig. 26A). The ostium is relatively narrow and subquadrate in shape. The height of the ostium is only slightly greater than the height of the cauda, but the length of the ostium is significantly shorter than the cauda. The narrow cauda is approximately 2.5 times as long as the ostium. The dorsal and ventral margins of the cauda are horizontal and essentially parallel. The posterior portion of the cauda is bent downward. A ridge-like crista superior occurs above the cauda and a linear, depressed area is located above the crista superior. There may have been a ventral furrow, but this region is not well preserved on the specimen in our sample. The outer face is concave and has a slightly irregular surface (Fig. 26B).

Remarks

The Catahoula Formation *Allomorone* sp. sagitta appears to be very closely related to what was previously reported as *Orthopristis americana* (Koken, 1888) from the Gulf Coast upper Eocene (Jackson Group), a taxon that was first reported by Koken (1888) as *Otolithus* (*Carangidarum*) *americana*. However, Schwarzhans *et al*. (2024) considered *Allomorone* different from *Orthopristis* because of the much shorter, downward section of the cauda that terminates away from the post-ventral margin on the sagitta of *Allomorone*. Unfortunately, the somewhat eroded specimen available to us is not sufficient to make a specific determination. *Allomorone* sp. otoliths are much more common in the Gulf Coastal Plain compared to the Atlantic Coastal Plain, as Müller (1999) only reported three specimens from the Eocene (as "Genus aff. *Orthopristis* sp.") in a sample of over 12 000 fossil otoliths collected from middle Eocene to Pliocene deposits in the Atlantic Coastal Plain. In contrast, *Allomorone americana* was more abundant in the upper Eocene (primarily Priabonian) Yazoo Clay otolith assemblage from Copenhagen,

Louisiana, representing 4.35% of the total specimens in a sample (Nolf & Stringer 2003; reported as *Orthopristis americana*). Green (2002) reported a significant occurrence of *A. americana* (18.17% of the total number of otolith specimens) in the middle Eocene (Bartonian) Moodys Branch Formation at the Heison Landing locality along the Ouachita River in Caldwell Parish, Louisiana (shown as *O. americana*). Ebersole *et al*. (2021) did not report *O. americana* from the Rupelian Glendon Limestone

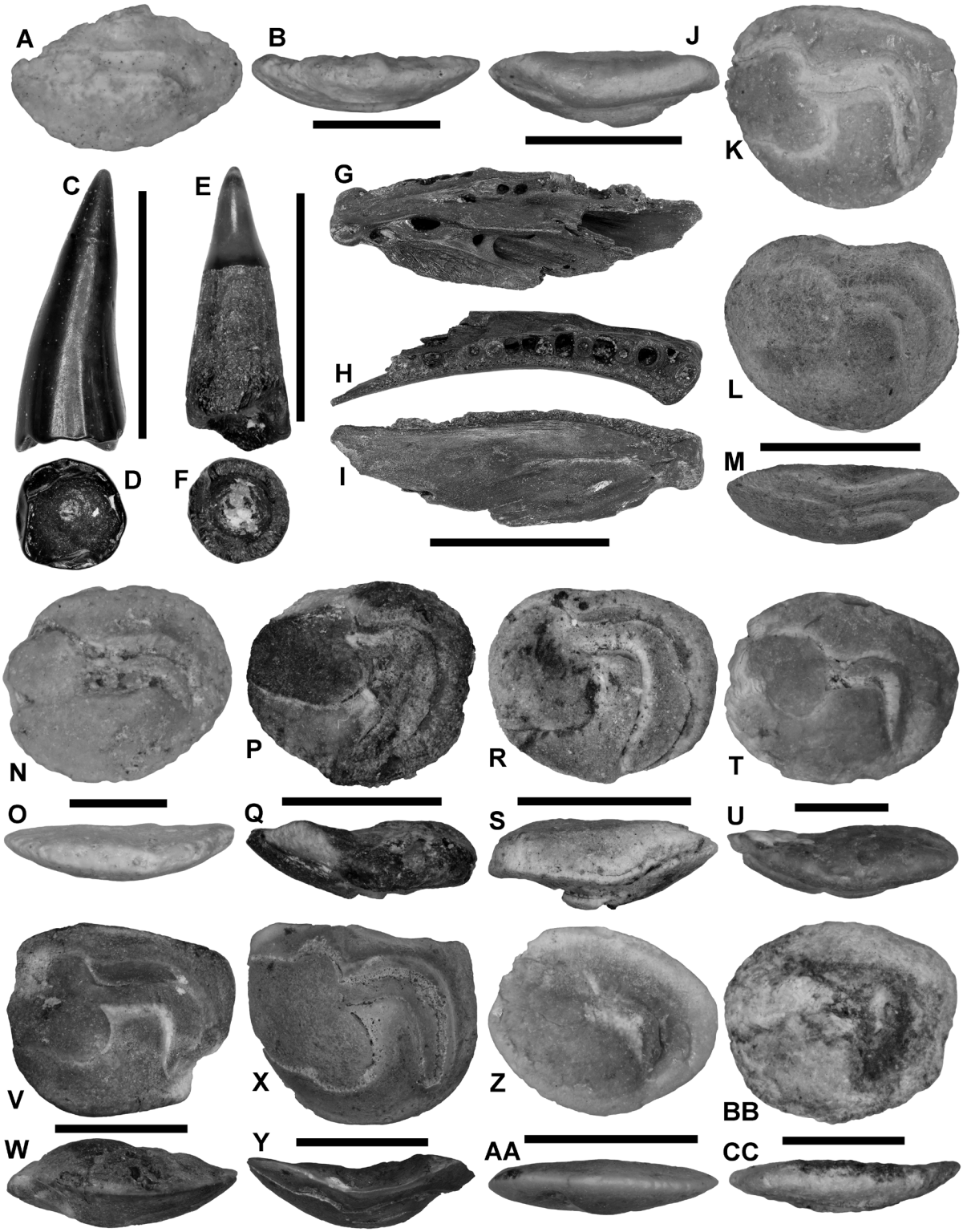

Member of the Byram Formation in Alabama, and it has not been reported from younger formations in the Gulf and Atlantic coastal plains (Stringer & Bell 2018; Stringer & Shannon 2019; Stringer & Hulbert 2020; Stringer & Starnes 2020; Stringer *et al*. 2020a, 2022b).

Family Lutjanidae Gill, 1861

Lutjanidae gen. et sp. indet.
Fig. 26C–I

Material examined

UNITED STATES OF AMERICA – **Mississippi** • 112 isolated teeth; Catahoula Formation; MMNS VP-7685 (4 teeth), MMNS VP-7685.1 (Fig. 26C–D), MMNS VP-7685.2 (Fig. 26E–F), SC2013.28.677 to 28.682, SC2013.28.683 (100 teeth) • 1 jaw; Catahoula Formation; MMNS VP-8341 (Fig. 26G–I).

Description

Specimen MMNS VP-8341 is an incomplete left dentary measuring roughly 4 cm in length and 1.5 cm in maximum height. In labial view, the oral and aboral margins are moderately convex. Much of the labial face is convex and smooth, and there are several large fenestrae penetrating the surface (Fig. 26G). Aborally, the jaw is thin and developed into a ridge-like structure bearing conspicuous oblique ridges. The anterior jaw margin is vertical and straight. Slightly posterior to this margin is a conspicuous constriction where the jaw measures only 7.5 mm in height. The lingual surface is smooth (Fig. 26I). In oral view, the jaw is convex antero-posteriorly, it is thickest at its blunt anterior end, and there is a single row of large tooth alveoli flanked by a medial tooth patch (Fig. 26H). All of the large alveoli occur along the labial margin and have a circular outline. The sizes of the alveoli demonstrate that the largest teeth were located anteriorly, but teeth decreased slightly in size towards the posterior end of the tooth row. The lingual tooth patch is widest anteriorly but narrows posteriorly, and it consists of numerous tiny and circular alveoli (Fig. 26H–I).

The isolated teeth attain up to 5 mm in total height. They are conical and straight to postero-medially curved to varying degrees (Fig. 26E and 26C, respectively). Well-preserved specimens show that the

Fig. 26 (page 88). *Allomorone* sp. (A–B), Lutjanidae gen. et sp. indet. (C–I), *Aplodinotus distortus* Nolf, 2003 (J–M), *A. gemma* (Koken, 1888) (N–S), Sciaenidae gen. et sp. indet. (T–W), *Sciaena*? *pseudoradians* (Dante & Frizzell in Frizzell & Dante, 1965) (X–AA), and *Sciaena*? *radians* (Koken, 1888) (BB–CC), remains. **A–B**. MMNS VP-12160, *Allomorone* sp., left otolith (reversed). **A**. Inner view. **B**. Dorsal view. **C–D**. MMNS VP-7685.1, Lutjanidae gen. et sp. indet., tooth. **C**. Profile view. **D**. Basal view. **E–F**. MMNS VP-7685.2, Lutjanidae gen. et sp. indet., tooth. **E**. Profile view. **F**. Basal view. **G–I**. MMNS VP-8341, Lutjanidae gen. et sp. indet., left dentary. **G**. Labial view. **H**. Oral view. **I**. Lingual. **J–K**. MMNS VP-7458.1, *Aplodinotus distortus*, left otolith (reversed). **J**. Dorsal view. **K**. Inner view. **L–M**. MMNS VP-7456.1, *A. distortus*, left otolith (reversed). **L**. Inner view. **M**. Dorsal view. **N–O**. MMNS VP-8712.2, *A. gemma*, right otolith. **N**. Inner view. **O**. Dorsal view. **P–Q**. MMNS VP-8430.1, *A. gemma*, right otolith. **P**. Inner view. **Q**. Dorsal view. **R–S**. MMNS VP-8430.2, *A. gemma*, left otolith (reversed). **R**. Inner view. **S**. Dorsal view. **T–U**. MMNS VP-8712.3, Sciaenidae gen. et sp. indet., left otolith (reversed). **T**. Inner view. **U**. Dorsal view. **V–W**. MMNS VP-8712.4, Sciaenidae gen. et sp. indet., right otolith. **V**. Inner view. **W**. Dorsal view. **X–Y**. MMNS VP-7445, *Sciaena*? *pseudoradians*, left otolith (reversed). **X**. Inner view. **Y**. Dorsal view. **Z–AA**. MMNS VP-8711.1, *S.*? *pseudoradians*, left otolith (reversed). **Z**. Inner view. **AA**. Dorsal view. **BB–CC**. MMNS VP-12076, *Sciaena*? *radians*, left otolith (reversed). **BB**. Inner view. **CC**. Dorsal view. Scale bars: A–B, N–O, T–U, BB–CC = 1 mm; C–D, P–Q, X–Y = 5 mm; E–F, R–S = 4 mm; G–I = 2 cm; J–M, V–W = 3 mm; Z–AA = 2 mm.

entire crown was covered by enameloid, but this is often only preserved on the upper one-half of the tooth. Interestingly, the apparently thinner enameloid covering along the lower one-half of the tooth is often a lighter color shade compared to the darker color of the upper one-half. Fine vertical fluting may occur on the posterior crown surface. Specimens that are ablated at the base show that the internal dentine is layered. Teeth have a circular basal outline, and the deep pulp cavity is framed by a thick wall of dentine (Fig. 24D, F).

Remarks

We compared the jaw and teeth described above to those of numerous extant fishes occurring in the Gulf of Mexico and found that they are very similar to representatives of Lutjanidae, particularly *Lutjanus*. The Catahoula Formation teeth are nearly identical to the large anterior teeth occurring on the premaxilla of *L. jocu* (Bloch & Schneider, 1801) (MSC 49315, SC uncurated specimen), but they are also similar to equivalent teeth of *L. synagris* (Linnaeus, 1758) (MSC 49478) and *L. campechanus* (Poey, 1860) (MSC 45233, MSC 49309). The fossil jaws differ by having a lingual tooth patch consisting of numerous tiny alveoli, as opposed to there being one or two rows of moderately-sized teeth in this region (as observed on the extant taxa noted above). Several interpretations could account for the variation in tooth size that we observed in the Catahoula Formation sample, including intra- and/or interspecific variation. It is possible that differences in tooth size are related to ontogeny within a single species, as the teeth of a 10 cm TL *L. campechanus* (MSC 45233) are simply smaller versions of teeth occurring in a 57.5 cm TL individual (MSC 49309). Additionally, the teeth along the jaws of one individual become smaller antero-posteriorly within the jaws. Although it is possible that the teeth and dentary available to us represent different species, there is currently no definitive evidence that more than one lutjanid taxon occurs within the Catahoula Formation.

Ebersole *et al.* (2019) reported teeth like those described above as Osteoglossidae indet. (i.e., bony tongues), derived from middle Eocene deposits in Alabama. However, a reexamination of these teeth as part of the current study leads us to believe that the Eocene teeth instead belong to Lutjanidae, a taxon that is common in the Gulf of Mexico today (see Hoese & Moore 1998). In contrast, extant osteoglossids are freshwater fish occurring in South America, Africa, and Southeast Asia to northern Australia (Nelson *et al.* 2016). Nevertheless, the lutjanid teeth in our Catahoula Formation sample represent the first Oligocene occurrence of this taxon in the Gulf Coastal Plain of the USA.

Order Acanthuriformes (sensu Nelson *et al.* 2016)
Suborder Sciaenoidei Betancur-R *et al.*, 2013
Family Sciaenidae Cuvier, 1829

Genus ***Aplodinotus*** Rafinesque, 1819

Type species

Aplodinotus grunniens Rafinesque, 1819, Extant.

Aplodinotus distortus Nolf, 2003
Fig. 26J–M

Material examined

UNITED STATES OF AMERICA – **Mississippi •** 19 sagittae; Catahoula Formation; MMNS VP-7449, MMNS VP-7461, MMNS VP-7456.1 (Fig. 26L–M), MMNS VP-8002.2, MMNS VP-8200.2, MMNS VP-8201.2, MMNS VP-8712 (8 specimens), MMNS VP-7458.1 (Fig. 26J–K), MMNS VP-7458.2, SC2013.28.760, SC2013.28.761, SC2013.28.793.

Description

The sagitta outline is somewhat rectangular (sensu Smale *et al*. 1995) in smaller specimens. Specimens larger than 5 mm show a marked distortion from the antero-dorsal to the posteroventral, which noticeably affects the overall shape. Furthermore, some of the larger specimens may show a hypertrophical development of the posteroventral margin, and there may also be an expansion of the antero-dorsal area. The margins are typically smooth. The inner face is somewhat convex and characterized by a very large, prominent heterosulcoid-type sulcus. The height of the cauda is slightly over 20% of the height of the ostium, and the cauda has a horizontal and downturned component. The outer face is not as convex as the inner face.

Remarks

Ontogenetic variation is apparent in our *A. distortus* otolith sample. For example, the ostium on juvenile specimens is much smaller in height, and the ventral margin of the sulcus has no expansion compared to adult specimens, where the ostium extends from near the antero-dorsal margin well down into the ventral field and is largest at the posterior portion. The ventral margin of the adult ostium curves distinctly upward toward the anterior margin and is subparallel to the anteroventral margin in larger specimens, and the posteroventral portion extends underneath the cauda. There are significant ontogenetic changes in the cauda, with the horizontal portion being significantly greater in length on smaller specimens compared adult specimens. Additionally, the downturned portion may have a greater length on large specimens, exceeding approximately 10 mm (see also Nolf 2003: pl. 4 fig. 4). The outer face ranges from nearly flat on small specimens to slightly more convex in larger specimens, and there is also greater convexity in the posterior portion than in the anterior. With respect to species identification, there is typically a wide area between the posterior of the ostium and the downturned portion of the cauda in *Aplodinotus distortus*, which is noticeably wider than that on *A. gemma* (see below). *Aplodinotus distortus* lacks the inframedian tip on the posterior margin occurring on *Sciaena*? *radians* sagittae.

Nolf (2003) named *Aplodinotus distortus* based on specimens from the Byram Formation (Oligocene, Rupelian) at the Keyes Iron and Metal locality near Vicksburg, Mississippi, USA. Specimens were recovered from other Byram Formation exposures in the Vicksburg vicinity, and otoliths were also obtained from the Rosefield Marl Beds of the Rosefield Formation (Oligocene, Rupelian) in Catahoula Parish, Louisiana (Stringer & Worley 2003). One of the current authors (GLS) has observed that specimens 10 mm in length are common in several of the Byram Formation localities in the Vicksburg, Mississippi area.

Although only 18 specimens of *Aplodinotus distortus* were recovered (including one tentatively referred to the species) from the Catahoula Formation at Jones Branch (4.4% of the otolith sample), the taxon is more abundant than *Sciaena*? *radians* but much less common than *S.*? *pseudoradians* and *A. gemma*. Like *S.*? *pseudoradians*, *S.*? *radians*, and *Aplodinotus gemma*, *A. distortus* is widespread in the Gulf Coastal Plain and is known from many Oligocene formations in Louisiana and Mississippi (Nolf 2003, 2013; Stringer & Worley 2003; Worley 2004).

Aplodinotus gemma (Koken, 1888)
Fig. 26N–S

Otolithus (*Sciandarum*) *gemma* Koken, 1888: 281.

Material examined

UNITED STATES OF AMERICA – **Mississippi •** 46 sagittae; Catahoula Formation; MMNS VP-7447, MMNS VP-7452, MMNS VP-7456.2, MMNS VP-7458.3, MMNS VP-7459.3, MMNS VP-8201.1, MMNS VP-8430 (2 specimens), MMNS VP-8430.1 (Fig. 26P–Q), MMNS VP-8430.2 (Fig. 26R–S),

MMNS VP-8712.2 (Fig. 26N–O), SC2013.28.771, SC2013.28.779, GLS otolith comparative collection (33 specimens).

Description

The sagitta outline is somewhat square to discoidal (sensu Smale *et al*. 1995). Larger specimens (greater than 5 mm) have a greater dorso-ventral height, and a more discoidal shape compared to smaller ones. The margins are generally smooth. The inner face is generally strongly convex and characterized by a very large, prominent heterosulcoid-type sulcus. The ostium extends from near the antero-dorsal margin well down into the ventral field and is largest at the posterior portion. The ventral margin of the ostium curves only slightly upward toward the anterior margin. The posteroventral portion of the ostium extends underneath the cauda. Generally, there is a very short distance between the posterior of the ostium and the downturned portion of the cauda. The height of the cauda constitutes approximately 25% of the height of the ostium, and the cauda has a horizontal and downturned component. The downturned portion of the cauda tends to be slightly curved. The outer face is only slightly convex, and that of larger specimens is often more irregular than on smaller specimens.

Remarks

Koken (1888) mentioned this species from the "Vicksburg; Red Bluff; Jackson River, Mississippi" and "Jackson and Vicksburg Beds," but the exact stratigraphic occurrence(s) for his specimens cannot be ascertained. However, *Aplodinotus gemma* is known from Oligocene formations (Mint Spring and Byram formations) in the vicinities of Vicksburg and Jackson in Mississippi (Nolf 2003, 2013; Stringer *et al*. 2020c). Specimens of *A. gemma* are also known from the Rosefield Marl Beds of the Rosefield Formation (Oligocene, Rupelian) in Catahoula Parish, Louisiana (Stringer & Worley 2003; Worley 2004) and from the Glendon Limestone Member of the Byram Formation of Alabama (Ebersole *et al*. 2021). The 46 *A. gemma* specimens from the Catahoula Formation constitute 11.2% of the total number of otoliths in the sample. This abundance is only exceeded by *Sciaena*? *pseudoradians* (see below).

Schwarzhans (1993) proposed the otolith-based genus *Frizzelithus* to accomodate *A. gemma*. However, this designation was based on only 20 large specimens, some of which were eroded. The present study has the advantage of including hundreds of sciaenid otoliths from the Oligocene of Alabama, Mississippi, and Louisiana, as well as an ontogenetic series. Whereas fig. 144 in Schwarzhans (1993) represents *Aplodinotus gemma*, figs 145–146 are significantly different in the shape of the ostium and the salient inframedian posterior tip, and are attributed to *Sciaena*? *radians* (Nolf 2003, 2013). The otolith in fig. 147 is much more elongate, has a greater distance between the ostium and downturned portion of the cauda, and the shape of the ostium differs greatly from that in fig. 144. The former matches *Sciaena*? aff. *pseudoradians* from the upper Eocene and *Sciaena*? *pseudoradians* from the Oligocene of the Gulf Coast. Several of the sciaenids of the Oligocene appear to be closely related to the extant *Aplodinotus grunniens* Rafinesque, 1819 (Nolf 2003, 2013; Ebersole *et al.* 2021; Fuelling *et al.* 2022), which is extremely common in eastern North America, and the Catahoula specimens are placed in this genus.

Genus ***Sciaena*** Linnaeus, 1758

Type species

Sciaena umbra Linnaeus, 1758, Extant.

Sciaena? ***pseudoradians*** (Dante & Frizzell in Frizzell & Dante, 1965)
Fig. 26X–AA

Corvina pseudoradians Dante & Frizzel in Frizzell & Dante, 1965: 707–708.

Material examined

UNITED STATES OF AMERICA – **Mississippi •** 134 sagittae; Catahoula Formation; MMNS VP-7445 (Fig. 26X–Y), MMNS VP-7446 (3 specimens), MMNS VP-7448 (3 specimens), MMNS VP-7451, MMNS VP-7453 (4 specimens), MMNS VP-7459.2, MMNS VP-7460.1, MMNS VP-8200.1 (9 specimens), MMNS VP-8711 (4 specimens), MMNS VP-8711.1 (Fig. 26Z–AA), MMNS VP-8935, SC2013.28.757, SC2013.28.758, SC2013.28.762, SC2013.28.764 to 28.770, SC2013.28.772, SC2013.28.774 to 28.776, SC2013.28.778, SC2013.28.781 to 28.783, SC2013.28.786, SC2013.28.794, SC2013.28.801, GLS otolith comparative collection (84 specimens).

Description

The outline of *Sciaena*? *pseudoradians* is primarily rectangular (sensu Smale *et al*. 1995), but the anterior and ventral margins are somewhat convex and rounded. The margins are typically smooth, and the inner face is moderately convex. The inner face is characterized by a very large, prominent heterosulcoid-type sulcus. The ostium is exceptionally large in length and height, especially compared to the cauda. The ostium extends from near the anterodorsal margin well down into the ventral field and is largest at the posterior portion. The posteroventral portion of the ostium extends noticeably underneath the cauda in larger specimens. The height of the cauda is only about 25% of the height of the ostium (i.e., much narrower in comparison). The cauda has a distinctive horizontal and downturned component. The horizontal portion appears to shorten in length compared to the downturned portion during ontogenetic development (Nolf 2003: pl. 2 figs 3–6). The outer face increases in irregularity with growth and is convex, but not as much as the inner face.

Remarks

Dante & Frizzell in Frizzell & Dante (1965) first named *Sciaena*? *pseudoradians* as *Corvina pseudoradians* based on specimens from the Byram Formation (Oligocene, Rupelian) in Mississippi, USA, and the holotype (USNM 23368) was illustrated by Nolf (2003: fig. 6). *Sciaena*? *pseudoradians* is known from numerous Oligocene formations in Mississippi, Louisiana, and Alabama (Nolf 2003; Stringer & Worley 2003; Worley 2004; Stringer *et al.* 2020c; Ebersole *et al*. 2021), and its presence is therefore not unexpected in the Catahoula Formation. *Sciaena*? *pseudoradians* is the most abundant otolith-based species in our Catahoula Formation sample (n = 134), including seven additional specimens tentatively assigned to the species. Nolf & Stringer (2003) identified *Sciaena*? aff. *pseudoradians* from the upper Eocene (primarily Priabonian) Yazoo Clay based on 78 specimens of the 5293 otoliths they examined (1.47% of the sample). *Sciaena* aff. *pseudoradians* was reported from the Eocene Clinchfield Formation in Georgia, where it represented 8% of the total number of specimens in the bulk sample. Lin & Nolf (2022) noted that *S.*? *pseudoradians* is known primarily from the lower Oligocene of the Gulf Coastal Plain, but they also noted that "imperfectly preserved" otoliths are known from the Eocene of Texas and Louisiana (Bartonian and Priabonian).

Sciaena*? *radians (Koken, 1888)
Fig. 26BB–CC

Otolithus (*Sciaenidarum*) *radians* Koken, 1888: 280.

Material examined

UNITED STATES OF AMERICA – **Mississippi •** 3 sagittae; Catahoula Formation; MMNS VP-8934, MMNS VP-12076 (Fig. 26BB–CC), SC2013.28.763.

Description

The outline of the sagitta is somewhat rectangular (sensu Smale *et al*. 1995), but the anterior, dorsal, and ventral margins are slightly convex and rounded to various degrees (Fig. 26BB). The margins are

typically smooth, and there is a highly characteristic inframedian tip on the posterior margin. The inner face is moderately convex (Fig. 26CC) and characterized by a very large and prominent heterosulcoid-type sulcus. The ostium is noticeably large in its length and height. The ostium extends from near the anterodorsal margin well into the ventral field and is largest at the posterior portion. The ventral margin of the ostium curves distinctly upward toward the anterior margin and is subparallel to the anteroventral margin. The posteroventral portion of the ostium extends conspicuously underneath the cauda, especially on larger specimens. The height of the cauda is about 30% of the height of the ostium. The cauda has a characteristic horizontal and downturned component. The horizontal and downturned portions are of similar length, but the downturned portion is usually slightly longer on the larger specimens (Nolf 2003: pl. 4 figs 1–3). The outer face becomes somewhat more irregular on larger specimens. The outer face is nearly flat on small specimens but is more convex on larger specimens, although it is not nearly as convex as the inner face.

Remarks

Koken (1888) originally named *Otolithus* (*Sciaenidarum*) *gemma* based on specimens labeled only as "Vicksburg" from Mississippi, USA. Unfortunately, Koken's type suite actually contained three different species, including *Sciaena*? *radians*, *S.*? *pseudoradians*, and *Aplodinotus gemma* (see discussion in Nolf 2003). Only three specimens of *Sciaena*? *radians* were recovered from the Catahoula Formation (less than 1% of the total specimens), and the species is the least common of the sciaenids within the otolith assemblage. Although "*S.*?" *radians* is widespread in the Gulf Coastal Plain and is known from many Oligocene formations in Mississippi, Louisiana, and Alabama (Nolf 2003, 2013; Stringer & Worley 2003; Worley 2004; Stringer *et al.* 2020c), the species is similarly rare in those assemblages.

Sciaenidae gen. et sp. indet.
Figs 26T–W, 27

Material examined

UNITED STATES OF AMERICA – **Mississippi** • 5761 isolated teeth; Catahoula Formation; SC2013.28.809 (Fig. 27F–H), SC2013.28.810, SC2013.28.811 (Fig. 27I–K), SC2013.28.812, SC2013.28.813 (79 teeth), SC2013.28.842 (5678 teeth) • 16 pharyngeals; Catahoula Formation; SC2013.28.684 (Fig. 27C–E), SC2013.28.685 to 28.689, SC2013.28.690 (9 specimens), SC2013.28.691 • 192 sagittae; Catahoula Formation; MMNS VP-7457 (2 specimens), MMNS VP-7460.2, MMNS VP-8712.3 (Fig. 26T–U), MMNS VP-8712.4 (Fig. 26V–W), MMNS VP-8933 (2 specimens), MMNS VP-8933.1 (Fig. 27A–B), SC2013.28.759, SC2013.28.773, SC2013.28.777, SC2013.28.780, SC2013.28.784, SC2013.28.785, SC2013.28.787, SC2013.28.790, SC2013.28.792, SC2013.28.798 to 28.800, SC2013.28.806 (6 specimens), SC2013.28.807 (12 specimens), GLS otolith comparative collection (154 specimens).

Description

The best-preserved sciaenid jaw element is an edentulous lower right pharyngeal (Fig. 27C–E). In aboral and oral views, the bone has a somewhat triangular outline. The symphyseal margin is rather straight and would have abutted (but not fused) with the left pharyngeal. The labial margin is relatively straight and intersects the symphyseal margin at a blunt anterior point. Posteriorly the labial margin extends away from the symphysis, and the distal margin is convex. The oral surface bears alveoli and broken tooth bases that are loosely arranged into rows that parallel the labial margin. The teeth are largest anteriorly, but teeth located at the distal one-third of the jaw were only about one-half as large. In symphyseal view, the symphyseal surface is high, especially medially, and the anterior end of the bone curves dorsally. The ventral strut that buttressed the bone against the cleithrum is incompletely preserved.

Isolated teeth consist of a moderately high crown and base that comprises one-third or less of the total tooth height (Fig. 27F–K). The crown is covered by a relatively thin layer of smooth enameloid that ends abruptly at the base (Fig. 27G, J). The occlusal surface of unworn teeth is weakly to moderately convex, but the crowns of worn teeth exhibit a flat surface with exposed dentine. The occlusal outline is polygonal (i.e., four-sided to six-sided; Fig. 27F, I), and the sides of the crown are flat and vertical. In basal view, a small and deep pulp cavity is framed by a thick wall of dentine (Fig. 27H, K).

Remarks

Herein included within undetermined sciaenid fishes are isolated teeth, pharyngeal tooth plates, and poorly preserved otoliths. The pharyngeal bones are largely abraded and incomplete, often hindering our ability to determine their location in the jaw let alone the taxon represented. The isolated teeth are reminiscent of several sciaenid species, and we could not conclusively determine that they are representative of any one of the taxa we identified by otoliths. The otoliths are not well enough preserved for us to assign them to a particular genus (i.e., Fig. 26T), and it is unclear whether they represent one of the taxa described herein. All of these specimens are included here for completeness.

Order Spariformes (sensu Nelson *et al.* 2016)
Family Sparidae Rafinesque, 1818

Genus ***Diplodus*** Rafinesque, 1810

Type species

Sparus annularis Linnaeus, 1758, Extant.

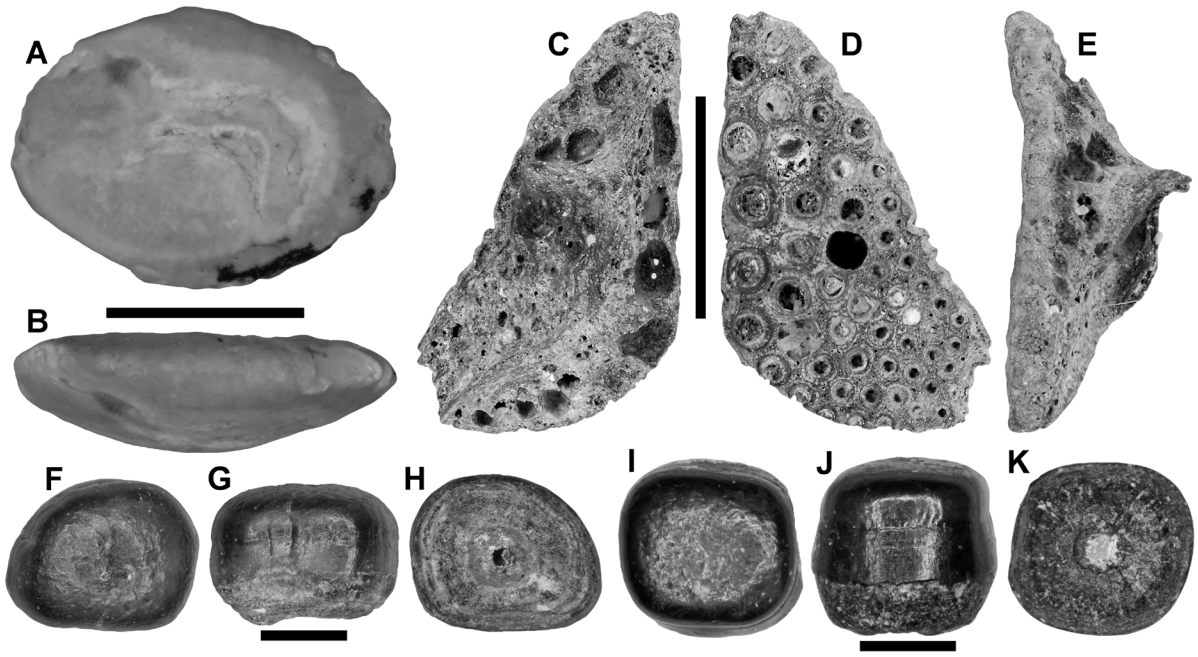

Fig. 27. Sciaenidae gen. et sp. indet., remains. **A–B**. MMNS VP-8933.1, right sagitta. **A**. Inner view. **B**. Dorsal view. **C–E**. SC2013.28.684, lower right pharyngeal. **C**. Aboral view. **D**. Oral view. **E**. Symphyseal view. **F–H**. SC2013.28.809, tooth. **F**. Occlusal view. **G**. Profile view. **H**. Basal view. **I–K**. SC2013.28.811, tooth. **I**. Occlusal view. **J**. Profile view. **K**. Basal view. Scale bars: A–B, F–K = 1 mm; C–E = 5 mm.

Diplodus sp.
Fig. 28

Material examined

UNITED STATES OF AMERICA – **Mississippi** • 183 isolated teeth; Catahoula Formation; SC2013.28.643 (Fig. 28A–C), SC2013.28.644 to 28.650, SC2013.28.651 (Fig. 28D–F), SC2013.28.652, SC2013.28.653, SC2013.28.654 (2 teeth), SC2013.28.655 (11 teeth), SC2013.28.656 (16 teeth), SC2013.28.657 (20 teeth), SC2013.28.658 (21 teeth), SC2013.28.659 (20 teeth), SC2013.28.660 (13 teeth), SC2013.28.661 (37 teeth), SC2013.28.662 (17 teeth), SC2013.28.663 (15 teeth).

Description

Isolated teeth are highly laterally compressed (labio-lingually) and approximately as tall (apico-basally) as they are elongated (mesio-distally). The crown constitutes the upper two-thirds of a tooth and is covered with smooth enameloid. The labial crown face is weakly convex and the lingual face weakly concave (Fig. 28C, F). In mesial/distal view, the crown may be lingually curved. In labial/lingual view, unworn teeth have a roughly rhomboidal outline. The mesial margin may be uniformly convex or sinuous, with the basal portion being most convex but transitioning apically to concave. The distal margin is sinuous, with the basal portion being most convex but transitioning apically to concave. The apical part of the crown is formed into a cusp-like projection (Fig. 28B). The crown tapers basally towards a narrow bony projection, and the crown foot is marked by the enameloid boundary (Fig. 28E).

Remarks

Our sample includes teeth that are worn to varying degrees. These teeth demonstrate that the cuspidate crown apex exhibits the initial signs of in vivo wear (polished and somewhat flattened wear facet), and with continued use the cusp is worn completely away to a flat, relatively horizontal surface that reveals the internal dentine (compare Fig. 28A to D). Some teeth are worn nearly to the crown base, indicating a long period of tooth retention within the jaws and possibly pointing to a durophagous diet.

Diplodus sp. was recently reported from the upper Rupelian Givhans Ferry Member of the Ashley Formation in Dorchester County, South Carolina by Cicimurri *et al.* (2022). These teeth are easy to distinguish from those of all other bony fishes by their laterally compressed crowns with sinuous anterior and posterior margins. Our Catahoula Formation teeth represent the first occurrence of this taxon from the Gulf Coastal Plain of the USA.

Genus ***Sparus*** Linnaeus, 1758

Type species

Sparus aurata Linnaeus, 1758, Extant.

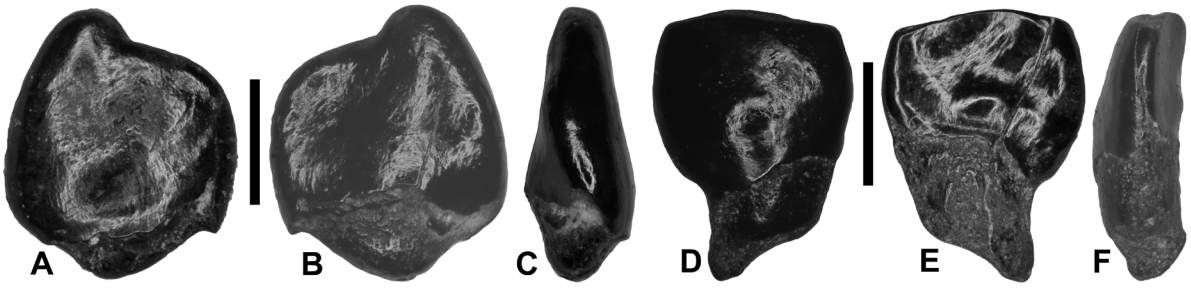

Fig. 28. *Diplodus* sp., teeth. **A–C**. SC2013.28.643, tooth. **A**. Outer view. **B**. Inner view. **C**. Anterior view. **D–F**. SC2013.28.651, tooth. **D**. Outer view. **E**. Inner view. **F**. Anterior view. Scale bars = 1 mm.

Sparus*? cf. *elegantulus (Koken, 1888)
Fig. 29A–B

Otolithus (*Pagelli*) *elegantulus* Koken, 1888: 279.

Material examined

UNITED STATES OF AMERICA – **Mississippi** • 1 sagitta; Catahoula Formation; MMNS VP-12077.

Description

The outline of MMNS VP-12077 is essentially a square. The margins are primarily irregular with varying indications of lobation, sinuosity, and smoothness. The height/length ratio is about 0.65. The inner face tends to be slightly and fairly evenly convex (Fig. 29B). A prominent heterosulcoid-type sulcus extends across approximately 85% of the inner face (Fig. 29A). The sulcus, which is located slightly dorsal, is essentially horizontal except for a very small, downwardly flexed posterior of the cauda. The ostium opens on the anterior margin. The dorsal and ventral margins of the ostium are approximately parallel. The posteroventral portion of the ostium does not extend underneath the cauda. The ostium is approximately 40% of the length of the cauda. The height of the cauda is approximately 50–60% of the height of the ostium. Approximately 80% of the cauda is horizontal with about 20% downturned. The downturned portion is approximately 45° from horizontal. There is an irregularly shaped, dorsal depression above the cauda and a faint ventral furrow located away from the ventral margin. The outer face is slightly concave and may be slightly irregular.

Remarks

The single specimen was tentatively assigned to *Sparus elegantulus* due to its preservation. The species was originally identified by Koken (1888) in the Gulf Coast Plain of the USA. *Sparus*? *elegantulus* is known from the Eocene of Alabama, Georgia, Louisiana, and Mississippi (Nolf & Stringer 2003; Nolf 2013; Stringer *et al.* 2022a). Within Oligocene deposits, the species has previously been reported from the Rupelian Glendon Limestone (NP22/23) in Mississippi (Stringer *et al.* 2020c) and from the Glendon Limestone Member of the Byram Formation (NP23) of Alabama by Ebersole *et al*. (2021). In the latter occurrence, the species was relatively abundant and represented 12.06% of the total otolith sample.

Sparidae gen. et sp. indet.
Fig. 29C–J

Material examined

UNITED STATES OF AMERICA – **Mississippi** • 1041 isolated teeth; Catahoula Formation; SC2013.28.664 to 28.666, SC2013.28.667 (6 specimens), SC2013.28.668 (Fig. 29I–J), SC2013.28.669, SC2013.28.670 (3 specimens), SC2013.28.671 (3 specimens), SC2013.28.672, SC2013.28.673 (4 specimens), SC2013.28.674 (4 specimens), SC2013.28.675, SC2013.28.676 (4 specimens), SC2013.28.903 (Fig. 29C–E), SC2013.28.904 (Fig. 29F–H), SC2013.28.907, SC2013.28.910 (1007 specimens).

Description

In addition to *Diplodus* sp., at least two other sparid tooth morphotypes occur in the Catahoula Formation. One morphotype, shown in Fig. 29C–H, is represented by low- and high-crowned specimens. Low-crowned specimens have a weakly to moderately convex occlusal surface (compare Fig. 29D to G) and circular to ovate occlusal outline (compare Fig. 29C to F). High-crowned specimens are cylindrical with a very convex occlusal surface and circular occlusal outline. Regardless of crown height, there is a conspicuous basal band that is distinguished by a weak cingulum (Fig. 29G). In basal view, a large pulp cavity is framed by a thick dentine wall with a thick external enameloid covering (Fig. 29E, H).

Fig. 29. Sparidae gen. et sp. indet., remains. **A–B**. MMNS VP-12077, left sagitta (reversed). **A**. Inner view. **B**. Dorsal view. **C–E**. SC2013.28.903, tooth. **C**. Occlusal view. **D**. Profile view. **E**. Basal view. **F–H**. SC2013.28.904, tooth. **F**. Occlusal view. **G**. Profile view. **H**. Basal view. **I–J**. SC2013.28.668, tooth. **I.** Profile view. **J.** Basal view. Scale bars: A–B = 1 mm; C–J = 2 mm.

Another morphotype is like that shown in Fig. 29I–J. These teeth are also of variable height, but all have a very convex labial face and less convex lingual face. In profile view, the crown is medially curved and the labial and lingual faces are asymmetrically divided by blunt carinae that may or may not reach the crown base (Fig. 29I). In basal view, the tooth base has a circular to slightly oval outline, and the central pulp cavity varies in size but is framed by a wall of dentine covered with thick external enameloid (Fig. 29J).

Remarks

Teeth within the jaws of extant Sparidae that we examined can be differentiated into incisiform, lateral, and molariform types. Incisiform teeth are located along the anterior margin of tooth plates, whereas lateral teeth occur along the lateral margins (i.e., Fig. 29I). Molariform teeth occur on the main body of a pharyngeal tooth plate and form most of a triturating surface (i.e., Fig. 29C, F). The lateral teeth identified as *Diplodus* sp. (see above) are easily separated from those assigned to Sparidae indet. by their thinness and sinuous anterior and posterior margins.

Order Lophiiformes Garman, 1899
Family Lophiidae Rafinesque, 1810

Lophiidae gen. et sp. indet.
Fig. 30

Material examined

UNITED STATES OF AMERICA – **Mississippi** • 229 teeth, MMNS VP-6995 (10 teeth), SC2013.28.581 (Fig. 30A–C), SC2013.28.582 (Fig. 30G–I), SC2013.28.583, SC2013.28.584 (Fig. 30D–F), SC2013.28.585, SC2013.28.586, SC2013.28.587 (Fig. 30J–L), SC2013.28.588 (8 teeth), SC2013.28.589 (15 teeth), SC2013.28.590 (36 teeth), SC2013.28.591 (15 teeth), SC2013.28.592 (51 teeth), SC2013.28.593 (87 teeth).

Description

The isolated teeth are tall, needle-like, and, in profile view, posteriorly curving to varying degrees (Fig. 30A, D, G, J). The crown is conical to somewhat laterally compressed, with the anterior face of the latter morphology being narrower than that of the posterior face (Fig. 30B, E, H). In anterior/posterior

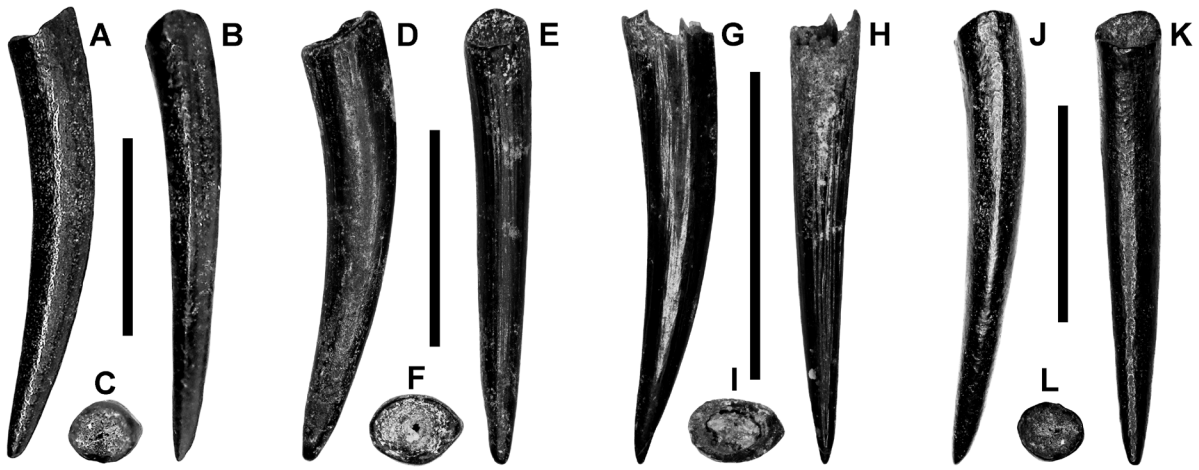

Fig. 30. Lophiidae gen. et sp. indet., remains. **A–C**. SC2013.28.581, tooth. **A**. Labial view. **B**. Posterior view. **C**. Basal view. **D–F**. SC2013.28.584, tooth. **D**. Lingual view. **E**. Posterior view. **F**. Basal view. **G–I**. SC2013.28.582, tooth. **G**. Labial view. **H**. Posterior view. **I**. Basal view. **J–L**. SC2013.28.587, tooth. **J**. Labial view. **K**. Posterior view. **L**. Basal view. Scale bars = 5 mm.

view, the crown may be weakly medially curved. Enameloid is not evident on any specimens, but the posterior surface bears numerous closely spaced, parallel vertical ridges extending up to three-quarters of the tooth height. The teeth have a labial carina that extents the height of the tooth. In basal view, the tooth has a circular to elliptical outline, and a circular pulp cavity is deep and framed by a thin wall of dentine (Fig. 30C, F, I, L).

Remarks

The fossil material we examined compares very well to an extant *Lophius americanus* Cuvier & Valenciennes, 1837 in the MSC collection (MSC 50198), as well as illustrations of Miocene material reported from elsewhere (Purdy *et al.* 2001: fig. 66c; Schultz 2006: pl. 1 figs 1b, 2b). The lophiid teeth are easily distinguished from the teeth of all other Catahoula Formation teleosts by their tall, needle-like and curved crown, posterior longitudinal ridges, labial carina, and circular basal outline. Additional extant lophiid comparative specimens are needed to further elucidate the taxonomic affinities of these remains.

Order Tetraodontiformes Berg, 1940
Suborder Tetraodontoidei Nelson *et al*., 2016
Family Tetraodontidae Bonaparte, 1831

Tetraodontidae gen. et sp. indet.
Fig. 31

Material examined

UNITED STATES OF AMERICA – **Mississippi •** 6 isolated jaws; Catahoula Formation; SC2013.28.604, SC2013.28.605 (Fig. 31A–C), SC2013.28.606, SC2013.28.607 (2 specimens), SC2013.28.608 (Fig. 31D–F).

Description

Specimen SC2013.28.608 is a right premaxilla measuring 4 mm in antero-posterior length, 1.5 mm in dorso-ventral height, and 1 mm in greatest medio-lateral width. In aboral view, the jaw is thickest

mesially but tapers distally, it has an arcuate appearance (convex labially), and the internal bony structure has a spongy appearance (Fig. 31F). In labial view, the jaw surface is convex and appears to consist of a uniform layer of shiny tissue (Fig. 31E). In oral view, much of the triturating surface is rather thin and the labial margin is sharp. In symphyseal view, the articular surface (for the left premaxilla) bears a series of fossae that are separated by thin dentine lamellae. Additionally, what appears to be a circular triturating pad occurs on the oral surface, just distal to the symphysis (Fig. 31D).

Also included in our sample are jaw fragments that are comprised of stacked rows of teeth. In labial view, the teeth are very low (apico-basally) and elongated (mesio-distally). Tooth length varies among the teeth in a row, and they have roughly rectangular outlines. The teeth in each row may butt directly against each other, or the tapered ends may overlap the end of the preceding/succeeding teeth (Fig. 31B). The teeth in successive rows may not perfectly overlie those in previous rows, and younger teeth may be longer or shorter than the tooth immediately below. In lingual view, the teeth are embedded in osteodentine (Fig. 31A).

Remarks

The specimens are very small, but SC2013.28.608 is similar to the premaxillae of fossil tetraodontoid taxa that have been described. The premaxilla of the Pliocene *Spheroides hyperostosis* Tyler *et al.*, 1992 bears a single triturating tooth on the oral surface, whereas that of the Oligocene *Archaeotetraodon winterbottomi* Tyler & Bannikov, 1994 has three. The premaxilla of *Eotetraodon* Tyler, 1980 is incompletely known, but the dentary or *E. tavernei* Tyler & Bannikov, 2012 bears two triturating teeth. *Lagocephalus striatus* Aguilera *et al.*, 2018 was recently described from the Middle Miocene strata of Panama, but the morphology of the triturating surface of the premaxilla is presently unknown. Similarly, the premaxilla morphology of *Leithaodon sandroi* Carnevale & Tyler, 2015 from the Middle Miocene of Austria is unknown. Unfortunately, the knob-like triturating pad of SC2013.28.608 is ablated and it is difficult to determine whether the triturating surface consists of one or two teeth. Additional specimens, particularly cranial material, are necessary to accurately determine the generic affinity of the Catahoula Formation pufferfish.

The jaws of two other groups of tetraodontiform fishes, Diodontidae and Triodontidae, have anterior beak-like structures, but these differ from the Catahoula Formation specimens by being composed of alternating stacked rows of sub-triangular teeth with pointed apices (Thiery *et al.* 2017). The Catahoula Formation pufferfish specimens are significant because, to our knowledge, they represent the first Oligocene record of Tetraodontidae in the Western Hemisphere.

Fig. 31. Tetraodontidae gen. et sp. indet., remains. **A–C**. SC2013.28.605, jaw. **A**. Lingual view. **B**. Labial view. **C**. Aboral view. **D–F**. SC2013.28.608, right premaxilla. **D**. Lingual view. **E**. Labial view. **F**. Aboral view. Scale bars: A–C = 1 mm; D–F = 2 mm.

Teleostei fam., gen. et sp. indet.

An additional 1127 teleost remains include isolated jaws like premaxillae and dentaries (n = 17), other cranial bones like quadrates and vomerines (n = 8), isolated teeth (n = 843), fin spines (n = 210), and vertebrae (n = 49). Our comparative sample of extant marine taxa did not allow us to assign these remains beyond Teleostei and are not discussed in further detail. These specimens were included in the total number of fish remains examined in our sample, but not counted among the remains identified to at least the ordinal level.

Discussion

Our evaluation of 13 551 fish fossils from the Catahoula Formation indicates that a rather diverse late Oligocene (Chattian) fauna is preserved within the fossiliferous horizon we sampled. The taxa we identified are largely based on teeth, jaw elements, scales, and fin spines, but our knowledge of the paleofauna is supplemented by a sample of 409 otoliths. Details regarding the Catahoula Formation fish assemblage are provided below, and the chondrichthyan and teleost taxa we identified are listed in Appendix 1 and Appendix 2, respectively.

Characteristics of the Catahoula fish assemblage

The 3605 elasmobranch teeth, scales, and caudal spines within our Catahoula Formation sample represent 29 taxa belonging to five orders and nineteen families. Sharks are more diverse than rays in this assemblage, with 19 taxa belonging to 12 families compared to 10 taxa within six families, respectively. Of the sharks, Carcharhiniformes is the most diverse group (12 taxa in five families), followed by Lamniformes (four genera in four families) and Orectolobiformes (three genera in three families). Myliobatiformes is the more diverse ray group and is represented by at least seven taxa, whereas there are three genera (within two families) of Rhinopristiformes.

Sharks and rays possess a polyphyodont dentition where teeth within the various files are continuously replaced throughout the lifetime of an individual (Rasch *et al.* 2016). The replacement rates, faster or slower, could impact our ability to determine abundance or rarity within the Catahoula Formation elasmobranch assemblage. Tooth replacement is relatively fast in some sharks, like *Ginglymostoma*, and may occur within ten days (Luer *et al*. 1990). Conversely, it may take more than a month for a tooth to be replaced in *Triakis* (Smith *et al*. 2009). Tooth abundance could also be affected by other factors, like regular death of individuals and scattering of large numbers of teeth, rather than regular replacement by living individuals. However, we can only presume that the numbers of specimens we recovered for each taxon reflects their scarcity or abundance within the Catahoula Formation fossil bed. Furthermore, the abundance/scarcity of a taxon within the Catahoula Formation is likely related to environmental and/or dietary preferences for the taxa we identified. Although we cannot rule out the possibility that our sample is influenced by preservation and/or collecting biases, we believe that the latter was mitigated by the small mesh sizes employed to recover remains (0.4 mm), which in addition to small elasmobranch and teleost fossils also includes foraminifera tests and ostracod valves.

Of the shark component, Carcharhiniformes is the most common group based on isolated teeth (n = 1729), followed by Lamniformes (n = 245) and Orectolobiformes (n = 21). Continuing this further, *Carcharhinus acuarius* (daggernose shark) is the most abundant elasmobranch, not just in the shark component but within the total elasmobranch sample (n = 986, 49% of the shark component and 27% of the total elasmobranch sample). Other common sharks include *Hemipristis intermedia* sp. nov. (n = 196, roughly 10% of the shark sample), *Carcharhinus elongatus* (n = 287, 14% of the shark sample), and *Carcharias cuspidatus* (n = 240, 12% of the shark sample).

Of the batoids, teeth of taxa with durophagous (crushing) dentitions are common but largely represented by lateral teeth and broken symphyseal teeth. These teeth represent at least three genera, but the highly worn and/or broken nature of 49.5% of the total sample (326 teeth out of 658 specimens) inhibits our ability to determine whether other taxa are represented. It does appear that presumed filter-feeding rays, represented by two genera (*Plinthicus* sp., *Paramobula fragilis*), are rare components of the Catahoula Formation fish assemblage, as they are represented by a total of three teeth. *Hypanus*? *heterodontus* sp. nov. is the most abundant of the Catahoula Formation batoids, and the 578 teeth we recovered comprise over 36% of the total batoid component. *Rhynchobatus* teeth are also common, with 246 teeth representing 15% of the batoid sample.

Of the 9937 Catahoula Formation bony fish fossils we examined, 96% of the sample consists of skeletal remains, particularly teeth but to a lesser extent jaws, scales, and fin spines. The remaining 4% of the sample includes otoliths. Together, these fossils indicate that at least 20 unequivocal bony fish taxa occur in the Catahoula Formation. One order, Siluriformes, is based on fin spines, but ten families have been identified based on teeth, jaws and/or scales. Three of these families, Albulidae, Sciaenidae, and Sparidae, are also known by otoliths. We presume that the teeth and jaw bones generically assigned to Sciaenidae and Sparidae represent any of the seven genera within these families that we identified by otoliths, although we cannot discount the presence of other species or even genera. Three additional families, Congridae, Cyclopsettidae, and Haemulidae, are known only by otoliths.

As noted above, there is a fundamental difference in the occurrence of bony fish teeth and otoliths in the Catahoula Formation fish assemblage. It is improbable, if not impossible, to equate the number of individual teeth to the number of individual fish represented in our sample. Bony fishes are primarily polyphyodont, and the tooth loss and replacement system is not well documented at the generic and especially at the species level. This is primarily due to a lack of obvious patterning in the mouth, accurately determining loss of teeth, and maintaining specimens long enough in a controlled environment to observe and document loss and replacement (i.e., Carr *et al*. 2021). Much of the literature on polyphyodont bony fishes has emphasized taxa with extreme morphological heterodonty (Fraser *et al*. 2012; Conway *et al*. 2015; Bemis *et al*. 2019; Kolmann *et al*. 2019). However, fishes with dissimilar tooth shapes, like laniary teeth, appear to have independent replacement patterns, and replacement may be maintained by a spatially and temporally driven development network (Wakita *et al*. 1977; Huysseune & Meunier 1994; Huysseune 1995; Bemis *et al*. 2005; Trapani *et al.* 2005; Carr *et al*. 2021). There appears to be a single pattern of tooth replacement in bony fishes with a simple dentition morphology, and there is evidence that some of the bony fishes with a simple dentition can shed as many as 3% of their total number of teeth per day (Carr *et al*. 2021). This phenomenon can profoundly impact the interpretation of taxonomic abundance based on isolated teeth in teleost paleofaunas.

In contrast, otoliths are paired elements and thus every right sagitta represents an individual fish (Schwarzhans 1978; Nolf 1985; Nolf & Stringer 1992; Campana 2004). In some instances, it has even been possible to determine the right and left otoliths from the same individual fish (Girard *et al.* 2005). With these premises set, it is evident that fish teeth are the most abundant of the bony fish skeletal remains in the Catahoula Formation at the Jones Branch locality (Appendix 2). The 5761 teeth from Sciaenidae are the most numerous of any of the fish skeletal remains identified at least to the ordinal level, including elasmobranchs (47% of the total fish assemblage, 65% of the bony fish tooth sample) and indicate that these fishes were common in the ancient Catahoula Formation environment. This is corroborated by the high proportion of sciaenid otoliths we identified (96% of the otolith sample). Other taxa are known by relatively few numbers of specimens and therefore appear to be uncommon to rare, including Cyclopsettidae (n = 3 otoliths), ?*Acanthocybium* sp. (n = 3 teeth), Tetraodontidae (n = 6 beak fragments), and Siluriformes (n = 8 fin spines). Albulidae (bonefishes) is represented by relatively few teeth (n = 48) and even fewer otoliths (n = 9), but we are not surprised by this apparent rarity given

the behavior, abundance, and distribution of these fishes in the present-day Gulf of Mexico (Hoese & Moore 1998; Froese & Pauly 2023) and their trophic niche (Crabtree *et al*. 1998; Reeves 2011). Snyder & Burgess (2016) characterized the preferred habitat as seagrass and carbonate sand bottoms in clear shallow water (often < 2 m). Those authors also noted that albulids are often found alone and feed primarily on crabs, shrimp, snails, clams, and worms.

Several of the bony fish taxa we identified, like *Sphyraena* sp., *Scomberomorus* sp., Lophiidae, and Sparidae (including *Diplodus* sp.), are represented by relatively large numbers of teeth. These taxa represent roughly 24% (n = 609), 7% (n = 175), 9% (n = 229), and 48% (n = 1224) respectively, of the remaining non-sciaenid teeth in our Catahoula Formation sample. Interestingly, we did not recover any otoliths of the former three taxa, but this may not be surprising given that fish like *Sphyraena* are upper trophic-level predators, and their otoliths are typically very rare in otolith assemblages (Nolf 1985, 2013; Nolf & Stringer 1992, 2003; Stringer *et al*. 2020b, 2023). For example, Schwarzhans (2019a) reported only two *Sphyraena* sp. specimens in his exhaustive study of approximately 25 000 otoliths from the Cenozoic of New Zealand. As the small otolith sample from the Catahoula Formation would make the occurrence of *Sphyraena* otoliths even less likely, the relative abundance of *Sphyraena* teeth warrants further comment.

Froese & Pauly (2023) reported that extant *Sphyraena* (Sphyraenidae) typically occur in brackish and marine waters in tropical and subtropical settings. Of the three species inhabiting the Atlantic Ocean and Gulf of Mexico, *S. barracuda* (Edwards, 1771), *S. borealis* DeKay, 1842, and *S. guachancho* Cuvier, 1829, their common depth ranges are 3–30 m, 10–65 m, and 0–100 m, respectively (Froese & Pauly 2023; Page *et al*. 2023). The first two species tend to be more solitary, but *S. guachancho* is reported as a schooling species that commonly occurs in turbid coastal waters over muddy bottoms. Additionally, Blaber (1982) reported that *S. barracuda* individuals under two years of age inhabit estuarine environments where they prey upon smaller fishes. Either or both scenarios could explain the abundance of *Sphyraena* sp. teeth in the Catahoula Formation fish assemblage. Further discussion of the depositional environment of the Catahoula Formation fossil bed is provided below.

Biostratigraphic and biogeographic implications of the Catahoula Formation fish assemblage

Our study is the first to focus on vertebrate marine fossils occurring in the Catahoula Formation, and this is the most comprehensive report on Oligocene fishes from the Gulf Coastal Plain. Although elasmobranchs and to a lesser extent teleosts have been described from Oligocene units of Virginia (Müller 1999) and South Carolina (Cicimurri & Knight 2009; Cicimurri *et al.* 2022), a systematic evaluation of Oligocene fish assemblages from the Gulf Coastal Plain has yet to be undertaken. The taxa that have been reported from other lithostratigraphic units in Mississippi, as well as in Louisiana and Alabama, are largely based on preliminary evaluations (i.e., Ebersole *et al*. 2021, 2024a) or focused only on otoliths (i.e., Worley 2004).

The Catahoula Formation fish assemblage is slightly younger than that of the Ashley Formation (Rupelian, ca 28.5 Ma), and slightly older than or temporally equivalent to the Chandler Bridge Formation (Chattian, ca 24.5 Ma) of South Carolina. The Old Church Formation of Virginia is somewhat older (29 Ma) than the fish assemblage reported from the Ashley Formation (Cicimurri *et al.* 2022; Weems *et al.* 2022). At the generic level, a comparison of the elasmobranch taxa from each of these units revealed a striking similarity, as 75% of the taxa occurring in the Catahoula Formation are also found in the Oligocene of the Atlantic Coastal Plain (Müller 1999; Cicimurri & Knight 2009; Cicimurri *et al.* 2022). At the species level, several of those from the Catahoula Formation occur in the Atlantic Coastal Plain, as, for example, *Paramobula fragilis*, which is present in the Old Church, Ashley, and Chandler Bridge formations. Alternatively, there are significant differences among the units, as *Galeocerdo platycuspidatum* sp. nov. occurs in Mississippi but *G. aduncus* is found in the Chandler Bridge Formation (Cicimurri &

Knight 2009). It is interesting to note that daggernose shark teeth are common in both the Catahoula Formation and Old Church Formation (based on SC2020.43), and this taxon also occurs in the Rupelian (NP23) Rosefield Formation of Louisiana (as *Isogomphodon* sp. in Cicimurri & Ebersole 2021). Some of the differences are likely related to environmental variations, as the Catahoula and Chandler Bridge Formations appear to have been deposited in rather shallow water, whereas the Ashley Formation formed further offshore at a depth of around 100 m (Cicimurri & Knight 2009; Cicimurri *et al.* 2022). Temporal age may also be a factor, as the lithostratigraphic units may be separated by up to several million years of time.

Our knowledge of the Oligocene bony fishes from the Atlantic and Gulf coastal plains is far from complete and largely based on either tooth-based taxa or otolith-based taxa. Some Catahoula Formation bony fish genera also occur in the Ashley Formation, including *Sphyraena* sp., *Acanthocybium* sp., and *Scomberomorus* sp. Additionally, the families Albulidae, Labridae, Sciaenidae, and Sparidae occur in both units and, except for Sciaenidae, have also been reported from the Chandler Bridge Formation (Cicimurri & Knight 2009; Cicimurri *et al.* 2022). Based on the teleost teeth contained within SC2020.43, all the families listed above also occur in the Old Church Formation. In their preliminary note on fossil fishes from the Glendon Limestone Member of the Byram Formation (Rupelian, Zone P19, NP23) of Alabama, Ebersole *et al.* (2021) documented teeth of *Albula* sp. and *Sphyraena* sp.

Oligocene bony fish diversity within many of the aforementioned units increases significantly when otolith-based taxa are included. Otoliths have been described from Oligocene units in Alabama, Louisiana, and Mississippi (Stringer *et al*. 2001, 2020c; Stringer & Worley 2003; Worley 2004; Ebersole *et al.* 2021), but otoliths are unknown from the Oligocene of South Carolina. Additionally, the taxa Müller (1999) reported from the Old Church Formation of Virginia need revision due to the obsolete classification scheme utilized, a task currently being undertaken by several of the present authors. Currently, the sciaenids *Aplodinotus gemma*, *A. distortus*, and *Sciaena*? *radians* are known only from the Oligocene of the Gulf Coastal Plain (Nolf 2003, 2013; Stringer & Mixon 2005; Ebersole *et al.* 2021; Fuelling *et al.* 2022; Lin & Nolf 2022). Unfortunately, none of the other Catahoula Formation otolith-based taxa are very diagnostic due to their extensive biostratigraphic ranges.

During our study of the Catahoula Formation fish assemblage, we found that otoliths were rare in the larger mesh size fractions (>4 mm mesh size or #5 soil screen), and most of the specimens were obtained from finer fractions generally between 0.4 mm and 0.85 mm mesh (#20 to #40 soil screen). The implications of the size disparities are discussed further below. Worley (2004) provided a comprehensive otolith study based on 446 otoliths recovered from the Oligocene Rosefield Formation (Rupelian, Zone P20, Zone NP23) from three sites in Catahoula Parish, Louisiana. Interestingly, the number of otoliths per kilogram of matrix was higher in the Rosefield Formation compared to the Catahoula Formation. The Rosefield Formation otolith assemblage is nearly twice as diverse as the Catahoula Formation (18 taxa versus 10 taxa), but two disparities stand out. Although both assemblages contain sciaenids, these fish comprise 36.32% of the total Rosefield Formation assemblage, whereas they constitute 96% of the Catahoula Formation assemblage. Additionally, the size of the Rosefield Formation otoliths ranges from 5 mm to 12 mm in length, but more than 99% of the Catahoula Formation specimens are less than 5 mm in length. These significant size differences in the otolith assemblages are believed to be directly related to paleoenvironmental conditions. The Rosefield Formation was shown to be more influenced by shallow, normal marine conditions (Worley 2004), whereas the Catahoula Formation otoliths indicate much shallower environments, including estuarine. The unusual size distribution of the otoliths in the Catahoula Formation assemblage is discussed in greater detail below.

The otolith taxa reported by Ebersole *et al.* (2021) from the Rupelian Glendon Limestone Member of the Byram Formation of Alabama included nine taxa, despite the much smaller matrix sample collected

and number of otoliths recovered (approximately 50 kg, 116 specimens) compared to the Catahoula Formation sample (122 kg, 373 specimens). Two significant differences are apparent between these otolith assemblages. Firstly, only 6.9% of the Glendon Limestone Member assemblage consisted of Sciaenidae, whereas 96% of the Catahoula Formation otolith sample is sciaenids. Secondly, 51% of the Glendon Limestone Member otolith sample consisted of Pleuronectiformes (i.e., Paralichthyidae). The pleuronectid representative in the Catahoula Formation, which is now placed in the family Cyclopsettidae, represents only 0.7% of the otolith assemblage we examined.

In summary, the Catahoula Formation otolith assemblage is distinctive and remarkable in that 99.2% of the total specimens in the otolith assemblage are smaller than 5 mm in length, and 96% of the total specimens consists of representatives in the family Sciaenidae. These peculiarities are believed to be directly related to the Catahoula Formation paleoenvironment and are discussed in the next section.

Paleoecology and depositional environment of the fossil deposit

The lithological and fossil evidence suggests that our fossil-bearing stratum was deposited in a subtropical, very nearshore, high-energy environment. The Jones Branch Catahoula Formation fossil bed we sampled is an argillaceous quartz sand. Grain size ranges from fine to coarse, and grain shape is variable. Most of the quartz consists of grains of colorless rock crystal that are sub-angular to very well-rounded (nearly spherical), but a small abraded, prismatic crystal was recovered. Angular grains of pink rose quartz are much less common, and glauconite is absent. Well-rounded grains indicate bimodal transport (i.e., tidal influence), and the presence of more angular grains and excellently preserved terrestrial mammal teeth suggest mixing of sediment transported a relatively short distance from the source. Starnes & Phillips (2016) reported that the basal Catahoula Formation represents deltaic deposits with both brackish water and terrestrial influences. Freshwater finely laminated clays preserve beautiful broadleaf and palmetto leaf fossils, whereas the sandy tidal channel beds contain oyster shell hash with marine and terrestrial vertebrate remains, and quartz and phosphatic pebbles.

With respect to the vertebrate fossils, the presence of terrestrial/brackish water vertebrates like gars, trionychid turtles, crocodilians, and terrestrial mammals (i.e., small rodents) indicates very close proximity to the shoreline and influx of sediment via distributary systems. If extant elasmobranchs provide a model for the environmental preferences of fossil species, the taxa we identified from the Catahoula Formation support a very nearshore marine environment. For example, tawny nurse sharks (*Nebrius*) are predominantly inshore inhabitants where water depth is between five and 30 m (Compagno *et al.* 2005). Daggernose shark teeth (*Carcharhinus acuarius*) are the most abundant selachian remains in our sample, and extant *C. oxyrhynchus* (Müller & Henle, 1839) prefers turbid waters near river mouths but can be found to depths of 40 m (Compagno *et al.* 2005). Stingray teeth tentatively identified as *Hypanus* are the most abundant batoid remains we recovered, and extant representatives of this genus occur at depths of nine to 25 m (Snelson *et al*. 1988; McEachran & de Carvalho 2002; Farmer 2004; Aguiar *et al.* 2009). At least three rhinopristiform rays occur in the Catahoula Formation, including wedgefish (*Rhynchobatus*) and sawfish (*Pristis* and *Anoxypristis*). Living representatives of the former taxon are often found in coastal waters to depths of 25 m (Compagno & Last 1999a), and those of the latter two taxa commonly occur in sub-tropical estuarine habitats (Stevens *et al.* 2008; Radkhah & Eagderi 2019). Cownosed rays (*Rhinoptera*) inhabit a variety of nearshore habitats in water depths up to 26 m (Compagno & Last 1999b).

Previous studies have demonstrated the use of bony fish otoliths as paleoenvironmental indicators. This has been especially true for younger geologic formations, like the Plio-Pleistocene units in the Gulf and Atlantic Coastal plains (Stringer & Bell 2018; Stringer & Shannon 2019; Stringer & Hulbert 2020; Stringer *et al.* 2020a, 2022b). Unfortunately, the relatively limited number of otolith-based taxa we recovered from the Catahoula Formation adversely impacts this usefulness, as none of the families are

particularly diagnostic of freshwater, brackish, or marine environments (Appendix 3), and only very general paleoenvironmental settings can be hypothesized based on taxonomic composition. Fortunately, taxonomic composition of otolith assemblages may not be the only indicator of depositional environment.

Analyses of thousands of otolith specimens from Oligocene formations in Louisiana, Mississippi, and Alabama (Nolf 2003, 2013; Stringer & Worley 2003; Worley 2004; Stringer *et al*. 2020c; Ebersole *et al*. 2021) have revealed that sagittae of *Sciaena*? *pseudoradians* are more commonly found in the 5–10 mm range, but specimens greater than 15 mm in length do occur. Based on growth series of modern sciaenid otoliths from the Gulf of Mexico, one-year-old *Sciaenops ocellatus* (Linnaeus, 1766) can reach up to 28 cm in length but have sagittae measuring approximately 15 mm. Additionally, sagittae of a one-year-old *Pogonias cromis* (Linnaeus, 1766) are approximately 10 mm, those of a one-year-old *Micropogonias undulatus* (Linnaeus, 1766) are around 10 mm, and otoliths of a one-year-old *Aplodinotus grunniens,* an extant freshwater inhabitant in North America, are approximately 5.90 mm in length (GLS pers. obs., 2024). These values provide some indication of the age of the sciaenid fishes represented in the Catahoula Formation otolith assemblage, which were apparently roughly one-year-old at the time of death. We note here that extant *Leiostomus* possesses relatively small otoliths, and one- to two-year-old *L. xanthurus* Lacépède, 1802 (approximately 140–220 mm total length) have otoliths around 6.5 mm in length (Bare 2001; Lombarte *et al.* 2006).

Of the 134 *Sciaena*? *pseudoradians* otoliths in our Catahoula Formation sample, only one specimen measures 10.27 mm in length (0.74% of the sample), whereas the remaining specimens (99.26% of the sample) measure 5.0 mm or less. More specifically, 24.43% of the otoliths measure less than 2.0 mm, 65.65% range between 2.1 and 3.0 mm, and 9.16% are between 3.1 and 5.0 mm in length. Based on extant analogs, 99.26% of the Catahoula Formation *S.*? *pseudoradians* otoliths represent juveniles, most likely very young at less than one year old. The restricted size distribution of the *S.*? *pseudoradians* sample is enigmatic and atypical of a shallow marine setting, where older juveniles, subadults, and adults generally occur. This phenomenon may be explained through the habitat preferences of extant *M. undulatus* and *L. xanthurus*, which are both common in the present-day Gulf of Mexico and could be considered as analogs for Oligocene *S.*? *pseudoradians*. If correct, then the size distribution of the *S.*? *pseudoradians* otoliths is indicative of lower-salinity upper reaches of estuaries as well as shallow soft-bottomed estuarine creeks and bays (Hales & Van Den Avyle 1989; Barbieri 1993; Barbieri *et al.* 1994; Bare 2001; Stringer & Shannon 2019).

As noted above, elasmobranchs are euryhaline animals that can be found at variable water depths. However, most of the taxa are indicative of shallow water, and many are quite common in estuarine environments. An estuarine paleoenvironment is supported by the abundance and size of the *S.*? *pseudoradians* otoliths and is congruent with the other Catahoula Formation otolith-based taxa. All the fossil fish taxa we identified, whether based on teeth, scales and spines, or otoliths, occur in present-day brackish and marine waters (Appendix 3). For example, Lepisosteidae occur in freshwater and brackish environments, Scombridae are freshwater to marine, whereas Sphyraenidae and Labridae are brackish to marine taxa, and taxa that are primarily/exclusively marine, like Lophiidae, are rare components (Froese & Pauly 2023). Although a brackish, estuarine environment is indicated by the Catahoula Formation fishes, this does not preclude proximity to and intrusion of shallow marine waters, which could also explain the presence of Congridae.

The large percentage of Sciaenidae teeth (70% of the tooth-based sample) is congruent with the high percentage of otoliths assigned to this family (95% of the total otolith sample), and we found that the families indicated only by skeletal remains are compatible with the paleoenvironment suggested by the otoliths. Our proposed paleoenvironment is corroborated by the sedimentological evidence, abundance of oysters, and the terrestrial and marine mammal species that were documented by Albright *et al.* (2018).

Additionally, examination of paleogeographic maps for the Oligocene (Smith *et al.* 1994; Scotese 2014; Blakey 2020) also indicates that our determination is feasible (Fig. 1).

The taxonomic composition of the Catahoula Formation fish assemblage, particularly the otolith-based taxa, provides important climatic data that are presented in Appendix 3. The climatic preferences of the bony fish families based on skeletal material largely overlaps with those taxa based on otoliths. The data in Appendix 3 show that the only climatic realm in which all the fish families would be found is tropical, but the occurrence of representatives of five families indicates subtropical and even temperate climates. A likely scenario for the Catahoula Formation climate therefore is tropical to subtropical, perhaps even warm temperate.

Conclusions

We examined more than 13 500 fish fossils that were recovered from the basal Catahoula Formation at a site in Wayne County, Mississippi. Forty-nine unequivocal taxa are represented by teeth, jaws, scales, fin spines, and/or otoliths. Twenty-nine elasmobranchs have been identified based on teeth, including a new species of *Hemipristis* (*H. intermedia*) and of *Galeocerdo* (*G. platycuspidatum*), two new species provisionally assigned to *Sphyrna* ("*S.*" *gracile* and "*S.*" *robustum*), and a new batoid species tentatively assigned to *Hypanus* (*H.*? *heterodontus*). The elasmobranch component of the assemblage is dominated by the daggernose shark, *Carcharhinus acuarius*, but *C. elongatus*, *H. intermedia* sp. nov., *Carcharias cuspidatus*, *Rhynchobatus* cf. *pristinus*, *H.*? *heterodontus* sp. nov., and durophagous myliobatids are also common. Twenty teleost taxa have been identified based on teeth, jaws, scales, fin spines, and otoliths, and this portion of the fish assemblage is dominated by sciaenids (drums) and to a lesser extent *Sphyraena* (barracuda). The first Oligocene western hemisphere record of Tetraodontidae is based on several beak fragments.

The fish paleofauna we report herein is indicative of an estuarine environment, which is consistent with previous lithological analyses indicating deltaic deposition. The Catahoula Formation fish assemblage is of Chattian (late Oligocene) age based on its stratigraphic occurrence (disconformably) above the Paynes Hammock Limestone, the latter being no younger than latest Rupelian based on planktonic foraminifers. The Catahoula Formation fossil horizon that we examined is slightly younger than the Old Church Formation of Virginia (ca 29 Ma) and the Ashley Formation of South Carolina (ca 28.5 Ma) and slightly older than or equivalent to the Chandler Bridge Formation of South Carolina (ca 25 Ma). Generically, and often at the species level, the taxa we identified in the Catahoula Formation occur in Atlantic Coastal Plain Oligocene units.

Acknowledgments

Our knowledge of the site would not have been possible without the contributions of A. Weller and R. Rains (Waynesboro, Mississippi, USA), who also assisted with field work and donated specimens to MMNS. Numerous other individuals assisted GEP with field work, processing bulk matrix, and other technical support, including Z. Weller, L. Weller, A. Weller, K. Irwin (formerly Arkansas Game and Fish Commission), D. Ehret (formerly Alabama Museum of Natural History, Tuscaloosa, Alabama), J. Rushing (Mississippi Gem and Mineral Society), L. Ritchie, R. Horn, K. Shannon, and B. Martin. Additional specimens were donated to MMNS by E. Mooney, J. McCraw, J. Dearman, and W. Collins. Volunteers G. and S. Kelly assisted DJC with microscopic sorting of Catahoula Formation matrix. K. Johnson (National Marine Fisheries Service), R. Taylor (formerly Florida Fish and Wildlife Conservation Commission, Fish and Wildlife Research Institute, St. Petersburg, Florida), and J. Hendon (Center for Fisheries Research and Development, Gulf Coast Research Laboratory, University of Southern Mississippi, Ocean Springs) generously provided modern fishes and otoliths as comparative specimens. D. Nolf (Royal Belgian Institute of Natural Sciences, Brussels) also supplied

modern and fossil otolith specimens to GLS. The Dauphin Island Sea Lab and Alabama Aquarium at Dauphin Island, AL are thanked for providing modern comparative specimens to MSC. Additionally, A.F. Bannikov (Russian Academy of Sciences) graciously provided insight into Oligocene *Acanthocybium* specimens. Thorough and critical reviews by W. Schwarzhans (Natural History Museum of Denmark, Zoological Museum, Copenhagen) and T. Reinecke (Bochum, Germany) improved an earlier version of this manuscript, and their time and effort are greatly appreciated. Reinecke also provided numerous photographs of fossil teeth that helped us make more accurate comparisons between the fossil Catahoula Formation and European taxa. Lastly, we wish to thank the editorial staff of the *European Journal of Taxonomy* for their time and effort in bringing this article to print.

References

Adnet S. & Cappetta H. 2008. New fossil triakid sharks from the Eocene of Prémontré, France, and comments on fossil record of the family. *Acta Palaeontologica Polonica* 53 (3): 433–448. https://doi.org/10.4202/app.2008.0306

Adnet S., Antoine P.-O., Hassan Baqri S.R., Crochet J.-Y., Marivaux L., Welcomme J.-L. & Metais G. 2007. New tropical carcharhinids (Chondrichthyes, Carcharhiniformes) from the late Eocene–early Oligocene of Balochistan, Pakistan: paleoenvironmental and paleogeographic implications. *Journal of Asian Earth Sciences* 30 (2): 303–323. https://doi.org/10.1016/j.jseaes.2006.10.002

Adnet S., Cappetta H. & Tabuce R. 2010. A Middle–Late Eocene vertebrate fauna (marine fish and mammals) from southwestern Morocco; preliminary report: age and palaeobiogeographical implications. *Geological Magazine* 147 (6): 860–870. https://doi.org/10.1017/S0016756810000348

Adnet S., Marivaux L., Cappetta H., Charrault A.-L., Essid E.M., Jiquel S., Khayati Ammar H. Marandat B., Marzougui W., Merseraud G., Temani R., Vianey-Liaud M. & Tabuce R. 2020. Diversity and renewal of tropical elasmobranchs around the Middle Eocene Climatic Optimum (MECO) in North Africa: new data from the lagoonal deposits of Djebel el Kébar, central Tunisia. *Palaeontologia Electronica* 23 (2): a38. https://doi.org/10.26879/1085

Adolfssen J.S. & Ward D.J. 2013. Neoselachians from the Danian (early Paleocene) of Denmark. *Acta Palaeontologica Polonica* 60 (2): 313–338.

Agassiz L. 1835. *Recherches sur les Poissons fossiles.* 5th livraison (June, 1835). Petitpierre, Neuchâtel, Switzerland. https://doi.org/10.5962/bhl.title.4275

Agassiz L. 1843. *Recherches sur les Poissons fossiles.* 15th and 16th livraisons (March 1843). Petitpierre, Neuchâtel, Switzerland. https://doi.org/10.5962/bhl.title.4275

Aguiar A.A., Valentin J.L. & Rosa R.S. 2009. Habitat use by *Dasyatis americana* in a south-western Atlantic oceanic island. *Journal of the Marine Biological Association of the United Kingdom* 89 (6): 1147–1152. https://doi.org/10.1017/S0025315409000058

Aguilera O., Rodrigues F., Moretti T., Bello M., Lopes R.T., Machado A.S., dos Santos T.M. & Béarez P. 2018. First Neogene Proto-Caribbean pufferfish: new evidence for Tetraodontidae radiation. *Journal of South American Earth Science*s 85 (1): 57–67. https://doi.org/10.1016/j.jsames.2018.04.017

Albright L.B. Jr, Phillips G., Starnes J.E., Stringer G.L. & Weller A. 2018. The Jones Branch local fauna: an early Arikareean mammalian assemblage from the Upper Oligocene Catahoula Clay, Wayne County, Mississippi. *Society of Vertebrate Paleontology Meeting Program and Abstracts* (76th Annual Meeting): 87. https://doi.org/10.1130/abs/2016SC-272418

Ameghino F. 1906. Les formations sédimentaires du Crétacé supérieur et du Tertiaire de Patagonie avec un parallèle entre leurs faunes mammalogiques et celles de l'ancien continent. *Anales del Museo nacional de Buenos Aires* 3 (8): 1–568.

Andrianavalona T.H., Ramihangihajason T.N., Rasoamiaramanana A., Ward D.J., Ali J.R. & Samonds K.E. 2015. Miocene shark and batoid fauna from Nosy Makamby (Mahajanga Basin, Northwestern Madagascar). *PLoS One* 10: e0129444. https://doi.org/10.1371/journal.pone.0129444

Applegate S.P. 1974. A revision of the higher taxa of orectoloboids. *Journal of the Marine Biological Association of India* 14 (2): 743–751.

Applegate S.P. & Espinosa-Arrubarrena L. 1996. The fossil history of *Carcharodon* and its possible ancestor, *Cretolamna*: a study in tooth identification. *In*: Klimley A.P. & Ainley D. (eds) *Great White Sharks. The Biology of Carcharodon carcharias*: 19–36. Academic Press, San Diego.

Arambourg C. 1952. Les vertébrés fossiles des gisements de phosphates (Maroc-Algérie-Tunisie). *Notes et Mémoires du Service géologique du Maroc* 92: 1–372.

Arratia G., Scasso R.A. & Kiessling W. 2004. Late Jurassic fishes from Longing Gap, Antarctic Peninsula. *Journal of Vertebrate Paleontology* 24 (1): 41–55. https://doi.org/10.1671/1952-4

Baghai-Riding N., Axsmith B. & Starnes J.E. 2018. Paleoclimate and taphonomic implications of a palynological sample from the Jones Branch interval, Catahoula Formation. *Botanical Society of America, Abstract*. https://doi.org/10.13140/RG.2.2.31388.21127

Ballen G. 2020. New records of the genus *Sphyraena* (Teleostei: Sphyraenidae) from the Caribbean with comments on dental characters in the genus. *Journal of Vertebrate Paleontology* 40 (6): e1849246. https://doi.org/10.1080/02724634.2020.1849246

Barbieri L. 1993. *Life History, Ppopulation Dynamics, and Yield-per-Recruit Modeling of Atlantic Croaker, Micropogonias undulatus, in the Chesapeake Bay Area*. Ph.D. thesis, School of Marine Science, College of William and Mary, Williamsburg, VA.

Barbieri L., Chittenden M. Jr & Jones C. 1994. Age, growth, and mortality of Atlantic croaker, *Micropogonias undulatus,* in the Chesapeake Bay region, with a discussion of apparent geographic changes in population dynamics. *Fishery Bulletin* 92 (1): 1–12.

Bare L. 2001. "*Leiostomus xanthurus*". Open Source Animal Diversity Web.
Available from https://animaldiversity.org/accounts/Leiostomus_xanthurus/ [accessed 16 Feb. 2023].

Barthelt D., Fejfar O., Pfeil F.H. & Unger E. 1991. Notizen zu einem Profil der Selachier-Fundstelle Walbertsweiler im Bereich der miozänen oberen Meeresmolasse Süddeutschlands. *Münchner geowissenschaftliche Abhandlungen Reihe A, Geologie und Paläontologie* 19: 195–208.

Bassani F. 1889. Ricerche sui pesci fossili di Chiavon. Strati di Sotzka – Miocene Inferiore. *Atti della reale Accademia delle Scienze fisiche e matematiche* 3 (6): 1–100.

Baut J.-P. & Génault B. 1999. Les elamobranches des sables de Kerniel (Rupélien), à Gellik, nord est de la Belgique. *Memoirs of the Geological Survey of Belgium* 45: 3–61.

Bemis K.E., Burke S., St. John C. & Bemis W.E. 2019. Tooth development and replacement in the Atlantic cutlassfish, *Trichiurus lepturus*, with comparisons to other Scombroidei. *Journal of Morphology* 280: 78–94. https://doi.org/10.1002/jmor.20919

Bemis W.E., Giuliano A. & McGuire B. 2005. Structure, attachment, replacement and growth of teeth in bluefish, *Pomatomus saltatrix* (Linnaeus, 1776), a teleost with deeply socketed teeth. *Zoology* (Jena) 108 (4): 317–327. https://doi.org/10.1016/j.zool.2005.09.004

Bennett E.T. 1830. Class Pisces. *In*: Raffles S. (ed.) *Memoir of the Life and Public Service of Sir Thomas Stamford Raffles, Particularly in the Government of Java, 1811–1816, and of Bencoolen and its Dependencies, 1817–1824; with Details of the Commerce and Resources of the Eastern Archipelago and Selections from his Correspondence*: 686–694. John Murray, London.

Berg L.S. 1937. A classification of fish-like vertebrates. *Izvestiya Akademii Nauk USSR, Seriya Biologischeskaya* 4: 1277–1280. [In Russian.]

Berg L.S. 1940. Classification of fishes, both recent and fossil. *Trudy Zoologiceskogo Instituta, Akademii Nauk SSR* 5 (2): 517. [In Russian.]

Betancur-R R., Broughton R., Wiley E., Carpenter K., López J., Li C., Holcroft N., Arcila D., Sanciangco M., Cureton J. II, Zhang F., Buser T., Campbell M., Ballesteros J., Roa-Varo A., Willis S., Borden W., Rowley T., Reneau P.C., Hough D., Lu G., Grande T., Arratia G. & Ortí G. 2013. *The Tree of Life and a New Classification of Bony Fishes.* Edition 1. PLoS Currents Tree of Life. Available from https://doi.org/10.1371/currents.tol.53ba26640df0ccaee75bb165c8c26288 [accessed 18 April 2013].

Blaber S.J.M. 1982. The ecology of *Sphyraena barracuda* (Osteichthyes: Perciformes) in the Kosi system with notes on the Sphyraenidae of other Natal estuaries. *South African Journal of Zoology* 17: 171–176.

de Blainville H.M.D. 1816. Prodrome d'une nouvelle distribution systématique du règne animal. *Bulletin des Sciences, par la Société philomatique de Paris* 1816: 105–112.

de Blainville H.M.D. 1818. Sur les ichthyolites ou les poissons fossiles. *Nouveau Dictionnaire d'Histoire naturelle* 37: 310–391.

Blakey R. 2020. *Cenozoic 30 Ma Paleo_Oligo. Global Paleogeography and Tectonics in Deep Time.* Deep Time Maps. Available from https://deeptimemaps.com [accessed 16 Aug. 2023].

Bleeker P. 1859. Enumeration speciorum piscium hujusque in Archipelago Indico observatarum, adjectis habitationibus citationibusque, ubi descriptiones earum recentiores reperiuntur, nec non species Musei Bleekeriani Bengalensibus, Japonicis, Capensibus Tasmanicisque. *Acta de la Société du Science d'Indo-Neerland* 6: 1–276.

Bloch M.E. 1793. *Naturgeschichte der ausländischen Fische*. Morino & Company, Berlin.

Bloch M.E. & Schneider J.G. 1801. *Systema Ichthyologiae Iconibus ex Illustratum. Post Obitum Auctoris Opus Inchoatum Absolvit, Correxit, Interpolavit*. J.G. Schneider, Berlin.
Available from https://www.biodiversitylibrary.org/page/5475805 [accessed 6 Jan. 2025].

Böhlke J.E. 1949. The systematic position of the apodal fish genus *Bathymyrus*. *Copeia* 1949 (3): 218.

Bolliger T., Kindlimann R. & Wegmüller U. 1995. Die marinen Sedimente (jüngere OMM, St. Gallen-Formation) am Südwestrand der Hörnlischüttung (Ostschweiz) und die palökologische Interpretation ihres Fossilinhaltes. *Eclogae Geologicae Helvetiae* 88 (3): 885–909.

Bonaparte C.L. 1831. *Saggio di una Distribuzione metodica degli Animali vertebrati*. Antonio Boulzaler, Rome. Available from https://www.biodiversitylibrary.org/page/33059956 [accessed 6 Jan. 2025].

Bonaparte C.L. 1838. Selachorum tabula analytica. *Nuovi Annali della Scienze Naturali Bologna* 1 (2): 195–214.

Bonaparte C.L. 1840a. Prodromis systematis ichthyologiae. *Nuovi Annali delle Scienze naturali Bologna* 4: 181–196, 272–277. Available from https://www.biodiversitylibrary.org/page/9325277 [accessed 6 Jan. 2025].

Bonaparte C.L. 1840b. *Iconografia della Fauna italica per le quattro Classi degli Animali vertebrati. Vol. III. Pesci.* Buttaoni and Canali, Rome. Available from https://www.biodiversitylibrary.org/page/47089297 [accessed 6 Jan. 2025].

Bonnaterre J.P. 1788. *Tableau encyclopédique et méthodique de trois Règnes de la Nature, Ichthyologie*. Panckoucke, Paris.

Bor T. 1990. A new species of mobulid ray (Elasmobranchii, Mobulidae) from the Oligocene of Belgium. *Contributions to Tertiary and Quaternary Geology* 27 (2–3): 93–97.

Bracher H. & Unger E. 2007. *Untermiozäne Haie und Rochen.* Altheim, Germany.

Breard S. & Stringer G.L. 1995. Paleoenvironment of a diverse marine vertebrate fauna from the Yazoo Clay (Late Eocene) at Copenhagen, Caldwell Parish, Louisiana. *Transactions of the Gulf Coast Association of Geological Societies* 45: 77–85.

Breard S. & Stringer G.L. 1999. Integrated paleoecology and marine vertebrate fauna of the Stone City Formation (Middle Eocene), Brazos River section, Texas. *Transactions of the Gulf Coast Association of Geological Societies* 49: 132–142.

Cadenat J. 1963. Notes d'ichthyologie ouest-africaine, 29. Notes sur requins de la famille des Carchariidae et formes apparentées de l'Atlangique ouest-africain (avec la description d'une espèce nouvelle: *Pseudocarcharias pelagicus*, classée dans un sous-genre nouveau). *Bulletin de l'Institut français d'Afrique noire* 25 (2): 526–537.

Campana S. 2004. Photographic atlas of fish otoliths of the Northwest Atlantic Ocean. *Canadian Special Publications of Fisheries and Aquatic Services* 133: 1–284. https://doi.org/10.1139/9780660191089

Campbell M.A., Chanet B., Chen J.-N., Lee M.-Y. & Chen W.-J. 2019. Origins and relationships of the Pleuronectoidei: molecular and morphological analysis of living and fossil taxa. *Zoologica Scripta* 48: 640–656. https://doi.org/10.1111/zsc.12372

Cappetta H. 1970. Les sélaciens du Miocène de la région de Montpellier. *Palaeovertebrata, Mémoire Extraordinaire* 1970: 1–139.

Cappetta H. 1980a. Modification du statut générique de quelques espèces de sélaciens Crétacés et Tertiaires. *Palaeovertebrata* 10 (1): 29–42.

Cappetta H. 1980b. Les sélaciens du Crétacé supérieur du Liban. II. Batoïdes. *Palaeontographica* A 168 (5–6): 149–229.

Cappetta H. 2012. *Chondrichthyes (Mesozoic and Cenozoic Elasmobranchii, Teeth).* Handbook of Palaeoichthyology Vol. 3E. Verlag Friedrich Pfeil, Munich.

Cappetta H. & Case G.R. 2016. A selachian fauna from the middle Eocene (Lutetian, Lisbon Formation) of Andalusia, Covington County, Alabama, USA. *Palaeontographica* A 307 (1–6): 43–103.

Cappetta H. & Stringer G.L. 2002. A new batoid genus (Neoselachii: Myliobatiformes) from the Yazoo Clay (late Eocene) of Louisiana, USA. *Tertiary Research* 21: 51–56.

Carnevale B. & Tyler J.C. 2015. A new pufferfish (Teleostei, Tetraodontidae) from the Middle Miocene of St. Margarethen, Austria. *Paläontologische Zeitschrift* 89: 435–447. https://doi.org/10.1007/s12542-014-0243-3

Carr E., Summers A. & Cohen K. 2021. The moment of tooth: rate, fate and pattern of Pacific lingcod dentition revealed by pulse-chase. *Proceedings of the Royal Society* B 288: e20211436. https://doi.org/10.1098/rspb.2021.1436

Carrillo-Briceño J.D., Maxwell E., Aguilera O.A., Sánchez R. & Sánchez-Villagra M.R. 2015. Sawfishes and other elasmobranch assemblages from the Mio-Pliocene of the South Caribbean (Urumaco Sequence, Northwestern Venezuela). *PLoS One* 10 (10): e0139230. https://doi.org/10.1371/journal.pone.0139230

Carrillo-Briceño J.D., Aguilera O.A., De Gracia C., Aguirre-Fernández G., Kindlimann R. & Sánchez-Villagra M.R. 2016. An early Neogene elasmobranch fauna from the southern Caribbean (western Venezuela). *Palaeontologia Electronica* 19.2.27A: 1–32.

Carrillo-Briceño J.D., Luz Z., Hendy A., Kocsis L., Aguilera O. & Vennemann T. 2019. Neogene Caribbean elasmobranchs: diversity, paleoecology and paleoenvironmental significance of the Cocinetas Basin assemblage (Guajira Peninsula, Colombia). *Biogeosciences* 16: 33–56. https://doi.org/10.5194/bg-16-33-2019

Case G.R. 1980. A selachian fauna from the Trent Formation, lower Miocene (Aquitanian) of eastern North Carolina. *Palaeontographica* A 171 (1–3): 75–103.

Casier E. 1946. La faune ichthyologique de l'Yprésien de la Belgique. *Mémoires du Musée royal d'Histoire naturelle de Belgique* 104: 3–267.

Casier E. 1949. Contributions à l'étude des poissons fossiles de la Belgique. VIII. Les pristidés éocènes. *Bulletin du Musée royal d'Histoire naturelle de Belgique* 25 (10): 1–53.

Chandler R.E., Chiswell K.E. & Faulkner G.D. 2006. Quantifying a possible Miocene phyletic change in *Hemipristis* (Chondrichthyes) teeth. *Palaeontologica Electronica* 9 (1): 1–14.

Ciampaglio C.N., Cicimurri D.J., Ebersole J.A. & Runyon K.E. 2013. A note on Late Cretaceous fish taxa recovered from stream gravels at site AGr-43 in Greene County, Alabama. *Bulletin of the Alabama Museum of Natural History* 31 (1): 84–97.

Cicimurri D.J. 2007. A partial rostrum of the sawfish *Pristis lathami* Galeotti, 1837, from the Eocene of South Carolina. *Journal of Paleontology* 81 (3): 597–601. https://doi.org/10.1666/05086.1

Cicimurri D.J. & Ebersole J.A. 2021. New Paleogene elasmobranch (Chondrichthyes) records from the Gulf Coastal Plain of the United States, including a new species of *Carcharhinus* de Blainville, 1816. *Cainozoic Research* 21 (2): 147–164.

Cicimurri D.J. & Knight J.L. 2009. Late Oligocene sharks and rays from the Chandler Bridge Formation, Dorchester County, South Carolina, USA. *Acta Paleontologica Electronica* 9 (1): 1–14.

Cicimurri D.J. & Knight J.L. 2019. Late Eocene (Priabonian) elasmobranchs from the Dry Branch Formation (Barnwell Group) of Aiken County, South Carolina, USA. *PaleoBios* 36: 1–31. https://doi.org/10.5070/P9361043964

Cicimurri D.J., Ciampaglio C.N. & Runyon K.E. 2014. Late Cretaceous elasmobranchs from the Eutaw Formation at Luxapalila Creek, Lowndes County, Mississippi. *PalArch's Journal of Vertebrate Paleontology* 11 (2): 1–36.

Cicimurri D.J., Ebersole J.A. & Martin G. 2020. Two new species of *Mennerotodus* Zhelezko, 1994 (Chondrichthyes: Lamniformes: Odontaspididae), from the Paleogene of the southeastern United States. *Fossil Record* 23: 117–140. https://doi.org/10.5194/fr-23-117-2020

Cicimurri D.J., Knight J.L. & Ebersole J.A. 2022. Early Oligocene (Rupelian) fishes (Chondrichthyes, Osteichthyes) from the Ashley Formation (Cooper Group) of South Carolina, USA. *Paleobios* 39: 1–38. https://doi.org/10.5070/P939056976

Cigala Fulgosi F. 1992. Addition to the fish fauna of the Italian Miocene. The occurrence of *Pseudocarcharias* (Chondrichthyes, Pseudocarchariidae) in the lower Serravalian of Parma Province, northern Apennines. *Tertiary Research* 14 (2): 51–60.

Ciobanu R. 1994. Addition to the Eocene selachian fauna of the Turnu Roşu (Porcesti). *Studia Universitatis "Babeş-Bolyai", Geologie* 4: 299–309.

Clayton A.A., Ciampaglio C.N. & Cicimurri D.J. 2013. An inquiry into the stratigraphic occurrence of a Claibornian (Eocene) vertebrate fauna from Covington County, Alabama. *Bulletin of the Alabama Museum of Natural History* 31: 60–73.

Coccioni R., Montanari A., Bice D., Brinkhuis H., Deino A., Frontalini F., Lirer F., Maiorano P., Monechi S., Pross J., Rochette P., Sagnotti L., Sideri M., Spirovieri M., Tateo F., Touchard Y., Van Simaeys S. & Williams G.L. 2018. The Global Stratotype Section and Point (GSSP) for the base of the Chattian Stage (Paleogene System, Oligocene Series) at Monte Cagnero, Italy. *Episodes* 41 (1): 17–32. https://doi.org/10.18814/epiiugs/2018/v41i1/018003

Collareta A., Merella M., Mollen F.H., Casati S. & DiCencio A. 2020. The extinct catshark *Pachyscyllium distans* (Probst, 1879) (Elasmobranchii: Carcharhiniformes) in the Pliocene of the Mediterranean Sea. *Neues Jahrbuch für Geologie und Paläontologie, Abhandlungen* 295 (2): 129–139.

Compagno L.J.V. 1973. Interrelationships of living elasmobranchs. *Zoological Journal of the Linnean Society* 53: 15–61.

Compagno L.J.V. 1984. FAO Species Catalogue. Vol 4: Sharks of the world, Part 2 – Carcharhiniformes. *FAO Fisheries Synopsis no. 125* 4 (2): 251–633.

Compagno L.J.V. & Last P.R. 1999a. Rhinobatiformes: Rhinidae (= Rhynchobatidae). *In*: Carpenter K.E. & Niem V.H. (eds). *The Living Marine Resources of the Western Central Pacific. Vol. 3. Batoid Fishes, Chimaeroids, and Bony Fishes, Part 1 (Elopidae to Linophyrnidae).* FAO Species Identification Guide for Fishery Purposes: 1418–1422. FAO, Rome.

Compagno L.J.V. & Last P.R. 1999b. Myliobatiformes: Rhinopteridae. *In*: Carpenter K.E. & Niem V.H. (eds) *The Living Marine Resources of the Western Central Pacific. Vol. 3. Batoid Fishes, Chimaeroids, and Bony Fishes, Part 1 (Elopidae to Linophyrnidae).* FAO Species Identification Guide for Fishery Purposes: 1520–1523. FAO, Rome.

Compagno L.J.V., Dando M. & Fowler S. 2005. *Sharks of the World*. Princeton Field Guides. Princeton University Press, Princeton, NJ.

Conway K., Bertrand N., Browning Z., Lancon T. & Clubb F.J. 2015. Heterodonty in the new world: an SEM investigation of oral jaw dentition in the clingfishes of the subfamily Gobiesocinae (Teleostei: Gobiesocidae). *Copeia* 103: 973–998. https://doi.org/10.1643/OT-15-234

Cope E.D. 1867. An addition to the vertebrate fauna of the Miocene period, with a synopsis of the extinct Cetacea of the United States. *Proceedings of the Academy of Natural Sciences of Philadelphia* 19: 138–156.

Cope E.D. 1869. Descriptions of some extinct fishes previously unknown. *Proceedings of the Boston Society of Natural History* 12: 310–317.

Cope E.D. 1871. Observations on the systematic relations of the fishes. *The American Naturalist* 5 (8/9): 579–593. https://doi.org/10.1086/270831

Cowman P.F., Bellwood D.R. & van Herwerden L. 2009. Dating the evolutionary origins of wrasse lineages (Labridae) and the rise of trophic novelty on coral reefs. *Molecular Phylogenetics and Evolution* 52 (3): 621–631. https://doi.org/10.1016/j.ympev.2009.05.015

Crabtree R., Stevens V., Snodgrass F. & Stengard F. 1998. Feeding habits of bonefish, *Albula vulpes* from waters of the Florida Keys. *Fishery Bulletin* 96 (4): 754–766.

Cuvier G.L.C.F.D. 1816. *Le Règne animal, distribué d'après son Organisation, pour servir de Base à l'Histoire naturelle des Animaux et d'Introduction à l'Anatomie comparée. Les Reptiles, les Poissons, les Mollusques et les Annélides*. Fortin, Masson et C^{ie}, Paris. https://doi.org/10.5962/bhl.title.39612

Cuvier G.L.C.F.D. 1825. *Recherches sur les Ossemens fossiles, où l'on rétablit les Caractères de plusieurs Animaux dont les Révolutions du Globe ont détruit les Espèces, Vol. III, 3rd edition*. Dufour & d'Ocagne, Paris. https://doi.org/10.5962/bhl.title.122964

Cuvier G.L.C.F.D. 1829. *Le Règne animal distribué d'après son Organisation pour servir de Base à l'Histoire naturelle des Animaux et d'Introduction à l'Anatomie comparée, Vol. II, 2nd edition*. Déterville, Paris. https://doi.org/10.5962/bhl.title.41460

Cuvier G.L.C.F.D. & Valenciennes M.A. 1832. *Histoire naturelle des Poissons. Vol. VIII*. F.G. Levrault, Paris.

Cuvier G.L.C.F.D. & Valenciennes M.A. 1837. *Histoire naturelle des Poissons. Vol. XII.* F.G. Levrault, Paris.

Daimeries A. 1889. Notes ichthyologiqes – V. *Annales de la Société royale malacologique de Belgique, Bulletin des Séances* 24: 39–44.

Dames W. 1883. Über eine tertiäre Wirbelthierfauna von der westlichen Insel der Birket-EI-Qrûn im Fajum (Aegypten). *Sitzungsberichte der königlich preussischen Akademie der Wissenschaften zu Berlin* 6: 129–153.

Dartevelle E. & Casier E. 1943. Les poissons fossils du Bas-Congo et des régions voisines. *Annales du Musée du Congo belge, Série A (Minéralogie, Géologie, Paléontolgie)* 2 (3): 1–200.

Dean M.N., Bizzarro J.J., Clark B., Underwood C.J. & Johanson Z. 2017. Large batoid fishes frequently consume stingrays despite skeletal damage. *Royal Society Open Science* 4: e170674. https://doi.org/10.1098/rsos.170674

DeKay J.E. 1842. *Zoology of New York, or the New York fauna; comprising detailed descriptions of all the animals hitherto observed within the state of New York, with brief notices of those occasionally found near its borders, and accompanied by appropriate illustrations. Part IV, Fishes*. Carroll and Cook, Albany, New York.

Deynat P.P. & Brito P.M.M. 1994. Révision des tubercles cutanés de raies (Chondrichthyes, Batoidea) du Bassin du Paraná, tertiaire d'Amérique du Sud. *Annales de Paléontologie* 80 (4): 237–51.

Dillon E.M., Norris R.D. & O'Dea A. 2017. Dermal denticles as a tool to reconstruct shark communities. *Marine Ecology Progress Series* 566: 117–134. https://doi.org/10.3354/meps12018

Dockery D. & Thompson D. 2016. *The Geology of Mississippi*. University Press of Mississippi, Jackson.

Ebersole J.A. & Cicimurri D.J. In press. Chapter 7: Fishes part I – Chondrichthyes (cartilaginous fish: sharks and rays) and Osteichthyes (bony fishes): osteological remains. *In*: Ting S., Smith L.E. & White C.D. (eds) *Vertebrate Fossils of Louisiana.* Special Publication of the Museum of Natural Science. Louisiana State University, Baton Rouge, LA.

Ebersole J.A. & Jacquemin S.J. 2018. A late Miocene (Hemphillian) freshwater fish (Osteichthyes) fauna from Mobile County, Alabama, USA. *Historical Biology* 31 (1): 3–45.

Ebersole J.A., Cicimurri D.J. & Stringer G.L. 2019. Taxonomy and biostratigraphy of the elasmobranchs and bony fishes (Chondrichthyes and Osteichthyes) of the lower-to-middle Eocene (Ypresian to Bartonian) Claiborne Group in Alabama, USA, including an analysis of otoliths. *European Journal of Taxonomy* 585: 1–274. https://doi.org/10.5852/ejt.2019.585

Ebersole J.A., Cicimurri D.J. & Stringer G.L. 2021. Marine fishes (Elasmobranchii, Teleostei) from the Glendon Limestone Member of the Byram Formation (Oligocene, Rupelian) at site AWa-9, Washington County, Alabama, USA, including a new species of gobiid (Gobiiformes: Gobiidae). *Acta Geologica Polonica* 71 (4): 481–518. https://doi.org/10.24425/agp.2020.134561

Ebersole J.A., Kelosky A.T., Huerta-Beltrán B.L., Cicimurri D.J. & Drymon J.M. 2023. Observations on heterodonty within the dentitions of Atlantic sharpnose sharks, *Rhizoprionodon terraenovae* (Richardson, 1836), from the northern Gulf of Mexico, USA, with implications on the fossil record. *PeerJ* 11: e15142. https://doi.org/10.7717/peerj.15142

Ebersole J.A., Cicimurri D.J., Stallworth L.M. & Gentry A.D. 2024a. Preliminary report on the fishes (Chondrichthyes & Teleostei) from the lower Oligocene (Rupelian) Red Bluff Clay at site AMo-9, Monroe County, Alabama, USA. *Palaeo Vertebrata* 2024: 1–24. https://doi.org/10.18563/pv.47.2.e2

Ebersole J.A., Cicimurri D.J., Stringer G.L., Jacquemin S.J. & Ciampaglio C.N. 2024b. Cretaceous fishes of Alabama: *Chiloscyllium* ver. 1. *In:* Ebersole J.A. (ed.) *Fossil Fishes of Alabama* 3 (10):1–4. https://doi.org/10.69737/YQPK1523

Engelbrecht A., Mörs T., Reguero M.A. & Kriwet J. 2017. Revision of Eocene Antarctic carpet sharks (Elasmobranchii, Orectolobiformes) from Seymour Island, Antarctic Peninsula. *Journal of Systematic Palaeontology* 15 (12): 969–990. https://doi.org/10.1080/14772019.2016.1266048

Farmer C.H. III. 2004. *Sharks of South Carolina*. South Carolina Department of Natural Resources, Charleston, SC.

Feldmann R.M. & Portell R.W. 2007. First report of *Costacopluma* Collins and Morris, 1975 (Decapoda: Brachyura: Retroplumidae) from the Eocene of Alabama, U.S.A. *Journal of Crustacean Biology* 27 (1): 90–96.

Fialho P., Balbino A. & Antunes M.T. 2019. Langhian rays (Chondrichthyes, Batomorphii) from Brielas, Lower Tagus Basin, Portugal. *Geologica Acta* 17 (7): 1–16. https://doi.org/10.1344/GeologicaActa2019.17.7

Fink S.V. & Fink W.L. 1981. Interrelationships of ostariophysan fishes (Teleostei). *Zoological Journal of the Linnean Society* 72: 297–353. https://doi.org/10.1111/j.1096-3642.1981.tb01575.x

Fink S.V. & Fink W.L. 1996. Interrelationships of ostariophysan fishes (Teleostei). *In*: Stiassny M.L.J., Parenti L.R. & Johnson G.D. (eds) *Interrelationships of Fishes*: 209–249. Academic Press, San Diego, CA.

Fitch J.E. 1966. Additional fish remains, mostly otoliths, from a Pleistocene deposit at Playa del Rey, California. *Contributions in Science, Los Angeles County Museum* 119: 1–16.

Fitch J.E. 1970. Fish remains, mostly otoliths and teeth, from the Palos Verdes Sand (Late Pleistocene) of California. *Contributions in Science, Los Angeles County Museum* 199: 1–41.

Fraser G., Britz R., Hall A., Johanson Z. & Smith M. 2012. Replacing the first-generation dentition in pufferfish with a unique beak. *Proceedings of the National Academy of Sciences* 109 (21): 8179–8184. https://doi.org/10.1073/pnas.1119635109

Fricke R., Eschmeyer W. & Van der Laan R. 2019. *Eschmeyer's Catalog of Fishes: Genera, Species, References*. Available from https://researcharchive.calacademy.org/research/ichthyology/catalog/fishcatmain.asp [accessed 17 Aug. 2023].

Frizzell D.L. & Dante J.H. 1965. Otoliths of some early Cenozoic fishes of the Gulf Coast. *Journal of Paleontology* 39 (4): 687–718.

Froese R. & Pauly D. 2023. *FishBase.* Ver. 2/2023. Available from http://www.fishbase.org [accessed 16 Aug. 2023].

Fuelling L., Jacquemin S., Stringer G., Smith A. & Ciampaglio C. 2022. Phylogeography and biogeography of the ubiquitous and unique sciaenid genus *Aplodinotus* in North America. *Historical Biology* 35 (4): 555–566. https://doi.org/10.1080/08912963.2022.2054713

Garman S. 1899. Reports on an exploration off the west coasts of Mexico, Central and South America, and off the Galapagos Islands, in charge of Alexander Agassiz, by the US Fish Commission steamer "Albatross," during 1891, Lieut. Commander Z.L. Tanner, USN, commanding. XXVI. The fishes. *Memoirs of the Museum of Comparative Zoology at Harvard College* 24: 3–431.

Garman S. 1908. New Plagiostomia and Chismopnea. *Bulletin of the Museum of Comparative Zoology at Harvard College* 51: 249–256.

Geoffroy Saint-Hilaire E. 1817. Poissons du Nil, de la Mer Rouge et de la Méditerranée. *Description de l'Egypte ou recueil des Observations et des Recherches qui ont été faites en Égypte pendant l'Expedition de l'Armée française, publié par les Ordres de sa Majesté l'Empereur Napoléon le Grand*: 18–27. Imprimerie Imperiale, Paris.

Gibbes R.W. 1849. Monograph of fossil Squalidae of the United States. *Journal of the Academy of Natural Sciences of Philadelphia, Series 2* 1: 191–206.

Gilbert C.R. 1967. A revision of the hammerhead sharks (family Sphyrnidae). *Proceedings of the United States National Museum* 119 (3539): 1–88.

Gill T. 1861. Catalogue of the fishes of the eastern coast of North America, from Greenland to Georgia. *Proceedings of the Academy of Natural Sciences of Philadelphia* 13: 1–63.

Gill T. 1862. Analytical synopsis of the order of Squali and revision of the nomenclature of the genera. *Annals of the Lyceum of Natural History of New York* 7 (32): 367–408. https://doi.org/10.1111/j.1749-6632.1862.tb00166.x

Gill T. 1885. Sub-class II. Teleostei. *In*: Kingsley J. (ed.) *The Standard Natural History, Vol. III. Lower Vertebrates*: 98–298. Cassino and Company, Boston, MA.

Gill T. 1893. Families and subfamilies of fishes. *Memoirs of the National Academy of Science* 6 (6): 127–138.

Girard C.F. 1858. Notes upon various new genera and new species of fishes in the museum of the Smithsonian Institution collected in connection with the United States and Mexico boundary survey: Major William Emory, Commissioner. *Proceedings of the Academy of Natural Sciences of Philadelphia* 10: 167–171.

Girard J., Heller N., Dering J., Scott S., Jackson H. & Stringer G. 2005. Investigations at the Conly Site, a Middle Archaic Period settlement in Northwest Louisiana. *Bulletin of the Louisiana Archaeological Society* 32: 5–77.

Glückman L.S. 1964. *Sharks of the Palaeogene and their Stratigraphic Significance.* Nauka Press, Moscow. [In Russian.]

Gonzalez-Pestana A., Acuña-Perales N., Coasaca-Cespedes J., Cordova-Zavaleta F., Alfaro-Shigueto J., Mangel J.C. & Espinoza P. 2017. Trophic ecology of the smooth hammerhead shark (*Sphyrna zygaena*) off the coast of northern Peru. *Fishery Bulletin* 115: 451–459. https://doi.org/10.7755/FB.115.2

Goodrich E.S. 1930. *Studies on the Structure and Development of Vertebrates*. Macmillan and Co., London. https://doi.org/10.5962/bhl.title.82144

Gottfried M.D. & Fordyce R.E. 2001. An associated specimen of *Carcharodon angustidens* (Chondrichthyes, Lamnidae) from the Late Oligocene of New Zealand, with comments on *Carcharodon* relationships. *Journal of Vertebrate Paleontology* 21 (4): 730–739.

Grande L. 2010. An empirical synthetic pattern study of gars (Lepisosteiformes) and closely related species, based mostly on skeletal anatomy. The resurrection of Holostei. *Copeia* 2A: 1–871.

Gray J.E. 1834. *Illustrations of Indian Zoology Chiefly Selected from the Collection of Major-General Hardwicke, F.R.S.* Volume 2: 88–102. Natural History Museum, London.

Gray J.E. 1851. *List of the Specimens of Fish in the Collection of the British Museum. Part I. Chondropterygii*. British Museum, London. https://doi.org/10.5962/bhl.title.20819

Green J.M. 2002. *A Comparison of Paleoecological Determinations Based on Vertebrate and Invertebrate Faunas from the Moodys Branch Formation (Upper Eocene) of Louisiana and Mississippi*. M.Sc. thesis, University of Louisiana at Monroe.

Greenwood P.H., Rosen D.E., Weitzmann S.H. & Myers G.S. 1966. Phyletic studies of teleostean fishes, with a provisional classification of living forms. *Bulletin of the American Museum of Natural History* 131: 339–456.

Griffith E. & Smith C. 1834. *The Class Pisces, Arranged by Baron Cuvier, with Supplementary Additions by Edward Griffith, F.R.S. etc., and Lieut.-Col. Charles Hamilton Smith, FR, LSS, etc., etc.* Whittaker and Co., London.

Hales L. & Van Den Avyle M. 1989. Species profiles: life histories and environmental requirements of coastal fishes and invertebrates (South Atlantic). *United States Fish and Wildlife Services Biology Report* 82: 1–24.

Hasse C. 1878. *Das natürliche System der Elasmobranchier auf Grundlage des Baues und der Entwicklung ihrer Wirbelsäule. Eine morphologische und paläontologische Studie.* Allgemeiner Theil: 1–76. Gustav Fischer, Jena, Germany. Available from https://www.biodiversitylibrary.org/page/8534667 [accessed 6 Jan. 2025].

Hay O.P. 1902. Bibliography and catalogue of the fossil Vertebrata of North America. *Bulletin of the United States Geological and Geographical Survey of the Territories* 179: 1–868. https://doi.org/10.5962/bhl.title.20094

Hay O.P. 1929. Second bibliography and catalogue of the fossil Vertebrata of North America. *Carnegie Institution of Washington* 390 (1): 1–916.

Haye T., Reinecke T., Gürs K. & Piehl A. 2008. Die Elasmobranchier des Neochattiums (Oberoligozän) von Johannistal, Ostholstein, und Ergänzungen zu deren Vorkommen in der Ratzeburg-Formation (Neochattium) des südöstlichen Nordseebeckens. *Palaeontos* 14 (2): 1–95.

Herman J., Hovestadt-Euler M. & Hovestadt D.C. 1992. Contributions to the study of the comparative morphology of teeth and other relevant ichthyodorulites in living suprapecific taxa of Chondrichthyan fishes. Part A: Selachii. No. 4. Order: Orectolobiformes. – Families: Brachaeluridae, Ginglymostomatidae, Hemiscylliidae, Orectolobidae, Parascylliidae, Rhiniodontidae, Stegostomatidae. Order: Pristiophoriformes – Family: Pristiophoridae. Order: Squatiniformes – Family: Squatinidae. *Bulletin de l'Institut royal des Sciences naturelles de Belgique, Biologie* 62: 193–254.

Herman J., Hovestadt-Euler M. & Hovestadt D.C. 2003. Contributions to the study of the comparative morphology of teeth and other relevant ichthyodorulites in living supraspecific taxa of chondrichthyan fishes. Part A: Selachii. Addendum to 1: Order Hexanchiformes – Family Hexachidae, 2: Order Carcharhiniformes, 2a: Family Triakidae, 2b: Family Scyliorhinidae, 2c: Family Carcharhinidae, Hemigaleidae, Leptochariidae, Sphyrnidae, Proscylliidae and Pseudotriakidae, 3: Order Squaliformes – Families Echinorhinidae, Oxynotidae and Squalidae. Tooth vascularization and phylogenetic interpretation. *Bulletin de l'Institut royal des Sciences naturelles de Belgique, Biologie* 73: 5–26.

Hildebrand S.F. & Schroeder W.C. 1928. Fishes of Cheseapeake Bay. *Bulletin of the United States Bureau of Fisheries* 43 (1): 1–366.

Hoese H. & Moore R. 1998. *Fishes of the Gulf of Mexico*. Texas A&M University Press, College Station, TX.

Höltke O., Maxwell E.E. & Rasser M.W. 2024. A review of the paleobiology of some Neogene sharks and the fossil records of extant shark species. *Diversity* 16 (3): e147. https://doi.org/10.3390/d16030147

Hovestadt D.C. 2020. Taxonomic adjustments of the Oligocene and Miocene Odontaspididae and Carchariidae based on extant specimens. *Cainozoic Research* 20 (2): 229–255.

Hovestadt D.C. 2022. A partial skeleton of *Carcharias cuspidatus* (Agassiz, 1843) (Chondrichthyes, Carchariidae) including embryos from the Oligocene of Germany. *Cainozoic Research* 22 (1): 25–36.

Hovestadt D.C. & Hovestadt-Euler M. 2013. Generic assessment and reallocation of Cenozoic Myliobatinae based on new information of tooth, tooth plate, and caudal spine morphology of extant taxa. *Palaeontos* 24 (1): 1–66.

Hovestadt D. & Steurbaut E. 2023. Annotated iconography of the type specimens of fossil chondrichthyan fishes in the collection of the Royal Belgian Institute of Natural Sciences. *RBINS Monographs in Natural Science* 1: 1–122.

Howe H.V. 1937. Large oysters from the Gulf coast Tertiary. *Journal of Paleontology* 11: 355– 366.

Huxley T.H. 1880. On the application of the laws of evolution to the arrangement of the Vertebrata and more particularly of the Mammalia. *Proceedings of the Zoological Society of London* 1880: 649–662.

Huysseune A. 1995. Phenotypic plasticity in the lower pharyngeal jaw dentition of *Astatoreochromis alluaudi* (Teleostei: Chichlidae). *Archives of Oral Biology* 40 (11): 1005–1014. https://doi.org/10.1016/0003-9969(95)00074-Y

Huysseune A. & Meunier F. 1994. Comparative study of lower pharyngeal structure in two phenotypes of *Astatoreochromis alluaudi* (Teleostei: Chichlidae). *Journal of Morphology* 221: 25–43. https://doi.org/10.1002/jmor.1052210103

Ikejiri T., Ebersole J.A., Blewitt H.L. & Ebersole S.M. 2013. An overview of Late Cretaceous vertebrates from Alabama. *Bulletin of the Alabama Museum of Natural History* 31 (1): 46–71.

Inoue J.G., Miya M., Miller M.J., Sado T., Hanel R., Hatooka K., Aoyama J., Minegishi Y., Nishida M. & Tsukamoto K. 2010. Deep-ocean origin of the freshwater eels. *Biology Letters* 6: 363–366. https://doi.org/10.1098/rsbl.2009.0989

Jacquemin S.J., Ebersole J.A., Dickinson W.C. & Ciampaglio C.N. 2016. Late Pleistocene fishes of the Tennessee River Basin: an analysis of a late Pleistocene freshwater fish fauna from Bell Cave (site ACb-2) in Colbert County, Alabama. *PeerJ* 4: e1648. https://doi.org/10.7717/peerj.1648

Jaekel O. 1895. Unter-tertiäre Selachier aus Südrussland. *Mémoires du Comité géologique de St. Pétersbourg* 9: 19–35.

Joleaud L. 1912. *Géologie et Paléontologie de la Plaine du Comtat et de ses Abords. Description des Terrains néogènes* 2: 255–285. Imprimerie Montane, Sicardi et Valentin, Monpellier, France.

Jordan D.S. & Evermann B.W. 1896. The fishes of North and Middle America: a descriptive catalogue of the species of fish-like vertebrates found in the waters of North America, north of the Isthmus of Panama. Part 1. *Bulletin of the United States National Museum* 47: 1–1240. https://doi.org/10.5962/bhl.title.46755

Jordan D.S. & Gilbert C.H. 1879. Notes on the fishes of Beaufort Harbor, North Carolina. *Proceedings of the United States National Museum* 1 (55): 365–388. https://doi.org/10.5479/si.00963801.1-55.365

Jordan D.S. & Gilbert C.H. 1880. Notes on a collection of fishes from San Diego, California. *Proceedings of the United States National Museum* 3 (106): 23–34.

Kajiura S.M. & Tricas T.C. 1996. Seasonal dynamics of dental sexual dimorphism in the Atlantic stingray *Dasyatis sabina*. *Journal of Experimental Biology* 199: 2297–2306. https://doi.org/10.1242/jeb.199.10.2297

Kaufman L.S. & Liem K.F. 1982. Fishes of the suborder Labroidei (Pisces: Perciformes): phylogeny, ecology, and evolutionary significance. *Breviora* 472: 1–19.

Kaup J. 1856. Uebersicht der Aale. *Archiv für Naturgeschichte* 22 (1): 41–77. https://doi.org/10.5962/bhl.part.11240

King D.J. & Wade B.S. 2017. The extinction of *Chiloguembelina cubensis* in the Pacific Ocean: implications for defining the base of the Chattian (upper Oligocene). *Newsletters in Stratigraphy* 50 (3): 311–339. https://doi.org/10.1127/nos/2016/0308

Klimley A.P. 1987. The determinants of sexual segregation in the scalloped hammerhead shark, *Sphyrna lewini*. *Environmental Biology of Fishes* 18 (1): 27–40. https://doi.org/10.1007/BF00002325

Klunzinger C.B. 1871. Synopsis der Fische des Rothen Meeres. Theil II. *Verhandlungen der kaiserlich-königlichen zoologisch-botanischen Gesellschaft in Wien* 21: 441–688. https://doi.org/10.5962/bhl.title.14760

Klunzinger C.B. 1880. Die von Müller'sche Sammlung australischer Fische in Stuttgart. *Sitzungsberichte der kaiserlichen Akademie der Wissenschaften, mathematisch-naturwissenschaftliche Classe* 80 (3–4): 325–430.

Koken E. 1888. Neue Untersuchungen an tertiären Fisch-Otolithen. *Zeitschrift der deutschen geologischen Gesellschaft* 40: 274–305.

Kolmann M., Cohen K., Bemis K., Summers A., Irish F. & Hernandez L. 2019. Tooth and consequences: heterodonty and dental replacement in piranhas and pacus (Serrasalmidae). *Evolution and Development* 21: 247–262. https://doi.org/10.1111/ede.12306

Last P.R., White W.T. & Séret B. 2016. Taxonomic status of maskrays of the *Neotrygon kuhlii* species complex (Myliobatoidei: Dasyatidae) with the description of three new species from the Indo-West Pacific. *Zootaxa* 4083 (4): 533–561. https://doi.org/10.11646/zootaxa.4083.4.5

Latham J.F. 1794. An essay on the various species of sawfish. *The Transactions of the Linnean Society of London* 2 (25): 273-282.

Laurito C.A. 1999. *Los Selaceos fossiles de la Localidad de Alto Guayacan (y otros Ictiolitos associados). Mioceno superior–Plioceno inferior de Limon, Costa Rica*. Privately published, San José, Costa Rica.

Lawley R. 1876. *Nuovi Studi sopra ai Pesci ed altri Vertebrati fossili delle Colline toscane*. Tipografia dell'Arte della Stampa, Florence.

Leidy J. 1855. Indications of twelve species of fossil fishes. *Proceedings of the Academy of Natural Sciences of Philadelphia* 7: 395–397.

Leidy J. 1877. Description of vertebrate remains, chiefly from the phosphate beds of South Carolina. *Journal of the Academy of Natural Sciences of Philadelphia* 8 (2): 209–261.

Leriche M. 1908. Note préliminaire sur des poissons nouveaux de l'Oligocène belge. *Bulletin de la Société belge de Géologie, de Paléontologie et d'Hydrologie* 22: 378–384.

Leriche M. 1910. Les poissons tertiaires de la Belgique III. Les poissons oligocènes. *Mémoires du Musée royal d'Histoire naturelle de Belgique* 5 (2): 229–363.

Leriche M. 1942. Contribution à l'étude des faunes ichthyologiques marines des terrains tertiaires de la Plaine côtière Atlantique et du centre des Etats-Unis. Les synchronismes des formations teriaires des deux côtés de l'Atlantique. *Memoires de la Société géologique de France* 45 (2–4): 1–110.

Lesson R.P. 1831. Poissons. *In*: Duperrey L.I. (ed.) *Voyage autor du Monde, exécuté par Ordre du Roi, sur la Corvette de la Majésté, La Coquille, pendant les Années 1822, 1823, 1824 et 1825.* Vol. 2 (1): 66–238. Arthus Bertrand, Paris. https://doi.org/10.5962/bhl.title.57936

Lesueur C.A. 1817. Description of three new species of the genus *Raja*. *Journal of the Academy of Natural Sciences of Philadelphia* 1: 41–45

Lesueur C.A. 1822. Description of a *Squalus*, of very large size, which was taken on the coast of New Jersey. *Journal of the Academy of Natural Sciences of Philadelphia* 2: 343–352.

Li P., Fu C., Saimaiti A., Chang H., Tian J., Chen L. & Qiang X. 2023. Magnetostratigraphy of early Oligocene–middle Miocene deposits in the Xunhua Basin on the Tibet Plateau, China, and their paleoclimate significance. *Minerals* 13 (5): e671. https://doi.org/10.3390/min13050671

Lim D.D., Mott P.J., Mara A.K. & Martin A.P. 2010. Phylogeny of hammerhead sharks (family Sphyrnidae) inferred from mitochondrial and nuclear genes. *Molecular Phylogenetics and Evolution* 55 (2): 572–579. https://doi.org/10.1016/j.ympev.2010.01.037

Lin C.-H. & Nolf D. 2022. Middle and late Eocene fish otoliths from the eastern and southern USA. *European Journal of Taxonomy* 814: 1–122. https://doi.org/10.5852/ejt.2022.814.1745

Linck H.F. 1790. Versuch einer Eintheilung der Fische nach den Zähnen. *Magazin für das Neueste aus der Physik und Naturgeschichte* 6 (3): 28–38.

Linnaeus C. 1758. *Systema Naturae per Regna Tria Naturae, Secundum Classes, Ordines, Genera, Species, cum Characteribus, Differentiis, Synonymis, Locis*. 10th edition, vol. 1. Laurentius Salvius, Holmiae [Stockholm]. https://doi.org/10.5962/bhl.title.559

Linnaeus C. 1766. *Systema Naturae sive Regna Tria Naturae, Secundum Classes, Ordines, Genera, Species, cum Characteribus, Differentiis, Synonymis, Locis.* 12th edition, vol. 1 (pt 1): 1–532. Laurentius Salvius, Holmiae [Stockholm].

Lombarte A., Chic O., Parisi-Baradad V., Olivella R., Piera J. & Garca-Ladona E. 2006. A web-based environment from shape analysis of fish otoliths. The AFORO database. *Scientia Marina* 70: 147–152. https://doi.org/10.3989/scimar.2006.70n1147

Lowe R.T. 1841. A paper from the Rev. R.T. Lowe, M.A., describing certain new species of Madeiran fishes, and containing additional information relating to those already described. *Proceedings of the Zoological Society of London* 8: 36–39.

Luer C.A., Blum P.C. & Gilbert P.W. 1990. Rate of tooth replacement in the nurse shark, *Ginglymostoma cirratum*. *Copeia* 1: 182–191. https://doi.org/10.2307/1445834

Matsubara K. 1936. A new carcharoid shark found in Japan. *Zoological Magazine, Tokyo* 48 (7): 380–382. https://doi.org/10.34435/zm002443

May J., Baughman W.T., McCarty J.E., Glenn R.C. & Hall W.B. 1974. Wayne County geology and mineral resources. *Mississippi Geological, Economic, and Topographical Survey, Bulletin* 117: 1–97.

McEachran J.D. & de Carvallo M.R. 2002. Batoid fishes. *In*: Carpenter K.E. (ed.) *The Living Marine Resources of the Western Central Atlantic. Vol. 1: Introduction, Molluscs, Crustaceans, Hagfishes, Sharks, Batoid Fishes and Chimaeras. FAO Species Identification Guide for Fisheries Purposes*: 508–530. FAO, Rome.

Mello W. & Brito P.M.M. 2013. Contributions to the tooth morphology in early embryos of three species of hammerhead sharks (Elasmobranchii: Sphyrnidae) and their evolutionary implications. *Comptes rendus Biologies* 336: 466–471. https://doi.org/10.1016/j.crvi.2013.04.017

Menner V.V. 1928. Les sélaciens du Paléogène de Manghyschlak, d'Emba et du versant oriental d'Oural. *Bulletin de la Société impériale des Naturalistes de Moscou, Section géologique* 6 (3–4): 292–338. [In Russian.]

von Meyer H. 1863. *Sphyraena Tyrolensis* aus dem Tertiär-Gebilde von Häring in Tyrol. *Palaeontographica* 10 (6): 305–308.

Mitchill S.L. 1815. The fishes of New York described and arranged. *Transactions of the Literary and Philosophical Society of New York* 1: 355–492.

Monsch K.A. 2005. Revision of the scombroid fishes from the Tertiary of England. *Transactions of the Royal Society of Edinburgh, Earth Sciences* 95: 445–489. https://doi.org/10.1017/S0263593300001164

Monsch K.A. & Bannikov A.F. 2012. New taxonomic synopses and revision of the scombrid fishes (Scombroidei, Perciformes), including billfishes, from the Cenozoic of territories of the former USSR. *Earth and Environmental Science Transactions of the Royal Society of Edinburgh* 102: 253–300. https://doi.org/10.1017/S1755691011010085

Müller A. 1999. Ichthyofaunen aus dem atlantischen Tertiär der USA. *Leipziger Geowissenschaften* 9/10: 1–360.

Müller J. 1836. Verleichende Anatomie der Myxinoiden, der Cyclostomen mit durchbohrtem Gaumen. Erster Theil. Osteologie und Myologie. *Abhandlungen der königlichen Akademie der Wissenschaften zu Berlin* 1834: 65–340.

Müller J. 1845. Über den Bau und die Grenzen der Ganoiden, und über das natürliche System der Fische. *Archiv für Naturgeschichte* 11 (1): 91–141.

Müller J. & Henle F.G.J. 1837. Gattungen der Haifische und Rochen nach einer von ihm mit Hrn. Henle unternommenen gemeinschaflichen Arbeit über die Naturgeschichte der Knorpelfische. *Berichte der königlichen preussischen Akademie der Wisssenschaften zu Berlin* 1837: 111–118.

Müller J. & Henle F.G.J. 1838. On the generic characters of cartilaginous fishes, with descriptions of new genera. *Magazine of Natural History and Journal of Zoology, Botany,* M*ineralogy, Geology and Meteorology* 2: 33–37, 88–91.

Müller J. & Henle F.G.J. 1839. *Systematische Beschreibung der Plagiostomen*: 29–102. Veit und Comp., Berlin. https://doi.org/10.5962/bhl.title.6906

Müller J. & Henle F.G.J. 1841. *Systematische Beschreibung der Plagiostomen*: 103–200. Veit und Comp., Berlin. https://doi.org/10.5962/bhl.title.6906

Naylor G.J.P., Caira J.N., Rosana K.A.M., Straube N. & Lakner C. 2012. Elasmobranch phylogeny: a mitochondrial estimate based on 595 species. *In*: Carrier J.C., Musick J.A. & Heithaus M.R. (eds) *Biology of Sharks and their Relatives* (2nd edition): 31–56. Taylor and Francis, Boca Raton, FL.

Nelson J., Grande T. & Wilson M. 2016. *Fishes of the World* (5th edition). John Wiley and Sons, Hoboken, NJ.

Nicholls E.L. & Russell A.P. 1990. Paleobiogeography of the Cretaceous Western Interior Seaway of North America: the vertebrate evidence. *Palaeogeography, Palaeoclimatology, Palaeoecology* 79: 49–169.

Nolf D. 1985. Otolithi piscium. *In*: Schultze H.-P. (ed.) *Handbook of Paleoichthyology, Volume 10*: 1–142. Gustav Fischer, Stuttgart and New York.

Nolf D. 2003. Revision of the American otolith-based fish species described by Koken in 1888. *Louisiana Geological Survey Geological Pamphlet* 12: 1–19.

Nolf D. 2013. *The Diversity of Fish Otoliths, Past and Present*. Monographs in Natural Sciences. Royal Belgian Institute of Natural Sciences, Brussels.

Nolf D. & Stringer G.L. 1992. Neogene paleontology of the northern Dominican Republic, 14. Otoliths of teleostean fishes. *Bulletins of American Paleontology* 102 (340): 45–81.

Nolf D. & Stringer G.L. 2003. Late Eocene (Priabonian) fish otoliths from the Yazoo Clay at Copenhagen, Louisiana. *Louisiana Geological Survey Geological Pamphlet* 13: 1–23.

Norman J.R. 1926. A synopsis of the rays of the family Rhinobatidae, with a revision of the genus *Rhinobatus*. *Proceedings of the Zoological Society of London* 1926 (4): 941–982.

Notabartolo di Sciara G. 1987. A revisionary study of the genus *Mobula* Rafinesque, 1810 (Chondrichthyes: Mobulidae) with the description of a new species. *Zoological Journal of the Linnean Society* 91 (1): 1–91. https://doi.org/10.1111/j.1096-3642.1987.tb01723.x

Notabarolo di Sciara G. 2020. The giant devil ray *Mobula mobular* (Bonnaterre, 1788) is not giant, but it is the only spinetail devil ray. *Marine Biodiversity Records* 13 (4): 1–5. https://doi.org/10.1186/s41200-020-00187-0

Noubhani A. & Cappetta H. 1997. Les orectolobiformes, carcharhiniformes et myliobatiformes (Elasmobranchii, Neoselachii) des bassins à phosphates du Maroc (Maastrichtien–Lutétien basal). Systématique, biostratigraphie, évolution et dynamique des faunes. *Palaeo Ichthyologica* 8: 1–327.

Page L., Bemis K., Dowling T., Espinoza-Pérez H., Findley L., Gilbert C., Hartel K., Lea R., Mandrak N., Neighbors M., Schmitter-Soto J. & Walker H. Jr. 2023. Common and scientific names of fishes from the United States, Canada, and Mexico, 8th edition. *American Fisheries Society Special Publication* 37: 1–439. https://doi.org/10.47886/9781934874691

Palacios-Barreto P., Mar-Silva A.D., Bayona-Vasquez N.J., Adams D.H. & Díaz-Jaimes P. 2023. Characterization of the complete mitochondrial genome of the Brazilian cownose ray *Rhinoptera brasiliensis* (Mylobatiformes, Rhinopteridae) in the western Atlantic and its phylogenetic implications. *Molecular Biology Reports* 50: 4083–4095. https://doi.org/10.1007/s11033-023-08272-0

Pälike H., Norris R.D., Herrle J.O., Wilson P.A., Coxall H.K., Lear C.H., Shackleton N.J., Tripati A.K. & Wade B.S. 2006. The heartbeat of the Oligocene climate system. *Science* 314: 1894–1898. https://doi.org/10.1126/science.1133822

Palmer D.K. 1934. The foraminiferal genus *Guembelina* in the Tertiary of Cuba. *Memorias de la Sociedad cubana de Historia natural "Felipe Poey"* 8 (2): 73–76.

Parmley D. & Cicimurri D.J. 2003. Late Eocene sharks of the Hardie Mine local fauna of Wilkinson County, Georgia. *Georgia Journal of Science* 61 (3): 153–179.

Patterson C. & Rosen D.E. 1977. Review of ichthyodectiform and other Mesozoic fishes and the theory of practice of classifying fossils. *Bulletin of the American Museum of Natural History* 158: 83–172.

Perez V. 2022. The chondrichthyan fossil record of the Florida Platform (Eocene–Pleistocene). *Paleobiology* 48 (4): 622–654.

Perez V., Godfrey S.J., Kent B.W., Weems R.E. & Nance J.R. 2018. The transition between *Carcharocles chubutensis* and *Carcharocles megalodon* (Otodontidae, Chondrichthyes): lateral cusplet loss through time. *Journal of Vertebrate Paleontology* 38 (6): e1546732. https://doi.org/10.1080/02724634.2018.1546732

Petean F.F., Yang L., Corrigan S., Lima S.M.Q. & Naylor G.J.P. 2024. How many lineages are there of the stingrays genus *Hypanus* (Myliobatiformes: Dasyatidae) and why does it matter? *Neotropical Ichthyology* 22 (1): e230046. https://doi.org/10.1590/1982-0224-2023-0046

Pfeil F.H. 1981. Eine nektonische Fischfauna aus dem unteroligozänen Schönecker Fischschiefer des Galon-Grabens in Oberbayern. *Geologica Bavarica* 82: 357–388.

De Pinna M.C.C. 1996. Teleostean monophyly. *In*: Stiassny M.L.J., Parenti L.R. & Johnson G.D. (eds) *Interrelationships of Fishes*: 147–162. Academic Press, San Diego.

Poey F. 1860. *Memorias sobre la Historia natural de la Isla de Cuba, acompañadas de Sumarios latinos y Extractos en francés. Vol. 2*: 97–336. Viuda de Barcina, Havana, Cuba. https://doi.org/10.5962/bhl.title.2485

Poey F. 1875. Enumeratio piscium cubensium (Parte III). *Anales de la Sociedad española de Historia natural* 5: 373–404. https://doi.org/10.5962/bhl.title.12630

Pollerspöck J. & Straube N. 2020. An identification key to elasmobranch species based on dental morphological characters. Part B: extant lamniform sharks (Superorder Galeomorphii: Order Lamniformes). *Bulletin of Fish Biology* 19: 27–64.

Pollerspöck J. & Unger E. 2023. "Beiträge zur Kenntniss der fossilen Fische aus der Molasse von Baltringen" – Revision zum 200. Geburtstag von Pfarrer Josef Probst. Teil Hayfische (Selachoidei A. Günther) (Probst 1878). *Jahreshefte der Gesellschaft für Naturkunde in Württemberg* 179: 197–255. https://doi.org/10.26251/jhgfn.179.2023.197-255

Priem M.F. 1912. Sur les poissons fossiles des terrains Tertiaires supérieurs du sud de la France. *Bulletin de la Société géologique de France, Series 4* 12: 213–245.

Probst J. 1877. Beiträge zur Kenntniss der fossilen Fische aus der Molasse von Baltrigen. II: Batoidei. *Jahreshefte des Vereins für vaterländische Naturkunde in Württemberg* 33: 69– 103.

Probst J. 1878. Beiträge zur Kenntniss der fossilen Fische aus der Molasse von Baltringen. Hayefische. *Jahreshefte des Vereins für vaterländische Naturkunde in Württemberg* 34: 113–154.

Probst J. 1879. Beiträge zur Kenntniss der fossilen Fische aus der Molasse von Baltrigen. Hayfische. *Jahreshefte des Vereins für vaterländische Naturkunde in Württemberg* 35: 127–191.

Puckridge M., Last P.R., White W.T. & Andreakis N. 2013. Phylogeography of the Indo-West Pacific maskrays (Dasyatidae, *Neotrygon*): a complex example of chondrichthyan radiation in the Cenozoic. *Ecology and Evolution* 3 (2): 1–16. https://doi.org/10.1002/ece3.448

Purdy R.W., Schneider V.P., Applegate S.P., McLellan J.H., Meyer R.L. & Slaughter B.H. 2001. The Neogene sharks, rays and bony fishes from Lee Creek Mine, Aurora, North Carolina. *Smithsonian Contributions to Paleontology* 90: 71–202. https://doi.org/10.5479/si.00810266.90.1

Quoy J.R.C. & Gaimard J.P. 1824. Chapter IX. Description des poissons. *In*: Freycinet L. (ed.) *Voyage autour du Monde, entrepris par Ordre du Roi. Exécuté sur les Corvettes de S.M. l'Uranie et la Physicienne, pendant les Années 1817, 1818, 1819 et 1820*: 1–328. Pillet Aîné, Paris. https://doi.org/10.5962/bhl.title.152367

Radkhah A.R. & Eagderi S. 2019. Threatened fishes of the world: *Anoxypristis cuspidata* (Latham, 1794) (Pristidae). *Journal of Fisheries* 7 (1): 681–684. https://doi.org/10.17017/j.fish.9

Rafinesque C.S. 1810. *Caratteri di alcuni nuovi Ggeneri e nuove Specie di Animali e Piante della Sicilia, con varie Osservazioni sopra i medesimi*. Part I: 5–69. Opuscolo del Sicilia, Palermo, Italy. https://doi.org/10.5962/bhl.title.104418

Rafinesque C.S. 1815. *Analyse de la Nature ou Tableau de l'Univers et des Corps organisés*. Giovanni Barravecchia, Palermo, Italy.

Rafinesque C.S. 1818. Description of three new genera of fluviatile fish, *Pomoxis, Sarchirus* and *Exoglossum. Journal of the Academy of Natural Sciences of Philadelphia* 1 (2): 417–422.

Rafinesque C.S. 1819. Prodrome de 70 nouveaux genres d'animaux découverts dans l'intérieur des États-Unis d'Amérique, durant l'année 1818. *Journal de Physique, de Chimie et d'Histoire naturelle* 88: 417–429.

Ranzani C. 1842. De nonnullis novis speciebus piscium. Opusculum tertium. *Novi Commentarii Academiae Scientiarum Instituti Bononiensis* 5: 307–338.

Rasch L.J., Martin K.J., Cooper R.L., Metscher B.D., Underwood C.J. & Fraser G.J. 2016. An ancient dental gene set governs development and continuous regeneration of teeth in sharks. *Developmental Biology* 415 (216): 347–370. https://doi.org/10.1016/j.ydbio.2016.01.038

Reeves S. 2011. "*Albula vulpes.*" Animal Diversity Web.
Available from https://animaldiversity.org/accounts/Albula_vulpes/ [accessed 11 Feb. 2023].

Regan C.T. 1923. The skeleton of *Lepidosteus*, with remarks on the origin and evolution of the lower Neopterygian Fishes. *Proceedings of the Zoological Society of London* 1923: 445–461.
https://doi.org/10.1111/j.1096-3642.1923.tb02191.x

Reinecke T. & Radwański A. 2015. Fossil sharks and batoids from the Korytnica clays, Early Badenian (Langhian, Middle Miocene), Fore-Carpathian Basin, central Poland – a revision and updated record. *Palaeontos* 28: 5–37.

Reinecke T., Stapf H. & Raisch M. 2001. Die Selachier und Chimären des Unteren Meeressandes und Schleichsandes im Mainzer Becken (Rupelium, Unteres Oligozän). *Palaeontos* 1: 1–73.

Reinecke T., Moths H., Grant A. & Breitkreutz H. 2005. Die Elasmobranchier des norddeutschen Chattiums, insbesondere des Sternberger Gesteins (Eochattium, Oligozän). *Palaeontos* 8: 1–135.

Reinecke T., von der Hocht F. & Gürs K. 2008. Die Elasmobranchier des Vierlandiums, Unteres Miozän, im Nordwestdeutschen Becken aus Bohrungen und glaziofluviatilen Geröllen ("Holsteiner Gestein") der Vierlande-Feinsande (Holstein) und der Kakert-Schichten (Niederrhein). *Palaeontos* 14: 1–54.

Reinecke T., Louwye S., Havekost U. & Moths H. 2011. The elasmobranch fauna of the late Burdigalian, Miocene, at Werder-Uesen, Lower Saxony, Germany, and its relationships with Early Miocene faunas of the North Atlantic, Central Paratethys and Mediterranean. *Palaeontos* 20: 1–170.

Reinecke T., Balsberger M., Beaury B. & Pollerspöck J. 2014. The elasmobranch fauna of the Thalberg Beds, Early Egerian (Chattian, Oligocene), in the Subalpine Molasse Basin near Siegsdorf, Bavaria, Germany. *Palaeontos* 26: 1–129.

Reinecke T., Mollen F.H., Seitz J.C., Motomura H., Hovestadt D. & Hoedemakers K. 2023. Iconography of jaws and representative teeth of extant rhinopristiform and dasyatoid batoids (Chondrichthyes, Elasmobranchii) for comparison with fossil batoid material. *Palaeontos* 34: 1–158.

Röse A.F. 1793. *Petri Artedi Angermannia-Sueci Synonymia Nominum Piscium fere Omnium. Ichthyologiae, pars IV, editio II*. A.F. Röse, Grypeswaldiae [Greifswald, Germany].

Rosen D.E. 1985. An essay on euteleostean classification. *American Museum Novitates* 2827: 1–57.

Rüppell W.P.E.S.E. 1837. *Neue Wirbelthiere zu der Fauna von Abyssinien gehörig: Fische des rothen Meeres*: 53–80. Siegmund Schmerber, Frankfurt am Main. https://doi.org/10.5962/bhl.title.53778

Santini F., Carnevale G. & Sorenson L. 2015. First timetree of Sphyraenidae (Percomorpha) reveals a Middle Eocene crown age and an Oligo–Miocene radiation of barracudas. *Italian Journal of Zoology* 82 (1): 133–142. https://doi.org/10.1080/11250003.2014.962630

Schultz O. 2006. An anglerfish, *Lophius* (Osteichthyes, Euteleostei, Lophiidae), from the Leitha Limestone (Badenian, Middle Miocene) of the Vienna Basin, Austria (Central Paratethys). *Beiträge zur Paläontologie* 30: 427–435.

Schwarzhans W. 1978. Otolith-morphology and its usage for higher systematical units, with special reference to the Myctophiformes. *Mededelingen van de Werkgroep voor Tertaire en Kwartaire Geologie* 15 (4): 167–185.

Schwarzhans W. 1993. A comparative morphological treatise of Recent and fossil otoliths of the family Sciaenidae (Perciformes). *In*: Pfeil F. (ed.) *Piscium Catalogus, Otolithi Piscium*. Verlag Dr. Friedrich Pfeil, Munich.

Schwarzhans W. 2019a. Reconstruction of the fossil marine bony fish fauna (Teleostei) from the Eocene to Pleistocene of New Zealand by means of otoliths. *Memorie della Società italiana di Scienze naturali e del Museo di Storia naturale di Milano* 46: 3–326.

Schwarzhans W. 2019b. A comparative morphological study of Recent otoliths of the Congridae, Muraenesocidae, Nettastomatidae and Colocongridae (Anguilliformes). *Memorie della Società italiana di Scienze naturali e del Museo di Storia naturale di Milano* 46: 327–354. https://doi.org/10.18563/pv.45.1.e1

Scwharzhans W., Stringer G.L. & Takeuchi G.T. 2024. The middle Eocene bony fish fauna of California, USA, reconstructed by means of otoliths. *Rivista italiana di Paleontologia e Stratigrafia* 130 (2): 373–473. https://doi.org/10.54103/2039-4942/22783

Schweitzer C., Feldmann R. & Stringer G.L. 2014. *Neozanthopsis americana* (Decapoda, Brachyura, Carpilioidea) from the middle Eocene Cane River Formation of Louisiana, USA, and associated teleost otoliths. *Scripta Geologica* 147: 163–183.

Scotese C. R. 2014. *Cenozoic Plate Tectonic, Paleogeographic, and Paleoclimatic Reconstructions, Maps 1–15.* The PALEOMAP Project PaleoAtlas for ArcGIS, ver. 2, vol. 1. PALEOMAP Project, Evanston, Illinois.

da Silva Rodrigues-Filho L.F., da Costa Nogueira P., Sodré D., da Silva Leal J.R., Silva Nunes J.L., Rincon G., Teixeira Lessa R.A., Sampaio I., Vallinoto M., Ready J.S. & Luna Sales J.B. 2023. Evolutionary history and taxonomic reclassification of the critically endangered daggernose shark, a species endemic to the Western Atlantic. *Journal of Zoological Systematics and Evolutionary Research* 2023: e4798805. https://doi.org/10.1155/2023/4798805

Smale M., Watson G. & Hecht T. 1995. Otolith atlas of southern African marine fishes. *Ichthyological Monographs of the J.L.B. Smith Institute of Ichthyology* 1: 1–253.

Smith A.G., Smith D.G. & Funnell B.M. 1994. *Atlas of Mesozoic and Cenozoic Coastlines*. Cambridge University Press, Cambridge, UK.

Smith M.M., Fraser G.J., Chaplin N., Hobbs C. & Graham A. 2009. Reiterative pattern of sonic hedgehog expression in the catshark dentition reveals a phylogenetic template for jawed vertebrates. *Proceedings of the Royal Society B* 276 (1660): 1225–1233. https://doi.org/10.1098/rspb.2008.1526

Snelson F.F., Williams-Hooper S.E. & Schmid T.H. 1988. Reproduction and ecology of the Atlantic stingray, *Dasyatis sabina*, in Florida coastal lagoons. *Copeia* 1988 (3): 729–739. https://doi.org/10.2307/1445395

Snyder D.B. & Burgess G.H. 2016. *Marine Fishes of Florida*. Johns Hopkins University Press, Baltimore, MD.

Soares K.D.A. & de Carvalho M.R. 2019. The catshark genus *Scyliorhinus* (Chondrichthyes: Carcharhiniformes: Scyliorhinidae): taxonomy, morphology, and distribution. *Zootaxa* 4601 (1): 1–147. https://doi.org/10.11646/zootaxa.4601.1.1

Springer S. 1940. A new species of the hammerhead shark genus *Sphyrna*. *Proceedings of the Florida Academy of Sciences* 5: 46–52.

Starks E.C. 1910. The osteology and mutual relationships of the fishes belonging to the family Scombridae. *Journal of Morphology* 21 (1): 77–99.

Starnes J. & Phillips G. 2016. Stratigraphy of the late Oligocene Jones Branch vertebrate fossil site, lower Catahoula Formation, Wayne County, Mississippi. *Geological Society of America, South-Central Section, Abstracts with Programs*: 48.

Stevens J.D., McAuley R.B., Simpendorfer C.A. & Pillans R.D. 2008. *Spatial Distribution and Habitat Utilisation of Sawfish (Pristis spp) in Relation to Fishing in Northern Australia.* CISRO Publishing, Clayton, VIC, Australia.

Storms R. 1894. Troisième note sur les poissons du terrain Rupélien. *Bulletin de la Société belge de Géologie, de Paléontologie et d'Hydrologie* 8: 67–82.

Stringer G.L. 1992. Late Pleistocene–early Holocene teleostean otoliths from a Mississippi River mudlump. *Journal of Vertebrate Paleontology* 12 (1): 33–41.

Stringer G.L. & Bell D. 2018. Teleostean otoliths reveal diverse Plio-Pleistocene fish assemblages in coastal Georgia (Glynn County). *Bulletin of the Florida Museum of Natural History* 56 (3): 83–108.

Stringer G.L. & Breard S. 1997. Comparison of otolith-based paleoecology to other fossil groups: an example from the Cane River Formation (Eocene) of Louisiana. *Transactions of the Gulf Coast Association of Geological Societies* 47: 563–570.

Stringer G.L. & Hulbert R.C. Jr. 2020. Fish otoliths provide further taxonomic and paleoecologic data for the late Pleistocene (Rancholabrean) Jones Girls Site, Georgia. *Eastern Paleontologist* 5: 1–15.

Stringer G.L. & Miller M. 2001. Paleoenvironmental interpretations based on vertebrate fossil assemblages: an example of their utilization in the Gulf Coast. *Transactions of the Gulf Coast Association of Geological Societies* 51: 329–338.

Stringer G.L & Mixon V. 2005. Exceptional foraminiferal and fish otolith preservation reveals environmental fluctuations in the Oligocene Byram Formation (Big Black River Locality, Mississippi). *Geological Society of America, Southeastern Section, Abstracts with Programs* 37 (2): 3.

Stringer G.L. & Shannon K. 2019. The Pliocene Elizabethtown otolith assemblage (Bladen County, North Carolina, USA) with indications of a primary fish nursery area. *Historical Biology* 32 (8): 1108–1119. https://doi.org/10.1080/08912963.2019.1566324

Stringer G.L. & Starnes J. 2020. Significance of late Miocene fish otoliths (*Micropogonias undulatus*) from a *Rangia johnsoni* bed in the Pascagoula Formation in the subsurface of Mississippi. *Southeastern Geology* 54 (1): 21–28.

Stringer G.L. & Worley L. 2003. Implications of recently discovered marine Oligocene vertebrates from the Rosefield Formation of Louisiana. *Abstracts with Programs, 106th Annual Meeing of the Texas Academy of Science, Nacogdoches, Texas, Feb. 27–Mar. 1, 2003*: 67.

Stringer G.L., Breard S.Q. & Kontrovitz M. 2001. Biostratigraphy and paleoecology of diagnostic invertebrates and vertebrates from the type locality of the Oligocene Rosefield marl beds, Louisiana. *Transactions of the Gulf Coast Association of Geological Societies* 51: 321–328.

Stringer G.L., Hulbert R., Nolf D., Roth P. & Portell R. 2017. A rare occurrence of matched otoliths and associated skeletal remains of *Apogon townsendi* (Osteichthyes) from the Caloosahatchee Formation (lower Pleistocene) of Florida. *Bulletin of the Florida Museum of Natural History* 55 (4): 89–103.

Stringer G.L, Ebersole J.A., Starnes J. & Ebersole S.M. 2020a. First Pliocene otolith assemblage from the Gulf Coastal Plain, Dauphin Island, Mobile County, Alabama, USA. *Historical Biology* 33: 2147–2170. https://doi.org/10.1080/08912963.2020.1773457

Stringer G.L., Schwarzhans W., Phillips G. & Lambert R. 2020b. Highly diversified Late Cretaceous fish assemblage revealed by otoliths (Ripley Formation and Owl Creek Formation, northeast Mississippi, USA). *Rivista italiana di Paleontologia e Stratigrafia* 126 (1): 111–155. https://doi.org/10.13130/2039-4942/13013

Stringer G.L., Starnes J.E., Leard J. & Puckett M. 2020c. Taphonomic and paleoecologic considerations of a phenomenal abundance of teleostean otoliths in the Glendon Limestone (Oligocene, Rupelian), Brandon, Mississippi. *Journal of the Mississippi Academy of Sciences* 65 (1): 101. https://doi.org/10.24425/agp.2020.134561

Stringer G.L., Parmley D. & Quinn A. 2022a. Eocene teleostean otoliths, including a new taxon, from the Clinchfield Formation (Bartonian) in Georgia, USA, with biostratigraphic, biogeographic, and paleoecologic implications. *Palaeovertebrata* 45: 1–20. https://doi.org/10.18563/pv.45.1.e1

Stringer G.L., Sadorf E. & Shannon K. 2022b. Late Pliocene (Yorktown Formation) teleostean otoliths from new locations in North Carolina, USA, and their relationship to other American assemblages. *Eastern Paleontologist* 10: 1–34.

Stringer G.L., Ebersole J.A., Starnes J.E. & Ebersole S.M. 2023. Additions to the Pliocene fish otolith assemblage from site AMb-2 on Dauphin Island, Alabama, USA, and their taxonomic and paleoecologic implications. *Paleoichthys* 7: 1–29.

Stults D.Z., Hermsen E. & Starnes J.E. 2024. Fossil seeds of *Passiflora* L.: an Oligocene record of a new species and a Pleistocene record of a modern species from the Gulf of Mexico Coastal Plain. *Review of Palaeobotany and Palynology* 324: e105093. https://doi.org/10.1016/j.revpalbo.2024.105093

Szabó M., Kocsis L., Tóth E., Szabó P., Németh T. & Sebe K. 2022. Chondrichthyan (Holocephali, Squalomorphi and Batomorphii) remains from the Badenian of southern Hungary (Tekeres, Mecsek Mountains): the first deepwater cartilaginous fishes from the Middle Miocene of the Central Paratethys. *Papers in Palaeontology* 8 (6): e1471. https://doi.org/10.1002/spp2.1471

Tanaka T., Fujita Y. & Morinobu S. 2006. Fossil shark teeth from the Namigata Formation in Ibara City, Okayama Prefecture, Central Japan and their biostratigraphical significance. *Bulletin of the Mizunami Fossil Museum* 33: 103–109.

Taylor R.L., Compagno L.J.V. & Struhsaker P.J. 1983. Megamouth – a new species, genus, and family of lamnoid shark (*Megachasma pelagios*, Family Megachasmidae) from the Hawaiian Islands. *Proceedings of the California Academy of Sciences* 43: 87–110.

Thiery A.P., Shono T., Kurokawa D., Britz R., Johanson Z. & Fraser G.J. 2017. Spatially restricted dental regeneration drives pufferfish beak development. *Proceedings of the National Academy of Sciences* 114 (22): E4425–E4434. https://doi.org/10.1073/pnas.1702909114

Tomita T., Yabumoto Y. & Kuga N. 2023. A new snaggletooth shark species, *Hemipristis tanakai* sp. nov. from the Ashiya Group (Oligocene), Northern Kyushu, Japan. *Paleontological Research* 28 (3): 273–278. https://doi.org/10.2517/PR220021

Trapani J., Yamamoto Y. & Stock D. 2005. Ontogenetic transition from unicuspid to multicuspid oral dentition in teleost fish: *Astyanax mexicanus*, the Mexican tetra (Ostariophysi: Characidae). *Zoological Journal of the Linnean Society* 145 (4): 523–538. https://doi.org/10.1111/j.1096-3642.2005.00193.x

Tuomey M. 1858. *Second Biennial Report of the Geology of Alabama*. N.B. Cloud, Montgomery, AL.

Türtscher J., López-Romero F.A., Jambura P.L., Kindlimann R., Ward D.J. & Kriwet J. 2021. Evolution, diversity and disparity of the tiger shark lineage *Galeocerdo* in deep time. *Paleobiology* 47 (4): 574–590. https://doi.org/10.1017/pab.2021.6

Tyler J.C. 1980. Osteology, phylogeny, and higher classification of the fishes of the Order Plectognathi (Tetraodontiformes). *National Oceanic and Atmospheric Administration, National Marine Fisheries Service, Technical Report, Circular* 434: 1–422.

Tyler J.C. & Bannikov A.F. 1994. A new genus of fossil pufferfish (Tetraodontidae: Tetraodontiformes) based on a new species from the Oligocene of Russia and a referred species from the Miocene of Ukraine. *Proceedings of the Biological Society of Washington* 107 (1): 97–108.

Tyler J.C. & Bannikov A.F. 2012. A new species of pufferfish, *Eotetraodon tavernei*, from the Eocene of Monte Bolca, Italy (Tetraodontidae, Tetraodontiformes). *Studi e Ricerche sui Giacimenti terziari di Bolca, Miscellanea Paleontologica* 11: 51–58.

Tyler J.C., Purdy R.W. & Oliver K.H. 1992. A new species of *Spheroides* pufferfish (Teleostei: Tetraodontidae) with extensive hyperostosis from the Pliocene of North Carolina. *Proceedings of the Biological Society of Washington* 105 (3): 462–482.

Underwood C.J., Ward D.J., King C., Antar S.M., Zalmout I.S. & Gingerich P.D. 2011. Shark and ray faunas of the Middle and Late Eocene of the Fayum area, Egypt. *Proceedings of the Geologists' Association* 122 (1): 47–66. https://doi.org/10.1016/j.pgeola.2010.09.004

Valenciennes M.A. 1822. Sur le sous-genre marteau, *Zygaena*. *Mémoires du Muséum d'Histoire naturelle* 9: 222–228.

Van der Laan R., Eschmeyer W. & Fricke R. 2014. Family-group names of Recent fishes. *Zootaxa* 3882 (1): 1–230. https://doi.org/10.11646/zootaxa.3882.1.1

Van der Laan R., Eschmeyer W. & Fricke R. 2017. Cumulative addenda to family-group names of Recent fishes. Addenda to and errata of: Van der Laan *et al.* (2014). Family-group names of Recent fishes.

Van Simaeys S., De Man E., Vandenberghe N., Brinkuis H. & Steurbaut E. 2004. Stratigraphic and palaeoenvironmental analysis of the Rupelian–Chattian transition in the type region: evidence from dinoflagellate cysts, foraminifera and calcareous nannofossils. *Palaeogeography, Palaeoclimatology, Palaeoecology* 208: 31–58. https://doi.org/10.1016/j.palaeo.2004.02.029

Vialle N., Adnet S. & Cappetta H. 2011. A new shark and ray fauna from the Middle Miocene of Mazan, Vaucluse (Southern France) and its importance in interpreting the paleoenvironment of marine deposits in the southern Rhodanian Basin. *Swiss Journal of Paleontology* 130: 241–258. https://doi.org/10.1007/s13358-011-0025-4

Villafaña J.A., Marramà G., Klug S., Pollerspöck J., Balsberger M., Rivadeneira M. & Kriwet J. 2020. Sharks, rays and skates (Chondrichthyes, Elasmobranchii) from the Upper Marine Molasse (middle Burdigalian, early Miocene) of the Simssee area (Bavaria, Germany), with comments on palaeogeographic and ecological patterns. *Paläontologische Zeitschrift* 94: 725–757. https://doi.org/10.1007/s12542-020-00518-7

Villalobos-Segura E. & Underwood C.J. 2020. Radiation and divergence times of the Batoidea. *Journal of Vertebrate Paleontology* 40 (3): e1777147. https://doi.org/10.1080/02724634.2020.1777147

Wainwright P.C., Smith W.L., Price S.A., Tang K.L., Sparks J.S., Ferry L.A., Kuhn K.L., Eytan R.I. & Near T.J. 2012. The evolution of pharyngognathy: a phylogenetic and functional appraisal of the pharyngeal jaw key innovation in labroid fishes and beyond. *Systematic Biology* 61 (6): 1001–1027. https://doi.org/10.1093/sysbio/sys060

Wakita M., Itoh K. & Kobayashi S. 1977. Tooth replacement in the teleost fish *Prionurus microlepidotus* Lacépède. *Journal of Morphology* 153: 129–141. https://doi.org/10.1002/jmor.1051530109

Walbaum J.J. 1792. *Petri Artedi Sueci Genera Piscium in Quibus Systema totum Ichthyologiae Proponitur*. Ichthyologiae. III. A.F. Röse, Grypeswaldiae [Greifswald, Germany].

Ward D.J. & Bonavia C.G. 2001. Additions to, and a review of, the Miocene shark and ray fauna of Malta. *The Central Mediterranean Naturalist* 3 (3): 131–146.

Weems R.E., Boessenecker R.W. & Sanders A.E. 2022. Cetacean remains from the lower Oligocene Old Church Formation of Virginia. *The Mosasaur* 12: 30–45. https://doi.org/10.5281/zenodo.8271554

Weiler W. 1938. Neue Untersuchungen an mitteloligozänen Fischen Ungarns. *Geologica Hungarica*, *Series Palaeontologica* 15: 1–30.

Westgate J.W. 1984. Lower vertebrates from the Late Eocene Crow Creek local fauna, St. Francis County, Arkansas. *Journal of Vertebrate Paleontology* 4 (4): 536–546.

Westgate J.W. 2001. Paleoecology and biostratigraphy of marginal marine Gulf Coast Eocene vertebrate localities. *In*: Gunnel G.F. (ed.) *Eocene Biodiversity: Unusual Occurrences and Rarely Sampled Habitats*: 263-297. Plenum Press, New York. https://doi.org/10.1007/978-1-4615-1271-4_11

White E.I. 1926. Eocene fishes of Nigeria. *Bulletin of the Geological Survey of Nigeria* 10: 1– 82. https://doi.org/10.1093/oxfordjournals.afraf.a100500

White E.I. 1955. Notes on African Tertiary sharks. *Bulletin of the Geological Survey of Nigeria* 5 (3): 319–325.

White E.I. 1956. The Eocene fishes of Alabama. *Bulletins of American Paleontology* 36: 123–150.

White E.I. & Moy-Thomas J.A. 1941. Notes on the nomenclature of fossil fishes. Part III. Homonyms M–Z. *Annals and Magazine of Natural History, Series 11* 7: 395–400. https://doi.org/10.1080/03745481.1941.9727941

Whitley G.P. 1929. Additions to the check-list of the fishes of New South Wales, 2. *Australian Zoologist* 5 (4): 353–357.

Wiley E.O. & Johnson G.D. 2010. A teleost classification based on monophyletic groups. *In*: Nelson J., Schultze H.-P. & Wilson M. (eds) *Origin and Phylogenetic Interrelationships of Teleosts*: 123–182. Verlag Dr. Friedrich Pfeil, Munich.

Winkler T.C. 1874. Deuxième mémoire sur des dents de poissons fossiles du terrain bruxellien. *Archives du Musée Teyler* 4 (1): 16–48.

Woodward A.S. 1889. *Catalogue of the Fossil Fishes in the British Museum*, Pt. I. British Museum (Natural History), London.

Worley L.E. 2004. *Paleoecologic and Evolutionary Implications of Bony and Cartilaginous Fishes from Oligocene Sites of the Rosefield Formation in Northwestern Catahoula Parish, Louisiana*. M.Sc. thesis, University of Louisiana at Monroe.

Yabumoto Y. & Uyeno T. 1994. Late Mesozoic and Cenozoic fish faunas of Japan. *Island Arc* 3 (4): 255–269. https://doi.org/10.1111/j.1440-1738.1994.tb00115.x

Manuscript received: 30 April 2024
Manuscript accepted: 10 October 2024
Published on: 28 March 2025
Topic editor: Marie-Béatrice Forel
Desk editor: Danny Eibye-Jacobsen

Copenhagen, Denmark; Naturalis Biodiversity Center, Leiden, the Netherlands; Museo Nacional de Ciencias Naturales-CSIC, Madrid, Spain; Leibniz Institute for the Analysis of Biodiversity Change, Bonn – Hamburg, Germany; National Museum of the Czech Republic, Prague, Czech Republic; The Steinhardt Museum of Natural History, Tel Aviv, Israël.

Appendices

Appendix 1. Taxonomic listing of Chondrichthyes identified from the Catahoula Formation in Wayne County, Mississippi. With each taxonomic ranking we provide the numbers of specimens for each type of remains recovered (i.e., teeth, caudal spines), as well as the percentages of the total chondrichthyan component that each taxon constitutes.

Catahoula Formation taxon	# teeth	# scales	# other	total # specimens (genus/species)	total # specimens (Division, Order, Family)	% elasmobranch assemblage (genus/species)	% elasmobranch assemblage (Division, Order, Family)
SELACHII				1995	2002	55.38	55.57
Selachii indet.	7				7		0.19
Orectolobiformes					21		0.57
Brachaeluridae					1		0.02
gen. indet.	1			1		0.02	
Hemiscylliidae					12		0.33
Chiloscyllium sp.	12			12		0.33	
Ginglymostomatidae					8		0.22
Nebrius sp.	8			8		0.22	
Lamniformes					245		6.79
Otodontidae					1		0.02
(*Otodus*) *Carcharocles* sp.	1			1		0.02	
Carchariidae					240		6.67
Carcharias cuspidatus	240			240		6.67	
Pseudocarchariidae					2		0.05
aff. *Pseudocarcharias* sp.	2			2		0.05	
Alopiidae					2		0.05
Alopias sp.	2			2		0.05	
Carcharhiniformes					1729		48.02
Hemigaleidae					193		5.36
Hemipristis intermedia sp. nov.	193			193		5.36	
Carcharhinidae					1344		37.35
Physogaleus contortus	15			15		0.41	
Physogaleus sp.	14			14		0.38	
Rhizoprionodon sp.	36			36		1	
Carcharhinus acuarius	986			986		27.42	
Carcharhinus elongatus	291			291		8.09	
Galeorhinus sp.	2			2		0.05	
Scyliorhinidae					30		0.82
Pachyscyllium distans	11			11		0.3	
Pachyscyllium sp.	19			19		0.52	
Sphyrnidae					116		3.22
"Sphyrna" gracile gen. et sp. nov.	31			31		0.86	
"Sphyrna" robustum sp. nov.	85			85		2.36	
Galeocerdonidae					46		1.27
Galeocerdo platycuspidatum sp. nov.	46			46		1.27	
BATOMORPHII				1215	1593	42.79	43.23
Batomorphii indet.		9	43		52		1.44
Rhinopristiformes					298		8.27
Rhinidae					246		6.84
Rhynchobatus cf. R. *pristinus*	246			246		6.84	
Pristidae					22		1.43
Pristis sp.	28		12	40		1.16	
Anoxypristis sp.			10	10		0.27	
Myliobatiformes					1243		33.52
gen. indet. (durophagous)	326				326	9.06	
Dasyatidae					582		16.18
Hypanus? *heterodontus* sp. nov.	578			578		16.07	
gen. et sp. indet.	3	1		4		0.11	
Myliobatidae					222		6.16
"*Myliobatis*" sp.	170		1	171		4.75	
"*Aetomylaeus*" sp.	49		2	51		1.41	
Rhinopteridae					110		3.05
"*Rhinoptera*" sp.	110			110		3.05	
Mobulidae					3		0.07
Plinthicus sp.	1			1		0.02	
Paramobula fragilis	2			2		0.05	
						42.79	
Euselachii indet.		10	9				
				total = 3210	**total = 3595**	**total = 98.17%**	**total = 98.8%**

Appendix 2. Taxonomic listing of Teleostei identified from the Catahoula Formation in Wayne County, Mississippi. With each taxonomic ranking we provide the numbers of specimens for each type of remains recovered (i.e., teeth, otoliths), as well as the percentages of the total bony fish component that each taxon constitutes.

Catahoula Formation taxon	# teeth	# scales	# jaw elements	# otoliths	# other	total # specimens (genus/species)	total # specimens (Division, Order, Family)	% bony fish assemblage (genus/species)	% bony fish assemblage (Division, Order, Family)
GINGLYMODI							173		1.96
Lepisosteiformes							173		1.96
Lepisosteidae							173		1.96
gen. indet.	109	64				173		1.96	
TELEOSTEOMORPHA							8628		97.18
Albuliformes							63		0.71
Albulidae							63		0.71
gen. indet.	48		6	9		63		0.71	
Anguilliformes							3		0.04
Congridae							3		0.03
Protanago nonsector				2		2		0.02	
gen. indet.				1		1		0.01	
Siluriformes							8		0.09
gen. indet.					8 (fin spine)	8		0.09	
Istiophoriformes							609		6.91
Sphyraenidae							609		6.91
Sphyraena sp.	609					609		6.91	
Pleruonectiformes							3		0.03
Cyclopsettidae							3		0.03
Syacium sp.				3		3		0.03	
Scombriformes							178		2.01
Scombridae							178		2.01
Acanthocybium sp.	3					3		0.03	
Scomberomorus sp.	175					175		1.98	
Labriformes							19		0.21
Labridae							19		0.21
gen. indet.	12				7 (tooth mass)	19		0.21	
Perciformes							114		1.17
Haemulidae							1		0.01
Allomorone sp.				1		1		0.01	
Lutjanidae							113		1.28
gen. indet.	112		1			113		1.28	
Acanthuriformes							6171		70.1
Sciaenidae							6171		70.1
Aplodinotus distortus				19		19		0.21	
Aplodinotus gemma				46		46		0.52	
Sciaena ? pseudoradians				134		134		1.52	
Sciaena ? radians				3		3		0.03	
gen. indet.	5761		16	192		5969		67.82	
Spariformes							1225		13.88
Sparidae							1225		13.88
Diplodus sp.	183					183		2.07	
Sparus ? cf. elegantulus				1		1		0.01	
gen. indet.	1041					1041		11.8	
Lophiiformes							229		2.6
Lophiidae							229		2.6
gen. indet.	229					229		2.6	
Tetraodontiformes							6		0.06
Tetraodontidae							6		0.06
gen. indet.			6			6		0.06	
Actinopterygii									
gen. indet.	843		17		276 (misc.)				
						total = 8801	**total = 8801**	**total = 99.88%**	**total = 99.14%**

Appendix 3. Habitat distribution and general climatic ranges of the families of otolith-based bony fishes from the Catahoula Formation at the Jones Branch locality. Key to superscripts: 1 = rarely freshwater or brackish; 2 = primarily marine with some brackish; 3 = primarily brackish and marine coastal waters; 4 = chiefly marine and rarely freshwater; 5 = mainly tropical to warm temperate; 6 = primarily marine with a few brackish.

Osteichthyan Family	Environmental Distribution			Climatic Range			
	Freshwater	Brackish	Marine	Tropical	Subtropical	Temperate	Arctic
Albulidae [1]							
Congridae [2]							
Cyclopsettidae [3]							
Haemulidae [4]							
Sciaenidae [5]							
Sparidae [6]							